# The role of poly(ADP-ribose) polymerase-1 in the MDM2-p53 DNA damage response pathway

**By**

**Paul Andrew Jowsey**

**University of Newcastle upon Tyne**
**Cancer Research Unit**

**A thesis submitted in part requirement for the degree of Doctor of Philosophy from the Faculty of Medicine, University of Newcastle upon Tyne**

**July 2003**

# ABSTRACT

p53 is a tumour suppressor protein that is stabilised and activated by DNA damage. DNA damage-induced p53 is able to bring about either cell cycle arrest or apoptosis by the induction of p53-responsive genes such as mdm2 and $p21^{waf-1}$. Mdm2 regulates p53 function by blocking the transcriptional transactivation domain of p53 and also by targeting p53 for degradation via an ubiquitin-mediated pathway. Increases in the levels and activity of p53 are brought about by post-translational modifications. The most widely studied modification of p53 is phosphorylation, mediated by several DNA damage-activated kinases. Poly(ADP-Ribose) Polymerase-1 (PARP-1) is also a DNA damage-activated enzyme which covalently modifies several target proteins by poly(ADP-ribosylation). It is well established that PARP-1 plays a key role in DNA base excision repair. More recently, several studies have implicated PARP-1 in the regulation of p53 function in response to DNA damage, although the nature of this relationship has been controversial.

This study aimed to clarify and investigate further the role of PARP-1 in p53 regulation using PARP-1 proficient and PARP-1 deficient mouse embryonic fibroblasts (MEFs) as well as a novel potent PARP-1 inhibitor (AG14361; $K_i < 6nM$). In this study, both primary and immortalised PARP-1 MEFs were used. Initial experiments revealed a tendency for $PARP\text{-}1^{+/+}$ MEFs to develop p53 mutations during immortalisation. Interestingly, $PARP\text{-}1^{-/-}$ MEFs retained wild-type p53, suggesting that the absence of PARP-1 bypasses the requirement for p53 to be mutated during the immortalisation of MEFs. As these cells could not be used to analyse p53 responses, experiments were performed on primary PARP-1 MEFs. However, the primary PARP-1 MEFs were found

to grow very slowly compared to their PARP-1 proficient counterparts. Interestingly, treatment of primary PARP-$1^{+/+}$ MEFs with AG14361 had a similar effect on cellular growth. This growth inhibition in the absence of PARP-1 was only evident in primary and not immortalised cells. It was therefore decided to stably transfect immortalised PARP-$1^{-/-}$ MEFs, expressing wild-type p53, with a plasmid construct containing PARP-1 to produce an isogenic cell line pair. These cells have been used, together with a human colorectal carcinoma cell line (HCT-116) and the potent PARP-1 inhibitor AG14361 to analyse the p53 response to different DNA damaging agents. In response to ionising radiation and ultra violet radiation, the absence of PARP-1 did not alter the induction or activity of p53. In response to the alkylating agent temozolomide, treatment of PARP-1 proficient MEFs with AG14361 potentiated the increase in p53 protein levels without affecting the transcriptional transactivation activity of p53, possibly due to an impaired repair of the DNA damage and hence increased signalling to p53 due to the persistence of DNA strand breaks. However, similar results were not obtained in the absence of PARP-1 protein (PARP-$1^{-/-}$ MEFs) or in HCT-116 cells treated with AG14361 The data presented do not support the hypothesis that PARP-1 is directly involved in the DNA damage induced regulation of p53. There may, however, be an altered p53 response in the absence of PARP-1 when cells are treated with particular DNA damaging agents, due to an impaired DNA repair pathway.

# Table of contents

# Acknowledgements

I would like to thank my supervisors, John and Barbara for their support and encouragement throughout my three years at Newcastle. In addition, I thank all members of staff, past and present, from the Cancer Research Unit. They all helped to make my time there enjoyable, even when things were not always going well. I am particularly grateful to Gillian who shared her expertise with the reporter gene assay used in this project and also for invaluable help, advice and words of encouragement both during my project and in the time since. I acknowledge the funding received from Cancer Research UK throughout the project.

On a personal note, I could not have reached this stage in my education without the earlier help and support from my late grandparents. I also owe huge thanks to my parents who have provided constant and unwavering encouragement and guidance from my early days at school. I hope they realise how much I appreciate all they have done for me.

My final note of thanks goes to my girlfriend, Emma who has stood by me for eight years, throughout my A-levels, undergraduate degree and PhD. She has been nothing other than loving and supportive even during the most frustrating and difficult of times. Without her I doubt that I could have reached the stage of completing a PhD thesis. Emma also recently gave birth to our first child, baby Grace, for which I will be eternally thankful. I hope she realises how much her being there means to me and that in the coming years I can repay the huge debt of thanks that I owe her.

# List of abbreviations

| | |
|---|---|
| A | adenosine |
| ADPr | adenosine diphosphate ribose |
| Amp | ampicillin |
| ARF | alternative reading frame |
| Asp | aspartic acid |
| ATP | adenosine triphosphates |
| Bcl-2 | B-cell leukaemia/lymphoma-2 |
| BER | base excision repair |
| Bp | base pair |
| BLAST | basic local alignment search tool |
| C | cytosine |
| CAK | cyclin activating kinase |
| CDK | cyclin dependent kinase |
| cDNA | complimentary deoxyribonucleic acid |
| CREB | camp response element binding protein |
| dATP | deoxyadenosine triphosphates |
| DBD | DNA binding domain |
| dCTP | deoxycytosine triphosphate |
| dGTP | deoxyguanosine triphosphates |
| dNTP | deoxynucleoside triphosphate |
| dTTP | deoxythymidine triphosphate |
| ddATP | dideoxyadenosine triphosphate |
| ddCTP | dideoxycytosine triphosphate |
| ddGTP | dideoxyguanosine triphosphates |
| ddNTP | dideoxynucleoside triphosphates |
| ddTTP | dideoxythymidine triphosphates |
| DMEM | Dulbecco s modified eagles medium |
| DMSO | dimethylsulfoxide |
| DNA | deoxyribonucleic acid |
| DNA-PK | DNA-dependent protein kinase |
| Dnase | deoxyribonuclease |
| DSB | double strand break |
| DTT | dithiothreitol |
| *E. coli* | *Escherichia coli* |
| ECL™ | enhanced chemiluminescence |
| EDTA | ethylenediaminetetraacetic acid |
| FBS | foetal bovine serum |
| G | guanosine |
| GST | glutathione *S*-transferase |
| HPV | human papilloma virus |
| HR | homologous recombination |
| HRP | horseradish peroxidase |
| IR | ionising radiation |
| LB | Luria-Bertani medium |
| MDM2 | murine double minute 2 |
| MMS | methyl methane sulphonate |
| MNNG | *N*-methyl-*N*-nitro-*N*-nitrosoguanidine |

| | |
|---|---|
| MNU | N-methyl-N-nitrosourea |
| mRNA | messenger ribonucleic acid |
| NAD | nicotinamide adenosine diphosphate |
| NHEJ | non-homologous end-joining |
| NER | nucleotide excision repair |
| PAGE | polyacrylamide gel electrophoresis |
| PARP-1 | poly(ADP-ribose) polymerase-1 |
| PARG | poly(ADP-ribose) glycohydrolas |
| PBS | phosphate buffered saline |
| RNA | ribonucleic acid |
| SCE | sister chromatid exchange |
| SDS | sodium dodecyl sulphate |
| TBST | tris buffered saline with 0.1% Tween20 |
| UV | ultra-violet radiation |
| v/v | volume to volume |
| w/v | weight to volume |
| XP | xeroderma pigmentosum |

# List of figures

# List of tables

# CHAPTER 1

# INTRODUCTION

## 1.1 GENERAL INTRODUCTION

The division of cells normally occurs in a highly ordered and controlled manner. This growth involves a stage during which the DNA of the cell is replicated in order for the cell to divide into two. As the DNA of a cell is replicated and one copy passed on to a daughter cell, it is essential that the integrity of the DNA be maintained. If the DNA does become damaged, this can lead to mutations to genes which can ultimately lead to cell death, or in the case of multicellular organisms, the formation of a cancerous cell. Several mechanisms exist to ensure that errors do not occur during DNA replication. In addition to errors occurring during replication, DNA damage can occur as a result of many exogenous factors such as ionising radiation, ultra-violet light, various classes of chemicals and even certain viruses. Again, cells possess mechanisms to counteract the effect of these agents. It is these mechanisms that are the focus of my research.

### 1.1.1 The cell cycle

The eukaryotic cell cycle is divided into four sections, as can be seen in the diagram below (figure 1.1). During S phase, synthesis of new DNA occurs. G1 (gap 1) and G2 (gap 2) are gaps of time during which the cell prepares itself for the next stage in the cycle. Mitosis is the phase during which the cell actually divides into two. There are two points at which this cycle is regulated:- the G1/S phase junction and the G2/M junction. Cells that are not cycling are said to be quiescent and in a phase known as G0. Stimulation of cells in this state to enter the cell cycle is provided by growth factors. Subsequent progression of a cell through the cycle is dependent upon a range of cell cycle control proteins, including cyclins and cyclin-dependent kinases.

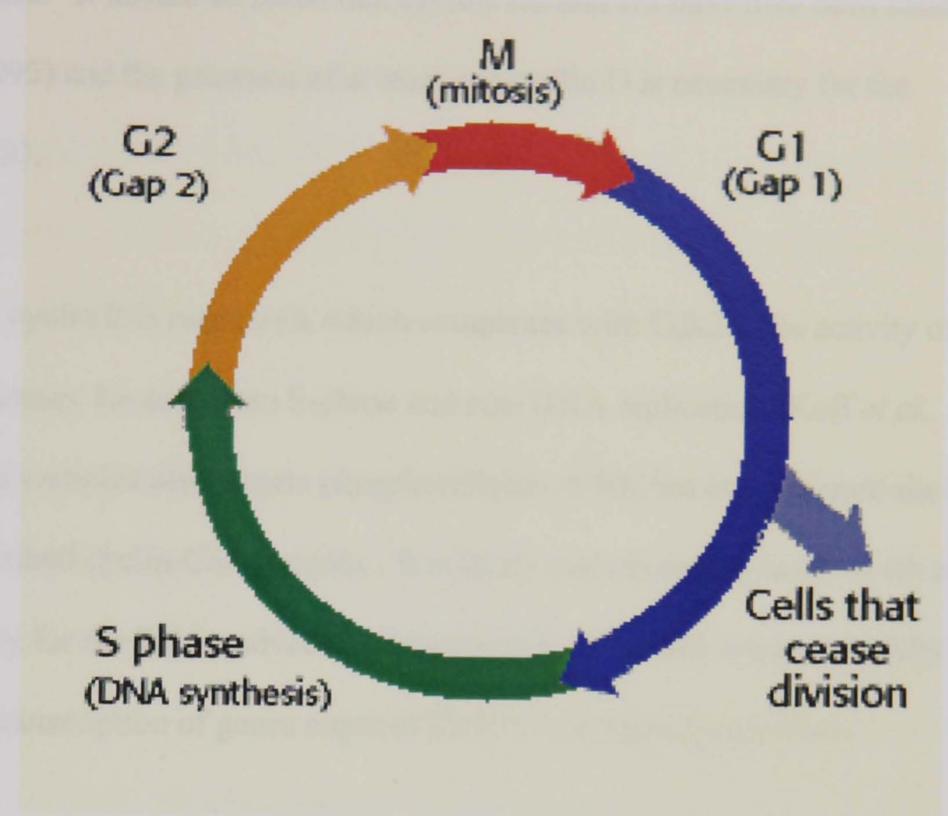


**Figure 1.1 Diagram summarising the eukaryotic cell cycle**

The activity of the kinases is dependent upon their binding to a specific cyclin (Solomon *et al.,* 1990) and as such the kinases are known as cyclin dependent kinases (Cdks). To date, six Cdks have been implicated in the cell cycle, and at least thirteen cyclins. The levels of particular Cdk-cyclin complexes oscillate throughout the cycle, with different complexes phosphorylating different target proteins dependent upon the stage in the cell cycle. For example, initial stimulation of a quiescent cell by the Ras-Raf-MAPK pathway results in the expression of cyclin D1 (Aktas *et al.,* 1997), which complexes with cdk4 or cdk6. The principal targets of these activated kinases are the retinoblastoma protein (Rb) (Kato *et al.,* 1993), which functions to bind and negatively regulate a transcription factor called E2F (Kovesdi *et al.,* 1997). E2F is a transcription factor (part of a family), which is required for progression of the cell through the G1-S phase transition and will be discussed in more detail in a later section. In addition two other Rb family members have been identified as targets of the cyclin D1/Cdk4/6 complex, namely p107 and p130, both of which are growth

inhibitory proteins It should be noted that cyclins D2 and D3 have also been identified (Sherr *et al.*, 1995) and the presence of at least one cyclin D is necessary for the completion of G1.

In mid-late G1, cyclin E is expressed, which complexes with Cdk2. The activity of this complex is necessary for entry into S-phase and also DNA replication (Koff *et al.*, 1992). This cyclin-Cdk complex also targets phosphorylation of Rb, but at a different site to the previously described cyclin-Cdk complex. It is likely that phosphorylation of Rb at several sites is necessary for the full inactivation of the protein. This will release and fully activate E2F, allowing transcription of genes required for G1 to S phase progression.

Cyclin A is expressed at the G1-S phase boundary and also complexes with Cdk2 (Elledge *et al.*, 1992). The activity of this complex is required for S phase transition and control of DNA replication (Heuvel and Harlow, 1993). One known substrate of the cyclin A-Cdk2 complex is Cdc6, which is required for the initiation of DNA synthesis. Upon phosphorylation, Cdc6 is exported from the nucleus, possibly to prevent re-replication of DNA (Petersen *et al.*, 1999). In addition, this complex phosphorylates HIRA (histone cell cycle regulation defective homologue A), a protein involved in the repression of histone gene transcription. Phosphorylation abolishes its repressor activity leading to increased histone transcription.

The final cyclin-Cdk complex to be discussed is cyclin B1-Cdk1, which is expressed in late S and G2 phases. Despite being expressed, the kinase remains inactive until late G2 when the activity is required for entry into mitosis (Nurse, 1990). This complex phosphorylates several kinds of lamins, leading to the breakdown of the nuclear envelope,

obviously an essential event in mitosis. Other essential events include condensation of the chromosomes, possibly *via* phosphorylation of histones and reorganisation of the cytoskeleton. In addition the cyclin B1-Cdk1 complex phosphorylates the TFIIH subunit of RNA polymerase II resulting in the global inhibition of transcription and translation that occurs during mitosis (Long *et al.*, 1998).

In conclusion, this section has briefly described the cyclins and kinases that are involved during each stage of the cell cycle. In addition, some of the targets of the kinases have been highlighted along with the likely relevance to that particular stage in the cell cycle. Efficient progression of the cell cycle is dependent upon regulation of both components of the complex. The factors involved in the regulation of cyclins and Cdks will be discussed in the following section.

### 1.1.2 Regulation of the cell cycle

There are several different mechanisms involved in the regulation of Cdk activity. All of these mechanisms are carefully orchestrated such that the cell is able to efficiently complete a cell cycle and also prepare itself for further proliferation. The regulatory mechanisms to be discussed in this section are phosphorylation, the inhibition of Cdk activity and the degradation of both components of the complex at specific points during the cycle.

Although stated earlier that the binding of a particular Cdk to a cyclin results in activation of the kinase, it should be noted that this only results in partial activation. An additional phosphorylation event is required for full activation of the kinase. This phosphorylation occurs at a site on the Cdks proximal to the ATP binding site and induces a conformational

change such that ATP is able to enter and bind the active site more readily (Jeffrey *et al.*, 1995). For each of the Cdks discussed, the phosphorylation occurs on a conserved threonine residue and is performed by Cdk-activating kinase (CAK). CAK is actually a complex itself, composed of Cdk7 and cyclin H. The phosphate group is subsequently removed by a phosphatase called KAP (kinase associated phosphatase; Hannon *et al.*, 1994).

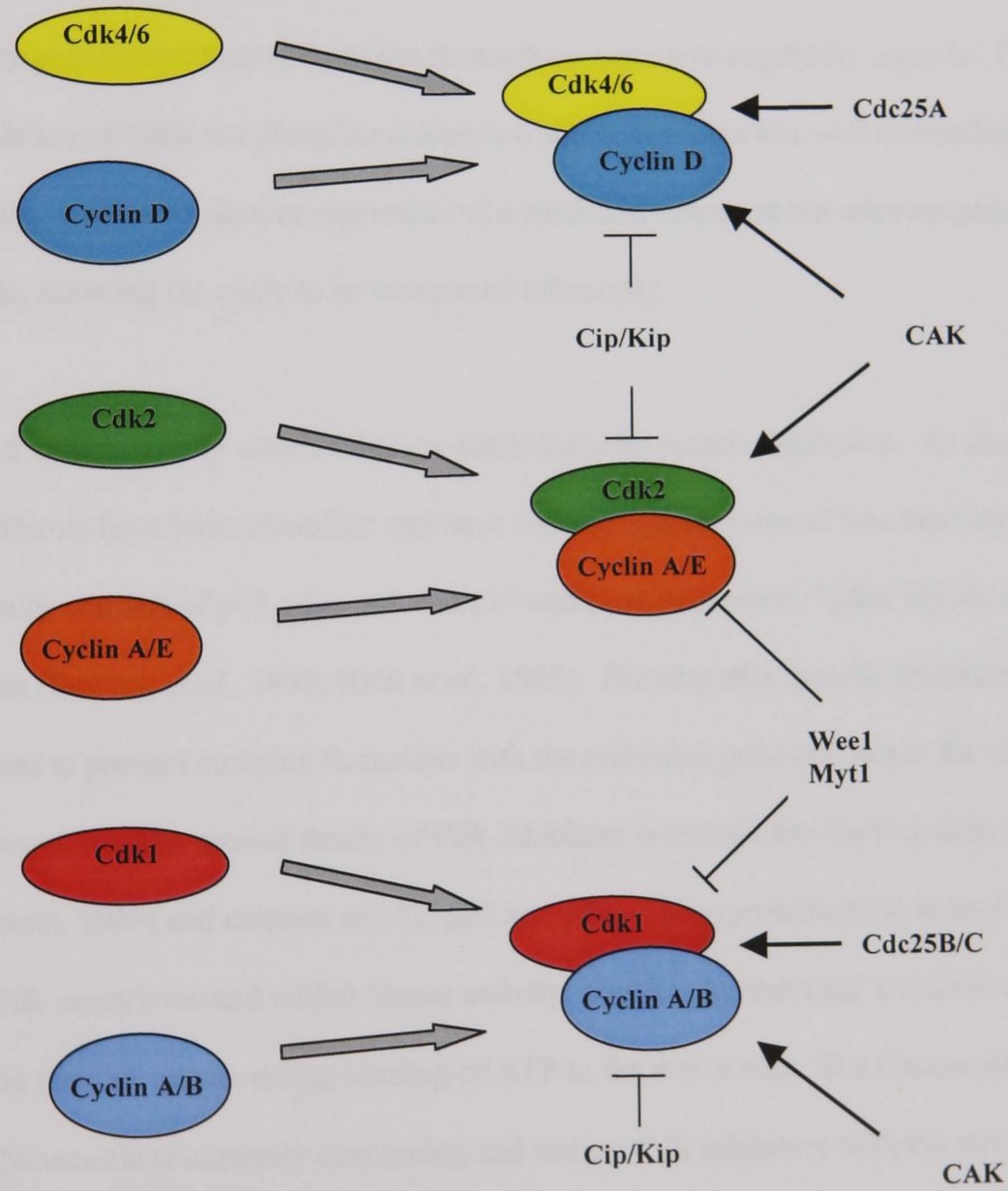


**Figure 1.2 Diagram summarising the regulation of cyclins and Cdks**

As well as being stimulatory, phosphorylation of Cdks can also have a negative regulatory effect (Morgan, 1995). For all of the Cdks discussed this inhibitory phosphorylation occurs near the N-terminal and involves a tyrosine residue. Cdk1 and Cdk2 also have a second threonine residue that is phosphorylated. The kinases responsible for the two phosphorylation events on Cdk1 and 2 have been identified as Wee1 and Myt1, which are bi-functional kinases, capable of phosphorylating both tyrosine and threonine residues (Parker *et al.,* 1992; Mueller *et al.,* 1995). The kinases responsible for the stimulatory or inhibitory phosphorylation of Cdks are themselves subject to regulatory signals. Therefore the regulation of Cdks *via* phosphorylation is a highly complex but well-controlled process that results in the activation or repression of a particular kinase at the relevant point in the cell cycle, allowing the cycle to be completed efficiently.

A second mechanism by which Cdks are inhibited is by protein inhibition. To date seven Cdk inhibitors have been identified and have been assigned to one of two families. The Ink4 family consists of p15, p16, p18 and p19 and bind monomeric Cdks, before complex formation (Serrano *et al.,* 1993; Hirai *et al.,* 1995). Binding of a specific inhibitor to a Cdk is believed to prevent complex formation with the relevant cyclin and hence the Cdk will remain inactive. The second family of Cdk inhibitors is termed the Cip/Kip family (Sherr and Roberts, 1995) and consists of p21, p27 and p57. These proteins bind to preformed cyclin-Cdk complexes and inhibit kinase activity, possible by inducing a conformational change in the Cdk or preventing binding of ATP to the active site. The Cancer Research Unit in Newcastle is currently developing and testing Cdk inhibitors with the aim of using them in cancer therapy. In theory, the tumour cells will then lack a kinase activity required for efficient cell cycle progression and hence the tumour cells will not be able to divide.

The final regulatory mechanism to be discussed is degradation. Degradation of cell cycle components is performed by two complexes, the Skp-Cullin-F-box (SCF) complex and the anaphase promoting complex (APC). Both complexes utilise the ubiquitin-proteosome pathway and act as E3 ligases for the degradation of target proteins. SCF acts late in G1, through S phase and in early G2, whereas APC is active at the end of G2 and mediates the transition through mitosis. The purpose of these degradation pathways is to remove the kinases or cyclins that have been induced or activated during the cell cycle. This allows the cell to 'reset' itself such that it can perform further rounds of cellular proliferation.

### 1.1.3 Cell cycle arrest

The previous sections have provided a brief overview of the cell cycle and highlighted some of the components required for this process. The principal aim of the cycle is to replicate the genome of a cell followed by division of the cell and DNA to form two daughter cells. Obviously in such a process it is essential that the integrity of the DNA be maintained to prevent mutations occurring. The accumulation of a variety of mutations over time can lead to the formation of a cancerous cell. If the DNA of a cell does become damaged, there are mechanisms allowing the cell cycle to be halted, allowing efficient repair of the DNA before resumption of the cell cycle. The cycle is actually controlled at two different stages; at the G1/S phase boundary and the G2/M phase boundary, both of which are known as cell cycle checkpoints.

During the G1-S phase transition, proteins necessary for DNA and deoxyribonucleotide synthesis are induced. A family of transcription factors, together called E2F, have been identified as being essential to this process. Binding of RB to E2F prevents E2F acting as a transcription factor. This inhibition can be alleviated by phosphorylation of RB,

breaking up the complex and freeing E2F. This phosphorylation can be performed by cyclin-CDK complexes, specifically cyclin D-Cdk4/6 and cyclin E-Cdk2. The G1/S phase checkpoint is mediated by a Cdk inhibitor called $p21^{waf-1}$, which binds to and inhibits the catalytic activity of the kinases involved in E2F activation. Inhibition of the kinases described earlier will result in Rb remaining in a hypophosphorylated state and hence will remain bound to E2F. This will in turn prevent transcription of genes necessary for progression to the next stage of the cell cycle. It should be noted that the expression of $p21^{waf-1}$ is mediated by p53, a DNA damage-inducible tumour suppressor protein, the regulation of which will be discussed in a later section (Section 1.2). The importance of the G1/S phase checkpoint is highlighted by the fact that virtually all tumour cells have lost the ability to undergo G1 arrest. In the majority of tumours, the lack of G1 arrest is attributed to functional inactivation of p53, the most common mechanism being mutation of the p53 gene.

The mechanisms behind the G2/M checkpoint are less well understood but are not believed to involve either $p21^{waf-1}$ or p53, as p53 mutant cells are capable of inducing a G2 arrest in response to DNA damage (Kastan *et al.*, 1991). As described earlier, cyclins A and B, along with Cdc2 are required for the transition from G2 into mitosis. Inhibitory phosphorylation of this Cdk on amino acid residues Thr14 and Tyr15 is thought to bring about cell cycle arrest at the G2/M checkpoint. The latter phosphorylation site is highly conserved, with identical regulation found in fission yeast (Nurse, 1990). In addition, mutation of this site to a non-phosphorylatable residue results in abrogation of the G2 arrest (Blasina *et al.*, 1997). The kinase responsible for this phosphorylation event has been identified as Wee1. The increased phosphorylation of Thr15 is potentiated by inactivation of the Cdc25 phosphatase, which targets the same residue. It should be noted

that Wee1 is activated by another protein kinase, Chk1. This kinase is initially activated in response to genotoxic stress thus providing a link between DNA damage and cell cycle arrest at the G2/M checkpoint.

### 1.1.4 Cancer, tumour suppressor genes and oncogenes

As described above cellular proliferation occurs *via* the cell cycle, which can be halted at one of two checkpoints in response to DNA damage. A disruption in the regulation of the cell cycle such that the cycle can no longer be suppressed or stopped leads to the formation of a cancerous cell. Such disruptions are caused by mutations to particular genes. Various chemicals, ionising radiation (IR), ultra violet light (UV) and environmental factors (e.g. chemicals inhaled due to smoking) can bring about these mutations. Cancerous cells are typified by their genomic instability, which is likely to promote a greater mutation rate in these cells, allowing them to evolve (Lengauer *et al.*, 1998).

A group of genes commonly mutated in cancers are oncogenes. These are mutated or abnormally expressed forms of normal cellular genes that induce or maintain the uncontrolled cellular proliferation associated with cancer, an example of which is the *ras* oncogene. Ras is a G-protein that normally cycles from an inactive state to an active state by changing the bound GDP to GTP. When in the active state, *ras* relays growth-promoting signals to the cell. Mutation of *ras* prevents the release of GTP from the protein and hence the protein is permanently active and cells continually grow and divide. Oncogenes can be carried by retroviruses (for example *v-src*) or may be produced due to mutation (as for *ras* described above). A second group of genes commonly mutated are tumour suppressor genes. Non-mutated tumour suppressor genes function to suppress cell growth and division (therefore they have an opposite effect to cellular proto-oncogenes).

This group includes the previously discussed RB gene, mutation of which prevents the regulation of E2F (Section 1.1.3). If, through mutation, Rb is unable to bind E2F, this will lead to cell cycle progression, even in the presence of DNA damage resulting in the accumulation of more genetic alterations. A second tumour suppressor gene, p53, is found to be mutated in around 50% of cancers. p53 is a transcription factor that brings about cell cycle arrest or apoptosis by activating a variety of genes, the details of which will be explained below.

## 1.2 P53 – tumour suppressor

P53 is the product of a tumour suppressor gene (reviewed in Ryan *et al.*, 2001 and Colman *et al.*, 2000) and is the most common target for genetic alterations in cancer, with around 50% of tumours possessing mutations in the p53 gene. It accumulates and is activated in response to DNA damage and subsequently functions as a transcription factor, stimulating transcription of various genes. These genes produce proteins that are involved predominantly in cell cycle arrest or the apoptotic pathway, depending upon the extent of DNA damage. The use of mouse model systems (Attardi & Jacks, 1999) and various mutant cell lines has led to a clearer elucidation of p53 function in the last decade.

### 1.2.1 The structure of p53

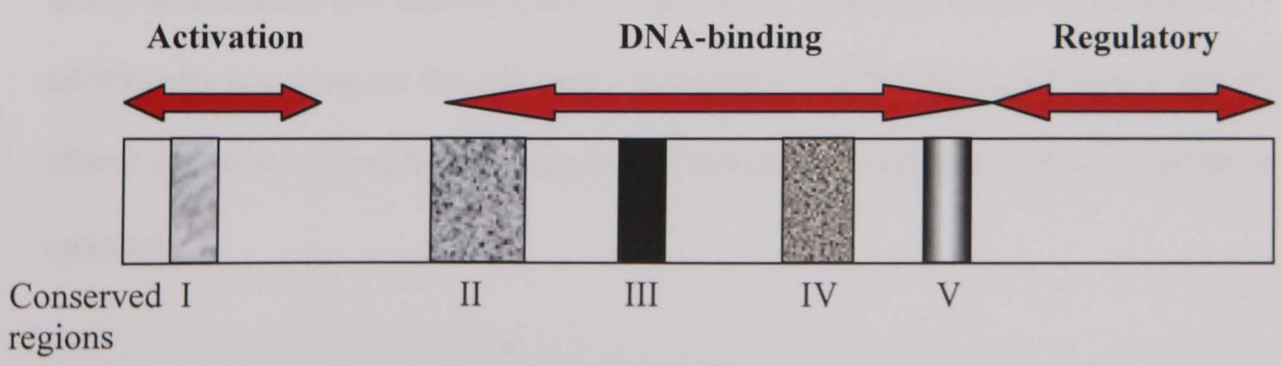


**Figure 1.3 The domain structure of p53**

P53 is a nuclear phosphoprotein consisting of 393 amino acids and has been described as having five conserved domains (figure 1.3). The N-terminal consists of a transcriptional transactivation domain, necessary for the interaction of p53 with the components of the transcriptional machinery. Amino acids F19, L22 and W23 have been shown to be essential for transcriptional activation by p53 *in vivo* (Lin *et al.*, 1994). These amino acids bind to two subunits of transcription factor IID *in vitro* (Lu & Levine, 1995; Thut *et al.*, 1995). The central domain of p53 consists of the sequence-specific DNA-binding domain. Native p53 is in the form of a tetramer (actually a dimer of a dimer). The amino acids necessary for this oligomerisation are residues 324-355, within the C-terminal, which form two α-helices and two β-sheets. The four α-helices come together to form a four-helix bundle, aided by hydrophobic interactions. The oligomerisation domain also contains a nuclear localisation signal (NLS). Finally, the C-terminus contains a domain that regulates the latent form of p53. Deletion of this domain, phosphorylation at S378 by protein kinase C or S392 by casein kinase II or binding of antibody PAb421, all activate site-specific DNA binding by the central domain of p53 (Hupp and Lane, 1994).

In a normal cycling cell, p53 is in an inactive form, bound to its negative regulator, Mdm2 (a product of a murine double minute gene, see Section 1.3). The importance of this interaction is highlighted by the fact that *mdm2* knockout mice die at the embryotic stage due to uncontrolled p53 activity (Jones *et al.*, 1995). The mice can be rescued by additionally knocking out the p53 gene. In response to DNA damaging agents, this p53-Mdm2 complex is disrupted resulting in p53 activation followed by cell cycle arrest or apoptosis.

### 1.2.2 Activation of p53

In response to DNA damage, p53 levels increase due to increased stability and hence increased half-life of the protein. In addition, p53 transcriptional transactivation activity increases, resulting in the increased expression of p53 target genes. Both of these effects are brought about by post-translational modifications of the p53 protein. p53 has been reported to be subject to several post-translational modifications such as phosphorylation, acetylation and sumoylation (see figure 1.4). With particular relevance to this study, p53 has also been shown to be a target for poly(ADP-ribosyl)ation, catalysed by the enzyme poly(ADP-ribose) polymerase-1 (PARP-1), although this is by no means a universal observation (see Section 1.4.6).

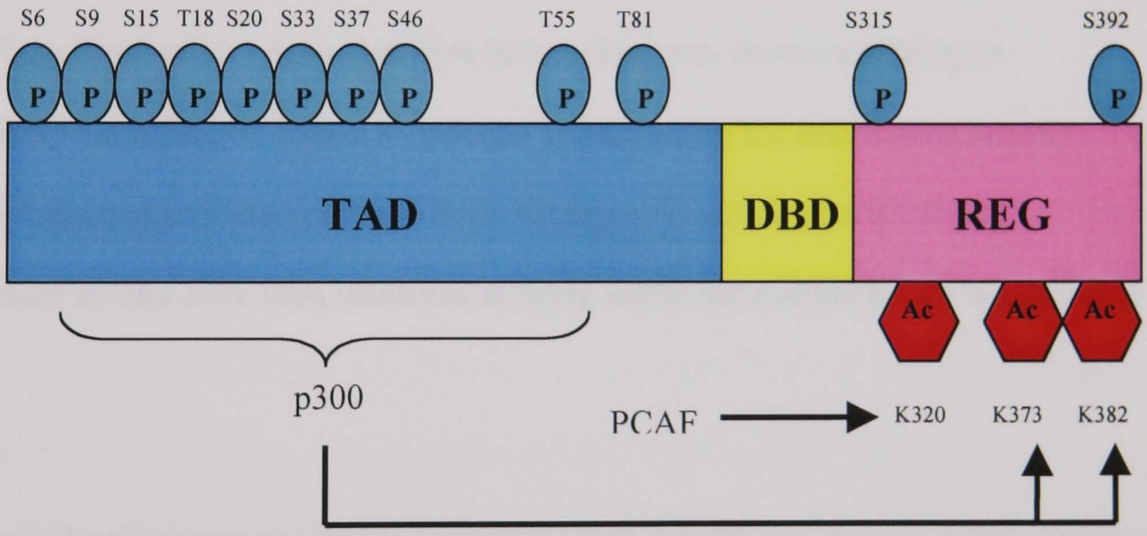


**Figure 1.4 Schematic diagram showing the post-translational modifications of p53**
The phosphorylation sites reported to date are shown in blue circles and the acetylation sites are shown in red hexagons. TAD = transcriptional activation domain; DBD = DNA binding domain and REG = regulatory domain. Mdm2 binds the N-terminal of p53, within the main cluster of putative phosphorylation sites

The initial step in p53 activation is the alleviation of the inhibition imposed by the binding of Mdm2. Mdm2 blocks the transcriptional transactivation domain of p53 and also targets p53 for degradation, the details of which will be discussed in a later section (Section 1.3.2). It is the process of phosphorylation that has been most widely implicated in disrupting the p53-Mdm2 complex and thus the activation of p53 (Martinez *et al.*, 1997; Meek, 1994).

The use of phosphorylation site-specific antibodies has led to the identification of several phosphorylation sites within the N-terminus of p53. To date eight N-terminal phosphorylation sites have been identified, consisting of serines 6, 9, 15, 20, 33, 37 and 47 as well as threonine 18. In addition two C-terminal phosphorylation sites have been identified, serines 315 and 392. It should be noted that phosphorylation at certain sites has only been observed in response to particular DNA damaging agents. For example, Ser37 is phosphorylated in response to UV, but not IR. As well as different phosphorylation sites being identified, different kinases have been shown to be responsible for these phosphorylations. Among the kinases implicated in the activation of p53 are the ataxia telangiectasia mutated kinase (ATM), the AT related kinase (ATR), checkpoint kinase 2 (Chk2) and casein kinase 1 (CK1) (Delia *et al.*, 2000; Banin *et al.*, 1998; Hirao *et al.*, 2000). These kinases have been identified by knocking out, down-regulating or constitutively activating the kinase in question and analysing the stabilisation (and/or phosphorylation) of p53 in response to DNA damage. As yet, no specific site or combinations of sites have been identified as being solely responsible for the activation of p53.

Attempts to identify important residues have involved substituting specific serine residues by alanine residues. Studies involving substitution of many of the serine residues resulted in no major defect in p53 stabilisation in response to DNA damage (Ashcroft *et al.*, 1999; Blattner *et al.*, 1999), suggesting that p53 stabilisation is not dependent upon phosphorylation. However, this suggestion may be flawed as one group failed to analyse p53 containing a Ser20 substitution (Ashcroft et al., 1999) and the other reported a partial stabilisation when all N-terminal serines were substituted (Blattner et al., 1999), although this latter group did not follow up their analysis by examining single-site mutants. Another

study (Chehab *et al.*, 1999) has proposed that phosphorylation of Ser20 brings about p53 stabilisation. This was based upon findings that substitution of Ser20 with Ala or Asp completely abrogates p53 stabilisation after exposure to IR or UV radiation. Furthermore, ATM and the related kinase ATR cannot directly phosphorylate p53 on Ser20. However, it is believed that one or the other is required for p53 stabilisation in response to IR or UV. Therefore, the authors (Chehab et al., 1999) proposed that ATM or ATR are required to phosphorylate and activate another kinase in response to DNA damage. The checkpoint kinases Chk1 and Chk2 have subsequently been identified as phosphorylating Ser20 (Shieh *et al.*, 2000; Chehab *et al.*, 2000) downstream of ATR/ATM.

Several studies have also identified Ser15 as being important in p53 activation in response to DNA damage (Appella *et al.*, 2001; Canman *et al.*, 1998). This residue is phosphorylated in an ATM-dependent manner in response to IR, leading to a disruption of the p53-Mdm2 complex. This will obviously increase the stability of p53 and lead to the induction in protein levels observed in response to IR. It should be noted that ATM-deficient cells show delayed p53 induction in response to IR (Delia *et al.*, 2000) but show an intact p53 response to UV. This further highlights the previously mentioned observation that some p53 phosphorylation sites are DNA damage-specific. Serine 15 has also been identified as a DNA-PK target, *in vitro* (Lees-Miller *et al.*, 1992; Shieh *et al.*, 1997; Silicano *et al.*, 1997). A subsequent study showed that cells lacking DNA-PK possess a transcriptionally inactive p53, with p53 being unable to bind DNA and therefore unable to activate transcription of target genes and bring about cell cycle arrest (Woo *et al.*, 1998). This study suggested that sites phosphorylated by DNA-PK may be vital in the activation of p53. However, these results could be described in one of the two cell lines studied by the presence of a mutation in the DBD of p53. Several subsequent studies have

contradicted the findings of Woo *et al.*, 1998, with p53 induction being shown to be independent of DNA-PK activity (Jimenez *et al.*, 1999; Burma *et al.*, 1999; Jhappan *et al.*, 2000).

The experimental data summarised above highlights the number of phosphorylation sites present on p53. However, to date Ser15 and Ser20 have been identified as perhaps the most important residues in p53 activation. As the sites are within the Mdm2-binding site of p53, the likely result is disruption of the p53-Mdm2 complex, possibly involving a conformational change of p53, or steric hindrance in formation of the complex. Full activation of p53 is likely to involve a combination of the identified phosphorylation sites. In addition, dephosphorylation by particular phosphatases is likely to play an important role in p53 regulation as phosphate groups must be removed to allow reassembly of the p53-Mdm2 complex. As yet, the phosphatases responsible for this activity have not been identified.

A second post-translational modification involved in the activation of p53 is acetylation. This reaction is performed by the CREB binding protein (CBP)/p300 and p300/CBP associated factor (PCAF). Antibody studies have identified target residues within the C-terminal of p53; Lys320 (PCAF), Lys373 (p300 and PCAF) and Lys382 (p300), with the observed effect of acetylation being increased DNA binding of p53 (Liu *et al.*, 1999). *In vitro*, p300 has actually been shown to bind to the N-terminal of p53, with residues between Leu22 and Phe54 being critical for this interaction (Scolnick *et al.*, 1997). In response to DNA damage (both IR and UV; Ito *et al.*, 2001), p53 and p300 colocalize to the nucleus in a stable DNA binding complex (Lill *et al.*, 1997). The mechanism behind the formation of nuclear aggregates of p300 and p53 is unclear. However, a recent study

identified a second nuclear export signal within the N-terminal of p53 (Zhang and Xiong, 2001), coinciding with the p300-binding motif. It is therefore possible that in response to DNA damage, p300 binds to p53, concealing this nuclear export signal, resulting in nuclear retention and accumulation of p53. Subsequent acetylation of the previously described C-terminal residues results in increased transcription of p53 target genes. To further highlight the complex nature of p53 activation, acetylation can be influenced by phosphorylation of particular residues. Ser15 phosphorylation increases the binding of p300 to p53 but is not an absolute requirement for acetylation to occur (Lambert *et al.*, 1998).

The data summarised thus far suggests that p300 and acetylation of p53 results in nuclear retention and increased DNA binding of the protein. Both of these observations would be consistent with a positive role for acetylation in p53 activation. However, there is also data suggesting a negative regulatory role for acetylation. Kawai *et al.*, 2001, suggest that the initial acetylation of p53 results in the previously described effects. However, upon induction of Mdm2, the authors propose that Mdm2 becomes a target for acetylation. This modification results in stabilisation of Mdm2 and a subsequent increase in the half-life of the protein. The ability of Mdm2 to target p53 for degradation (see Section 1.3.2) is thus augmented and p53 levels begin to decrease. This model is consistent with the transient nature of the increase in p53 levels that are observed in response to DNA damage, thus allowing the cell to resume DNA replication and re-enter the cell cycle. It is likely that further mechanisms such as dephosphorylation of critical p53 residues are also involved in the reduction of p53 levels usually observed 6-24 hours after DNA damage.

### 1.2.3 P53 and the cell cycle

The cell cycle has been described in Section 1.1.1. If DNA is damaged, it is essential that cells harbouring this damage are not allowed to progress through the cell cycle, which would result in the copying of a damaged template, leading to mutations in the newly synthesised DNA.

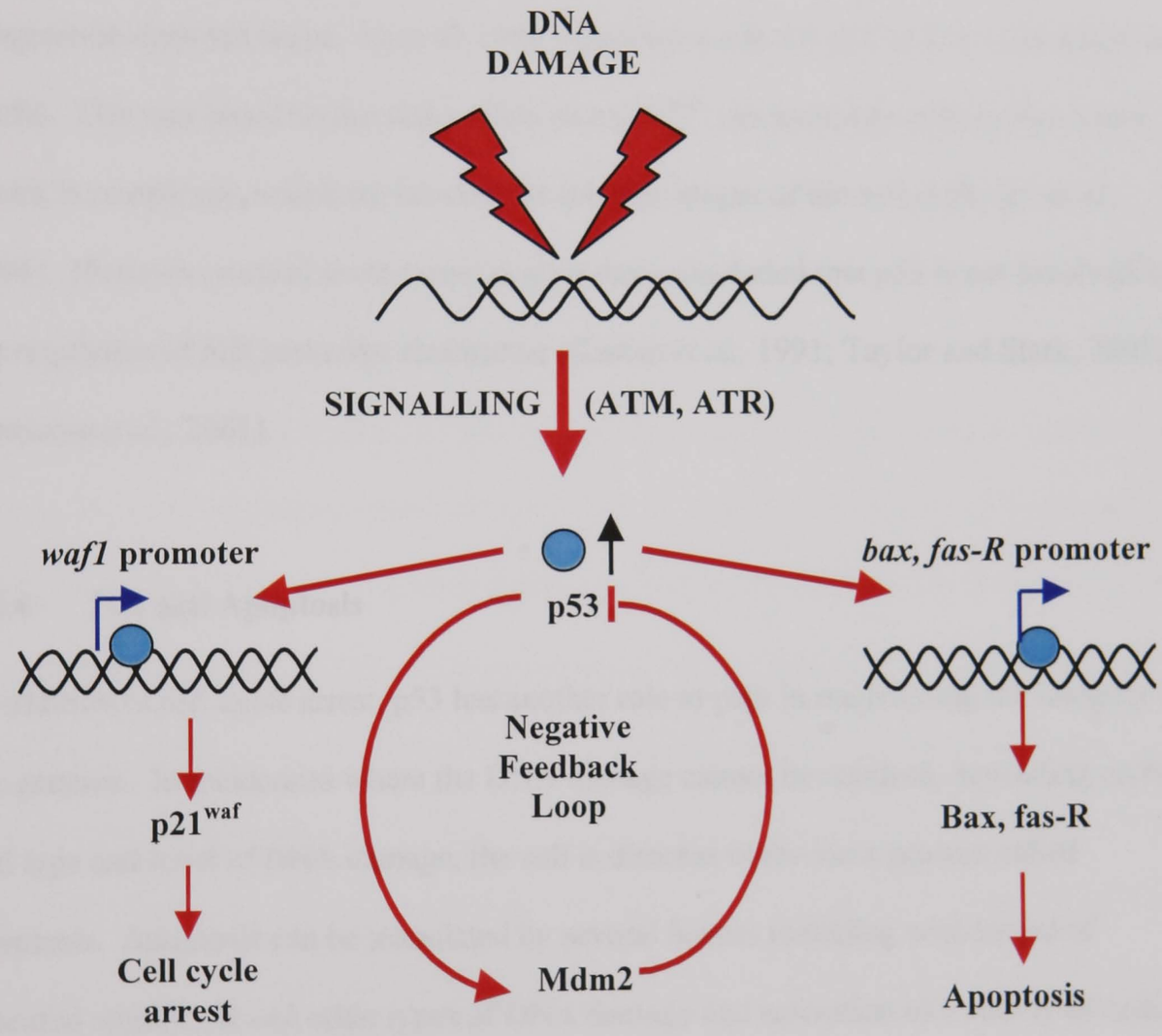


**Figure 1.5 Diagram summarising the major functions of p53**

P53 is activated in response to DNA damage (see figure 1.5) and is essential for slowing or halting the cell cycle to allow the efficient repair of this damage by repair enzymes. This is illustrated by the susceptibility of p53 knockout mice to tumour formation (Donehower *et al.*, 1992). p53 mediates transcription of several genes, the products of which are able to

bring about cell cycle arrest (Kuerbitz *et al.*, 1992) at the G1/S phase checkpoint. Perhaps one of the most important genes activated by p53 is *waf1* (El Deiry *et al.*, 1993). This gene produces a small Cdk inhibitor called $p21^{waf1}$ and brings about cell cycle arrest at the G1/S phase junction. It is believed that this protein binds to cyclin-CDK complexes (in particular Cdk2/cyclin E), inhibiting the kinase activity (Dulic *et al.*, 1994). This prevents phosphorylation of the RB-E2F complex; hence E2F is not released and cell cycle progression does not occur. Li *et al,* 1994, proposed a role for p53 in cell cycle arrest at G2/M. This was based on the observation that $p21^{waf1}$ can associate with cyclin A and cyclin B complexes, which are involved in the later stages of the cell cycle (Li *et al.*, 1994). However, several more recent studies have concluded that p53 is not involved in the regulation of this particular checkpoint (Kastan *et al.,* 1991; Taylor and Stark, 2001; Koniaras *et al.,* 2001).

### 1.2.4 P53 and Apoptosis

In addition to cell cycle arrest, p53 has another role to play in maintaining the integrity of the genome. In incidences where the DNA damage cannot be repaired, depending on the cell type and level of DNA damage, the cell is directed to die *via* a process called apoptosis. Apoptosis can be stimulated by several factors including withdrawal of essential stimuli, IR and other types of DNA damage and activation of a variety of cellular receptors. The response itself is characterised by the activation of a particular family of proteolytic enzymes called caspases, which then activate further caspases *via* cleavage (Saikumar *et al.,* 1999; Wolf and Green, 1999). Events downstream of catalytic cleavage include nuclear condensation and fragmentation of the DNA (Enari *et al.*, 1998; Martin & Green, 1995). In most cases, the initial stimuli converge on a common pathway, as suggested by the ability of Bcl-2 to inhibit apoptosis. Apoptosis can occur *via* both p53-

dependent and p53-independent mechanisms. For the purposes of this thesis I will focus on the p53-dependent mechanism. The exact processes involved have not yet been elucidated. However, several genes with an apoptotic function have been shown to be p53-inducible.

As described previously, p53-dependent cell death is mediated by caspases. These caspases are activated by the release of apoptogenic factors, such as cytochrome c from the mitochondria. Permeabilisation of the mitochondrial membrane allows the release of cytochrome c and is controlled by the pro- or anti- apoptotic members of the bcl-2 family. It is believed that p53 signalling to the pro-apoptotic Bax protein initiates the release of cytochrome c from mitochondria. Release of cytochrome c allows the formation of the apoptosome, consisting of the adaptor protein, Apaf-1 and caspase nine, which is activated upon recruitment to the complex. This caspase in turn cleaves and activates caspase-3 and –7 leading to the execution of cell death (Zou *et al.,* 1997; Li *et al.,* 1997; Saleh *et al.,* 1999; Hu *et al.,* 1999). The process described above is known as intrinsic apoptosis. A second pathway exists, called extrinsic apoptosis, which relies upon the stimulation of cellular receptors known as death receptors. There are several members of the death receptor family including CD95, Fas, TRAIL and DR5. Ligation of the receptors by their respective ligands results in formation of the death inducing signalling complex (DISC) composed of the adaptor protein FADD and caspase-8. Subsequent activation of this caspase sets in motion the cascade of caspase activation observed in intrinsic apoptosis.

It should be noted that the membrane expression of several of the death receptors mentioned earlier can be regulated by p53 (reviewed in Vousden and Lu, 2002). For instance, DR5, a member of the TNFR family has been identified as a possible participant in the p53-dependent apoptotic pathway (Sheikh *et al.*, 1998; Wu *et al.*, 1997). The Fas

gene has also been shown to contain a p53 binding consensus sequence. The same study showed that certain chemotherapeutic drugs up-regulate Fas only in the presence of wild type p53 (Muller *et al.*, 1997). Fas and TNF-R1 both contain a loosely conserved (~28%) region near the C-terminus, which has been called the death domain. It is this domain that interacts with intracellular proteins to initiate the apoptotic pathway. An important step in the apoptotic pathway is the release of reactive oxygen species (ROS), which are powerful activators of both mitochondrial damage and apoptosis (Johnson *et al.*, 1996; Lotem *et al.*, 1996). Several genes can bring about the release of such species, including p53-induced genes (PIGs). One such gene, PIG3, was shown to contain p53-binding sites in its promoter (Polyak *et al.*, 1997).

This section on p53 has described the factors involved in the activation of p53 in response to DNA damage. It is clear that several factors are involved, including phosphorylation and acetylation, with both modifications occurring on several residues. Less is known about how these modifications are reversed although this is undoubtedly a very important step in the overall regulation of p53. This section has also described some of the downstream effects of p53 activation, that is cell cycle arrest and apoptosis. The fact that p53 is able to induce such vital cellular processes as these, highlights how important it is to deduce the processes involved in the regulation of p53. Fundamental to the regulation of p53 and hence to these downstream effects is the negative regulation imposed by Mdm2. Mentioned only briefly in this section, the details involved in how Mdm2 interacts with p53 and the consequence of this interaction will be discussed in the following section (Section 1.3). In addition, the regulation of Mdm2 itself by another tumour suppressor protein, $p14^{ARF}$ will be discussed in terms of the implications on p53 activity.

## 1.3 Mdm2

Murine double minute 2 (*MDM2*) is a proto-oncogene that was first discovered as the gene responsible for the spontaneous transformation of an immortalised murine cell line called BALB/c 3T3 (Fakharzadeh *et al.*, 1991). The *MDM2* gene is approximately 25-kb in size and can give rise to Mdm2 polypeptide of varying size due to alternative splicing of the mRNA transcript (Olson *et al.*, 1993; Sigalas *et al.*, 1996; Haines *et al.*, 1994). In addition, the *MDM2* gene has two different promoters, termed P1 and P2, which can initiate transcription at different transcriptional start sites (Barak *et al.*, 1994). Despite the presence of several different sized Mdm2 polypeptides, resulting from alternative splicing and post-translational cleavage, it is unclear whether they perform individual functions or whether their functions overlap.

### 1.3.1 The structure of Mdm2

The largest form of human Mdm2 spans 491 amino acids and contains several domains, which are conserved. The N-terminal region of the protein is necessary for binding to p53 and mediates the best-characterised function of Mdm2, the binding to and inhibition of p53 (figure 1.6).

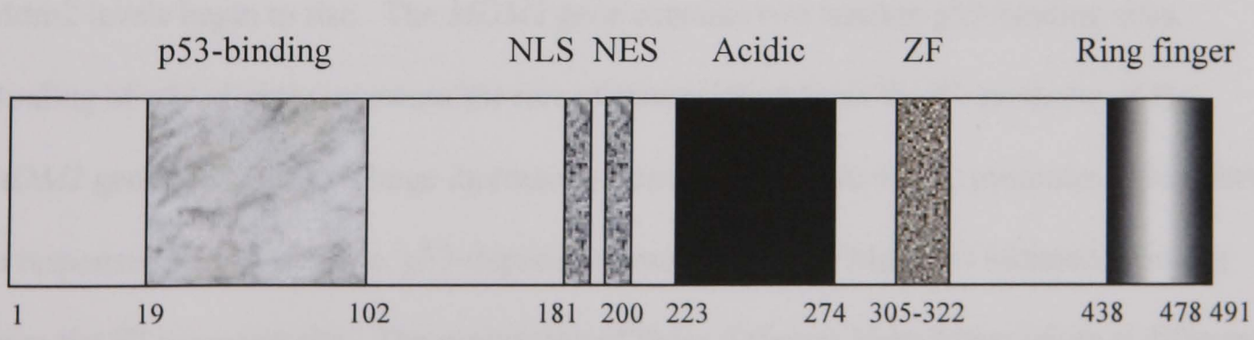


**Figure 1.6 The domain structure of Mdm2**
NLS = nuclear localisation signal, NES = nuclear export signal and ZF = zinc finger domain

In addition, the N-terminal region has been implicated in binding to the transcription factor E2F1 (Martin *et al* 1995). The next conserved regions in the Mdm2 sequence are responsible for the shuttling of Mdm2 between the nucleus and the cytoplasm (Roth *et al.*, 1998b), with the nuclear localisation signal and the nuclear export signal being adjacent to each other in the sequence. It is believed that shuttling from the nucleus to the cytoplasm is necessary for the efficient regulation of p53 function. The centre of the protein contains a highly acidic region responsible for the interaction of Mdm2 with the ribosomal protein L5 and 5S ribosomal RNA. The remaining conserved regions are a zinc finger domain, a caspase-3 cleavage site, three putative DNA-dependent protein kinase (DNA-PK) phosphorylation sites and finally two zinc fingers in a ring conformation at the C-terminus. This C-terminus is also thought to be involved in regulating p53 levels by acting as a ubiquitin ligase leading to the degradation of p53 (Honda *et al.*, 1997), which will be discussed in more detail later.

### 1.3.2 The regulation of p53 by Mdm2

Expression of Mdm2 is induced in response to activated p53 (Barak *et al.*, 1993). The induction in response to p53 is not an immediate one, with at least an hour needed before Mdm2 levels begin to rise. The *MDM2* gene contains two tandem p53-binding sites. Binding of p53 slightly increases the rate of transcription from the P1 promoter of the *MDM2* gene but leads to a large increase in transcription from the P2 promoter. Therefore, in response to DNA damage, p53-dependent transcription of Mdm2 is initiated primarily from the P2 promoter site. The production of these different Mdm2 transcripts at different rates may be significant to the function or regulation of the Mdm2 protein. It should be noted that the two promoter sites are conserved in the human and mouse Mdm2 genes, perhaps indicating the importance of having two distinct promoter sites.

Once produced, Mdm2 binds p53, as illustrated by the fact that the two proteins can be coimmunoprecipitated (Chen *et al.*, 1993b) (figure 1.7). The binding involves the insertion of an amphipathic α-helix of two and a half turns from p53 into the cleft of Mdm2. The formation of the α-helix structure is induced as the two proteins come close together. Van der Waals interactions form between the α-helix of p53 and several hydrophobic and aromatic amino acids in the cleft of Mdm2. Mutational analysis has revealed amino acid residues D68, C77, G58 and V75 of Mdm2 as being critical for the formation of the complex (Freedman *et al.*, 1997).


**Figure 1.7 The p53-Mdm2 complex**
The panel shows Phe19, Trp23 and Leu26 of p53 inserted into a deep cleft of Mdm2.

Chen *et al* (1995) showed that the expression of the N-terminal domain of Mdm2 could block the activity of p53 in both cell culture and also in an *in vitro* transcription assay (Chen *et al.*, 1995). The basis for this inhibition was, until recently, thought to be mediated primarily by the binding of Mdm2 to the same region of p53 necessary to contact various proteins involved in transcription. Without these interactions, p53 is unable to

initiate transcription (Li *et al.*, 1993; Lu & Levine, 1995; Thut et al., 1995). Mdm2 can be thought of as acting rather like a competitive enzyme inhibitor, with Mdm2 competing with various components of the transcription machinery for binding to a particular site on the p53 protein.

Recent evidence has suggested a second mechanism by which Mdm2 inhibits p53 activity. Roth *et al* (1998) demonstrated that human Mdm2 contains a nuclear export signal (NES). When mutated in this region, the mutant hdm2 demonstrated an enhanced inhibition of p53, as demonstrated by a reduction in the expression of a p53-dependent reporter gene (Roth *et al.*, 1998a). In addition, immunoblotting analysis of cells transfected to express p53 and hdm2 (either wild type or NES mutant) showed no change in p53 levels when the mutant hdm2 was expressed. This was in total contrast to the near disappearance of p53 upon expression of the wild type hdm2. Roth *et al* (1998) also showed that prior treatment of cells with a proteosome inhibitor (N-carbobenzoxy-leucyl-leucyl-leucinal) abolished the ability of either wild type or mutant hdm2 to reduce the amount of cellular p53. These findings indicate that hdm2 nuclear export is necessary for the proteosome-mediated degradation of p53. Honda *et al* (1997) suggested that Mdm2 may function as an E3 ubiquitin ligase for p53, with Mdm2 binding to p53 and then ubiquitinating p53 and itself. Mutagenesis studies have demonstrated that the conserved residue Cys464 on Mdm2 is necessary for both transferring ubiquitin to p53 (Honda *et al.,* 1997) and for mediating p53 degradation in cultured cells (Kubbatat *et al.,* 1999). Ubiquitinated proteins are then directed towards the 26S proteasome where they are degraded.

From what has been discussed, it is clear that an autoregulatory feedback loop is operating to regulate the levels of p53 in the cell. However, it is also necessary to regulate the loop

itself such that p53 levels are able to rise at the appropriate time. Under normal circumstances a basal level of both Mdm2 and p53 is present in cells, mostly in the form of a complex. In this situation p53 is unstable and thus has a short half-life of approximately 20 minutes. However, in response to DNA damage, p53 levels rise (on average 2-6 hours after DNA damage) due to increased stability of p53. In order for this rise to occur, it is necessary to alleviate the inhibition imposed upon p53 by Mdm2. The most obvious way to achieve this is to disrupt the interactions between the two proteins.

### 1.3.3 The role of Mdm2 phosphorylation in p53 activation

Evidence exists that the p53-Mdm2 complex can be disrupted by phosphorylation of p53 at Ser 15 after γ-irradiation (Shieh et al., 1997). This phosphorylation is performed by a kinase called ATM. A recent study (Khosravi *et al.*, 1999) has also shown that this kinase can phosphorylate Mdm2 after treatment of cells with IR or radiomimetic chemicals. However, in this study the expression of mutant p53 (with Ser 15 substituted by Ala) in p53-null and p53/ATM-null backgrounds did not prevent ATM-dependent stabilisation of p53. This showed that phosphorylation of Ser 15 alone cannot account for the stabilisation of p53. Further studies showed that treatment of cells with IR produced a faster migrating form of Mdm2, a change that occurred well before p53 induction (Khosravi *et al.*, 1999). This change was subsequently shown to be due to ATM-dependent phosphorylation of Mdm2. A more recent study using site directed mutagenesis (Maya *et al.*, 2001) demonstrated that Ser395 of Mdm2 is a target for ATM dependent phosphorylation. Furthermore, this study showed that phosphorylation of this residue resulted in nuclear accumulation of p53. It is therefore apparent that ATM may act on both members of the p53-Mdm2 complex so as to stabilise p53.

A second method by which p53 could be stabilised in response to DNA damage is by the destabilisation of Mdm2. Evidence shows that Mdm2 levels decrease rapidly after exposure to UV in a p53-independent manner, before the induction of p53 (Wu & Levine, 1997). This destabilisation of Mdm2 would give rise to an increase in p53 levels such that p53 can promote transcription of proteins involved in cell cycle arrest, allowing repair of any damaged DNA. A similar effect in terms of Mdm2 down-regulation has also been observed in response to hypoxia and several DNA damaging chemotherapeutic agents (Ashcroft *et al.,* 2000; Alarcon *et al.,* 1999). The principal mechanism for the decrease in Mdm2 levels was a reduction in the expression of the *Mdm2* gene. However, some studies have suggested that the observed decrease in Mdm2 levels is due to an inability of the antibody used in Western blot analysis to recognise a particular epitope. For example, Toledo *et al,* 2000, demonstrated that Mdm2 is rapidly phosphorylated in response to DNA damage in an ATM-dependent-manner. If a particular antibody (SMP 14, recognising amino acid resdues 154-167) is used to detect Mdm2 then there is an apparent decrease in Mdm2 levels. However, if a different antibody (AB-1), with a different epitope site, is used then Mdm2 levels do not decrease. The authors suggest that the initial antibody used recognises an epitope containing a phosphorylation site and hence the antibody is unable to recognise the modified Mdm2 upon Western blot analysis. The same study also showed no change in Mdm2 mRNA levels and no change in the rate of Mdm2 protein degradation. Despite this apparently conflicting set of data, there is a growing body of evidence suggesting that Mdm2 is a target for phosphorylation, with the likely outcome being the activation of p53.

It should be noted that a p53-binding protein with homology to Mdm2 has been identified (Shvarts *et al.*, 1996). This protein is called mdmX and is able to bind p53 and prevent

p53 transactivation (Jackson & Berberich, 2000). However, it does not possess the Mdm2 properties of being able to facilitate nuclear export or bring about p53 degradation. Expression of mdmX can reverse Mdm2-induced degradation whilst maintaining inhibition of p53 transactivation. The authors (Jackson & Berberich, 2000) propose that this represents a mechanism whereby undamaged cells can retain a nuclear pool of p53.

It should be noted that mdmx null mice are embryonic lethal (Parant *et al.*, 2001), as are Mdm2 null mice. In addition, they can also be rescued by additionally knocking out or mutating p53.

### 1.3.4 The regulation of Mdm2 by $p14^{ARF}$

$p14^{ARF}$ is the product of a tumour suppressor gene ($p19^{ARF}$ in mice) that functions to negatively regulate the activity of Mdm2 (Pomerantz *et al.*, 1998). Inhibition of Mdm2 results in the activation of p53 and subsequent cell cycle arrest, hence $p14^{ARF}$ is only tumour suppressive in the presence of wild type p53. The mechanism by which $p14^{ARF}$ activates p53 has been the focus of intensive research in the last 4 years. Presently, $p14^{ARF}$ is believed to act *via* two mechanisms. Firstly, Honda and Yasuda, 1999 demonstrated that binding of $p14^{ARF}$ to Mdm2 abolished the E3 ligase activity of Mdm2 hence protecting p53 from ubiquitin-mediated degradation. Protein localisation studies have also revealed that Mdm2 is sequestered in the nucleus in response to $p14^{ARF}$ activation (Tao and Levine, 1999; Weber *et al.*, 1999). This is a likely consequence of $p14^{ARF}$ binding to Mdm2 and concealing the NES. This will in turn prevent the shuttling of Mdm2 into the cytoplasm, which is an essential step in the regulation of p53, as ubiquitin-mediated degradation only occurs in the cytoplasm. Both of the mechanisms described will have the effect of activating p53.

### 1.3.5 The oncogenic properties of Mdm2

Thus far only overexpression of Mdm2 and subsequent binding to p53 has been discussed in relation to the oncogenic properties of Mdm2. However, there is evidence for alternative oncogenic mechanisms of Mdm2. For instance, the transfection of NIH 3T3 cells with any of five alternatively spliced forms of Mdm2 (designated a-e), which all lack part of the p53-binding domain, generated transformed foci at a high frequency (Sigalas *et al.*, 1996). In addition, in the same study the alternatively spliced Mdm2 variants were found more frequently in poorly differentiated and late-stage tumours. Only splice variant e retained normal p53 binding, therefore the increased transforming capacity of the other four splice variants cannot be attributed to a p53-dependent effect.

It is also of note that Mdm2 is thought to be able to bind to both the transcription factor E2F (Martin *et al.*, 1995) and the retinoblastoma protein, RB (Xiao *et al.*, 1995). E2F functions to drive the cell cycle through S-phase, with RB functioning to negatively regulate this activity. Mdm2 has been shown to activate an E2F reporter gene and as such may play a role in progression through the cell cycle. This could possibly represent a p53-independent mechanism by which Mdm2 can be oncogenic. It should be noted that E2F and RB bind to the N-terminal domain of Mdm2. As all of the Mdm2 splice variants contain N-terminal deletions (in particular variants a-d with large deletions), it is unlikely that they are still able to bind either E2F or RB. The potential role of these splice variants in the formation of certain cancers is currently unknown.

A high percentage of tumours (around 50%) retain wild type p53 activity. Jones *et al* (1995) found that knocking out the Mdm2 gene in mice resulted in early embryonic lethality. This lethality could be prevented by additionally knocking out the p53 gene.

Therefore, removing Mdm2 activity from cells expressing wild type p53 results in death of those cells (Jones *et al.*, 1995). This offers a potential target for the treatment of tumours expressing wild type p53. One such strategy of 'removing' Mdm2 activity is to block the binding of Mdm2 to p53. Proof of principle that such approaches may be effective has been provided by the introduction of a synthetic peptide modelled to bind the p53-binding site of Mdm2 (Bottger *et al.*, 1997). Alternatively, microinjection of a monoclonal antibody raised against the p53-binding site of Mdm2 can be used to block complex formation (Chen *et al.*, 1993a). However, such molecules do not enter cells easily, if at all and therefore are not suitable for therapy. Future directions include the design of smaller molecules able to achieve the same effect. Other potential treatments for tumours with wild type p53 include stabilising p53 by blocking the nucleo-cytoplasmic shuttling of Mdm2. This can be achieved by transfecting target cells with NLS-rex, an inhibitor of nuclear protein export.

Previous sections have aimed to highlight the importance of the tumour suppressor protein p53 in the regulation of genomic stability. By inducing cell cycle arrest or apoptosis, p53 allows repair of DNA damage or removal of a highly damaged cell by apoptosis before mutations are propagated. Therefore the mechanisms involved in the activation of p53 are vital for maintaining normal cellular function. Thus far phosphorylation, acetylation and regulation by Mdm2 have all been described as regulatory mechanisms. However, data exists in the literature suggesting a further regulatory function performed by the DNA damage-inducible enzyme poly(ADP-ribose) polymerase-1 (PARP-1). As will be described in the following sections PARP-1 is involved in DNA repair and has been reported to post-translationally modify a variety of nuclear proteins, including p53.

## 1.4 Poly(ADP-Ribose) Polymerase-1

PARP-1 is a nuclear enzyme involved in the detection of DNA strand breaks (for reviews see (D'Amours *et al.*, 1999; Oliver *et al.*, 1999). The occurrence of such breaks results in the rapid activation of PARP-1 and the subsequent poly(ADP-ribosyl)ation of several nuclear proteins (Althaus & Richter, 1987). The reaction involves the transfer of the ADP-ribose moeity from $NAD^+$ to target proteins and occurs in three steps. The reaction is initiated by the mono-ADPribosylation of target proteins, followed by elongation and branching. Target proteins identified *in vitro* include several involved in chromatin structure, DNA metabolism and cell cycle control, for example, DNA polymerases α and β and DNA ligases I and II (Yoshihara *et al.*, 1985 and Ohashi *et al.*, 1986). Observations made *in vitro* should be interpreted with caution as these proteins may not be targets for poly(ADP-ribosyl)ation under physiological conditions. The major acceptors of poly(ADP-ribose) identified *in vivo* are histones and PARP-1 itself (Ogata *et al.*, 1981; Adamietz and Rudolph, 1984). The result of poly(ADP-ribosyl)ation differs depending upon the protein involved. The effect on proteins with a particular relevance to this study will be discussed later.

### 1.4.1 Structure of PARP-1

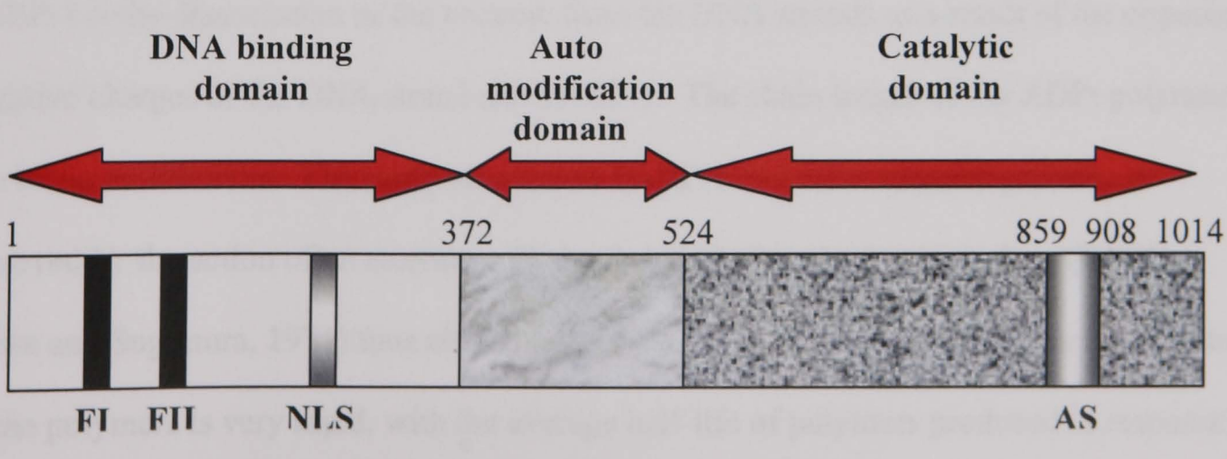


**Figure 1.8 Schematic diagram showing the domain structure of PARP-1**
FI and FII represent the zinc fingers of PARP-1; NLS = Nuclear localisation signal and AS = Active site

Human PARP-1 consists of 1,014 amino acids and contains three major structural domains (Alkhatib *et al.*, 1987; Kurosaki *et al.*, 1987) (see fig 1.8). The N-terminal of the protein comprises the DNA binding domain (DBD), which contains two zinc fingers, termed FI and FII (Mazen *et al.*, 1989) and a high proportion of basic amino acids (believed to be involved in the enzyme's interaction with DNA). Unlike the vast majority of zinc fingers in proteins, those of PARP-1 do not recognise specific DNA sequences, rather they recognise altered structures such as strand breaks (both single stranded and double stranded breaks). It is this strand break recognition which activates PARP-1, with activity being increased up to 500-fold (Wielckens *et al.*, 1983). DNA protection experiments have suggested that PARP-1 binds DNA strand breaks in the form of a dimer, with seven nucleotides either side of a single strand break being protected from nucleolytic digestion (Gradwohl *et al.*, 1990; Menissier de Murcia *et al.*, 1989).

The central region of PARP-1, located between amino acid residues 374 and 525 comprises the automodification domain. PARP-1 binds tightly to DNA strand breaks, is rapidly activated and poly(ADP-ribosyl)ates other DNA-bound proteins as well as itself. This poly(ADP-ribosyl)ation results in the addition of many ADP-ribose (ADPr) units, carrying negative charge, to the target protein. The effect of this automodification upon PARP-1 is the dissociation of the enzyme from the DNA strands as a result of the opposing negative charges of the DNA strand and PARP-1. The chain length of the ADPr polymers can be up to 200 units. The chain attached to PARP-1 and other targeted proteins is removed by the action of an enzyme called poly(ADP-ribose) glycohydrolase (PARG; Miwa and Sugimura, 1971) thus allowing the proteins to re-bind to DNA. The catabolism of the polymers is very rapid, with the average half-life of polymers produced in response to DNA damage being less than 1 minute (Wielckens *et al.*, 1983). The automodification

domain prevents the permanent activation of PARP-1 when it encounters DNA strand breaks and thus plays a vital regulatory role and may be important in allowing other repair enzymes to access the strand break.

The C-terminal domain of PARP-1 consists of residues 526-1014 and comprises the catalytic domain of the enzyme (Kurosaki *et al.,* 1987), involved in the nick-binding poly(ADP ribose) synthesis. As described earlier, PARP-1 binds DNA strand breaks as a dimer and is subsequently automodified. The observation that the ADPr polymers are elongated at their distal extremity suggests that the automodification is intermolecular, with one half of the dimer targeting the other half during catalysis (Alvarez-Gonzalez, 1988). The catalytic reaction involves the transfer of the ADP-ribose moiety from $NAD^+$ to target proteins *via* the γ-carboxy groups of glutamic acid residues (Riquelme *et al.,* 1979 and Burzio *et al.,* 1979). The polymer is then elongated and branched, with the individual residues being joined by glycosidic bonds (see figure 1.9). As described above, the polymer is degraded by PARG, an enzyme possessing both endo and exoglycosidase activity that hydrolyses the glycosidic bonds between ADPr units. The most proximal ADP-ribose unit is removed by an enzyme called ADP-ribosyl protein lyase. This step appears to be the rate-limiting step in ADPr metabolism (Wielckens *et al.,* 1982).

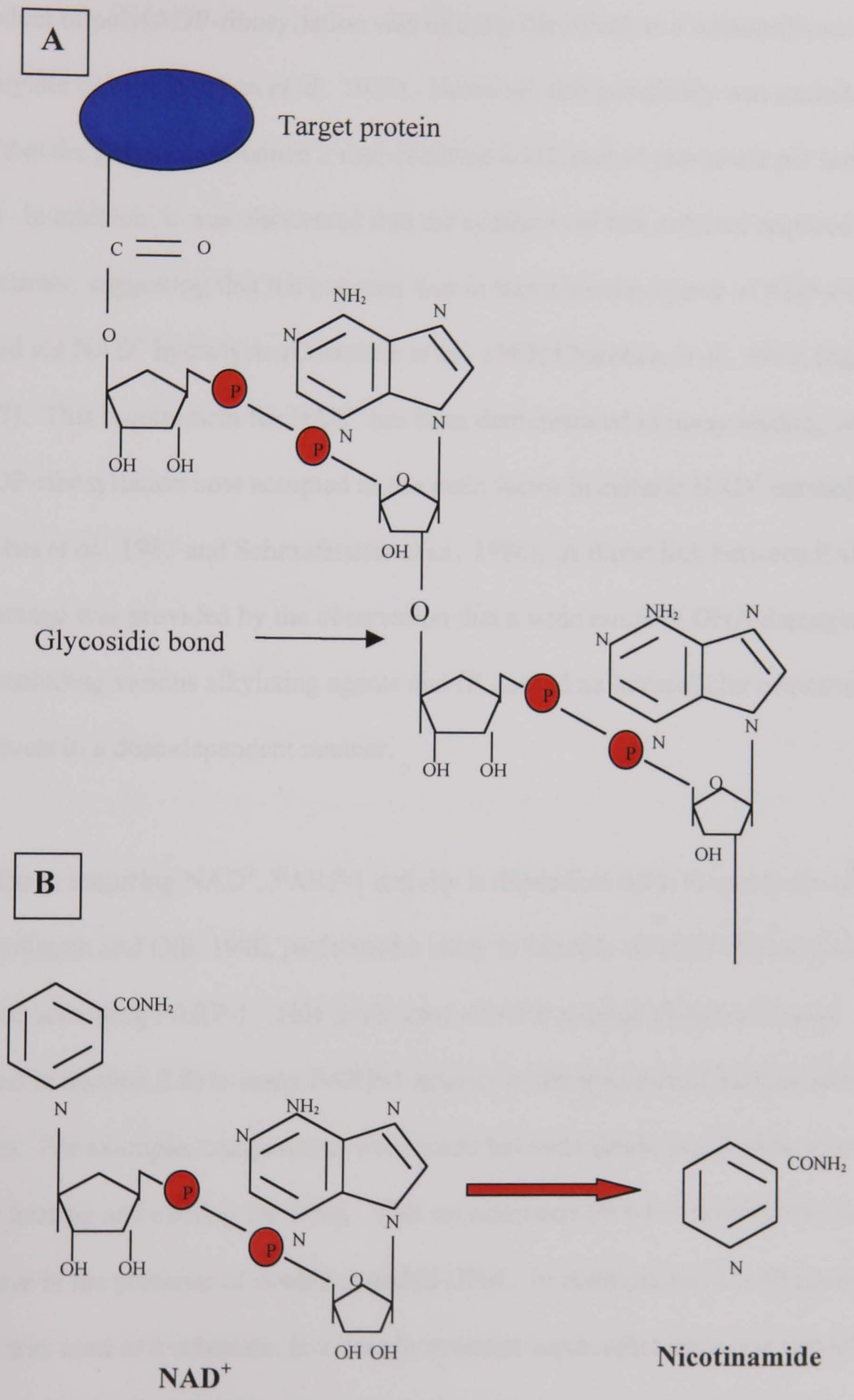


**Figure 1.9 The structure of ADPr polymer and hydrolysis of $NAD^+$**
Diagram A shows two ADPr units linked by a glycosidic bond, joined to a target protein. B shows the hydrolysis of $NAD^+$, with the subsequent release of nicotinamide.

### 1.4.2 The activation of PARP-1

The product of poly(ADP-ribosyl)ation was initially identified as a homopolymer of riboadenylate units (Chambon *et al.,* 1963). However, this possibility was excluded by the finding that the polymer contained 2 mol of ribose and 2 mol of phosphate per mol of adenine. In addition, it was discovered that the synthesis of this polymer required $NAD^+$ as a precursor, suggesting that the polymer was in fact a homopolymer of ADP-ribose units generated *via* $NAD^+$ hydrolysis (Chambon *et al.,* 1963; Chambon *et al.,* 1966, Sugimura *et al.,* 1967). This requirement for $NAD^+$ has been demonstrated in many studies, with poly(ADP-ribosyl)ation now accepted as the main factor in cellular $NAD^+$ catabolism (Wielckens *et al.,* 1983 and Schraufstatter *et al.,* 1986). A direct link between PARP-1 and DNA damage was provided by the observation that a wide range of DNA damaging agents, including various alkylating agents and IR caused an intracellular decrease in $NAD^+$ levels in a dose-dependent manner.

In addition to requiring $NAD^+$, PARP-1 activity is dependent upon the presence of DNA ends. Benjamin and Gill, 1980, performed a study to identify what DNA structures are capable of activating PARP-1. This study used a PARP permeabilised cell assay (described in Section 2.9) to assay PARP-1 activity in the presence of various DNA substrates. For example, comparisons were made between single and double-stranded DNA by heating and cooling the DNA. This revealed that PARP-1 activity was increased much more in the presence of double stranded DNA. In addition, the *E. coli* plasmid, pBR322 was used as a substrate, in a double stranded supercoiled state and also after digestion with certain restriction enzymes. Use of these enzymes allowed the generation of substrates with a known number of specific strand breaks (for example, single or double stranded breaks could be generated). The results generated clearly showed a lack of

PARP-1 activation, even at high concentrations, when closed circle or supercoiled plasmid DNA was used, presumably due to a lack of DNA ends. In contrast, digestion of the plasmid DNA with agents inducing single or double stranded breaks resulted in a marked increase in PARP-1 activity, highlighting the absolute requirement of DNA strand breaks for PARP-1 activation. The finding that PARP-1 requires DNA strand breaks for activation led to the hypothesis that PARP-1 functions in repair of this damage. Numerous studies have been performed investigating the role of PARP-1 in the repair, some of which will be described in the following section (1.4.3).

As described previously in this section, PARP-1 activation causes a decrease in the intracellular levels of $NAD^+$ (reviewed in d'Amours *et al.,* 1999). In response to certain damaging agents, at high doses, the level of $NAD^+$ can drop to approximately 10% of its normal level (Skidmore *et al.,* 1979 and Rankin *et al.,* 1980). As a consequence of this, the levels of ATP within cells also drops, as the synthesis of one molecule of $NAD^+$ requires at least two molecules of ATP (depending upon the particular synthetic pathway used). In addition, a decrease in $NAD^+$ levels inhibits glyceraldehydes-3-phosphate dehydrogenase activity, which is required to resynthesise ATP during glycolysis (Goodwin *et al.,* 1978). Therefore, activation of PARP-1 by high doses of IR brings about a reduction in the cellular levels of ATP. This ATP depletion has been shown to bring about a switch in the mode of cell death in response to DNA damage, from apoptosis to necrosis (Eguchi *et al.,* 1997 and Leist *et al.,* 1997). This is due to the absolute requirement of ATP for the efficient execution of apoptosis. Necrotic death is characterised by cell lysis and the release of inflammatory factors which cause damage to neighbouring cells (reviewed in Szabo, 1998). This is in contrast to apoptotic cell death, which is localised to the particular damaged cell(s). The death of cells *via* necrosis is responsible for the pathological

complications associated with ischemia and with some forms of diabetes. Therefore, a major area of research is currently involved in the development of PARP-1 inhibitors, which may be used in patients who have suffered ischaemia. The aim is to inhibit PARP-1 and prevent the intracellular depletion of $NAD^+$ and hence protect cells from switching to the necrotic mode of cell death. Interestingly, studies with PARP-1 deficient mice show that these animals are protected from post-ischaemia damage compared to the PARP-1 proficient animals (Szabo *et al.,* 1996 and Masutani *et al.,* 1999). It should be noted that PARP-1 proficient cells appear to have evolved a mechanism to prevent massive depletion of $NAD^+$ during cell death. For example, once a cell is commited to apoptosis, PARP-1 is rapidly cleaved and inactivated by caspase-3 (Lazebnik *et al.,* 1994). This cleavage separates the DBD of PARP-1 from the catalytic domain and hence the catalytic activity can no longer be activated by DNA strand breaks. A characteristic of apoptotic cell death is chromosomal degradation, which would obviously generate many DNA ends. Under normal circumstances, these ends would massively activate PARP-1 and possibly cause a switch from apoptosis to necrosis. Therefore, cleavage of PARP-1 early in apoptosis prevents this from occurring thus preventing cells undergoing necrotic cell death, which can result in damage to neighbouring healthy cells.

### 1.4.3 PARP-1 and DNA repair

An initial role for PARP-1 in DNA repair was proposed by Durkacz *et al.,*1980, who showed that the repair of damage induced by the monofunctional alkylating agent, dimethyl sulphate, was significantly slowed in the presence of a PARP-1 inhibitor, 3-aminobenzamide (3-AB). In the last decade, many genetic and biochemical studies have been performed involving PARP-1 to try and clarify the role it performs in DNA repair. The principal aim of these studies was to remove PARP-1 protein and/or activity from

whole animals or various cell types and observe the response to various DNA damaging agents. Several techniques have been used to remove PARP-1 from the system being studied. These include a dominant-negative strategy involving the overexpression of the DBD of PARP-1 (Kupper *et al.*, 1995) such that it binds to DNA breaks in competition with the native PARP-1 and hence poly(ADP-ribosyl)ation does not occur. Other methods include the use of PARP-1 inhibitors (e.g. Boulton *et al.*, 1995; Griffin *et al.*, 1995) expression of an antisense RNA construct and knocking out the PARP-1 gene (e.g. de Murcia *et al.*, 1997; Masutani *et al.*, 1999; Wang *et al.*, 1995).

Before describing the putative role of PARP-1 in DNA repair, some of the pathways involved in the process of DNA repair will be discussed. This is particularly relevant to this study as a variety of DNA damaging agents have been used, which in turn produce different forms of DNA damage. A description of the forms of damage and their repair will be provided below.

#### 1.4.3.1 Base excision repair

Base excision repair (BER) involves the repair of damage induced by oxidative, alkylating and other DNA damaging agents (McCullough *et al.*, 99). Figure 1.10 summarises this repair pathway. Damage induced includes the formation of covalent bonds between, for example, an alkylating agent and the base. Common lesions include 3-methyladenine and 8-hydroxyguanine. Enzymes called DNA glycosylases diffuse along the minor groove of the DNA. They are able to recognise specific types of damaged nucleotide and excise the altered base *via* cleavage of the glycosidic bond between the base and deoxyribose. Human cells possess many glycosylases, with each one being capable of recognising and removing a particular modified base. At this stage the backbone of the DNA helix remains

intact. An apurinic (AP) endonuclease then nicks the damaged DNA strand upstream of the abasic site to produce a 3' OH. This produces a single stranded DNA break (shown in figure 1.9), which may be important in the activation of PARP-1 and other DNA damage response proteins to be discussed later. The gap in the DNA is ultimately filled by the extension of the 3' OH, by a DNA polymerase followed by excision of the abasic site. The repair process is completed by the ligation of the DNA ends.

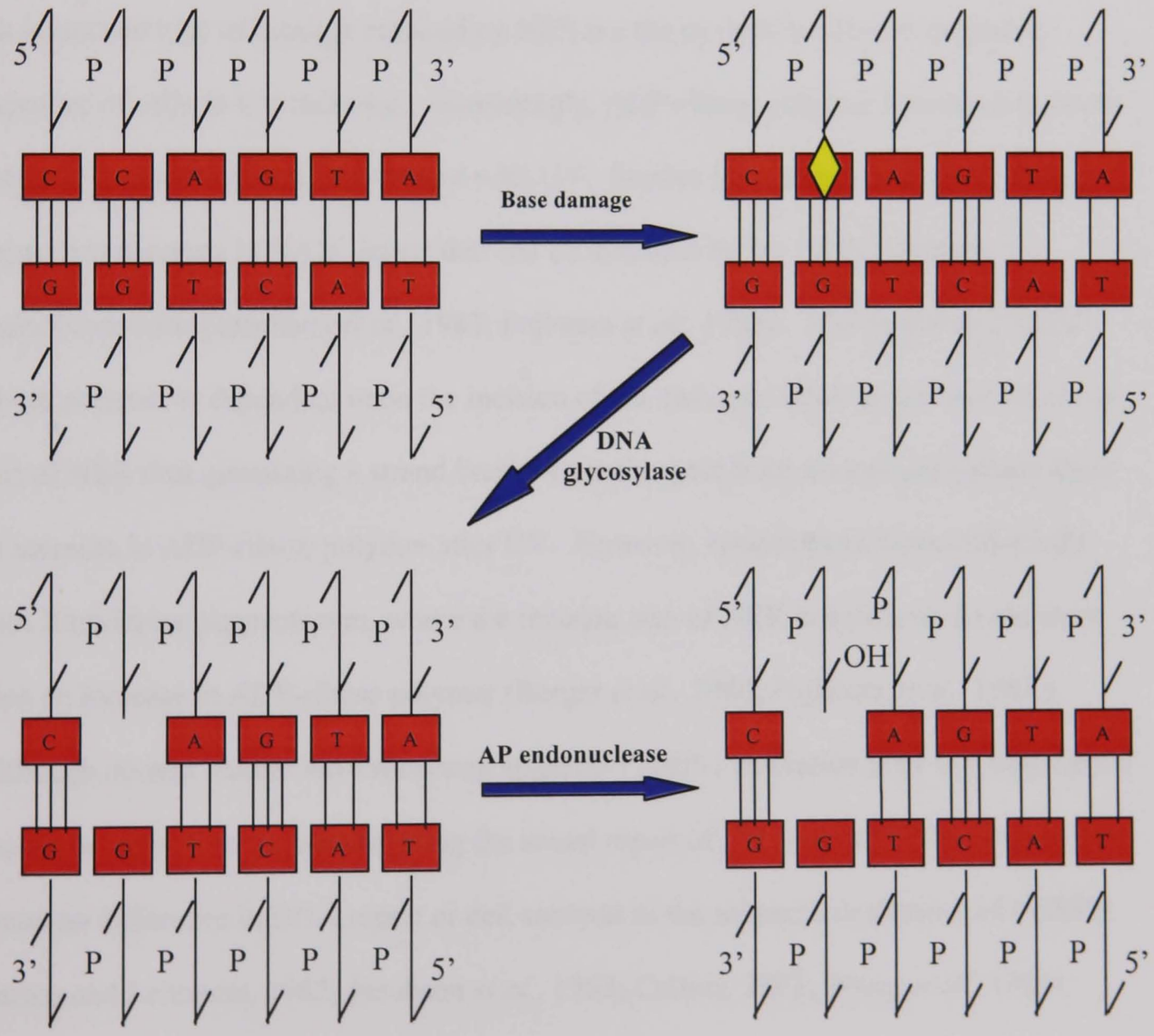


**Figure 1.10 Diagram showing the formation of a SSB during BER**

### 1.4.3.2 Nucleotide excision repair

A second repair pathway, called nucleotide excision repair (NER) serves to remove a whole oligonucleotide at sites containing damaged base(s), which result in alteration of the normal helical structure of the DNA. A multiprotein complex is responsible for recognition of such sites, followed by incision of the DNA strand, displacement of the oligonucleotide and finally filling of the gap by DNA polymerisation and ligation (Muller *et* al., 98). The repair complex contains several XP proteins, identified as being defective in the human condition xeroderma pigmentosum, characterised by a sensitivity to UV light. An important type of damage repaired by NER are the pyrimidine dimers caused by exposure of cells to UV radiation. Interestingly, ADP-ribose polymer formation has been detected in permeabilised cells treated with UV. Studies have also shown a UV dose-dependent decrease in $NAD^+$ levels that can be inhibited by the PARP inhibitor 3-aminobenzamide (Jacobson *et al.,* 1983; Fujiwara *et al.,* 1983). This synthesis of ADP-ribose polymer is dependent upon the incision of the damaged DNA strand that occurs as part of NER thus generating a strand break. Lymphocytes from normal individuals show an increase in ADP-ribose polymer after UV. However, lymphocytes from individuals with Xeroderma pigmentosum, where the incision step of NER is deficient, do not show such an increase in ADP-ribose polymer (Berger *et al.,* 1980; Fujiwara *et al.,* 1983 ). Although several studies have shown an apparent PARP-1 activation after UV radiation, it should be noted that studies analysing the actual repair of UV-induced DNA damage have found no difference in DNA repair or cell survival in the presence or absence of PARP-1 (James and Lehmann, 1982; Jacobson *et al.,* 1983; Collins, 1985; Wang *et al.,* 1995).

### 1.4.3.3 Double strand break repair

The final form of DNA damage to be discussed is double strand breaks (DSBs) which result from exposure to ionising radiation. Ionising radiation is a form of DNA damage

that induces both single and double stranded DNA breaks. In addition, free radicals (reactive oxygen species, for example, hydroxyl radicals and hydrogen peroxide) are produced, which can chemically modify DNA bases via oxidation e.g. 8-hydroxyguanine, which is repaired by BER, as are thymine glycols, produced by oxidation of a thymine base and 8-hydroxyguanine. The most cytotoxic lesions induced by IR are considered to be DSBs. If repaired inefficiently, this type of break frequently leads to mutations, in particular chromosomal translocations (Richardson and Jasin, 2000) or apoptosis (Rich *et al.,* 2000). As such it is important to the normal (i.e. non mutated) survival of the cell that DSBs are recognised and repaired as efficiently as possible. Two pathways are involved in the repair of DSBs, homologous recombination (HR) and non-homologous end-joining (NHEJ), with the latter being the predominant pathway in mammalian cells (Chu, 1997).

During HR (reviewed in Jackson, 2002), the damaged chromosome aligns with and retrieves genetic information from an undamaged DNA molecule with which it shares sequence homology. In humans, a set of proteins termed the 'RAD50' group have been described, which are extensively involved in HR (Wood *et al.,* 2001). Briefly, a complex containing Rad50 resects one strand of the DSB in the 5' to 3' direction. The resultant 3' single stranded DNA tail is then bound by Rad51, which interacts with an undamaged DNA template and locates a homologous region on the undamaged chromosome. Rad51 then catalyses strand invasion by the single-stranded DNA into the undamaged DNA duplex resulting in displacement of one of the strands. The 3'terminus of the damaged DNA is then extended by a DNA polymerase, using the undamaged strand of DNA as a template. Upon completion, the DNA crossovers (Holliday junctions) are cleaved and ligated to yield two intact DNA molecules.

Efficient recognition and repair of DSBs by NHEJ (reviewed in Jackson, 2002) is dependent upon a heterodimeric protein called Ku, consisting of 70 and 86kDa subunits. Biochemical studies have revealed that Ku binds to DSBs in a non-sequence-dependent manner (Dynan and Yoo *et al.,* 1998). Binding of Ku leads to recruitment and activation of a catalytic subunit, the DNA-dependent protein kinase catalytic subunit (DNA-PKcs) to form a trimeric complex. The catalytic subunit shares C-terminal sequence homology with two previously discussed DNA damage response kinases, ATR and ATM. Ku also recruits XRCC4 and DNA ligase IV to the DSB, with the latter bringing about direct ligation of the DNA ends. Prior to this ligation it is likely that the ends of the DNA require processing by nucleases. In addition to the recruitment of a DNA ligase to the site of damage, it is possible that the DNA-PK complex performs other functions. For example, binding of Ku to the DSB may protect the DNA ends from further damage initiated by nucleases. Alternatively, the recruitment of the bulky DNA-PK complex and subsequent phosphorylation of nearby proteins may decondense chromatin structure, aiding the access of other DNA damage response proteins to the site of damage.

Although a precise role for PARP-1 in HR or NHEJ has not been described, several studies discussed below have shown that the lack of PARP-1 leads to hypersensitivity in response to IR. It is possible that a subset of breaks produced by IR (distinct from DSBs) are reliant upon PARP-1 for repair (Durkacz *et al.,* 1980). As described earlier in this section, certain lesions induced by IR e.g. thymine glycols and 8-hydroxyguanine are repaired by the BER pathway. Therefore, persistence of these breaks due to lack of PARP-1 may be sufficient to sensitise cells to IR. Alternatively, PARP-1 may have a direct role to play in the cellular response to IR. For example, PARP-1 has been shown to bind to double strand breaks and

therefore may perform a protective role, preventing further damage to the DNA ends by nucleases.

The types of DNA damage mostly responsible for the activation of PARP-1 *in vivo* are SSBs. This type of damage is usually repaired by the base excision repair pathway (BER) and this is the type of repair with which PARP-1 has been implicated. Satoh and Lindahl (1992) demonstrated that the repair of SSBs in a cell-free BER assay is dependent upon the presence of $NAD^+$, the substrate of PARP-1 (Satoh & Lindahl, 1992). Furthermore, inhibition of poly(ADP-ribosyl)ation in this assay resulted in a decreased repair of SSBs. In addition, inhibitor studies have shown that the base recognition and excision steps of BER are not influenced by PARP-1. Shall, 1984, showed that the formation of DNA breaks during BER was not affected by treatment with a PARP-1 inhibitor but that the subsequent re-joining of the break was retarded. As might be expected, this suggests that PARP-1 is not required until a strand break has been generated by the repair process, to which PARP-1 can bind and become activated.. In addition, this and other studies indicate that PARP-1 is not absolutely required for BER. Rather PARP-1 appears to increase the efficiency of BER such that the strand breaks are repaired more quickly in the presence of PARP-1.

Studies of PARP-1-deficient animals or cell lines initially suggested that PARP-1 was not involved in base excision repair. For example, it was reported that mice inactivated in both PARP-1 alleles were able to repair and transcribe alkylated plasmids introduced into cells derived from the mice (Wang et al., 1995), suggesting that PARP-1 is not involved in the repair of alkylation damage. However, it may be that the plasmid is repaired but the actual kinetics are slower in the absence of PARP-1. Therefore, depending upon the time scale

for repair, the role of PARP-1 in BER in this particular assay may have been missed. In addition, the plasmid DNA used in these studies is not in the same state as normal cellular DNA, as the plasmid is not tightly coiled around histone proteins.

Subsequent studies have led to the consensus of opinion that PARP-1 deficient mice are hypersensitive to monofunctional alkylating agents and IR. Whole body exposure of the mice to IR (8Gy) or treatment with the alkylating agents MNNG, MNU (75mg/Kg) or MMS (100μM) led to far greater death in the PARP-1 knockout animals compared to the PARP-1 proficient counterparts (de Murcia et al., 1997; Masutani et al., 1999; Wang *et al.*, 1997). Examination of PARP-$1^{-/-}$ mice after 8Gy IR treatment revealed that the mice died due to acute radiation toxicity to the small intestine (de Murcia *et al.*, 1997). Similar results have been obtained in cells derived from these mice, where colony forming assays after IR exposure or alkylating agent treatment have shown a marked decrease in colony formation (and hence cell survival) in the PARP-$1^{-/-}$ MEFs compared to PARP-$1^{+/+}$ MEFs. It should be noted that the alkylating agents used are potent PARP-1 activators in wild type mice. In addition DNA damage induced by MNU treatment and γ-irradiation of PARP-$1^{-/-}$ mice led to an increase in sister chromatid exchange (SCE) indicative of the genetic instability caused by the suppression of poly(ADP-ribosyl)ation reactions (de Murcia *et al.*, 1997).

Although it is now widely accepted that PARP-1 plays a role in BER, it is not clear as to what that role might be. Several theories exist, each of which is supported by different lines of evidence. It may be that PARP-1 has overlapping roles involving aspects of each of the proposed mechanisms. One proposed mechanism is based on the very rapid binding of PARP-1 to DNA strand breaks. It has been suggested that PARP-1 subsequently

recruits several other DNA-damage repair proteins to the site leading to the initiation of repair. Supporting evidence includes the identification of a BER complex consisting of PARP-1, XRCC1, DNA ligase III and DNA polymerase β (Caldecott *et al.*, 1996; Kubota *et al.*, 1996; Masson *et al.*, 1998). Central to this complex is the putative scaffold protein, XRCC1, upon which the other components of the complex bind. PARP-1 was first found to bind XRCC1 *via* a yeast two hybrid screen (Masson *et al.*, 1998), where human PARP-1 cDNA was fused to the LexA-encoding DNA binding domain and used as bait to screen a HeLa cell cDNA library fused with the activation domain of Gal4. This screen identified XRCC1 as a factor to which PARP-1 binds. Subsequent *in vivo* experiments using glutathione S-transferase (GST)-tagged fusion proteins showed that the interaction was *via* the BRCT domains of the respective proteins. Interestingly, the association of PARP-1 with XRCC1 was found to dramatically decrease the catalytic activity of PARP-1, without affecting the nick-binding function of this enzyme. This finding would be consistent with the recruitment model as one would not expect a complex to form in the vicinity of automodified PARP-1 due to electrostatic repulsion and also steric hindrance. Therefore, to allow the complex to form, the activity of PARP-1 is down-regulated, possibly before being switched on again, by an as yet unidentified mechanism, to allow dissociation of the enzyme from the DNA and repair of the SSB.

Another possible mechanism is based on the structure of chromatin. In this state the DNA of the cell is tightly wound around histone molecules into a very compact structure. DNA damage may allow access of PARP-1 to the site of damage. Poly(ADP-ribosyl)ation of nearby histones (Kreimeyer *et al.*, 1984) may decondense the DNA (Althaus, 1992), allowing access to the bulky complexes associated with the repair of DNA (see figure 1.11). This model of 'histone shuttling' was based on initial studies by Althaus and

colleagues who demonstrated that poly-ADPr turnover renders DNA susceptible to nuclease digestion when core histones are incubated with the DNA. In addition, degradation of the ADPr polymer by PARG abolishes the nucleolytic digestion of the DNA. These observations were described in terms of a relaxation of chromatin structure due to modification of histones by ADPr polymer. This negatively charged polymer results in dissociation of histones from DNA due to electrostatic repulsion causing localised relaxation of the chromatin structure and hence nucleolytic digestion of the DNA in this assay. Degradation of the polymer by PARG would prevent any electrostatic repulsion between the histones and DNA and hence the chromatin structure would remain intact and the DNA would be protected from nucleolytic digestion.

Further evidence for this proposed mechanism is the observation that the repair of damage in non-transcribed regions of the genome requires PARP-1 activity, whereas repair of transcribed regions does not require PARP-1 activity (Ray *et al.*, 1996). In transcribed regions of the genome, the DNA is already in a relaxed state to allow efficient gene transcription by RNA polymerase. Therefore, ADP-(ribosyl)ation is perhaps not required to decondense the DNA. However, in non-transcribed regions, where the DNA is tightly coiled around histones, PARP-1 activity may be necessary to decondense the DNA and allow access of other repair enzymes to the site of damage. In PARP-1-deficient mice treated with alkylating agents or γ-radiation, despite the presence of DNA damage, the DNA would remain in a highly condensed state. Therefore these mice exhibit hypersensitivity to the DNA-damaging agents mentioned due to the persistence of unrepaired DNA (de Murcia et al., 1997; Wang et al., 1997) and subsequent induction of cell death.

A further mechanism by which PARP-1 may mediate DNA repair is *via* a signalling pathway. PARP-1 activation is an immediate response to DNA damage, resulting in a rapid modification of several proteins at the site of damage (including histones and PARP-1 itself). The formation of ADP-ribose polymers may act as the initiating step in a signalling cascade resulting in the activation of downstream effectors involved in co-ordinating the cellular response to DNA damage. Supporting this model are studies suggesting a functional relationship between PARP-1 and p53, the details of which will be discussed in Section 1.4.6. In addition, PARP-1 has been shown to be capable of activating a DNA damage response kinase (DNA-PK; Ruscetti *et al.*, 1998), which has been implicated in the phosphorylation of p53 during the cellular response to DNA damage (Woo *et al.*, 1998). As well as being involved in the repair of SSBs it should be noted that PARP-1 has also been implicated in DSB repair (Weinfeld *et al.*, 1997 and Boulton *et al.*, 1999), although less data is currently available concerning PARP-1's involvement in this process.

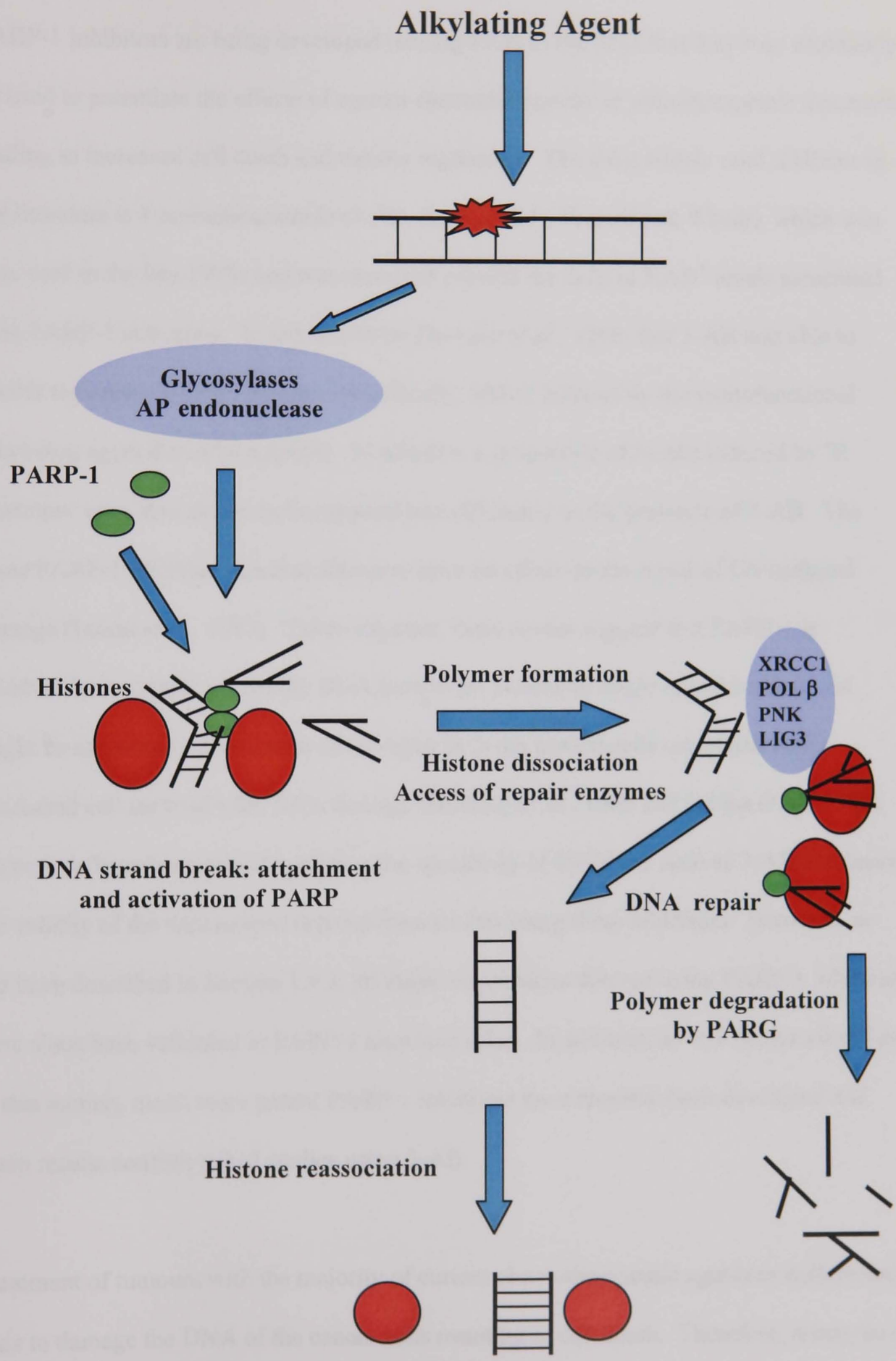


**Figure 1.11** Diagram summarising a potential role for PARP-1 in BER

### 1.4.4 PARP-1 inhibitors

PARP-1 inhibitors are being developed (see fig 1.12) in the hope that they may eventually be used to potentiate the effects of current chemotherapeutic or radiotherapeutic treatments leading to increased cell death and tumour regression. The most widely used inhibitor in the literature is 3-aminobenzamide (3-AB, developed by Purnell and Whish), which was first used in the late 1970s and was shown to prevent the drop in $NAD^+$ levels associated with PARP-1 activation. It was shown by Durkacz *et al.,* 1980, that 3-AB was able to inhibit the repair of DNA damage (specifically, SSBs) induced by the monofunctional alkylating agent dimethyl sulphate. In addition, a proportion of breaks induced by IR treatment were also shown to be repaired less efficiently in the presence of 3-AB. The same PARP-1 inhibitor was also shown to have no effect on the repair of UV-induced damage (James *et al.,* 1982). Taken together, these results suggest that PARP-1 is involved in the repair of specific DNA lesions (in particular single strand breaks). As might be expected, a decrease in DNA repair in 3-AB treated cells correlated with a decreased cell survival after DNA damage (Durkacz *et al.,* 1980 and Nduka *et al.,* 1980). Objections have been raised regarding the specificity of inhibitors such as 3-AB and hence the validity of the conclusions derived from studies using these inhibitors. However, as has been described in Section 1.4.3, all major conclusions derived using PARP-1 inhibitors have since been validated in PARP-1 knockout mice. In addition, as will be described later in this section, much more potent PARP-1 inhibitors have recently been developed and again results confirm initial studies using 3-AB.

Treatment of tumours with the majority of current chemotherapeutic agents or radiotherapy aims to damage the DNA of the cancer cells resulting in cell death. Therefore, it may be of therapeutic benefit to be able to potentiate the effects of chemo- or radio-therapy within

tumour cells. Treatment of tumour cells with an inhibitor of a DNA repair pathway would be expected to achieve such an objective. Therefore, there is a great deal; of interest in developing potent PARP-1 inhibitors that can be used for this purpose. The Cancer Research Unit in Newcastle has developed and tested a variety of novel inhibitors. Initial pre-clinical studies have characterised several potent PARP-1 inhibitors (Griffin, 1996; Griffin et al., 1995; Suto *et al.*, 1991). Boulton *et al* 1995 demonstrated that the PARP-1 inhibitor 8-hydroxy-2-methylquinazolin-4-one (NU1025) potentiated the cytotoxicity of the monofunctional alkylating agent temozolomide, correlating with an inhibition of SSB repair. This study showed both a decrease in clonogenic survival and an increase in DNA strand breaks when the cell cultures were incubated with NU1025 at 300μM prior to, and following exposure to ionising radiation and temozolomide. It is of note that both of the DNA damaging agents used in this study (i.e. temozolomide and IR) are currently used in the treatment of certain cancers, therefore any potentiation observed in the presence of a potent PARP-1 inhibitor may be therapeutically beneficial to these patients. The PARP-1 inhibitor used in this study, AG14361 ($k_i$ < 6nM, made in a collaboration between the Cancer Research Unit and Pfizer GRD, CA) is approximately 1000-fold more potent than 3-AB ($k_i$ = 5.7μM) and has also been tested within the Cancer Research Unit. Figure 1.12 shows the structures of the PARP-1 inhibitors discussed above.

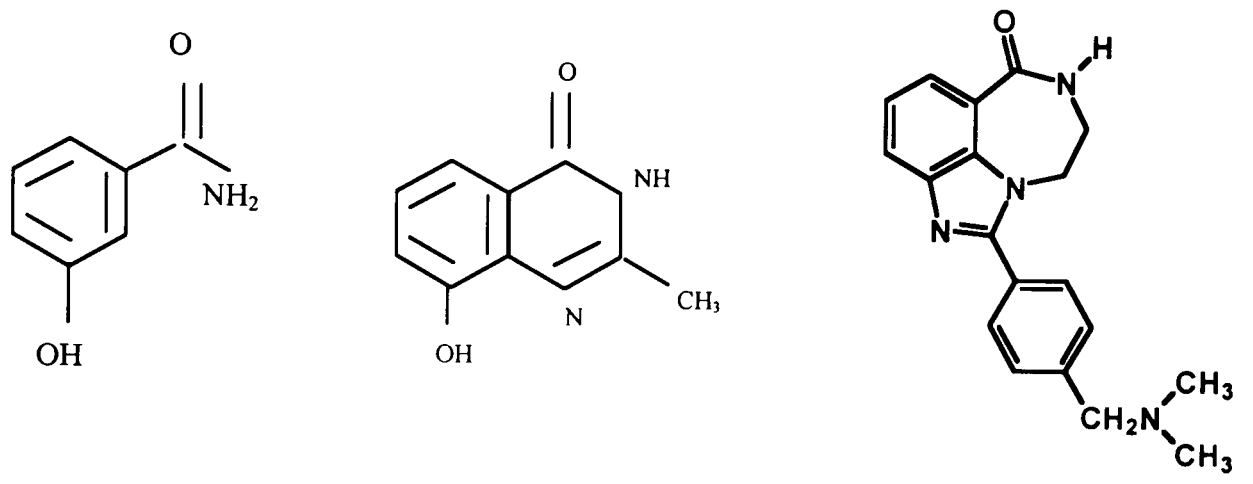


**Figure 1.12 The structure of a variety of PARP-1 inhibitors**
From left to right, 3-AB, NU1025 and AG14361

Unpublished data (Cancer Research Unit) has shown that treatment of a range of PARP-1 proficient human tumour cells with 0.4μM AG14361 resulted in a large potentiation of IR- and temozolomide induced damage (Drug Development Group, Cancer Research Unit), associated with a decrease in cell survival. Also, in response to IR, PARP-$1^{+/+}$ MEFs treated with 0.4μM AG14361 showed a dose dependent decrease in cell survival, as measured by clonogenic survival assays. At a dose of 6Gy IR, cell survival had decreased by 50% in the inhibitor-treated PARP-$1^{+/+}$ MEFs. In the same experiment, PARP-$1^{-/-}$ MEFs were shown to be much more sensitive to IR treatment than the PARP-$1^{+/+}$ MEFs. Approximately 90% of PARP-$1^{+/+}$ MEFs were killed at a dose of 5Gy, whereas a dose of only 1.5Gy was required to kill the same number of PARP-$1^{-/-}$ MEFs. It should be noted that the treatment of PARP-$1^{-/-}$ MEFs with 0.4μM AG14361 did not potentiate the effects of IR in these cells. This concentration of 0.4μM AG14361 should be compared to the concentration of 3mM 3-AB used in the study of Durkacz *et al.*, 1980 to highlight the potency of these new inhibitors. In addition, local studies in nude mice have shown that treatment with AG14361 results in significant regression of human tumour xenografts in response to IR, temozolomide and irinotecan (unpublished data). It should be noted that

PARP-1 inhibitors may also be useful in reducing the harmful side effects of current cancer treatments, caused by damage to non-cancerous cells. As well as being used in the treatment of cancers PARP-1 inhibitors may be useful in the treatment of ischaemia and certain types of diabetes, as described in Section 1.4.2.

### 1.4.5 Additional functions of PARP-1

The previous section (Section 1.4.4) has described the requirement for PARP-1 in cell survival after certain types of DNA damage. In addition, a variety of models have been proposed for the precise function of PARP-1 in the repair of these DNA lesions. These models have been based on evidence spanning back initially to the 1980s. However, additional functions of PARP-1 have been described, for example PARP-1 has been implicated in the control of cellular transcription and also in the regulation of the transcription factor NF-κB (reviewed in Chiarugi, 2002 and Shall and de Murcia, 2000).

A role for PARP-1 in transcriptional control was initially proposed based on the identification of PARP-1 as a factor that could increase the specificity of initiation of RNA polymerase II (Matsui *et al.*, 1980; Slattery *et al.*, 1983). Subsequent studies have produced a body of evidence showing that PARP-1 can have stimulatory or inhibitory effects on transcription, dependent upon the cell type, the gene being transcribed and the transcription factors involved (Ziegler and Oei, 2001). For example, PARP-1 was found to stimulate transcription in human cell extracts, but only if the PARP-1 remained catalytically inactive by excluding $NAD^+$ from the assay. Consistent with this finding is the identification of PARP-1 as a binding partner to a variety of transcription factors, including Oct-1, TEF-1 and AP-2 (Nie *et al.*, 1998; Butler *et al.*, 1999 and Kannan *et al.*, 1999). Addition of $NAD^+$ to the previously described assay resulted in silencing of RNA

polymerase II-dependent transcription due to protein modification by poly(ADP-ribose). During the formation of ADPr, PARP-1 is likely to become automodified and hence binding to the previously described transcription factors (Oct-1, TEF1 and AP-2) will be abolished. In addition, several other transcription factors have been identified as targets for poly(ADP-ribosyl)ation, including the TATA-binding protein and Yin Yang 1, with the likely result of dissociation of these proteins from transcription complexes or DNA promoter sequences hence the inhibition of transcription.

The precise role of PARP-1 in transcriptional control is likely to be complex, with PARP-1 able to bind DNA itself, bind to various transcription factors and also to poly(ADP-ribosyl)ate several transcription factors. One model for the role of PARP-1 has been proposed by Ziegler and Oei, 2001, who proposed that the functions of PARP-1 in DNA repair and transcription are combined in response to genotoxic stress. They suggested that upon exposure to DNA damage, PARP-1 rapidly binds to the DNA strand lesions (such as SSBs). As a consequence of this binding PARP-1 is catalytically activated and automodifies itself. This has recently been shown to increase the rate of ongoing transcription elongation (Vispe *et al.*, 2000). At the same time, PARP-1 targets various transcription factors for poly(ADP-ribosyl)ation, preventing the binding of these factors to promoter sites and hence preventing the initiation of transcription. It is obviously beneficial to prevent transcription of potentially damaged areas of the genome. Having shut down transcription, PARP-1 is able to perform its role in DNA repair, possibly by relaxing the localised chromatin structure and allowing access of repair enzymes to the lesion. After repair, the ADPr bound to PARP-1 and transcription factors is removed by PARG, allowing the cell to resume normal physiological processes.

Studies involving the use of PARP-1 inhibitors have implicated PARP-1 in the innate immune response under certain circumstances. For example, exposure of bone marrow macrophages to lipopolysaccharide (LPS) induces nitric oxide formation, which can be blocked by treatment of cells with the PARP-1 inhibitor 3AB (Hauschildt *et al.,* 1991). Nitric oxide is generated by the product of the inducible nitric oxide synthase gene (iNOS). Subsequent studies have revealed that the inhibition of PARP-1 brought about an inhibition in transcription of the iNOS gene, mediated by the transcription factor NF-κB (Le Page *et al.,* 1998). This study demonstrated clearly that the ability of NF-κB to function as a transcription activator of the iNOS gene was impaired in the absence of PARP-1. The transcription factor NF-κB is vital to many cellular processes, including DNA damage and repair and immune responses and is activated by a wide variety of agents, for example, IR, UV, tumour necrosis factor-α (TNF-α) and various mitogens. Once activated, NF-κB induces the expression of several immune response genes and is also crucial in preventing the initiation of apoptosis (reviewed in Foo and Nolan, 1999). As such an understanding of the regulation of this protein could prove very useful in deciphering the steps involved in various cellular pathways and also the treatment of certain diseases.

Studies involving PARP-1 knockout cells have further highlighted the functional relationship between PARP-1 and NF-κB. PARP-$1^{-/-}$ cells exhibited greater sensitivity to TNF-α cytotoxicity compared to PARP-$1^{+/+}$ cells, a difference which was attributed to an inability to induce NF-κB expression in the absence of PARP-1 (Oliver *et al.,* 1999). Identical results were obtained after exposure of cells to hydrogen peroxide. This same study also demonstrated impaired NF-κB function in PARP-1 knockout mice, where these animals were protected against the whole animal toxicity of LPS, again attributed to an inability to induce NF-κB and hence reduced expression iNOS and nitric oxide. Although

there is clear evidence supporting a role for PARP-1 in the expression of NF-κB, the exact mechanisms involved are not clear, although PARP-1 has been detected in a stable nuclear complex bound to both the p65 and p50 subunits of NF-κB (Hassa and Hottinger, 1999).

The fact that PARP-1 is able to induce the expression of the transcription factor NF-κB supports the hypothesis that PARP-1 is able to influence transcription of various genes. As described in this section PARP-1 has been shown to have both positive and negative effects on the rate of transcription, putatively by binding to or ADP-ribosylating a variety of transcription factors. The following section discusses in detail the potential role of PARP-1 in the regulation of another transcription factor, p53, which has turned out to be a controversial area of research. It is this regulation that is the focus of this thesis.

### 1.4.6 PARP-1 and p53

PARP-1 is activated immediately in response to DNA damage and has been implicated in signalling to several molecules, perhaps most significantly, p53. The effect of PARP-1 upon p53 is an area of research where a lot of contradiction still exists. Several groups have reported an altered p53 induction in PARP-1-deficient cells, whereas others have reported an unchanged p53 induction. However for a lot of the studies, different cell lines were used as well as different DNA-damaging agents.

For example Menissier-de Murcia *et al.* 1997 demonstrated an accumulation of p53 after treatment of PARP-1 knockout cells (splenocytes disrupted in exon 4) with an alkylating agent whereas p53 induction did not occur in the PARP-$1^{+/+}$ cells (de Murcia *et al.*, 1997). It is perhaps surprising that the PARP-1 proficient cell line showed no evidence of a p53 induction in response to DNA damage. This result is in accordance with Lu and Lane

(1993) who demonstrated an increased p53 induction after x-ray irradiation of mouse prostate cells treated with 3-AB, a PARP-1 inhibitor (Lu & Lane, 1993). These results were explained in terms of a persistence of DNA strand breaks in the absence of PARP-1 activity due to inefficient repair of the DNA. It was hypothesised that these breaks would relay greater activation signals to p53 and hence an increased response was observed. A recent study using the aforementioned de Murcia knockout cells demonstrated a differential requirement for PARP-1 in the p53 response to different DNA damaging agents (Valenzuela *et al.*, 2002). More precisely, primary PARP-$1^{-/-}$ MEFs showed a reduced p53 induction after exposure to ionising radiation but showed an increased p53 induction after treatment with an alkylating agent compared to PARP-$1^{+/+}$ MEFs. The authors proposed that the observed response to IR was due to impaired activation of ATM in the PARP-1 knockout cells, leading to the observed decrease in p53 Ser15 phosphorylation and hence a decrease in p53 activation. In response to the alkylating agent, a greater p53 response was observed in the PARP-1 knockout MEFs, possibly due to inefficient BER and hence persistence of strand breaks. A second set of PARP-1 knockout MEFs disrupted in exon 2 (Wang *et al.*, 1995) showed a reduced induction but normal activation and function of p53 in response to adriamycin and IR (Agarwal *et al.*, 1997). The authors proposed that the accumulation of p53 can occur *via* PARP-1 dependent and PARP-1 independent pathways but that the activation of p53 is predominantly independent of PARP-1. The final set of PARP-1 knockout MEFs are disrupted in exon 1 of the PARP-1 locus. These cells exhibit identical p53 responses (both induction and activity) to the PARP-1 wild type counterparts after treatment with 8Gy IR (Masutani *et al.*, 1999).

Simbulan-Rosenthal *et al.* (1998a) used the expression of PARP-1 antisense RNA to remove PARP-1 activity from cells (Burkitt's Lymphoma AG876). In response to ionising

radiation, the absence of PARP-1 activity led to a prolonged p53 response but with the magnitude of the response being unaffected compared to PARP-1 proficient cells. This study is in accordance with Lu and Lane, 1993 and de Murcia *et al.,* 1997, who showed that lack of PARP-1 potentiates the p53 response to DNA damage. Other results (Whitacre *et al.,* 1995; Wang *et al.,* 1998) show the opposite, with the absence of PARP-1 (through down-regulation or inhibition) showing decreased basal levels of p53 as well as a failure to activate p53 in response to various DNA damaging agents.

The studies summarised above highlight the controversy that exists in terms of the role (if any) of PARP-1 in the regulation of p53. However, if PARP-1 is ultimately found to modulate p53 activity, the next step will be to elucidate the precise mechanisms involved. To date, it has been shown that p53 can be poly(ADP-ribosyl)ated *in vitro* when p53 is incubated with purified PARP-1 (Wesierska-Gadek *et al.,* 1996b; Mendoza-Alvarez, 2001). The latter study also showed that this modification of p53 diminished the ability of p53 to bind to its DNA consensus sequence, as illustrated by gel-shift assays. The results of these studies should be interpreted with care, as activated PARP-1 may be able to target many proteins in cell-free systems, with accessibility to glutamic acid residues likely to be the limiting factor. In addition, cell free systems do not represent the normal physiological environment for proteins. For example, within cells p53 is able to bind DNA and Wesierska-Gadek *et al.,* 1996b demonstrated *in vitro* that p53 bound to DNA is not susceptible to poly(ADP-ribosyl)ation. Therefore, cell free reactions showing that p53 is a target for ADP-ribosylation do not necessarily mean this is true *in vivo*. Free ADP-ribose polymer has also been shown to physically interact with p53 (Malanga *et al.*, 1998). The binding was found to involve three domains of 23-26 amino acids on p53 and was subsequently shown to impair the ability of p53 to bind specific sequences of DNA. A

subsequent study has identified specific sequence motifs within ADP-ribose binding proteins (Pleschke *et al.*, 2000) by blotting particular sequences onto nylon membrane and incubating with purified radiolabelled polymer. Thorough washing followed by autoradiography revealed the ability of particular sequences to bind ADP-ribose polymer. Proteins found to possess such sequence motifs include p53, p21, Ku70 (part of DNA-PK) and XRCC1. A mechanism whereby ADP-ribose polymer is able to interact with components of DNA repair pathways may be consistent with the model of PARP-1 recruiting DNA damage response proteins to the site of the damage. For example, if PARP-1 were to bind a strand break and automodify itself, it is possible that the polymer produced is able to recruit other proteins to the site that are needed for efficient repair of the break.

In addition to p53 being subject to poly(ADP-ribosyl)ation, a physical interaction between PARP-1 and p53 has been demonstrated by co-immunoprecipitation. It should be noted, however, that this interaction may not be direct. Rather, PARP-1 and p53 may be part of a nuclear protein complex. It would be interesting to analyse the immunoprecipitation reactions for the presence of other proteins by gel electrophoresis followed by silver-staining. Wesierska-Gadek *et al.*, 2000 demonstrated co-immunoprecipitation of p53 with PARP-1 in cultured cells expressing wild type as well as mutant p53. Interestingly, using rat cells expressing the temperature sensitive mutant of p53 ($p53^{135Val}$), PARP-1 was sequestered in the cytoplasm at the restrictive temperature (37°C). It should be noted that at this temperature, the p53 is cytoplasmic. Therefore, the only way the normally nuclear PARP-1 could enter the cytoplasm is in a complex with p53. Transfer of the cells to 32°C (p53 should be nuclear at this temperature) results in both proteins accumulating in the nucleus. This finding is in accordance with Vaziri *et al.*, 1997, who showed binding of

PARP-1 to p53 *in vitro* and *in vivo*. This interaction was observed in cells treated with IR as well as untreated samples. It has also been suggested that PARP-1 may act to protect p53 from proteolytic degradation. This is based on the location of a putative poly(ADP-ribosyl)ation site near a proteolytic cleavage site on p53.

It is obvious that a lot more research needs to be performed investigating all aspects of the relationship of PARP-1 with p53. What will result is likely to be a complicated picture involving several aspects of the processes described above and likely several additional mechanisms.

### 1.4.7 The PARP family

The first intimation that more than one PARP protein existed came from studies showing that the PARP-1 knockout cells were still able to synthesise ADP-ribose polymer (Shieh *et al.*, 1998). Around the same time, studies analysing stress responses in plants led to the identification of a sequence, homologous to PARP-1, which has subsequently been described as PARP-2 (Babiychuk *et al.*, 1998, Berghammer *et al.*, 1999). A sequence corresponding to PARP-2 was also discovered in PARP-$1^{-/-}$ MEFs (Ame *et al.*, 1999). Further analysis by Ame and co-workers revealed that PARP-2 was a protein of 62kDa in mass, which possessed 60% homology to the C-terminal catalytic domain of PARP-1. Like PARP-1, this protein is able to bind and is activated by breaks in DNA strands. However, it should be noted that the DNA binding domain of PARP-2 is distinct from that of PARP-1. Therefore, the two enzymes may bind to different substrates and hence may have differing biological roles within cells. Despite this possibility, a recent study has implicated PARP-2 in the BER pathway (Schreiber *et al.*, 2002). This group showed that PARP-2 knockout MEFs are impaired in BER. This was exemplified *in vivo* using the

single cell gel electrophoresis assay (COMET assay) and treatment with MNU (an alkylating agent). A significant delay (2 hours) in rejoining of DNA strand breaks was observed in the PARP-2 knockout MEFs compared to their wild type counterparts. The same study was also able to demonstrate binding of PARP-2 to XRCC1 and PARP-1 suggesting that PARP-2 may have a role in BER as part of a multi-protein complex.

In addition to PARP-2, six other PARP family members have now been described, all of which contain sequence homology to the catalytic domain of PARP-1 (which is now described as the PARP signature sequence). Included in this family of PARP proteins is tankyrase (PARP-5), which is localised at telomeres and has been shown to synthesise ADP-ribose polymer (Smith *et al.,* 1998). It is believed that tankyrase may play a role in preserving the length of telomeric DNA. Also, a PARP protein was discovered as a component of the vault complex (Kickhoefer *et al.,* 1999), a ribonucleotide assembly that is ubiquitously expressed in eukaryotes. The vault complex forms a barrel-like structure and has been implicated in cellular transport. It has been shown that other components of this complex can be ADP-ribosylated by Vault-PARP (Kickhoefer *et al.,* 1999). It is possible that this modification alters the conformation of the vault complex such that transport capabilities are altered. Further analysis is needed of the other PARP family members before their functions are elucidated.

The identification of several proteins capable of poly(ADP-ribosyl)ation has perhaps complicated the interpretation of previous studies analysing the effect of poly(ADP-ribosyl)ation on various cellular functions. Previous studies have assigned any effect observed to the activity of PARP-1, however, it is now clear that some of these effects may be due to the activity of alternative PARP proteins. It will therefore be necessary to dissect

the role of the individual PARPs by knocking out the particular gene or by the development of inhibition strategies which specifically target specific PARP proteins.

## 1.5 Aims of this study

This introductory chapter has aimed to highlight the importance of p53 in the regulation of cellular functions in response to DNA damage. Having established the importance of these functions, it was necessary to summarise the data regarding the regulation and activation of this protein. Studies have been summarised demonstrating the role of Mdm2, phosphorylation and acetylation in the overall regulation of p53 function. The latter sections have addressed the potential role of PARP-1 in the DNA damage-induced activation of p53. Data has been described highlighting the controversial nature of this particular area of research.

**The principal aim of this study was to investigate the hypothesis that PARP-1 functions as an upstream regulator of p53 function. The methods used to address this hypothesis were two-fold.**

- Mouse embryonic fibroblasts disrupted in exon 4 of the PARP-1 locus were used along with their wild-type counterparts to analyse the requirement for PARP-1 protein on p53 activation

- A novel potent PARP-1 inhibitor (AG14361), developed in a collaboration between Pfizer GRD and the Drug Development Group of the Cancer Research Unit in Newcastle was used to inhibit PARP-1 activity in PARP-1 proficient MEFs and human cell lines to analyse the effect of blocking PARP-1 activity on the

ability of DNA damage to activate p53. In addition, a human tumour colorectal cell line with wt p53 was used to study the effects of the PARP-1 inhibitor

It should be noted that the use of PARP-1 knockout cells and a PARP-1 inhibitor represent very different strategies for the removal of PARP-1 activity from cells. For example, when using inhibitors, PARP-1 protein is still present and is therefore still able to bind to DNA strand breaks. However, this binding is likely to become irreversible as the catalytic function and hence the automodification and ensuing dissociation from DNA of PARP-1 is prevented. Therefore the strand breaks produced by DNA damage are likely to be 'protected' by PARP-1 and may conceal the breaks from other DNA damage-responsive proteins, such as ATM. This effect in itself may modulate 'normal' p53 activity. In contrast the PARP-$1^{-/-}$ MEFs do not possess any PARP-1 protein, therefore the strand breaks should be 'visible' to other proteins.

During the course of this study, a second hypothesis was formulated and tested. This was based on the observation that two independently derived immortalised clones of PARP-$1^{+/+}$ MEFs possessed p53 mutations. However, the PARP-$1^{-/-}$ MEFs were found to express wild type p53.

**It was therefore hypothesised that the absence of PARP-1 bypassed the requirement for MEFs to mutate p53 during immortalisation.**

- This hypothesis was tested by growth selection for spontaneously transformed independent colonies of primary PARP-1 MEFs and analysing the p53 status of the cells after immortalisation.

- During the course of these experiments, cumulative growth curves were plotted for each of the primary PARP-1 MEF colonies, leading to several observations regarding the growth rate of these cells and the consequences for DNA-damage induction of p53.

# CHAPTER 2

# MATERIALS AND METHODS

## 2.1 Tissue culture

### 2.1.1 Cell lines

Mouse embryonic fibroblasts (MEFs) were cultured from the embryos of mice kindly provided by Gilbert de Murcia (Ecole Superieure de Biotechnologie de Strasbourg). The MEFs were of a PARP-1 wild-type genotype (PARP-$1^{+/+}$) or a PARP-1 knockout genotype (PARP-$1^{-/-}$). The knockout MEFs were produced by the insertion of a targeting vector into embryonic stem cells. This targeting vector resulted in the insertion of a neomycin resistance cassette into exon 4 of the PARP-1 gene *via* homologous recombination (de Murcia *et al.*, 1997). These stem cells were then microinjected into blastocysts, giving rise to chimaeric offspring. These mice were then bred to produce mice homozygous for the disruption of the PARP-1 gene. Disruption of the PARP-1 gene, lack of PARP-1 expression and lack of PARP-1 activity have all been confirmed in these cells (de Murcia *et al.*, 1997).

During this study, both primary and immortalized MEFs were used. Primary cells are produced by the homogenisation of embryos and the derived cells are not grown beyond passage 5. Primary cells will eventually reach a stage where they cease growing, called senescence (reviewed in Itahana *et al.*, 2001). In time, a population of immortalized cells will begin to grow from these cells, presumably by mutation of a gene controlling cellular growth or cell cycle arrest. Typically, immortalized cells show an increased growth rate and also have an infinite lifespan compared to primary cells.

A further cell line used was HCT-116, a human colorectal tumour cell line. Previous studies within the department have shown that these cells have wild-type p53

characteristics, with an induction of p53 protein in response to DNA damage. In addition, the p53 is transcriptionally active, with induction of p53 target genes such as mdm2 and $p21^{waf-1}$ also being observed (results within this thesis; also confirmed by Farnie, G, PhD thesis, Cancer Research Unit, University of Newcastle upon Tyne). In addition to the wild-type HCT-116 cells, a 'degraded p53' cell line has also been used for the validation of p53-responsive techniques (Section 2.7). These cells are called HCT-116 N7 and are stably transfected with a plasmid containing the human papilloma virus (HPV) E6 protein, which targets p53 for degradation, and hence these cells express only very low levels of p53.

Some experiments have also been performed on a human ovarian carcinoma cell line, A2780. Like the HCT-116 cells, they show wild type p53 activity and were used in repeats of the experiments mentioned above with the aim of eliminating any possible cell-line specific observations.

### 2.1.2 Growth conditions

Mouse embryo fibroblasts were grown in high glucose Dulbecco's Minimum Essential Medium (DMEM) supplemented with 10% (v/v) foetal bovine serum (FBS) and 0.01% (w/v) penicillin/streptomycin. The human cell lines used (HCT-116, HCT-116 N7 and A2780) were grown in RPMI 1640 medium supplemented with the same concentrations of FBS and antibiotics. All culture medium, antibiotics and FBS were obtained from Gibco-BRL, Paisley, UK. All cells were maintained at 37°C in a humidified atmosphere containing 5% carbon dioxide. Cell lines were routinely grown in 15cm tissue culture plates (Nunc, Illinois, USA) until 70-80% confluent before being sub-cultured (passaged).

### 2.1.3 Sub-culturing of cells

To passage adherent cells, the medium was aspirated from the plate and the cells rinsed in phosphate buffered saline (PBS). 3ml of 0.25% (w/v) trypsin in PBS.EDTA (0.02% w/v EDTA) was added to the cells until they had lifted from the plate and the resultant suspension added to an equal volume of medium. Where necessary, to prevent clumping of the cells, the suspension was passed through a 19-gauge needle. Cells were then counted using a haemocytometer and an appropriate number plated out for specific experiments or placed back into 15cm tissue culture plates as routine subculture.

### 2.1.4 Mycoplasma testing

Cells were routinely tested for mycoplasma infection (once a month) according to DelGiudice and Happs, 1978

### 2.1.5 Drug preparation and storage

A variety of drugs were used in DNA damage experiments (see Section 2.1.6). The PARP-1 inhibitor (AG14361, produced in a collaboration between the Cancer Research Unit and Pfizer GRD) was made up as a 10mM stock in 100% DMSO (Sigma, Poole, UK). This was then diluted 1:10 in PBS before being frozen in 100µl aliquots at –20°C.

Temozolomide (a gift from Professor MGF Stevens, Cancer Research Laboratories, University of Nottingham, UK) was prepared as a 200mM stock in 100% DMSO and frozen in aliquots of 500µl at –20°C.

### 2.1.6 DNA damage experiments

Cells to be analysed by Western blotting were plated out in 5cm tissue culture plates. Cells were prepared according to the protocol above (Section 2.1.3) before addition of $5 \times 10^5$ cells to each plate. Six plates were required for each treatment, corresponding to time points of Untreated, 1h, 2h, 3h, 6h and 24h. The cells were grown at 37°C for 24 hours before treatment with the relevant DNA damaging agent. When using the PARP-1 inhibitor, AG14361, it was added to the cells 15mins prior to DNA damage treatment. For a plate containing 5ml of medium, 5µl of a 1mM AG14361 (in 10% DMSO; Sigma, Poole, UK) stock was added, to give a final concentration of 1µM AG14361 and 0.01% DMSO. The 1mM stock was dissolved in 10% DMSO, therefore control (untreated) cells were treated with 5µl of 10% DMSO as 'solvent controls'. Cells were treated with three types of DNA damaging agents. IR was administered at three doses; 2, 5 and 10Gy (using a Gamma Cell 1000 Elite, dose rate 3.64Gy/min). Alternatively, cells were treated with a dose of UV radiation; 20, 50 or $100J/m^2$ using a UV Stratalink machine (Stratalink, La Jolla, USA). Finally, cells were treated with the alkylating agent, temozolomide at three different concentrations; 0.25, 0.5 or 1mM temozolomide. Samples for the relevant time points were taken and processed according to Section 2.5.2.

DNA damage experiments were also performed on cells to be analysed by a luciferase assay, which will be discussed in Section 2.7

### 2.1.7 SulfurRhodamine B assay (SRB)

SRB assays (Skehan *et al.*, 1990) are used to estimate the growth of cells. The principle involves the growth of cells over time followed by the fixing of cells with 50% (w/v)

trichloroacetic acid (TCA) (Sigma, Poole, UK) at various time points. The cells can then be stained with SRB, a bright pink aminoxanthene dye, which stains total protein. SRB contains two sulfonic groups that bind amino acids under mildly acidic conditions. Therefore, the more cells present, the more protein and hence the more intense the staining effect. Excess stain is removed before solubilising the bound stain in relevant buffer. This results in the production of a purple solution, the optical density of which can be measured and is proportional to the number of cells originally present in the wells. This technique is commonly used to derive growth curves for cell lines and also to demonstrate any growth inhibitory effect of any treatments (e.g. drugs) being used.

### 2.1.8 Growth curves

The basic method involved plating cells into 96-well tissue culture plates (Nunc, Illinois, USA) at a variety of cellular concentrations (ranging from $0.625 \times 10^4$ cells/ml – $2 \times 10^5$ cells/ml). For growth curves ten wells were used for each cellular concentration. Therefore one plate was set up, with six different cellular densities, for each time point. The outer wells of the plate were not used for growing cells, instead they contain 100µl of medium to minimise any 'edge effect'. For growth curves the cells were grown over the course of a week and one plate of cells fixed by the addition of 25µl 50% TCA every 24h. These plates were stored at 4°C for at least 24h before rinsing several times with distilled $H_2O$. After the plates had dried, 100µl of 0.4% (w/v) SRB (in 1% acetic acid) (Sigma, Poole, UK) was added to each well for 30mins. Excess stain was removed by washing with 1% acetic acid (BDH, Poole, UK). Again the plates were allowed to dry before solubilising the bound stain in 100µl of 10mM Tris.HCl, (pH 10.5) (Sigma, Poole, UK) for 30 minutes on a plate shaker. Each plate was then analysed on a plate reader where the absorbance of each well is read at 540nm. The data is then analysed using computer

software (Microsoft Excel) and the data plotted with absorbance against time of growth. The mean of the ten replicates of a particular cell density was calculated along with the standard error for that set of data. This process is repeated for all cell densities at all time points and the data plotted in the form of a line graph to generate growth curves.

### 2.1.9 Growth inhibition assays

Growth inhibition assays were performed to show that the concentration of AG14361 used in DNA damage experiments did not inhibit cellular growth during the time course of experiments. Like growth curves, the assay was set up by plating cells into 96-well tissue culture plates. However, cells were plated out at only one concentration. The effects of drugs on growth inhibition were analysed over 72hrs. Therefore cells were plated out at a density such that they will be growing exponentially during this time. This optimum density was estimated from the growth curves previously derived for each cell line and was found to be $2 \times 10^4$/ml. Cells (90µl) were left overnight to adhere to the plates before addition of 10µl of AG14361 at final concentrations of 0.1, 1, 10 or 100µM. Each dilution was prepared by diluting a 10mM stock of AG14361 (in 100% DMSO) with culture medium. AG14361 was diluted 1:10 upon addition to the well, therefore, concentrations of 1, 10, 100 and 1000µM were prepared. The DMSO content was adjusted during dilution such that the two lower AG14361 concentrations contained 0.1% DMSO whereas the two higher AG14361 concentrations contained 10% DMSO. Upon addition to the well, the final DMSO concentration will be either 0.01% or 1%, depending upon the concentration of AG14361. Therefore, solvent controls were also included on each plate consisting of cells grown in 0.01% or 1% DMSO. Five replicates of each AG14361 concentration (or solvent control) were set up on each plate. Plates were then processed according to the

SRB assay protocol at 24, 48 and 72h. The data was analysed using Microsoft Excel software and the results plotted on graphs (see Section 2.1.7).

### 2.1.10 Immortalization of mouse embryonic fibroblasts

During cell culture primary MEFs grow at a constant growth rate. After a certain number of cellular divisions (typically between 15 and 25), the growth rate of the cells slows dramatically. At this stage, the cells adhere to the tissue culture plates but have withdrawn from the cell cycle. Cells are said to have reached senescence. Eventually, a sub-population of cells begins to exit the senescent phase and begin to grow rapidly (Todaro and Green, 1963). A common feature of such cells is the mutation of the tumour suppressor, p53, which confers immortality on the outgrowing population.

MEFs were derived from homogenised day 13.5 embryos. These cells were then grown according to the 3T3 protocol (Todaro and Green, 1963). Briefly, 1 x $10^6$ cells were placed into a 10cm tissue culture plate. The cells were grown according to Section 2.1.2 for 3 days, before the cells were trypsinised, counted and 1 x $10^6$ cells plated into a fresh 10cm plate. The aim of the experiment was to investigate the p53 status of immortalized PARP-$1^{+/+}$ and PARP-$1^{-/-}$ MEFs, or more specifically to investigate the hypothesis that mutation of p53 during immortalisation is affected by PARP-1. This hypothesis was based on data described in Section 4.2. For such a study it is necessary to derive several independent colonies of immortalised PARP-$1^{+/+}$ and PARP-$1^{-/-}$ and to analyse the p53 status of these colonies. Therefore, 5 plates of primary PARP-$1^{+/+}$ and 5 plates of primary PARP-$1^{-/-}$ MEFs were grown. In addition 5 further plates of PARP-$1^{+/+}$ MEFs were grown in medium containing 1μM AG14361. It was important to treat each plate as an individual

population of cells such that cross contamination did not occur. The cells were grown, with routine sub-culturing until they reached the senescent phase. At this stage, the plates were analysed by microscopic inspection for the presence of transformed cells (evident in the form of dense colonies of smaller cells) and the medium changed every three days. If transformed areas were present, the plate was trypsinised and the cells re-plated into a fresh 10cm plate, to allow the outgrowth of spontaneously transformed (immortalised) MEFs.

The cells were counted every three days (as or when sub-cultured) and this data was subsequently used to produce cumulative growth curves. This involves sequential addition of the individual cell counts to provide a total cell number produced from the original 1 x $10^6$ cells.

### 2.1.11 Stable transfection

A plasmid containing the cDNA for human PARP-1 (see Chapter 4 for details) was stably transfected into an immortalised PARP-$1^{-/-}$ MEF cell line. The principle of stable transfection is the initial introduction of the plasmid into cells followed by the integration of the plasmid into the host genome *via* recombination. In theory, the integrated DNA will remain as part of the host genome and will therefore be passed on to daughter cells during cellular replication. Ideally, the plasmid to be transfected into cells should contain a selectable marker, as well as the PARP-1 sequence. For example, if the plasmid also contained an antibiotic resistance gene, then after transfection the cells should be grown in medium supplemented with the relevant antibiotic. This would allow only antibiotic-resistant cells to grow and hence only cells that have taken up the plasmid. The plasmid

used in this study did not contain an antibiotic resistance gene therefore cells were co-transfected with a second plasmid, pCR3, which contained a neomycin resistance gene. However, it had been overlooked that the PARP-1 knockout MEFs already possessed resistance to this antibiotic (see Chapter 4, Section 4.2.4), which was the probable reason for only one colony of stably transfected cells being isolated.

#### 2.1.11.1 Optimisation of transfection

The optimisation involved altering the ratio of volume of transfection reagent (FuGENE 6, Roche, Basel, Switzerland) to mass of plasmid DNA such that maximum expression of the plasmid was achieved. Three different ratios were tried, 3:2 (µl of FuGENE 6:µg of DNA), 3:1 and 6:1. Immortalised PARP-$1^{-/-}$ MEFs were plated into six 35mm tissue culture plates at 1.5 x $10^5$ cells and incubated at 37°C for 24 hours. The cells were then transfected with both the PARP-1 plasmid (pPARP32; a gift from Alexander Burkle, Dept of Gerontology, Newcastle General Hospital) and the antibiotic resistance plasmid (pCR3, neomycin resistance gene). A transfection mix (3:2 ratio) was prepared by adding 3µl of FuGENE 6 to 100µl of serum free DMEM. After 5 minutes, 1µg of PARP-1 plasmid and 1µg of pCR3 were added. This mixture was incubated for at least 15 minutes before adding to one of the plates. Other transfection mixes were prepared corresponding to ratios of 3:1 and 6:1 and added to two other plates of cells. Three blanks were also prepared, corresponding to the pPARP32 plasmid without PARP-1. All plates were incubated at 37°C for 24 hours before lysing the cells in sodium dodecyl sulphate (SDS) lysis buffer (see Section 2.5.2). Protein assays were performed on each of the samples and 50µg ran on a polyacrylamide gel before Western blotting and subsequent probing of the membrane with an anti-PARP-1 antibody (Section 2.5). PARP-1 expression was found to be highest in the 3:2 ratio sample.

### 2.1.11.2 Stable transfection of PARP-1$^{-/-}$ MEFs

PARP-1$^{-/-}$ MEFs were plated out and transfected according to Section 2.1.10.1 with a 3:2 ratio of transfection reagent:plasmid DNA. However, after 24 hours incubation with transfection reagent, the cells were trypsinised and counted. Cell numbers ranging from 100 to 100000 were then plated out into 15cm tissue culture plates. The aim is to separate cells sufficiently such that they can adhere to the plate as a single cell and begin to form a homogenous colony of cells without being contaminated by other cells added to the plate. It took approximately 10-14 days for distinct colonies to become visible on the plates. Colonies were then isolated using sterile cloning rings (Sigma, Poole, UK). Briefly, the medium was aspirated from the plate and the cells rinsed in PBS. The edge of a cloning ring was then coated with sterile petroleum jelly and the ring carefully placed over the colony. Sufficient pressure was applied such that the petroleum jelly formed an airtight seal between the base of the cloning ring and the tissue culture plate. 100µl of trypsin was then added to the colony and left for 5 to 10 minutes. After the cells had lifted from the surface of the plate (this was checked microscopically), they were added to 500µl of medium in the well of a 24-well tissue culture plate. Each isolated colony was then observed daily and when sufficiently grown, split into two 35mm tissue culture plates. One plate was used for Western blot analysis for PARP-1 expression and the other was allowed to continue growing. Colonies that turned out to be negative for PARP-1 expression were discarded. The one positive colony that was isolated was bulked up and due to the problem of lack of antibiotic selection, mentioned earlier, was re-plated out for colonies. This was to ensure that the isolated colony was a homogenous population of cells. Ten colonies were analysed for PARP-1 expression, all of which were positive. The stable transfectant was then bulked up further and aliquots frozen in liquid nitrogen.

## 2.2 Nucleic acid extraction

### 2.2.1 Preparation of plasmid DNA

#### 2.2.1.1 Transformation of E.coli cells with plasmid DNA

Ready-competent E.coli strain JM109 cells (Promega, Madison, USA) were defrosted on ice before separating into 50µl aliquots. 2µl of plasmid DNA was added to the cells and the mixture left on ice for 20 minutes (all plasmids prepared contained an ampicillin resistance gene). The cells were then heat-shocked for 45-50 seconds at 42°C before being placed back on ice for 2 minutes. 950µl of SOC medium (2% tryptone-B, 0.5% yeast extract B, 0.05% NaCl, 0.5% $MgSO_4.7H_2O$ supplemented with 20mM glucose) was added. The mixture was then incubated for 90 minutes at 37°C in a rotary incubator at 150rpm. Finally, volumes ranging from 1-20µl of this mixture were streaked for single colonies onto agar plates and the plates incubated overnight at 37°C. The agar plates contained 10% tryptone (w/v), 10% sodium chloride (w/v), 5% yeast extract (w/v) and 1.5% agar (w/v). The agar was sterilised by autoclaving before the addition of 50µg/ml ampicillin and pouring into petri dishes. Any ampicillin resistant colonies that had grown should possess the desired plasmid. Therefore, a colony was picked and grown up in 5ml of LB supplemented with ampicillin at 37°C overnight. Plasmid DNA was then extracted from this sample using a Wizard™ mini-prep kit (Qiagen, Crawley, UK).

#### 2.2.1.2 Plasmid DNA preparation

Miniprep kits have been designed for efficient purification of plasmid DNA from bacterial cultures. The basis of the kit used in this study (Wizard kit, Qiagen, Crawley, UK) is the alkaline lysis of bacteria followed by purification of DNA *via* binding to silica membranes

and subsequent elution of the DNA into buffer. Bacterial cells are lysed in a solution containing SDS, which solubilises phospholipids and proteins hence causing lysis of the cellular membrane. In addition, the solution contains sodium hydroxide, which denatures both chromosomal and plasmid DNA. The smaller, less complex plasmid DNA is solubilised first. The incubation time is optimised for the solubilisation of plasmid DNA alone, before addition of a buffer containing guanidium chloride (a chaotropic salt) and acetic acid. The acetic acid neutralizes the sodium hydroxide thus bringing about a rapid change in pH. This pH change in turn causes precipitation of SDS in solid complexes with chromosomal DNA, proteins and cell debris. The solid material is removed *via* centrifugation, with the resultant supernatant containing the plasmid DNA. This supernatant is then applied to a silica membrane within a spin-column (supplied within the Wizard kit). DNA binds to silica in high concentrations of chaotropic salt (in this case guanidium chloride), possibly through the formation of cation bridges with the negatively charged silica. Upon centrifugation, the plasmid DNA binds strongly to the silica and hence is purified from solution. The plasmid DNA can then be solubilised by simply passing distilled water across the membrane, thus reducing the salt concentration and hence the plasmid DNA is eluted.

Plasmid DNA was extracted using the Wizard *plus SV* kit according to the manufacturer's instructions (Qiagen Plasmid Purification Handbook). Larger stocks of plasmid were produced by growing up larger quantities of transformed bacteria followed by the use of a Mega-prep kit (Qiagen, Crawley, UK), which was used according to the manufacturers protocol.

The plasmid was then restriction digested with an appropriate enzyme to demonstrate isolation of a DNA fragment corresponding to the relevant insert (Section 2.4.1.1). In certain circumstances it is the excised fragment that is required, therefore this fragment must be purified by separating it from the remainder of the original plasmid present in the sample. This is achieved by separation of the different sized DNA fragments using agarose gel electrophoresis (Section 2.3) and subsequent purification of the relevant fragment from the agarose gel.

### 2.2.1.3 Purification of DNA fragments from agarose gel

As described above, DNA fragments are separated using agarose gel electrophoresis. The fragments can then be visualised under UV light and the relevant band excised using a sharp, clean scalpel. As much of the excess agarose is removed as is possible without losing any of the DNA fragment. Any area that is not fluorescent under UV light does not contain any DNA and hence can be removed. The DNA fragment is then purified from the residual agarose using a gel extraction kit from Qiagen (QIAquick$^{TM}$). This kit relies upon the adsorption of DNA to a silica membrane (in a spin column) in the presence of high salt. Upon centrifugation of the column, the relevant buffer washes any contaminant through the membrane with the DNA remaining attached. The DNA can then be eluted from the column into distilled $H_2O$.

## 2.2.2 Extraction of genomic DNA from cell pellets

Isolation of cellular DNA initially requires lysis of cells, usually in a buffer containing a detergent, such as SDS, NP-40 or Triton X-100. In addition, it is important that the DNA isolated does not contain protein contamination. Therefore, the lysis buffer is

supplemented with proteinase K. Further removal of contaminants is achieved by chloroform extraction and subsequent precipitation of the DNA from the aqueous phase using isopropanol.

PARP-$1^{+/+}$ and PARP-$1^{-/-}$ MEFs were grown in 15cm tissue culture dishes until 80% confluent. Cells were trypsinised and 1 x $10^7$ cells spun down for 5 minutes at 1000 rpm before rinsing in PBS. Cells were then again spun down and resuspended in 5ml of reagent B (see appendix A) containing 50µl of proteinase K (final concentration of 10µg/ml) in a 50ml Falcon tube. The pellets were homogenised by pipetting and the samples placed in a rotary incubator overnight at 37°C.

The next day the sample was examined to ensure complete homogenisation before addition of 1250µl of sodium perchlorate. The samples were placed on a multi-tube roller at room temperature for 15 minutes before being transferred to a 65°C waterbath for 30 minutes. An equal volume of chloroform (6.25ml, BDH, Poole, UK) was then added and the samples mixed for 25 minutes at room temperature. Each sample was then centrifuged at 2500rpm (Mistral 2000i) for 15 mins. The upper aqueous phase of each sample was then transferred to a fresh Falcon tube containing an equal volume of isopropanol (BDH, Poole, UK). Repeated inversion of the tubes should result in the precipitation of the DNA in the form of fine white threads. The DNA was spun down at 2500rpm (Mistral 2000i) for 5 minutes and washed twice with 75% ethanol (BDH, Poole, UK). Excess ethanol was then removed and the pellet allowed to air dry for approximately one hour. Finally, the pellet was dissolved in 200 - 800µl of distilled $H_2O$, depending upon the size of the pellet. It should be noted that when using the DNA in applications involving restriction enzyme

digestion, it is best to avoid dissolving the DNA in 1 x Tris-EDTA as the EDTA may interfere with the efficiency of the restriction enzyme.

### 2.2.3 Extraction of cellular RNA

The major consideration when producing or working with RNA is the elimination of ribonucleases (Rnases) that will readily degrade the isolated RNA. It is therefore necessary to wash any equipment with Rnaseaway$^{TM}$ (Qiagen, Crawley, UK) before use and to bake any glassware used at 200°C for three or four hours. Both of these methods are effective at inactivating Rnases. RNA was produced using the Rneasy mini kit (Qiagen, Crawley, UK). This technique combines the selective binding properties of silica-gel membranes with the speed of microspin technology. Basically, the buffer system used is high salt and allows the selective binding of RNA longer than 200 bases to the silica gel membrane. Biological samples are initially lysed in a highly denaturing guanidine isothiocyanate-containing buffer, which immediately inactivates Rnases and hence ensures isolation of intact RNA. Addition of ethanol provides appropriate binding conditions before addition of the sample to an Rneasy mini spin column. Total RNA binds to the membrane, with subsequent washing steps removing any contaminants. The final step is the elution of the RNA from the membrane *via* the addition of Rnase free water.

Cells were grown in 15cm tissue culture plates before being trypsinised and counted. 1 x $10^7$ cells were then spun down (1000rpm for 5 mins) and rinsed in PBS. The supernatant was carefully aspirated. Incomplete removal of the supernatant may interfere with the subsequent lysis step and also dilute the sample, which may alter the optimum conditions

for binding of RNA to the Rneasy membrane. RNA was then isolated from the cell pellet according to the manufacturers protocol (Qiagen, RNeasy® mini handbook).

### 2.2.3.1 Assessment of RNA integrity

The quality of the isolated RNA was assessed by electrophoretic analysis of the RNA sample. 2μg of RNA (estimated by spectrophotometric analysis, see section 2.2.4) was made up to 10μl in distilled $H_2O$ before addition of 3μl of loading buffer (see appendix A). This sample was then analysed on a 1.2% agarose gel containing 0.25μg/ml of ethidium bromide (Sigma, Poole, UK) at 50V for 2 hours. The RNA was then visualised under UV illumination and photographed. Two bands should be clearly visible, one at 5kb and the other at 1.9kb. These correspond to the 28S rRNA and the 18S rRNA, respectively. In addition, the upper band should be approximately 2.5 times more intense than the lower band for good quality RNA.

## 2.2.4 Estimation of nucleic acid concentration and purity

The concentration and purity of nucleic acids is estimated by measuring the optical density at two wavelengths, 260 and 280nm using a spectrophotometer. The spectrophotometer is corrected to zero at each wavelength by measuring the absorbance of a 'blank', for example 500μl of distilled $H_2O$. The nucleic acid samples to be analysed were diluted 1:100 in distilled $H_2O$ by adding 5μl of sample to 495μl of water. This solution was mixed before being placed in a quartz cuvette for optical density analysis. The reading at 260nm provides the concentration of nucleic acid. An OD of 1 at 260nm corresponds to a concentration of 50μg/ml for double stranded DNA, 40μg/ml of single stranded DNA or RNA and approximately 30μg/ml of single stranded oligonucleotide. The ratio of the

readings at 260 and 280nm provide an indication of the purity of the nucleic acid. For DNA, $OD_{260nm}/OD_{280nm}$ should be 1.8. For pure RNA the ratio should be 2.0.

### 2.2.5 Nucleic acid storage

Once isolated, cellular DNA and plasmid DNA are stable and were stored at 4°C or –20°C. However, RNA is less stable than DNA and, as such was stored at –80°C.

## 2.3 Agarose gel electrophoresis

This technique is used to separate nucleic acids based upon their size. The gel itself consists of a matrix of polysaccharide molecules through which the nucleic acids are able to migrate. Therefore, it is the size of the nucleic acids that dictates how fast they can move through the matrix of the gel, with smaller nucleic acids able to migrate faster. The application of an electric current to the gel and subsequent movement of the negatively charged nucleic acids towards a positive electrode brings about the migration. The agarose content of gels can be varied depending upon the sizes of the nucleic acids being analysed. For instance, when analysing small molecules, the agarose content is increased which in turn leads to decreased pore size within the gel. Addition of ethidium bromide to both the gel and the running buffer allows visualisation of the DNA as ethidium bromide intercalates DNA and fluoresces when exposed to UV light.

The agarose gel is prepared by dissolving the required amount of agarose in tris-borate EDTA (TBE) buffer (see appendix A). The size of fragments being detected in this study required the preparation of a 0.8% gel (therefore 0.8g of agarose was dissolved in 100ml of TBE). It was necessary to boil the mixture to allow efficient solubilisation of the agarose.

This was achieved by gently heating the buffer in a conical flask in a microwave oven. The gel was allowed to cool to approximately $50^0$C before addition of ethidium bromide (0.1μg/ml final concentration). The gel was poured into a gel-casting tray and allowed to solidify.

Samples were prepared *via* the addition of one fifth loading buffer (see appendix A) before loading into the wells of the gel. Also included on the gel was a standard molecular weight marker (1kb marker, Gibco-BRL, Paisley, UK) to provide an indication of the size of fragments in the gel. The running buffer for the gel consisted of 1 litre of TBE containing ethidium bromide at a final concentration of 0.1μg/ml. The gel was run at 80V for approximately five hours, or until the bromophenol blue had migrated near to the edge of the gel. Gels were visualized under UV light and photographed using a BioVision gel imaging system, which also allowed digital storage of images.

## 2.4 Southern blotting

Southern blotting (Southern, 1975) is a technique used to detect a specific fragment of DNA within a sample containing entire genomic DNA, rather like finding a needle in a haystack. The technique involves the purification of genomic DNA before digesting the DNA with a specific restriction endonuclease. This will result in a mixture of fragments of DNA of a variety of sizes, which can then be separated by running the DNA through an agarose gel. The DNA is then denatured to form single-stranded DNA by soaking the gel in sodium hydroxide before transfer of the DNA to a nylon membrane. This allows efficient binding of the probe to target sequences. The exact positions of the DNA in the gel are preserved upon transfer to the membrane. To detect the DNA fragment of interest,

a single stranded oligonucleotide is produced that is complimentary to the sequence of interest. This oligonucleotide is then radiolabelled with $^{32}P$ and allowed to hybridise with homologous sequences on the membrane. Probe bound non-specifically to the membrane is removed in several washing steps before visualisation of the membrane using phosphorimagery.

This technique can be used to analyse the copy numbers of particular genes, for example, the amplification of a gene called MycN in neuroblastoma. Alternatively, Southern blotting can be used as a molecular biology tool to confirm disruption of a particular gene. For example, Southern blotting has been used in this study to confirm disruption of the PARP-1 gene *via* insertion of a neomycin resistant cassette into exon 4 of the PARP-1 locus. This results in the insertion of an extra *Eco*R1 site, which produces a smaller fragment of DNA upon *Eco*RI digestion. Therefore Southern blotting should result in the probe detecting different sized bands in the PARP-1 wild type and knockout MEFs (see Chapter 3, Section 3.2.3).

### 2.4.1 Preparation of probe for Southern blotting

The probe for PARP-1 has been inserted into a BlueScript plasmid. The plasmid was prepared and purifed according to section 2.2.1. In order to prepare the probe for Southern blotting, it is necessary to excise the relevant fragment of DNA using restriction enzyme digestion.

#### 2.4.1.1 Restriction endonuclease digestion

Restriction endonucleases are naturally occurring enzymes, present in bacteria and act to protect the bacterium from phage infection. The basis of this defence mechanism is the

ability of the endonucleases to recognise specific sequences of phage DNA, normally between 4 and 8bp long, and to cut the DNA at this site. Restriction endonucleases have been purified from bacteria and are now commonly used as molecular biology tools within the laboratory. For example, it is possible to manipulate DNA by removing a sequence using, for example *Eco*R1. A different sequence, also isolated using *Eco*R1 may then be inserted into this site, with the process being aided by the complementary ends of DNA left by the endonuclease. This is the basis for the cloning of different genes into the multiple cloning sites of expression vectors.

The plasmid containing the PARP-1 probe was prepared and purified. The restriction digestion was performed in a final volume of 40µl, consisting of 27µl of distilled water, 2µl of 10x *Eco*R1 reaction buffer, 2µl of *Eco*R1 (20U), 2µl of *Xba*1 (20U), 2µl of *Xba*1 reaction buffer and 5µl (20µg) of DNA (all restriction enzymes and buffers were from GibcoBRL, Paisley, UK). The reaction components were thoroughly mixed before collection *via* brief centrifugation. The reactions were incubated in 1.5ml Eppendorf tubes overnight at 37°C. The efficiency of the reaction was then checked by running 1µl of the reaction mix on a 0.8% agarose gel. The 1µl sample was added to 9µl of loading buffer (see appendix A) before analysis by gel electrophoresis. For each restriction digest sample, an uncut sample of plasmid DNA was included on the gel. The migration of the bands in each sample was compared to a molecular weight marker, also included on the gel. This allows confirmation that the size of the excised band and hence the probe to be used for Southern blotting was of the correct size (0.8kb). A clear shift should be apparent between the uncut plasmid DNA and the digested sample. The 0.8kb fragment was excised and purified according to Section 2.2.1.3

### 2.4.1.2 Radiolabelling of probe

Radiolabelling of the PARP-1 probe is essential for the final detection step involved in Southern blotting. The method used is based on a random primer extension DNA synthesis (Feinberg and Vogelstein, 1983). The reaction mixture contains dNTP without dATP, [$\alpha^{32}$P]-dATP (Amersham, Buckinghamshire, UK), probe DNA and the Klenow fragment of DNA polymerase-1 (GibcoBRL, Paisley, UK). During the ensuing reaction, the polymerase will synthesise new probe DNA, incorporating radiolabelled dATP into the probe sequence.

Approximately 10ng of PARP-1 probe was added to distilled water such that the final volume was 30µl. The mixture was heated to 100°C for 5 mins to denature the DNA. After cooling, 10µl of reaction mixture (containing all dNTPs except dATP, see appendix A), 1µl of bovine serum albumin (BSA, from 2mg/ml stock) (Sigma, Poole, UK) and 1µl of Klenow fragment (10 units, GibcoBRL, Paisley, UK) were added. After thorough mixing, the mixture was centrifuged briefly before finally adding 5µl [$\alpha^{32}$P]-dATP and incubating overnight at room temperature in a lead-lined container.

### 2.4.1.3 Purification of labelled probe

As well as containing labelled probe, the mixture will contain other fragments of radiolabelled DNA and free nucleotides. It is therefore necessary to purify the probe by passing the mixture down a Nick™ column containing Sephadex SG50 (Pharmacia). This technique uses size exclusion chromatography to separate fragments of DNA based upon their size. When the mixture is placed on the column, the larger fragments of DNA are eluted first followed by smaller fragments and free nucleotides.

Before adding the probe mixture, the column was washed with 5ml of 1 x TE (see appendix A) to equilibrate the column. The probe mixture was then added directly to the column before adding 200µl of 1 x TE. The eluant was collected in a 1.5ml eppendorf. Subsequent volumes of 200µl 1 x TE were added to the column and the eluant collected each time. This procedure was normally repeated 10 times such that the end result was ten different tubes containing different fractions from the column. A 2µl sample from each tube was then placed in a fresh eppendorf and subjected to scintillation counting (Wallac 1410, Pharmacia). This provides a measurement of the radioactive counts in each sample. The size of the PARP-1 probe is such that it usually eluted in fractions 3 and 4. The radioactivity in each sample can be estimated by multiplying the scintillation value by the dilution factor, 100.

### 2.4.2 Restriction enzyme digestion of total cellular DNA

The sensitivity of Southern blotting is such that, in general, 10µg of genomic human DNA is required for the detection of a single copy of target sequence within a sample. A volume containing 20µg of DNA from each sample was placed into a 1.5ml eppendorf tube. The lid was punctured several times with a needle and the DNA was dried down by vacuum centrifugation using a Speedvac SV100 (Savant), at a temperature of 65°C. After one hour all water should have evaporated from each sample. Each pellet of DNA was then subjected to *Eco*RI digestion for 24 hours. The components of the reaction are 34µl of distilled $H_2O$, 4µl of 10 x reaction buffer (buffer #3, Gibco BRL, Paisley, UK) and 2µl (20 units) of *Eco*RI (Gibco BRL, Paisley, UK). Samples were mixed thoroughly before incubating for 24 hours at 37°C

### 2.4.3 Gel electrophoresis of digested genomic DNA

It is necessary to ensure the complete digestion of the genomic DNA before transferring the DNA onto a membrane. This was achieved by mixing 1µl of the overnight digest with 5µl of distilled $H_2O$ and 4µl of loading buffer (see appendix A). This sample was then analysed on a 0.8% mini agarose gel at 50 volts for 1-2h before visualising the DNA under a UV light. If the DNA was completely digested then there should be an even smear of DNA down the gel with only one band, corresponding to satellite DNA. If the DNA was incompletely digested, there will be no satellite bands present and also the DNA will accumulate near the wells of the gel, due to the predominantly large fragments of DNA within the sample. In this situation more restriction enzyme and buffer should be added to the original sample followed by a further 24 hours incubation.

Upon efficient digestion of the DNA, 10µl of loading buffer was added to the original reaction mix, to give a final volume of 50µl containing 20µg of digested genomic DNA. Half of this was then loaded onto a 0.8% agarose gel and the sample electrophoresed for 5hrs at 80V. The DNA was then transferred to nylon membrane.

### 2.4.4 Transfer of the DNA fragments onto nylon membrane

Prior to transfer, the gel containing the digested DNA was exposed to UV for 5mins to fragment the DNA and improve the transfer to the membrane. At the same time, the gel was photographed alongside a ruler to allow estimation of the size of any bands on the membrane (by comparing the scale on the ruler to the molecular weight marker on the gel). The gel was then denatured in 1M NaOH, 2.5M NaCl for 30 minutes followed by neutralization in 3M NaAOc, pH 5.5 for a further 30 minutes. Neutralization brings the pH

of the gel down to below 9, which increases the binding of the DNA to the membrane. Transfer of the DNA from the gel to HybondN membrane (Amersham, Bucks, UK) was achieved by capillary flow using the system depicted in figure 2.1. An upturned agarose gel casting tray was placed in a large glass dish (approx $30cm^2$) filled with 20xSSC (see appendix A). Strips of 3MM Whatmann filter paper were laid over the tray and into the 20XSSC to act as a wick. Four pieces of clingfilm were laid over the edges of the casting tray and glass dish, to prevent evaporation of the buffer. The agarose gel was then placed on top of the casting tray such that the edges of the gel slightly overlapped the clingfilm. The HybondN membrane was then laid slowly on top of the gel. Three pieces of Whatmann 3MM filter paper (Whatmann, Maidstone, Kent), soaked in 20xSSC were placed on top of the membrane before a stack of absorbent towels (approx 10cm in height). Bubbles were eliminated at each stage during the assembly of the system *via* rolling with a glass pipette. The transfer occurs overnight, caused by the gradual upward flow of the 20xSSC buffer through the apparatus and into the paper towel wick. During this process, the DNA is eluted from the gel and binds to the nylon membrane. After blotting, the DNA was covalently attached to the membrane by exposing the membrane to $12,000\mu J/cm^2$ UV using a Stratalink machine. It should be noted that the membrane was only handled with tweezers, and where possible, contacting only the edge of the membrane.

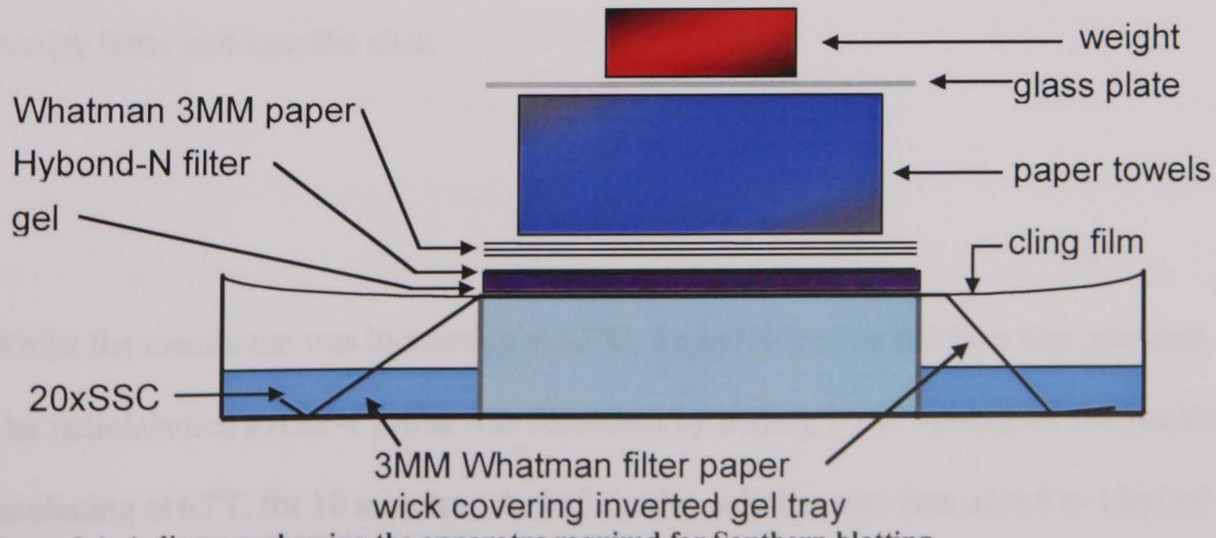


**Figure 2.1 A diagram showing the apparatus required for Southern blotting**

### 2.4.5 Hybridisation of the probe to the membrane

The final step in the process of Southern blotting is the binding of the radiolabelled probe to the target DNA sequence bound to the nylon membrane. This was achieved by performing a hybridisation reaction. Gilbert's solution (see appendix A) and sonicated salmon sperm DNA (10mg/ml) were pre-warmed to 65°C in a waterbath. 150µl of salmon sperm DNA was added to 15µl of 1M NaOH in a 1.5ml eppendorf tube. The tube was heated at 65°C for 10 mins in order to denature the DNA. This mixture was then added to 15ml of Gilbert's solution (see appendix A) to form the prehybridisation solution. The nylon membrane was rinsed briefly in 2 x SSC (see appendix A) before being sealed into a plastic bag containing the prehybridisation solution. Prior to sealing, all air bubbles were expelled from the bag by rolling with a glass pipette. This ensures that all areas of the membrane are exposed to the solution. The bag was then placed in a glass dish containing water, within a 65°C waterbath for at least 1hr with agitation. The plastic bag remains immersed in the heated water at all times by laying absorbent paper on top of the bag. The glass container was also covered with clingfilm to prevent evaporation of the water. The aim of the prehybridisation step is to prevent non-specific binding of the probe to the membrane. Instead, the salmon sperm DNA, included in the prehybridisation solution, will occupy these non-specific sites.

Whilst the membrane was incubating at 65°C, the hybridisation solution was prepared. The radiolabelled PARP-1 probe was denatured by adding $1/10^{th}$ volume of 1M NaOH and incubating at 65°C for 10 minutes. As before, this solution was then added to 15ml of

Gilbert's solution. Approximately 1.5 x $10^7$ counts are required per 15ml of Gilbert's solution (estimated from scintillation counting of the labelled probe). The prehybridisation solution was poured from the opened plastic bag and replaced with the hybridisation solution. The bag was resealed and placed back in the dish of water at 65°C overnight.

The next morning, the hybridisation solution was discarded and the membrane washed three times in a solution of 0.2xSSC/0.2%SDS (see appendix A). Each wash was for 15 minutes and was performed in a glass dish at 70°C in a shaking waterbath. These washing steps should remove any unbound probe from the membrane before it is resealed in a plastic bag and exposed to a phosphor storage screen overnight.

### 2.4.6 Use of PhosphorImager

A phosphorImager™ (Molecular Dynamics) was used to locate and measure the radioactive signal on the Southern blot membranes. As described in the previous section, the membrane was sealed into a plastic bag and exposed to a phosphor storage screen overnight. The screen itself is composed of fine crystals of $BaFBr:Eu^{++}$ in an organic binder. High-energy radiation (emitted from the radiolabelled $^{32}P$ on the membrane) excites an electron in the $Eu^{++}$ ions into the conduction band, which is then trapped in the $BaFBr^-$ complex. Loss of an electron results in $Eu^{++}$ becoming $Eu^{+++}$. Exposure of the screen to a helium-neon laser beam on the phosphorImager results in the liberation of an electron from the excited $BaFBr^-$ complex. This electron then reduces $Eu^{+++}$ back to $Eu^{++}$, releasing a photon at 390nm as it returns to the ground state. It is this photon which is detected by the phosphorImager and is processed by computer software to provide a digital

image on a computer screen. Image analysis was performed by ImageQuant software (Molecular Dynamics).

## 2.5 Polyacrylamide gel electrophoresis and Western blotting

### 2.5.1 Polyacrylamide gel electrophoresis (PAGE):

The process of PAGE allows the separation of proteins based upon their size. The separation depends upon the relative migration of different sized proteins through the matrix of a gel in response to an externally applied electric current. For example, a large protein will migrate through the pores of a gel significantly slower than a smaller protein. Therefore, electrophoresis leads to the formation of a 'ladder' of proteins down a gel, with each band corresponding to a particular protein. Samples for electrophoresis are prepared in a buffer containing SDS, which acts to denature proteins by coating them with a negative charge, leading to electrostatic repulsion in folded regions. In addition, this charge is necessary for the migration of proteins through the gel, towards a positive electrode. The buffer also contains β-mercaptoethanol to further denature proteins by reduction of disulphide bonds. Finally a blue dye, 2-bromophenol blue is added to the samples to visualise progress of the samples through the gel such that migration can be stopped at the necessary time.

The acrylamide content of gels can be changed to allow for more efficient resolution of a particular protein band, depending upon the size of the protein in question. For example, high molecular weight proteins are better-resolved using low percentage acrylamide gels, and vice-versa.

### 2.5.2 Sample preparation:

To prepare samples for Western blot analysis, cells ($2 \times 10^5$ or $5 \times 10^5$) were grown in 2cm or 5cm tissue culture plates, respectively. After relevant treatment (for example, with a DNA damaging agent), cells were lysed in SDS lysis buffer (see appendix A). In addition, the lysis buffer was supplemented with a variety of protease inhibitors; aprotinin, leupeptin, pepstatin A and trypsin inhibitor (all from Sigma, Poole, UK). For cells in 2cm plates, 50µl of SDS lysis buffer was used and 100µl for 5cm plates. Briefly, the medium was removed by aspiration before rinsing the cells in PBS. Aspiration of the PBS was followed by addition of the SDS lysis buffer. Samples were collected using cell scrapers (Costar) and placed into 0.5ml eppendorf tubes. Samples were then boiled for 5 minutes to promote the denaturation of proteins. At this stage the cell lysate was very viscous and difficult to pipette, due to the presence of DNA within the samples. To overcome this problem the samples were sonicated (Soniprep 150, MSE) for 10 seconds at 10 units, which shears the DNA and makes the sample more manageable. When comparing levels of a particular protein in a time course experiment it is necessary to load equal amounts of total protein from each sample onto the gel. This was achieved by performing a protein assay on each individual sample and, according to the protein concentration, adjusting the volumes of each sample loaded onto the gel. After assaying protein content, 2.5µl of 100% β-mercaptoethanol and 2.5µl of 1% bromophenol blue was added to 50µl samples at final concentrations of 5% and 0.05%, respectively. For 100µl lysates, 5µl of β-mercaptoethanol and bromophenol blue were added.

### 2.5.3 Pierce BCA protein assay:

Protein content of the cell lysates was estimated using a Pierce BCA protein assay kit (Pierce, Illinois, USA). The basis of this assay is the production of $Cu^{1+}$ from a reaction

between cysteine, tryptophan or tyrosine (present in protein samples) and $Cu^{2+}$ (present in one of the added reagents). Bicinchoninic acid is used as a sensitive detection reagent, and produces a soluble purple product in a reaction with $Cu^{1+}$. The optical density of the samples is then measured at 562nm and higher values represent high $Cu^{1+}$ and hence high protein content in the original samples.

The assay was performed in 96-well plates and required the addition of several standards of known protein concentration. Each standard was loaded in quadruplicate, with protein concentrations ranging from 0 – 2mg/ml. Volumes of 10µl were loaded into each well. Samples of unknown protein concentration were diluted 1:10 or 1:20 before loading, also in quadruplicate. A working reagent consisting of 50 parts buffer A to 1 part buffer B was prepared and 190µl added to each well, to give a total volume of 200µl. The plate was then covered in plastic film and agitated for 30 seconds before incubation at 37°C for 30 minutes. The OD (562nm) of each sample was analysed on a microtitre plate reader. The resulting protein concentration data was analysed and graphically presented using Protein Concentration Analysis Software (Life Science International, UK).

### 2.5.4 Gel electrophoresis:

Precast 4-20% gradient polyacrylamide Tris-Glycine gels (1 mm thickness, 10 x 10 cm, 10 well configuration, EC6025, Gibco BRL, Paisley, UK) were used for all protein electrophoresis work. Volumes of cell lysate containing 50µg of total protein were added to the gel. In addition, 4µl of seeblue molecular weight marker (Gibco BRL, Paisley, UK) was loaded. The marker consists of a mixture of proteins of known molecular weights, which can be used to estimate the molecular weight of any proteins detected in the cell

lysates. Gels were processed in Novex X-Cell gel tanks (Gibco BRL, Paisley, UK) containing 800 ml of electrode running buffer (see appendix A). The gels were then connected to an electrical power supply (250/2.5 Powerpack, Bio-Rad, California, USA) and ran at 180 volts for approximately 90 minutes (until the blue dye had ran to the bottom of the gel). Upon completion, gels were carefully removed from their plastic casing and prepared for protein transfer *via* Western blotting.

## 2.6 Western blotting:

Once separated on a gel, the protein constituents of a particular sample can then be transferred to a nitrocellulose membrane in a process called Western blotting (Burnette, 1981). Again, this technique, like Southern blotting, is based upon the application of an electric current and subsequent electrostatic transfer of the proteins from the gel to a membrane. The membrane is then incubated in a solution containing a specific primary antibody raised against the protein of interest. This antibody is in turn recognised by a species-specific secondary antibody conjugated to a horseradish peroxidase enzyme. The final step involves detection of the protein-antibody complex *via* enhanced chemiluminescence (ECL). This process basically involves the addition of ECL reagents to the membrane and subsequent production of light *via* a reaction performed by the horseradish peroxidase enzyme (see figure 2.2). This light is detected by exposing X-ray film to the membranes in an X-ray cassette. The film is then developed to show a black band corresponding to the protein of interest. The intensity of the band can be measured using image analysis computer software and is representative of the levels of the particular protein in the original sample applied to the acrylamide gel.

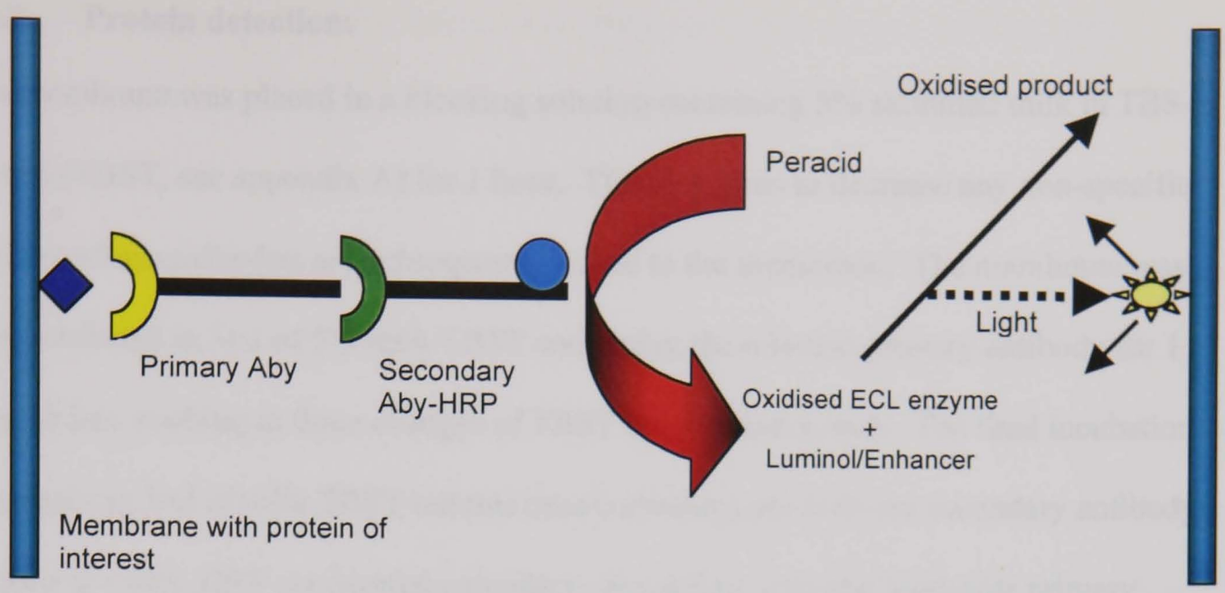


**Figure 2.2 Diagram summarising the principles of Western blotting**

### 2.6.1 Protein transfer

The components used for each Western blot are two glass fibre pads, two pieces of 3mm filter paper and one piece of HybondC membrane (Amersham, Bucks, UK). All components were pre-soaked for 30 minutes in transfer buffer (see appendix A). The components were then assembled together in a blotting cassette, with the gel adjacent to the membrane and placed into a blotting module (Mini Trans, Bio-Rad, California, USA). The Western blot was then ran at 30 volts for 15-18 hours or 65 volts for 1 hour. Upon completion, the membrane was removed from the cassette and subjected to staining with Ponceau S solution (Sigma, Poole, UK). This solution stains total protein and therefore provides an indication of whether the samples have ran through the gel correctly and also if the subsequent blotting procedure has been successful. Ponseau S can also provide an indication of the total protein in each lane, therefore, if the earlier protein assay was correct, each lane should be stained to approximately the same extent. The Ponseau S stain was removed by several washes of the membrane in distilled water.

### 2.6.2 Protein detection:

The membrane was placed in a blocking solution containing 5% skimmed milk in TBS-Tween (TBST, see appendix A) for 1 hour. This step aims to decrease any non-specific binding when antibodies are subsequently added to the membrane. The membrane was then incubated in 3ml of 5% milk TBST containing the relevant primary antibody for 1 hour before washing in three changes of TBST for 5 minutes each. The final incubation was again in 3ml of milk TBST but this time containing the relevant secondary antibody (mouse or rabbit HRP conjugated secondary, depending upon the particular primary antibody used) (Dako, Glostrup, Denmark). Details of the antibodies used and their concentrations are provided in the table below (table 2-1). The membrane was then washed in TBST for 1 hour, with the buffer being changed every 5 minutes. The final step in the Western blotting procedure involves detection of the protein *via* ECL detection.

### 2.6.3 ECL protein detection

The ECL Western blotting detection system (Amersham, Bucks, UK) is based upon a light emitting reaction catalysed by the horseradish peroxidase (HRP) enzyme conjugated to the secondary antibody. The ECL reagents added to the membrane contain a variety of chemicals, which react to produce light in the reaction described below.

The reaction exploits the HRP/hydrogen peroxide catalysed oxidation of a cyclic diacylhydrazide called luminol in alkaline conditions. Upon oxidation, luminol is in an excited state and subsequently decays to a lower energy ground-state *via* a light-emitting pathway. The ECL reagents also contain phenols, which enhance the light output by approximately 1000-fold (Amersham ECL™ product information booklet).

The methodology used in ECL detection is very simple, the excess TBST was first removed from the nitrocellulose membrane using absorbent paper. The two ECL reagents were mixed in a 1:1 ratio for 1 minute before being added to the membrane for a further minute. Excess ECL reagent was removed from the membrane using absorbent towel and the membrane then wrapped in Sarin-wrap. The membrane was then placed in an X-ray cassette and exposed to X-ray film under infra red light conditions in a dark room. Exposure times vary depending upon the primary antibody being used and the abundance of the protein being detected, but ranged between 10 seconds and 20 minutes. The film was removed and developed in an automated continuous roller processor (X-ray Film Processor, RGII, Fuji Ltd, Japan). Membranes that were to be re-probed with an alternative antibody were stored in TBS at 4°C.

| **Target Protein** | **Antibody** | **Epitope** | **Dilution** | **Source** |
|---|---|---|---|---|
| PARP-1 | H-250<br>Rabbit polyclonal | C-terminal | 1:1000 | Santa Cruz Biotechnology<br>Santa Cruz, USA |
| Mdm2 | Clone 14<br>Mouse monoclonal | C-terminal | 1:1000 | Dr John Anderson<br>Dept Pathology<br>University of Newcastle upon Tyne |
| p53 | CM5<br>Rabbit polyclonal | polyclonal | 1:1000 | Novocastra Laboratories, Newcastle upon Tyne, UK |
| Actin | AC40<br>Mouse monoclonal | C-terminal | 1:1000 | Sigma, Poole, UK |

**Table 2-1 Table of the antibodies used to detect various proteins**

## 2.7 Luciferase reporter gene assay

A reporter gene assay is a technique involving the introduction of plasmid DNA into cells. The plasmid usually contains a gene downstream of a promoter site, the expression of which can be measured. For example, the reporter gene used in this study is a luciferase gene. This gene was inserted into a pGL3 plasmid. In addition, a p53 responsive promoter

(The P2 site of the *Mdm2* gene) has been ligated into the plasmid upstream of the luciferase gene (Laing, H, PhD thesis, Cancer Research Unit, University of Newcastle upon Tyne). Therefore, introduction of this plasmid into cells should result in the expression of luciferase in a p53-dependent manner. In addition, when included in DNA damage response experiments, expression of luciferase should be increased due to increased transcriptional activity of p53. The luciferase produced can subsequently be measured using a luminometer (Becton Dickinson, Oxford, UK)

Introduction of the luciferase plasmid into cells is achieved using transient transfection. Transfection is a common research technique involving the introduction of foreign DNA into cells and monitoring protein expression. In contrast to stable transfection, the foreign DNA is not required to be integrated into the genome. Transient transfection can be achieved using a variety of methods, including calcium phosphate coprecipitation, electroporation, the use of viral vectors and cationic liposome mediated transfection. The transfection method used in this study involved a reagent called FuGENE 6 (Roche, Basel, Switzerland), a multi-component lipid-based transfection reagent that complexes with and transports DNA into the cell during transfection.

When trying to transiently transfect a cell line it is first necessary to optimise the conditions needed for transfection and expression of the plasmid. This work was performed by a colleague in the Cancer Research Unit, who developed and validated the luciferase gene reporter assay as part of a PhD course (Gillian Farnie, PhD thesis, University of Newcastle upon Tyne). The basic transfection procedure involves the plating of a particular number of cells into a 35mm tissue culture plate. The cells are allowed to

grow overnight before addition of the transfection reagent/plasmid DNA mix. The expression of the reporter gene is then monitored over time. Therefore the factors to be optimised are the cell number plated out, the amount of transfection reagent per plate, the ratio of transfection ratio to plasmid DNA(s) and the time at which optimum expression occurs. It should be noted that in addition to a luciferase plasmid, a plasmid encoding β-galactosidase is simultaneously transfected into the cells. This gene is under the control of a cytomegalo virus (CMV) promoter, which is not DNA damage-inducible and is included to act as an internal control for transfection efficiency. For example when using luciferase production as a measure of p53 activity, it is important to demonstrate that any increase in luciferase is not simply due to increased transfection of the luciferase plasmid in that particular sample. Therefore, the results from luciferase experiments are plotted as a ratio of luciferase/β-galactosidase.

### 2.7.1 Preparation of luciferase/β-galactosidase plasmids

Both plasmids were prepared and purified according to previously described techniques (Section 2.2.1). Briefly, *E.coli* JM109 cells were transformed with the plasmid DNA and plated out under the selection of the relevant antibiotic. The plasmid was then purified using DNA mini and mega-prep kits (Section 2.2.1.2). Isolation of the plasmid was confirmed using agarose gel electrophoresis. Stock solutions of 0.2mg/ml of each plasmid were prepared in distilled water.

### 2.7.2 Transient transfection of plasmids

As described earlier, the conditions for transient transfection of the plasmids into the cell lines used in this study have been optimised by Gillian Farnie (Cancer Research Unit, University of Newcastle upon Tyne).

Cells were trypsinised and counted. $1.5 \times 10^5$ cells were then placed in 2ml of medium in a 35mm tissue culture plate (Nunc, Illinois, USA). For each time point of an experiment, three plates were used. Therefore upon luciferase analysis, it was possible to measure the standard error of a particular sample and hence get a measure of the statistical significance of any changes observed. For a typical DNA damage response experiment, 15 plates were used, corresponding to time points of untreated, 1h, 2h, 3h and 6h. The cells were grown for 24 hours before addition of the transfection reagent, which contained the following:

| | |
|---|---|
| Per plate | 2µl of FuGENE 6 |
| | 100µl of serum free culture medium |

FuGENE 6 was added to the serum free medium in a 20ml Universal and left for 5 minutes. It is important that during addition the FuGENE 6 reagent does not come into direct contact with the plastic of the tube as this can adversely affect transfection efficiency.

| | |
|---|---|
| Per triplicate | 5µl of 0.2mg/ml luciferase plasmid |
| | 1µl of 0.2mg/ml β-galactosidase plasmid |

The relevant volume of each plasmid is then added to the serum free medium/FuGENE 6 mixture. After gentle mixing (no vortexing), the solution was left for 15 minutes. 100µl of the mixture was then added to each plate of cells for 24h.

After 24h transfection, the cells were ready for treatment with particular DNA damaging agents +/- AG14361. Samples were taken at the required time points by the removal of culture medium and addition of 200µl of lysis buffer to the plate (part of the Dual Light™ assay kit, Perkin Elmer, Conneticut, USA). After 5 minutes, the samples were collected by washing the lysis buffer over the surface of the plate twice before transfer to a 0.5ml eppendorf microfuge tube. Samples were stored at –20°C prior to analysis.

### 2.7.3 Analysis of samples

Samples were analysed by measuring the levels of both luciferase and β-galactosidase in each sample. Measurement involved the use of a Dual Light™ assay kit and a luminometer. The analysis was performed in black and white 96-well plates (Wallac) by adding 5µl of each sample to an individual well. The plate was then inserted into the luminometer and the luciferase and β-galactosidase values measured after the automated addition of various reagents. These reagents were supplied as part of the Dual Light Assay kit.

#### 2.7.3.1 Principles of the Dual Light Assay™

The transcription of the plasmids transfected into cells results in the expression of both luciferase and β-galactosidase. The levels of expression of each of these enzymes can be

monitored using the dual light assay kit. This involves adding various reagents (supplied within the kit) to a sample of cell lysate. The reagents contain substrates for the enzymes. Upon catalysis, light is emitted from the reaction. It is the intensity of this light which is measured by the luminometer and should be proportional to the amount of luciferase or β-galactosidase within the cellular sample. The reaction resulting in the production of light is summarised below:

$$\text{ATP + D-Luciferin + } O_2 \xrightarrow{\text{LUCIFERASE}} \text{Oxyluciferin + AMP + PPi + } CO_2 \text{ + LIGHT}$$

Briefly, 25µl of buffer A is added to a well followed by a 15 second delay. 100µl of buffer B is then added to the same well and the light measured after a further 15 seconds. To measure the β-galactosidase, the samples are left for approximately 1 hour after the addition of buffers A and B before adding 100µl of accelerator II solution. After a 15 second delay, the light intensity is measured. All readings are converted into a ratio of luciferase/β-galactosidase and analysed using Microsoft Excel software.

## 2.8 Measurement of poly(ADP-ribose) polymerase activity

Two methods have been used for the measurement of PARP-1 enzyme activity in this study. The basis of both methods described in this section is the introduction of a short double stranded oligonucleotide into cells to simulate DNA strand breaks and hence activate PARP-1. Both techniques require the prior permeabilisation of cells by suspending cells in a buffer containing digitonin (a mild detergent). This makes membranes 'leaky' and hence both oligonucleotide and exogenously added $NAD^+$ are able

to freely enter cells, but macromolecules such as PARP-1 cannot exit the cell. In the first technique described, the reaction mix also includes γ-[$^{32}$P] labelled $NAD^+$, which acts as a substrate for PARP-1. This leads to the production of [$^{32}$P] labelled ADP-ribose on various target proteins, which can be precipitated with TCA and bound to filters. Scintillation counting will then provide an estimation of the radioactive content of each sample and hence a measure of the PARP-1 activity.

The second technique discussed does not involve the use of radioactivity; rather an immunoblotting method is used to detect the ADP-ribose polymer that is bound to a nylon membrane and subsequently probed with a monoclonal antibody directed specifically against ADP-ribose polymer.

### 2.8.1 Incorporation of radiolabelled $NAD^+$ into permeabilised cells

#### 2.8.1.1 Preparation of $^{32}$P-labelled $NAD^+$

The $NAD^+$ used in this assay actually consists of a cocktail of normal (non-radioactive) $NAD^+$ mixed with a small amount of [$^{32}$P]-$NAD^+$. A 600mM stock solution of β-$NAD^+$ (Sigma) was prepared in distilled $H_2O$. The precise concentration of this solution was determined using spectrophotometry by measuring the OD at 260nm. 1mM $NAD^+$ has an absorbance of 18 OD units therefore it is possible to prepare a working solution of 600μM from the concentrated stock. The $NAD^+$ was diluted in distilled $H_2O$. To this a small volume of [$^{32}$P]-$NAD^+$ (Amersham pharmacia biotech) was added (2 - 5μl depending upon the activity of the [$^{32}$P]).

### 2.8.1.2 Permeabilisation of cells

The relevant number of cells was prepared by trypsinisation and counting (1 x $10^6$ per assay). This suspension was spun down at 1500rpm for 5 minutes and the pellet rinsed in ice cold PBS. The cells were spun again, the supernatant removed and the cells resuspended in 1.5ml of digitonin (150µg/ml in sterile $H_2O$). After 15 minutes incubation on ice, 13.5ml of ice-cold isotonic buffer was added (see appendix A). Permeabilisation of the cells was confirmed by staining a small number (5µl) with trypan blue (5µl). The suspension was loaded onto a haemocytometer and the cells viewed under a microscope. Trypan blue can enter permeabilised cells and hence stain them blue. For efficient permeabilisation, > 99% of cells should be stained blue. After permeabilisation, cells were kept on ice and assayed immediately.

### 2.8.1.3 PARP-1 assay

The following components were included in the reaction mix: 10µl of palindromic double stranded oligonucleotide (CGGAATTCCG, prepared at 200µg/ml in Tris.HCl, pH 7.8), 50µl of $NAD^+$ cocktail (prepared as described in Section 2.8.1.1), 8µl of DMSO or DMSO containing AG14361 and 37µl of distilled water. The sequence of the oligonucleotide used is such that it forms a hairpin structure due to the complementary nature of the bases in each half of the oligo. The formation of a hairpin produces a double-stranded DNA end at one extreme of the oligonucleotide. The reaction components were pre-incubated at 26°C in a shaking waterbath and the reaction started by the addition of 300µl of permeabilised cell suspension (1 x $10^6$ cells). The initiation of individual reactions was staggered by 10 seconds. The reaction was performed for 5 minutes before the addition of 2ml of ice cold 10% TCA (w/v), 10% sodium pyrophosphate (w/v) (both from Sigma, Poole, UK). The actual reaction performed is summarised below:

$$\beta NAD^{+} + \text{protein acceptor} \xrightarrow{\text{PARP-1}} (\text{ADP-ribose})_n\text{-protein} + \text{nicotinamide}$$

The TCA will precipitate high molecular weight material, including poly(ADP-ribosyl)ated proteins, whereas low molecular weight radiolabelled $NAD^+$ will remain in solution. Assay blanks, to correct for non-specific binding of the radiolabel to the filter were also prepared by adding 2ml of TCA before the cells, thereby preventing initiation of reaction. All tubes were incubated for 1 hour on ice.

The precipitated macromolecules were then bound to 25mm (GF/C) microfibre filters (Whatman International Ltd, Maidstone, Kent) using a Millipore filtration apparatus (Whatman International Ltd, Maidstone, Kent). Soluble components are able to pass straight through the filters therefore, only large insoluble molecules, including poly(ADP-ribosyl)ated proteins will remain bound to the filters. The filters were soaked in 1% TCA (1% w/v TCA, 1% w/v sodium pyrophosphate) and placed onto the filter holder. The funnel assembly was placed on top and the individual samples added to the funnels. Each sample was rinsed 4 times with 1% TCA, under gentle suction pressure. Each filter was removed and allowed to dry before being placed in liquid scintillation vials (20ml, Packard Instrument Company, USA). 10ml of scintillation fluid was added to each filter followed by thorough shaking of the vials. To provide a measurement of the specific activity of the radiolabel, 2µl of the $NAD^+$ cocktail was added to 20ml of scintillation fluid. All samples were analysed on a β-particle scintillation counter (Wallac Scintillation Products) for 3 minutes. All data points were performed in triplicate.

#### 2.8.1.4 Analysis of results

The first step in the analysis of the raw data was to calculate the number of counts representing 1pmol of $NAD^+$. This was achieved by calculating the mean DPM of the three standards ($S_M$), which are the samples containing only $NAD^+$ cocktail and scintillant. This figure was then divided by the concentration of $NAD^+$ used (600μM), to give value C:

$$S_M/4000 = DPM/pmol\ NAD^+$$

The amount of $NAD^+$ incorporated into the TCA precipitate is representative of the level of ADP-ribose polymer formation. Therefore, the pmol $NAD^+$ present in each of the samples (P) after the 5 minutes incubation was calculated.

The mean of the $T_0$ samples, $T_{0M}$, was determined and subtracted from each of the sample counts, removing the non-specific background counts:

$$P - T_{0M} = P_0$$

The values of $P_0$ were then divided by the number of DPM equivalent to 1pmol $NAD^+$ (C, calculated earlier):

$$P_0/C = pmol\ NAD^+ \text{ in each sample, } C_S$$

As the volume of cells added to each sample was 300μl, $C_S$ represents the pmol $NAD^+$/300μl of cell suspension. Therefore, to determine the pmol $NAD^+$ in 1ml of cell suspension ($1 \times 10^6$ cells), $C_S$ was multiplied by 3.33. The cell count taken prior to the experiment was then utilized to allow the final result to be represented as :

$$Pmol\ NAD^+ \text{ incorporated}/10^6 \text{ cells}/5min$$

### 2.8.2 Immuno dot-blot measurement of PARP-1 activity

This technique was developed and validated based on an assay described by Affar *et al.*, 1998. It involves the initial permeabilisation of cells to allow entry of $NAD^+$ and double

stranded oligonucleotide. The oligonucleotide used is the same as that in Section 2.8.1.3. Detection of ADP-ribose polymer is by antibody binding. The reaction was performed for 6 minutes and was stopped by the addition of an excess of PARP-1 inhibitor, AG14361. The samples were then bound to nylon membrane using a 96-well dot-blot manifold and a vacuum pump. The membrane was finally probed with a mouse monoclonal antibody directed against ADP-ribose polymers (clone 10H, a gift from Alexander Burkle, Department of Gerontology, Newcastle General Hospital). This antibody is a mouse monoclonal, raised against ADP-ribose polymer of chain length 10 – 50 units. No cross-reactivity with other macromolecules such as RNA or DNA has been detected. In addition the antibody does not detect monomers of ADP-ribose and NAD (Kawamitsu *et al.*, 1984; Menard and Poirier, 1987; Kupper *et al.*, 1990).

#### 2.8.2.1 Permeabilisation of cells

The required cell number was prepared by trypsinisation and cell counting. The suspension was spun at 1000rpm for 5 minutes at 4°C and the cells rinsed in ice-cold PBS. After a second identical spin, the cell pellet was resuspended in permeabilisation buffer (see appendix A) at a density of $3 \times 10^6$ cells/100µl. Each reaction required $5 \times 10^5$ cells. This suspension was left on ice for 1 minute before the addition of 4ml of ice-cold permeabilisation buffer/100µl of cells. The cells were then spun down at 1000rpm for 10 minutes at 4°C and the pellet resuspended in ice-cold permeabilisation buffer at a density of $5 \times 10^5$cells/53µl (therefore 53µl per reaction).

#### 2.8.2.2 PARP-1 assay

The following reaction components were added to $5 \times 10^5$ (53µl) cells on ice: 13µl of double stranded oligonucleotide (13µl of 384.6µg/ml oligo gives a final concentration of 50µg/ml) and 34µl of 3 x reaction buffer (appendix A) to give a total volume of 100µl. 1µl

of 100μM AG14361 (in 1% DMSO) or 1% DMSO, as control, was also included in the relevant samples. The reaction was initiated by the addition of cells and transfer of the tubes to a shaking waterbath at 30°C. Initiation of reaction was staggered by 10 seconds and the reaction stopped by adding 400μl of 1.25μM AG14361 (final concentration 1μM) and transferring the tubes to ice. Each tube contains 5 x $10^5$ cells in a total volume of 500μl. Therefore, the concentration of cells is 1000 cells/μl. Optimisation studies have shown that 1000 cells is the optimum number to load onto the membrane. 1μl of reaction mix was added to 19μl of PBS and this was in turn added to Hybond N membrane (Amersham, Bucks, UK) which is assembled into the dot blot apparatus on top of a piece of Whatman filter paper. The sample was passed through the membrane by vacuum aspiration. The negatively charged polymer binds to the membrane. The membrane is then rinsed with 200μl of 10% TCA (w/v), 2% sodium pyruvate (w/v) and 400μl of 70% ethanol (v/v, ethanol/$H_20$) before the dot-blot apparatus is disassembled and the membrane rinsed several times in PBS.

#### 2.8.2.3 Detection of ADP-ribose polymer

The membrane was incubated in a solution of 5% dried skimmed milk in PBST (phosphate bufferes saline, containing 0.1% Tween20, see appendix A) for 1 hour. This step is to reduce any non-specific binding of the antibody in subsequent steps as proteins in the milk will bind to such sites and hence prevent binding of the antibody. The membrane is then incubated in the primary antibody (10H at a concentration of 2.5μg/ml in 3ml of 5% milk-PBST) for 3h before being washed 3 times in PBST for 5 minutes each and transferred to the relevant secondary antibody (goat anti mouse, HRP-conjugated, 1:3000 in 5% milk PBST; Dako, Glostrup, Denmark) for 1 hour. After thorough washing in PBS, the blot was visualised using ECL (Amersham, Bucks, UK, see Section 2.6.3).

## 2.9 DNA sequencing

The sequencing of cDNA is a means of analysing the nucleotide sequence of a particular gene, which can in turn be used to evaluate the amino acid sequence of the resultant protein. The precise amino acid sequence determines the secondary and tertiary structure of a protein. Therefore any sequence changes are likely to result in disruption of structure in some way, by interfering with the formation of essential chemical bonds between amino acids in the folded protein. This is likely to bring about an altered protein function or even abolishment of the function altogether.

In this study, only the coding region of the gene of interest was sequenced. Therefore it is necessary to initially isolate cellular mRNA (Section 2.2.3) and then produce cDNA using the RNA as a template.

### 2.9.1 First strand cDNA synthesis

The production of cDNA from a cell relies heavily upon the initial isolation of an intact, pure sample of RNA. This RNA is then able to act as a template for a reverse transcriptase enzyme, which produces DNA from sequences of RNA.

cDNA has been produced in this study using The SUPERSCRIPT$^{TM}$ First-Strand Synthesis System (Gibco BRL, Paisley, UK), which is effective when using amounts of total RNA ranging from 1ng to 5μg. This technique is based on the polymerase chain reaction (Section 2.10.2) and, as such requires the initial binding of primers to the RNA before elongation of the primers by a reverse transcriptase enzyme. Random hexamer primers were used in this study. With this method, all RNAs in a population are templates for first-

strand cDNA synthesis. This helps to ensure that the mRNA of interest is reverse transcribed and subsequent PCR reactions on the cDNA using designed primers will specifically amplify the region of interest. Other types of primers may be used, for instance oligo(dT) primers bind to the poly(A) tails of mRNA. However, only 1-2% of total RNA possesses such tails and therefore, the cDNA yield is lower using this method. The bound primers are then elongated using a SUPERSCRIPT II RNase $H^-$ reverse transcriptase (RT) that has been modified to optimise the production of cDNA. This enzyme has been genetically modified to eliminate the Rnase activity, which is associated with other RTs. This Rnase activity would obviously degrade the mRNA during first-strand synthesis. In addition, SUPERSCRIPT II RT is not significantly inhibited by ribosomal and transfer RNA and can therefore be used to efficiently synthesise cDNA from a total RNA preparation. Finally, the enzyme exhibits increased thermal stability and may be used at temperatures up to 50°C. The combination of all these factors results in greater full-length cDNA synthesis and higher cDNA yield when compared to other RTs.

### 2.9.2 The polymerase chain reaction

The process of DNA sequencing relies heavily on a common research technique known as the polymerase chain reaction (PCR). This involves the amplification of a target sequence of DNA using a pair of oligonucleotides (called primers) complementary to regions flanking the target sequence of DNA. One primer binds to the sense strand and the other to the antisense strand of DNA. Basically these oligonucleotides bind the complementary flanking sequence and a DNA polymerase, included in the reaction mix, extends the ends of the primers using the original DNA sequence as a template. By adjusting the temperature accordingly, it is possible to repeat this reaction many times and hence

amplify the number of copies of the target sequence in the original sample. The reaction is explained in more detail in figure 2.3.

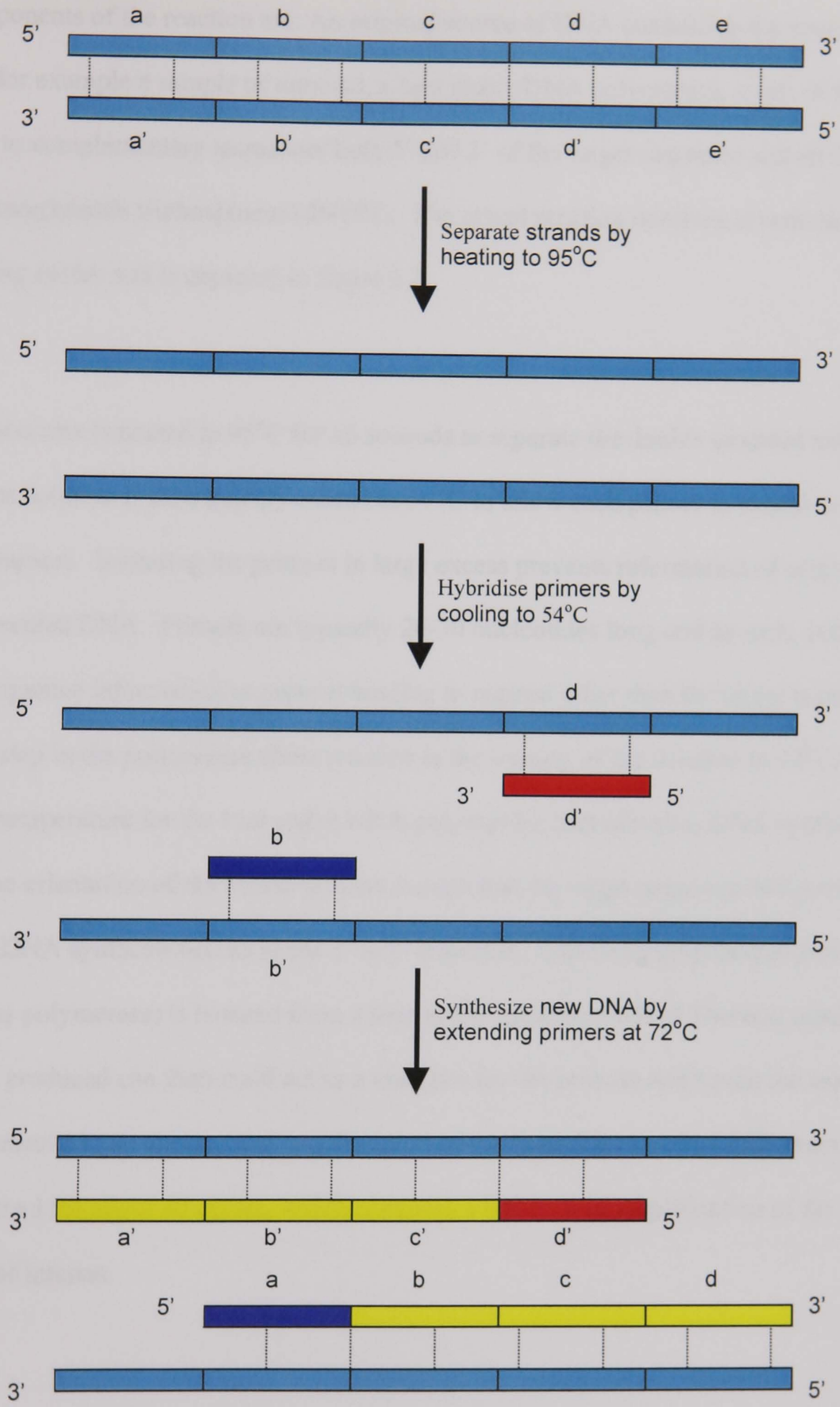


**Figure 2.3 Diagram summarising the polymerase chain reaction**
Original DNA is shown in turquoise, complimentary primers in blue and red and newly synthesised DNA is shown in yellow. Newly synthesised DNA is able to act as a template in subsequent cycles of the above reaction.

The components of the reaction are: An original source of DNA containing the sequence of interest (for example a sample of tumour), a heat stable DNA polymerase, a pair of primers that bind to complementary sequences both 3' and 5' of the target sequence and all four deoxyribonucleoside triphosphates (dNTPs). The actual reaction involves several heating and cooling cycles and is depicted in figure 2.3

The reaction mix is heated to 95°C for 15 seconds to separate the double stranded target DNA. The solution is then quickly cooled to 54°C to allow each primer to anneal to target DNA sequences. Including the primers in large excess prevents reformation of original double stranded DNA. Primers are typically 20-30 nucleotides long and as such, contain enough sequence information to prevent binding to regions other than the target sequence. The final step in the polymerase chain reaction is the heating of the solution to 72°C, the optimum temperature for the heat stable DNA polymerase thus allowing DNA synthesis to occur. The orientation of the bound primers is such that the target sequence will always be copied as DNA synthesis occurs in the 5' to 3' direction. The DNA polymerase used (called *Taq* polymerase) is isolated from a heat stable bacterium called *Thermus aquaticus*. The DNA produced can then itself act as a template for the primers and hence the reaction described results in an exponential amplification of the target DNA. Most PCR reactions are performed for about 30 cycles, which produces a billion fold amplification of the sequence of interest.

It is often necessary to optimise a PCR procedure to increase the yield and specificity of the reaction. For example, the concentration of magnesium chloride frequently needs to be modified. For example if a particular PCR reaction has too low a magnesium

concentration then the yield of PCR product is lowered. Alternatively, high magnesium may increase the amplification of non-specific PCR products. The reaction mix used here produced a good yield of the desired PCR product and hence optimisation of the reaction was not required.

The cDNA used in the PCRs has been derived from PARP-1 MEFs. The process involves the initial isolation of cellular RNA followed by production of the corresponding cDNA by RT-PCR. The PCR reaction was performed originally using a 'standard recipe', the components of which are listed below.

| | |
|---|---|
| 1µl | 1 OD stock of each primer of a particular pair |
| 4.2µl | $H_2O$ |
| 2.5µl | Reaction buffer |
| 0.15µl | *Taq* polymerase |
| 1.075µl | dNTP mix (0.1mM final concentration) |
| 5µl | $MgCl_2$ (final concentration 1.5mM) |
| 10µl | cDNA (diluted 1/10 from original stock) |

The reaction components were mixed thoroughly and heated to 94°C for 3 minutes. This was followed by 30 cycles of (94°C for 1min, 58°C for 2mins and 72°C for 3mins). After 30 cycles the temperature was held at 4°C

It is also important to prepare a 'blank' PCR reaction. This tube contained all components of the reaction except for the cDNA. Instead, 10µl of distilled water was added to the

reaction mix. This ensures that any PCR products are actually a product of the target DNA and not just some contaminant DNA that has somehow entered the reaction.

To demonstrate that the PCR reaction has been successful, it was necessary to analyse the products on an agarose gel, alongside a molecular weight marker. Comparison of PCR products to the marker will reveal whether the products are of the correct predicted size. Ideally, if the PCR reaction has been efficient and specific, only one band should be present in each lane. In addition, it is important that no bands are present in the lanes corresponding to the blank PCR reactions. The fragments of DNA were then purified from the agarose gel (Section 2.2.1.3).

#### 2.9.2.1 Design of PCR primers

The primers used were designed using DNA STAR software, which uses certain criteria when selecting a sequence for a primer. Generally, primers are between 18 and 30 base pairs long, which should ensure that the primers contain enough sequence information to eliminate non-specific binding of the primers. In addition the primer pair should not contain complimentary sequences as this may lead to primer self-annealing and thus prevent binding of primers to the target DNA. Ideally, primers should contain 45 – 55% of G or C bases. These bases form three hydrogen bonds compared to two for AT base pairs. This increases the binding efficiency of the primers. However, long stretches of Gs and Cs should be avoided in primers as this can promote non-specific binding. Likewise, for long stretches of As and Ts. Finally, it is best if the 3' end of the primer contains several GC residues. It is the 3' end that is extended during synthesis and the presence of G and C

bases at this point help clamp the primer to the DNA and can increase the efficiency of initiation and also increase the length of the PCR product.

### 2.9.2.2 Primer synthesis

All primers were kindly produced by Helen Atkins (Cancer Research Unit, University of Newcastle upon Tyne), using an automated Applied Biosystems model 392 oligosynthesiser (Applied Biosystems, California, USA). When synthesised, the oligonucleotides, which were dissolved in ammonia, were in the unreactive phosphodiester form, with their bases protected by amide groups. Before use, it was necessary to deprotect the oligonucleotides by heating at 55°C for 10 to 12 hours.

### 2.9.2.3 Primer quantification

The deprotected oligonucleotides were placed into 1.5ml Eppendorf tubes in 400µl aliquots. The DNA was dried down by piercing the lids of the tubes with a 21G needle and spinning in a vacuum centrifuge (Savant, Speedvac SC100) for approximately one hour. The primers were then resuspended in 400µl of sterile distilled $H_2O$. After thorough mixing, the concentration of the primers was determined according to Section 2.2.4 and diluted to a working concentration of 12pmol/µl (1OD). Reconstitited primers were stored at –20°C.

## 2.9.3 Dye terminator cycle sequencing

The common method for the sequencing of DNA is the Sanger dideoxy method (Sanger, 1981 Science). In a standard PCR reaction, dNTPs are included which are used by the DNA polymerase to extend the bound primer. However, the sequencing reaction also includes ddNTPs (dideoxyribonucleoside triphosphates), which lack the 3' hydroxy terminus that is essential for elongation of the DNA strand. Therefore, when a ddNTP is

incorporated into a PCR product, no further elongation takes place. This results in the production of a mixed population of DNA fragments, all of different lengths, depending upon where the PCR was terminated. The ratio of dNTPs to ddNTPs is optimised such that long PCR products can be produced as well as only very small PCR products. The particular sequencing kit used in this study relies on the fact that each of the ddNTPs used contains a different fluorescent tag whose excitation and emission spectrum is in the near infrared region. The reaction mixes are then ran through a gel (that will separate the fragments based upon their size) and the separated bands of DNA are then detected by their fluorescence as they emerge from the gel. For example, termination at A may give a red fluorescence and termination at C may give a blue signal. Detection of the fluorescent signal by an automated sequencing machine (Beckman CEQ 2000) allows for the sequence to be derived as each of the fragments emerges from the gel. It should be noted that each sequencing reaction contains only one of a primer pair. This ensures that every double stranded DNA product from a standard PCR reaction is analysed in both the sense and antisense direction during sequencing.

2µl of the purified PCR products from Section 2.10.2 were added to 5µl of $H_2O$ and 3µl of loading buffer (see appendix A) and analysed on a 1% agarose gel to confirm the purification of fragments of the desired size. These products were then used in the following sequencing reaction mix:

| | |
|---|---|
| Distilled $H_2O$ | 5µl |
| 10 x reaction buffer | 2µl |
| dNTP mix | 1µl |
| ddUTP dye terminator | 2µl |
| ddGTP dye terminator | 2µl |

| | |
|---|---|
| ddCTP dye terminator | 2µl |
| ddATP dye terminator | 2µl |
| DNA polymerase | 1µl |
| cDNA | 1µl |
| primer (1OD stock) | 2µl |

All components were supplied in a CEQ$^{TM}$2000 Dye Terminator Cycle Sequencing Kit (Beckman Coulter) except for the cDNA and primers. The reaction was performed in 200µl PCR tubes according to the following thermal cycling program:

| | |
|---|---|
| 96°C | 20 secs |
| 50°C | 20 secs |
| 60°C | 4 mins |

for 30 cycles followed by holding at 4°C

Each of the sequencing reactions was then transferred to a 0.5ml eppendorf tube containing 4µl of Stop Solution (1.5M NaOAc + 50mM EDTA) and 1µl of 20mg/ml glycogen. The salt and glycogen present facilitate subsequent precipitation of the DNA from the reaction mix. It is important that the stop solution is prepared immediately before use and that it is kept at room temperature otherwise the EDTA may precipitate out of solution. The components were mixed thoroughly before addition of 60µl of ice cold 95% (v/v) ethanol/$H_2O$ and mixed thoroughly to aid optimal precipitation of the DNA. The samples are then centrifuged at 14000rpm (Eppendorf 5417R) at 4°C for 15 minutes. After spinning, a pellet should be visible in the base of each tube. The supernatant is carefully removed with a micropipette before washing the pellet a further two times in ice cold 70%

ethanol. After each wash the samples are centrifuged at 14000rpm at 4°C for 5 minutes. The purpose of the washing steps is to remove the residual salts in the sample. Since salts are preferentially loaded on the CEQ, fewer sequencing fragments will be loaded. In addition, it is important not to leave the samples in ethanol for too long as this may actually cause precipitation of the salts that you are trying to remove. After the final washing step, as much ethanol as possible was removed from the pellet before allowing the DNA to air dry for approximately one hour. It is important to allow the pellet to dry completely as residual ethanol will suppress the signal on the CEQ. Finally, the DNA pellet was thoroughly resuspended in 40µl of deionised formamide and the sample transferred to a CEQ sample plate. A drop of mineral oil was then placed on top of each sample. The oil protects the dyes and hence increases their stability. The plate is loaded into the CEQ and the samples analysed.

### 2.9.4 Analysis of sequencing data

The sequencing data derived from the CEQ was saved onto a CD and analysed using CEQ sequence analysis software. The raw data is in the form of a trace of peaks of 4 different colours, one for each of the four bases. From this trace, the software predicts a sequence of bases and displays the sequence on the screen.

The sequence produced was copied and pasted into a BLAST2 sequence alignment program (available on the world wide web through www.NCBI.com). The sequence was aligned to a wild type murine p53 sequence that had been deposited previously into the BLAST database (accession # X01237). The program aligned the inputted sequence to the previously published sequence and complementary sequences are shown alongside each

other, with matching bases joined by lines. Any abnormalities in the inputted sequence are highlighted by the lack of a line between bases. These areas may be due to the CEQ being unable to read that particular area of sequence. Such areas can be checked by analysing the results from the complementary strand of DNA. For example, imperfect areas of sequence on the sense strand of a particular DNA fragment can be validated using the sequencing information from the antisense strand of the same fragment. In addition, abnormalities in sequence should be referenced back to the actual raw data derived from the sequencing machine. On occasions, the sequencing software does not recognise a particular peak as a base even though the raw data clearly shows a peak corresponding to a particular base. Alternatively, any mismatched bases in the inputted sequence may actually be due to a mutation at this point. Again, the raw data should be checked and the sequencing data of the other strand analysed. For a homozygous mutation (where both copies of the gene have been mutated), both the sense and antisense strand will show exactly the same mutation. In the presence of a heterozygous mutation (where one copy of the gene remains wild type), the raw data trace should show two peaks at that point, one on top of the other.

# CHAPTER 3

# CHARACTERIZATION OF THE PARP-1 MEFs AND THE PARP-1 INHIBITOR, AG14361

## 3.1 Introduction and objectives

The principal aim of this project was to test the hypothesis that p53 is regulated by PARP-1 in response to DNA damage. The obvious way to test this hypothesis is to remove PARP-1 from cells and investigate the DNA damage-induced p53 response. Several techniques have been used to remove PARP-1 activity from cells. These include the use of antisense RNA, a dominant-negative strategy involving the overexpression of the DNA binding domain of PARP-1, use of small molecule inhibitors of PARP-1 and finally knocking out the PARP-1 gene (Simbulan-Rosenthal *et al.,* 1998; Lu and Lane, 1993; Wang *et al.,* 1998; Agarwal *et al.,* 1997; de Murcia *et al.*, 1997; Masutani *et al.,* 1999). All strategies have been successful to a large extent in removing PARP-1 activity. However, there is currently no consensus of opinion on the subsequent effect of loss of PARP-1 function and/or protein on p53 induction and activity. The data presented in this thesis compared two techniques for removing PARP-1 activity:- knockout cells (de Murcia *et al.*, 1997) and a potent PARP-1 inhibitor (AG14361, provided by Pfizer GRD). It should be noted that the PARP-1 knockout cells are mouse embryonic fibroblasts, disrupted in exon 4 of the PARP-1 gene (Figure 3.1). Other groups have also produced mice disrupted in exon 1 (Masutani *et al.,*1999) and exon 2 (Wang *et al.*, 1997), and again p53 studies on cells derived from these mice are not consistent. The inhibitor used in this study, AG14361, was developed by the Experimental Therapeutics Group (University of Newcastle upon Tyne) in collaboration with Pfizer GRD. It is a competitive inhibitor (i.e. competes with $NAD^+$ for the active site of PARP-1) and has been shown to have a $k_i < 6nM$ in cell-free assays. As such, it is approximately 1000-fold more potent than the archetypal PARP-1 inhibitor, 3-aminobenzamide ($k_i = 5.7\mu M$).

The aim of this chapter was to confirm that the PARP-1 knockout cell lines obtained from Gilbert de Murcia were disrupted in the PARP-1 gene, and to demonstrate the loss of PARP-1 protein and enzyme activity. In addition, the effects of AG14361 alone on enzyme activity and on cell growth were studied, using the SRB assay (Section 2.1.7). This chapter contains results showing the effectiveness of the strategies used to remove PARP-1 activity from cells. These include Southern blots and enzyme assays. In addition, SRB assays are presented showing that AG14361 alone has no growth inhibitory effect during the time-scales of experiments (24 – 72 hours). Finally, results are presented showing the development, validation and optimisation of two techniques used to estimate levels of poly(ADP-ribosyl)ation within cells. These techniques were set up to evaluate the ability of AG14361 to inhibit PARP-1 in PARP-1 proficient MEFs and human HCT-116 cells. Also, these techniques were used to confirm that the disruption of PARP-1 in the PARP-$1^{-/-}$ MEFs resulted in the loss of PARP-1 enzyme activity.

## 3.2 Results

### 3.2.1 Disruption of exon 4 in PARP-1 MEFs

Figure 3.1 shows the disruption of the PARP-1 gene by the insertion of PGK-neo (phosphoglycerate kinase promoter) into exon 4 of the PARP-1 locus (de Murcia *et al.*, 1997). The disruption of PARP-1 in exon 4 leaves a significant part of the PARP-1 gene intact, with both zinc fingers of PARP-1 being encoded by regions upstream of exon 4. Importantly, studies using Northern blotting and Western blotting with antibodies recognising the zinc finger domains did not detect any truncated version of PARP-1 in PARP-$1^{-/-}$ MEFs (Trucco *et al.*, 1998). The wild type PARP-1 gene contains two *Eco*RI sites, which upon digestion give rise to a fragment of 9.6kb. The disruption of the PARP-1

gene introduces an extra *Eco*RI site into the PARP-1 locus and hence upon *Eco*RI digestion, produces a fragment of 3.3kb. Therefore, Southern blotting should produce bands at the corresponding sizes when using the radiolabelled probe (shown in figure 3.1).

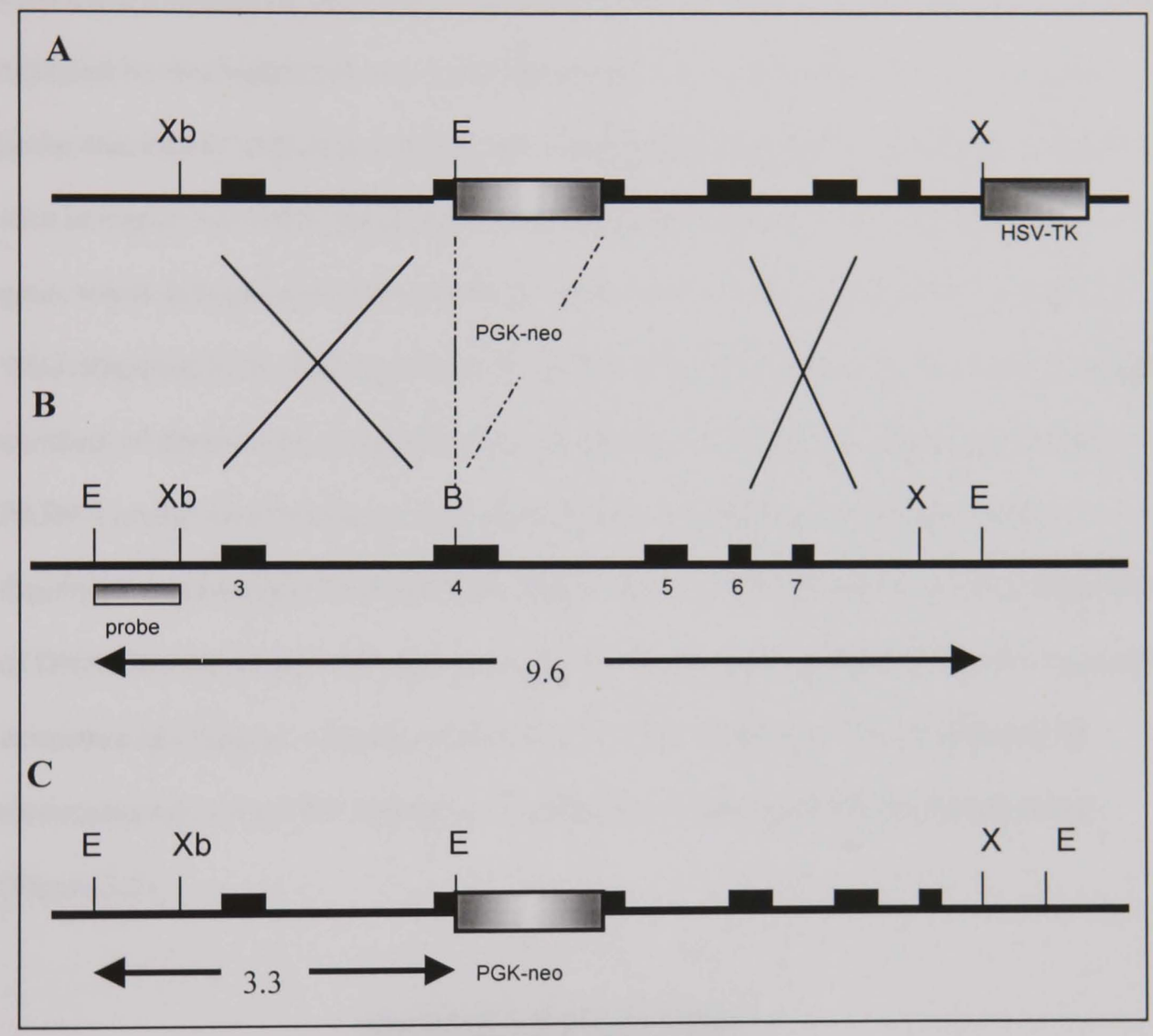


**Figure 3.1 Disruption of exon 4 in PARP-1$^{-/-}$ MEFs.**
The wild type PARP-1 locus has two EcoR1 (E) sites, separated by 9.6kb. The insertion of a neomycin resistance cassette (PGK-neo) into exon 4 in the PARP-1 knockout MEFs results in the insertion of an extra *Eco*R1 site. The highlighted 5' probe detects different sized genomic DNA fragments in the PARP-1$^{+/+}$ and PARP-1$^{-/-}$ MEFs. Xb = *Xba*I restriction site
(Diagram adapted from de Murcia *et al.*, 1997)

### 3.2.2 Preparation of the probe for Southern blotting:

The plasmid containing the probe for Southern blot analysis of genomic DNA from wild-type and knockout mouse tissue and MEFs was kindly provided by Gilbert de Murcia (Ecole Superieure de Biotechnologie de Strasbourg). The probe consisted of a 0.8kb

*Eco*RI – *Xba*I genomic fragment. E.*coli* JM109 cells were transformed with the plasmid and streaked onto agar plates supplemented with ampicillin. Resistant colonies were picked and bulked up initially in 50ml of LB. The plasmid was then purified from these cells using a mini-prep kit (Qiagen) and digested with *Eco*RI. The resultant products were analysed by electrophoresis on a 0.8% agarose gel. A band corresponding to the 0.8kb probe was clearly seen alongside the uncut plasmid sample (data not shown). As can be seen in Figure 3.1, centre panel, the 0.8kb probe should bind to the 5' end of the PARP-1 gene, which is intact in both the PARP-$1^{+/+}$ and PARP-$1^{-/-}$ MEFs and should recognise a 9.6kb fragment in the wild-type DNA and a 3.3kb fragment in the knockout DNA. Greater numbers of transformed *E.coli* cells were grown in 500ml LB and larger stocks of the PARP-1 probe were produced using a mega-prep kit (Qiagen) followed by *Eco*R1 digestion. Agarose gel electrophoresis again confirmed the isolation of a 0.8kb fragment of DNA. Several such bands were excised from the gel and the DNA purified using a gel extraction kit (Qiagen). Finally, a sample of purified PARP-1 probe was checked by electrophoresis on a 0.8% agarose gel confirming the success of the purification step (Figure 3.2).

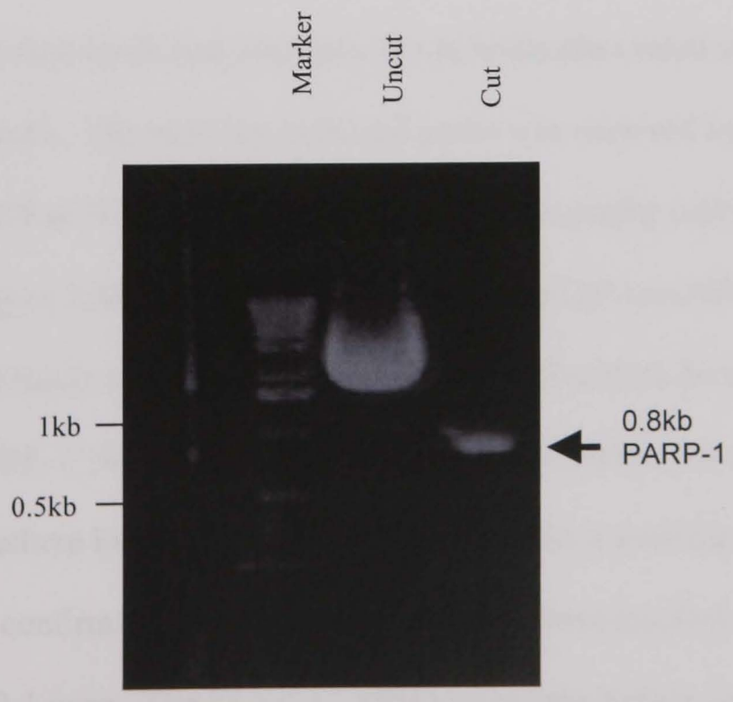


**Figure 3.2 Agarose gel showing uncut pBS plasmid and *Eco*RI digested and purified 0.8kb fragment**

### 3.2.3 Southern blotting

After preparation of the PARP-1 probe, it was necessary to isolate genomic DNA from the PARP-1 MEFs and perform *Eco*RI digestion of the DNA before separating the fragments on an agarose gel. DNA extraction and purification was performed on pellets of 1 x $10^7$ cells (PARP-$1^{+/+}$ and PARP-$1^{-/-}$ immortalised MEFs). 20μg of DNA for each cell line was then digested overnight with *Eco*RI. 1μg of the digestion was checked by electrophoresis on a 0.8% agarose mini-gel to confirm efficient digestion of the DNA. If the DNA was not properly digested extra restriction enzyme and buffer was added to the sample and again left overnight. Inefficient digestion is indicated by a gathering of high molecular weight DNA near the top of the gel. Instead, the DNA should be well-spread down the length of the gel and there should also be a clear band corresponding to satellite DNA about two-thirds of the way down the gel. Once efficient digestion was confirmed, 10μg of DNA was separated on a 0.8% agarose gel (figure 3.3A) before being transferred, by capillary blotting, to Hybond-N membrane (Section 2.4.4).

The membrane was then incubated overnight in a hybridisation solution containing [$^{32}$P]-labelled PARP-1 probe. The next day, unbound probe was removed by thorough washing in 0.2xSSC/0.2%SDS at 70°C before performing autoradiography using a phosphorimager (Section 2.4.6). Figure 3.3B shows the resultant Southern blot autoradiograph for the PARP-1 MEFs and bands can clearly be seen at the expected sizes for the PARP-$1^{+/+}$ (9.6kb) and the PARP-$1^{-/-}$ MEFs (3.3kb). A sample from a Balb/c mouse strain was also included on the Southern blot to act as a positive control for a wild type PARP-1 locus. This Southern blot confirms that a fragment of DNA has been inserted into and hence disrupted the PARP-1 gene. The PARP-$1^{-/-}$ MEFs were then further characterized to show lack of both PARP-1 protein and activity (see below).

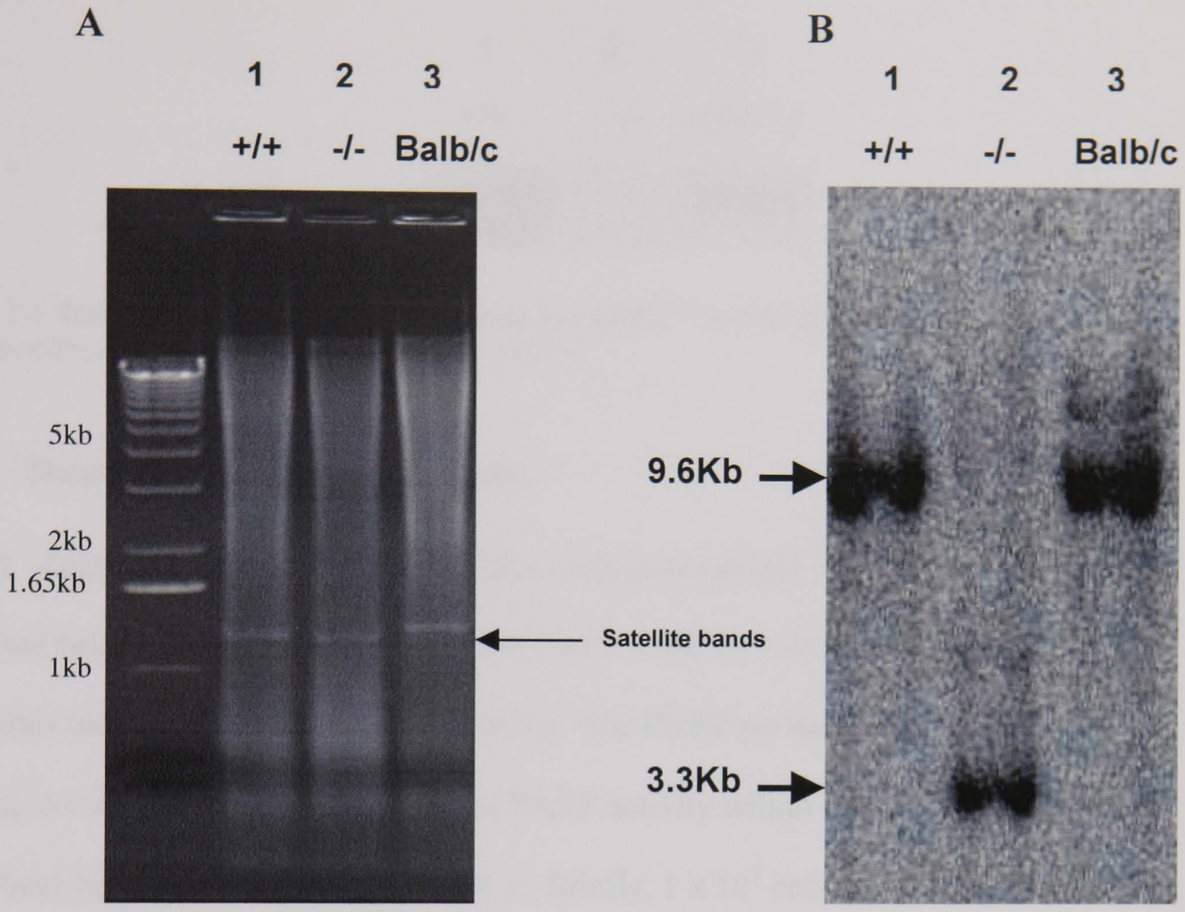


**Figure 3.3 Southern blot of PARP-1$^{+/+}$ and PARP-1$^{-/-}$ MEFs**
A. Ethidium bromide stained garose gel showing *Eco*R1 digestion of genomic DNA. Efficient digestion was confirmed by the presence of satellite bands. B. Southern blot of *Eco*RI-digested DNA from cell pellets (lanes 1 and 2) and from mouse tail section (lane 3). M = 1kb ladder molecular weight standard.

### 3.2.4 Western blot analysis of PARP-1 expression in PARP-1 MEFs

To confirm the absence of PARP-1 protein in the PARP-1$^{-/-}$ MEFs, Western blotting was performed, as described in Section 2.6. Samples of both wild type and knockout MEFs were lysed in SDS lysis buffer and 50µg of protein separated by electrophoresis on a 4-20% polyacrylamide gradient gel. The proteins were transferred to nitrocellulose membrane and the membrane probed with a rabbit polyclonal antibody raised against PARP-1 (H-250, recognises c-terminal of PARP-1, corresponding to residues 764 – 1014; Santa Cruz Biotechnology). A positive control of purified PARP-1 was also included on the gel. As can be seen in figure 3.4, the PARP-1$^{-/-}$ MEFs contained no detectable PARP-1 protein.

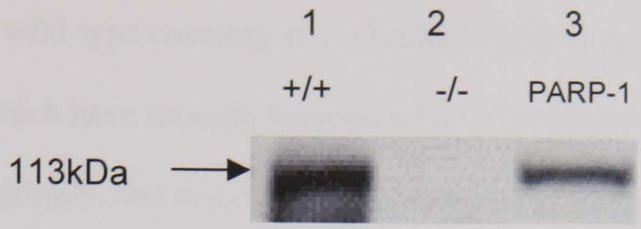


**Figure 3.4 Western blot showing PARP-1 protein in PARP-$1^{+/+}$ and PARP-$1^{-/-}$ MEFs.**
Lane three contains a positive control of purified PARP-1

### 3.2.5 Measurement of PARP-1 activity:

#### 3.2.5.1 Incorporation of [$^{32}$P]-$NAD^+$ into acid-precipitable material

The final step in the characterization of the PARP-1 MEFs involved the use of an enzymatic assay, measuring PARP-1 activity. The PARP permeabilised cell assay is a technique commonly used to measure the PARP activity within cells. The details of this assay have been described in Section 2.8.1. Briefly, 1 x $10^7$ cells are permeabilised in isotonic buffer supplemented with digitonin. The cells are then spun down and resuspended in a buffer containing [$^{32}$P]-labelled $NAD^+$ and a short double stranded oligonucleotide. This oligonucleotide simulates DNA strand breaks and hence stimulates PARP activity. Radiolabelled $NAD^+$ is then used as a substrate, resulting in the production of [$^{32}$P]-labelled ADP-ribose polymer covalently attached to proteins. The protein-bound polymer is precipitated, bound to a filter and then detected and quantified by scintillation counting. The PARP inhibitor AG14361 was also included in some samples. Figure 3.5 shows an example of a PARP-permeabilised cell assay performed in PARP-$1^{+/+}$ and PARP-$1^{-/-}$ MEFs. In the wild-type cells, the oligonucleotide greatly stimulated PARP-1 activity, with activity rising from 108 to 621 (fmol NAD incorporated per $10^6$ cells/minute). In addition this activity was completely abolished by treatment of cells with 1μM AG14361 (an activity of only 14fMol NAD incorporated per $10^6$ cells/minute was measured), showing the effectiveness of AG14361 in inhibiting PARP-1 activity. Figure

3.5 also shows that the PARP-1 knockout cells possessed approximately 5% PARP activity compared to their wild-type counterparts. This activity may be attributed to alternative PARP proteins, which have recently been described (for example PARP-2, V-PARP and tankyrase). Interestingly, this activity was independent of the presence of oligonucleotide and was completely abolished by treatment of cells with 1μM AG14361. This suggests that AG14361 is not just specific for PARP-1, but also inhibits alternative PARP enzymes. It should be noted that permeabilised cells are not in the normal physiological state and, as such it could be argued that this assay does not demonstrate the entry and activity of the PARP-1 inhibitor in intact cells. However, previous studies within the department have involved treating intact cells with AG14361 before washing the cells with PBS (to remove residual inhibitor) and subsequently performing the permeabilised cell assay in the absence of added inhibitor. These experiments demonstrated complete inhibition of PARP-1 probably due to the inhibitor being very tightly bound to PARP-1 prior to the permeabilisation process (Stephany Veuger, Cancer Research Unit, University of Newcastle upon Tyne, unpublished results) and therefore not diffusing out of the cell.

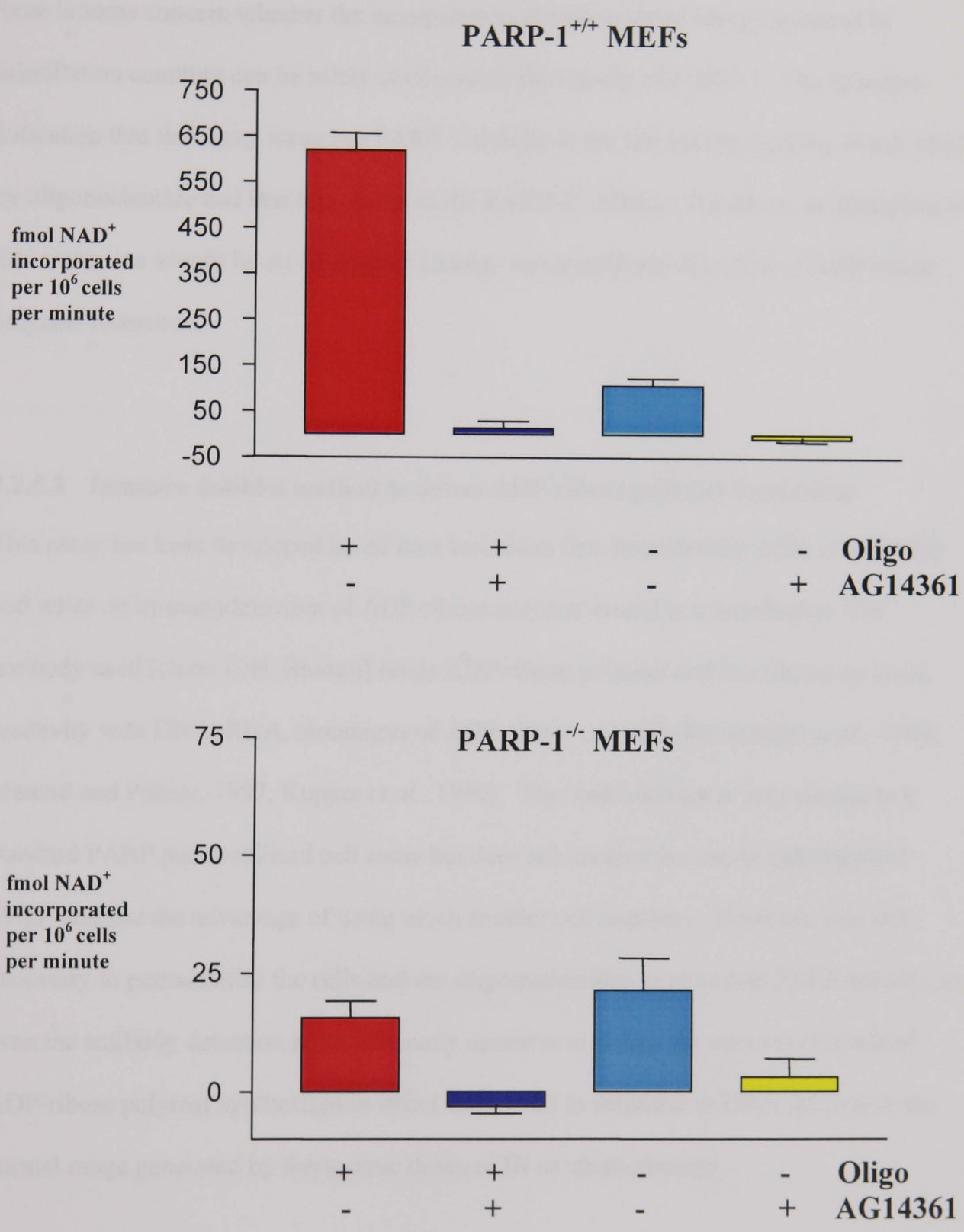


**Figure 3.5 PARP Permeabilised cell assay measuring the incorporation of radiolabelled $NAD^+$**
The results for PARP-$1^{+/+}$ MEFs are shown in the upper chart and the PARP-$1^{-/-}$ MEFs in the lower chart. Each set of results shows the effects of the presence or absence of double stranded oligonucleotide and 1μM AG14361 on PARP-1 activity.

Although this method is commonly used and effectively shows the inhibitory activity of AG14361, it does have limitations, which will be described in Section 3.3.2. For example, there is some concern whether the incorporation of radioactivity being measured by scintillation counting can be solely attributed to the activity of PARP-1. The strongest indication that this assay measures PARP-1 activity is the fact that the activity is activated by oligonucleotide and that it is absent in the PARP-$1^{-/-}$ MEFs. Therefore, confirmation of this assay was sought by an alternative strategy using antibody detection of ADP-ribose polymer formation.

### 3.2.5.2 Immuno dot-blot method to detect ADP-ribose polymer formation:

This assay has been developed based on a technique first described by Affar *et al* (1998) and relies on immunodetection of ADP-ribose polymer bound to a membrane. The antibody used (clone 10H, Biomol) binds ADP-ribose polymer and has shown no cross reactivity with DNA, RNA, monomers of ADP-ribose or NAD (Kawamitsu *et al.,* 1984; Menard and Poirier, 1987; Kupper *et al.,* 1990). The methodology is very similar to a standard PARP permeabilised cell assay but does not involve the use of radiolabelled $NAD^+$ and has the advantage of using much smaller cell numbers. However, it is still necessary to permeabilise the cells and use oligonucleotides to stimulate PARP activity, as even the antibody detection is insufficiently sensitive to detect the very small levels of ADP-ribose polymer synthesised in intact cells, even in response to DNA damage in the normal range generated by therapeutic doses of IR or chemotherapy.

Briefly, $5 \times 10^5$ cells were permeabilised, as before, in isotonic buffer supplemented with digitonin. Cells were then spun down and resuspended in a reaction buffer containing

$NAD^+$. Double-stranded oligonucleotide was also included in the reaction to stimulate PARP-1 activity. The reaction was performed at 30°C for 6 minutes and was stopped by the addition of an excess of AG14361 and transfer of the samples to ice. Samples were then vacuum aspirated onto Hybond-N membrane (Amersham) *via* a dot-blot manifold and the membrane probed with the clone 10H ADP-ribose polymer-specific mouse monoclonal antibody (full details of this method can be found in Section 2.8.2).

During the development and validation process, a variety of experimental factors have been varied. These included the concentrations of $NAD^+$ and oligonucleotide used as well as the number of cells bound to the membrane. In addition, purified ADP-ribose polymer has been used to show that the signal generated by ECL detection decreases with dilution of the polymer standard. The effect of each of these factors will be discussed in the section below. All initial experiments were performed on HCT-116 colorectal cells.

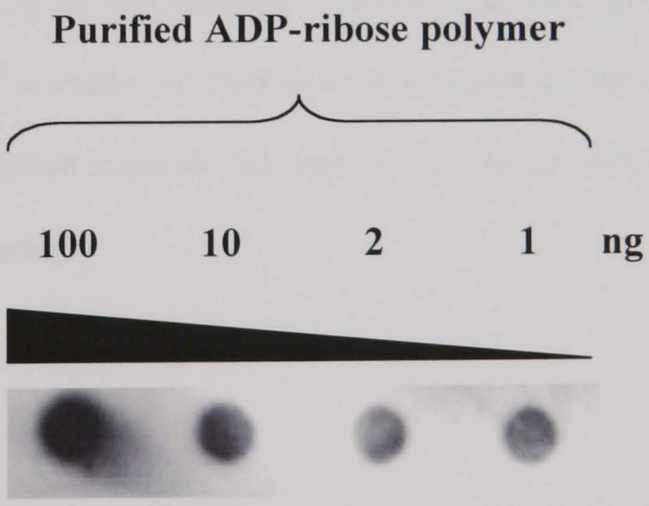


**Figure 3.6 Dot blot showing the ADP-ribose antibody used is sensitive to levels of purified polymer**

Figure 3.6 shows that the dot blot procedure is sensitive to detection of purified polymer. By diluting the polymer added to the membrane, the signal intensity of the dot is decreased, i.e. the signal intensity is dose-dependent.

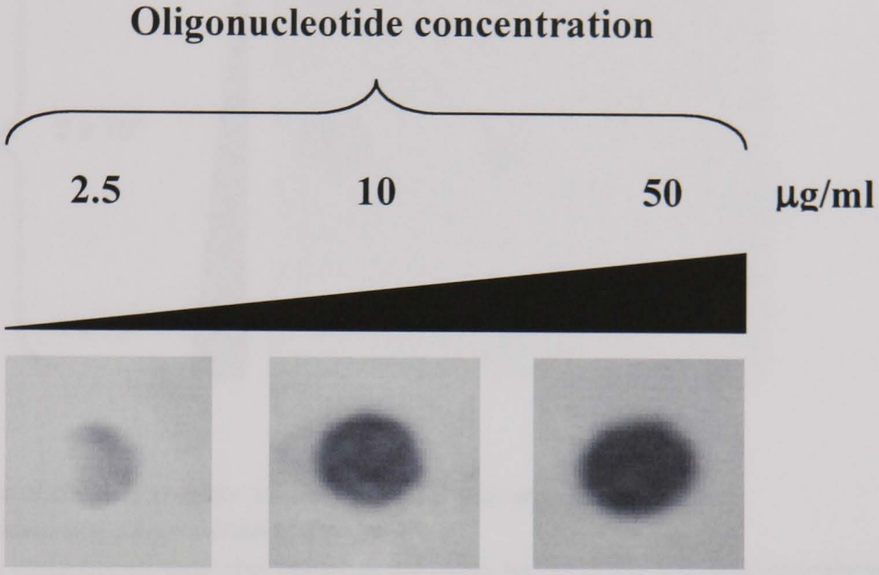


**Figure 3.7 Optimisation of oligonucleotide concentration**

Figure 3.7 shows that increasing the concentration of double stranded oligonucleotide results in an increase in signal intensity, attributable to an increase in PARP-1 activity. Based on this result, it was decided to use an oligonucleotide concentration of 50µg/ml in all subsequent dot-blot experiments.

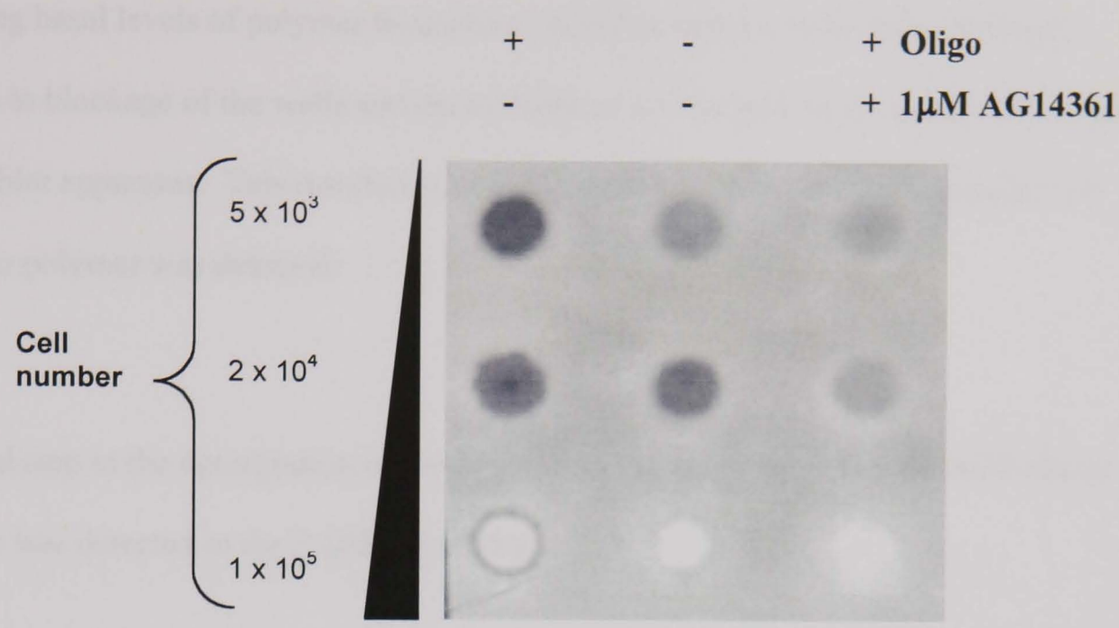


**Figure 3.8 Optimisation of the cell number added to the dot blot membrane**
Oligonucleotide was included at a concentration of 50μg/ml

The next factor to be optimised was the number of cells to be added to the membrane such that maximum sensitivity was achieved. The aim was to achieve maximum signal intensity in the + oligo sample, whilst maintaining maximum differentiation between these samples and the inhibitor-treated samples. Figure 3.8 shows that the optimum cell number appears to be 5000 as these samples clearly showed polymer formation in the oligonucleotide-treated samples. In addition, this polymer formation was abolished when 1μM AG14361 was included. Increasing cell number resulted in loss of this differentiation to a certain degree. This may be due to the oligonucleotide treated sample already being at a saturation point in terms of signal intensity. In addition, the samples without oligo show a basal level of ADP-ribose polymer formation, possibly as a consequence of the permeabilisation process, which has previously been shown to induce DNA strand breaks and hence activate PARP-1. Therefore, adding extra cells would only add to the basal levels of polymer being detected and hence the increase in signal intensity in the (–oligo) samples; but since the (+ oligo) signal was already saturated, leads to a loss of differentiation. This suggestion was further supported by the fact that AG14361 prevented this apparent increase in polymer

formation in the (–oligo +AG14361) samples (data not shown). This was due to AG14361 inhibiting basal levels of polymer formation. Addition of even more cells (100,000) resulted in blockage of the wells and the inability of the samples to be aspirated through the dot-blot apparatus. This resulted in no polymer being bound to the membrane and hence no polymer was detected.

The final step in the optimisation of the dot blot assay was to show that no ADP-ribose polymer was detected in the PARP-$1^{-/-}$ MEFs

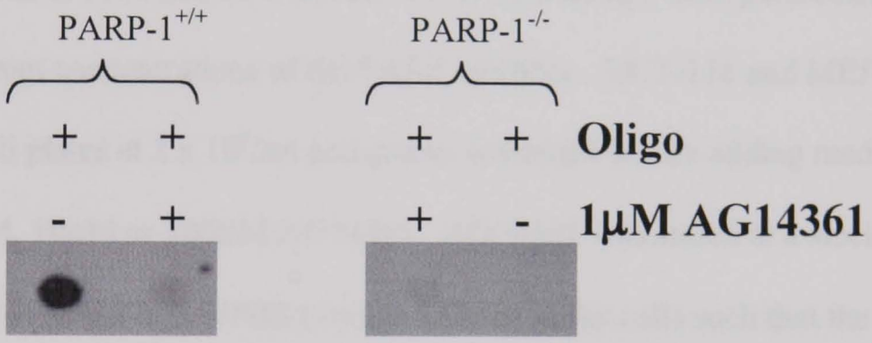


**Figure 3.9 Dot blot assay showing lack of ADP-ribose polymer formation in PARP-$1^{-/-}$ MEFs**

As can be seen in figure 3.9, little or no ADP-ribose polymer was formed in the PARP-1 knockout cells, even in the presence of oligonucleotide. PARP-1 proficient cell lines were also assayed in parallel to act as positive controls.

The above experiments confirm that the PARP-1 MEFs to be used in experiments are of the correct genotype and phenotype. In addition, treatment of cells with a potent PARP-1 inhibitor, AG14361 ($k_I < 6nM$) has been shown to be an effective alternative strategy for the removal of PARP activity from cells. Before using the inhibitor in DNA damage response experiments, it was necessary to show that AG14361 alone did not have an effect

on basal p53 levels over time. In addition, AG14361 should not have any effect on cellular growth during the course of the experiment, since it has been demonstrated through the construction of PARP-1 knockout mice that PARP-1 is not essential for normal development and growth. However, it is possible that the use of a chemical inhibitor of PARP-1 could have non-specific effects on the growth of cells.

### 3.2.6 Cytotoxicity studies of AG14361 alone

#### 3.2.6.1 SRB assays showing growth of cells after treatment with AG14361

To investigate the growth of cells treated with AG14361, SRB assays were performed on cells treated with different concentrations of the PARP inhibitor. HCT-116 and MEF cells were plated into 96-well plates at 2 x $10^4$/ml and grown overnight before adding medium containing 0.1μM, 1μM, 10μM or 100μM AG14361. AG14361 was stored at a stock concentration of 10μM in 10% DMSO/PBS (v/v) and added to the cells such that the final concentration of DMSO was 0.01 or 1%. In addition, plates contained two controls consisting of 0.01% and 1% DMSO. Plates were fixed at 24 hour time points (24h, 48h and 72h) before being washed and stained with SRB. The plates were analysed on a plate reader and the results plotted to show the effect of different concentrations of AG14361 on cell growth. As can be seen in figure 3.10, 1μM AG14361 (the concentration used in all subsequent DNA damage experiments) had no short-term effect on cell growth compared to the DMSO controls (0.01%). This was true for both PARP-1 MEFs and also HCT-116 colorectal cells. Higher concentrations of AG14361 (10 and 100μM) were growth inhibitory, due to some non-specific effects of the PARP inhibitor, which only become significant when AG14361 is used at a high concentration. It should be noted that the two higher concentrations of AG14361 had to contain a final DMSO of 1% for solubility

purposes. However, the lower concentrations of AG14361, 0.1 and 1μM contained a final DMSO concentration of 0.01% DMSO, as in the DNA damage experiments. Therefore, to control for possible effects of the DMSO, cells were grown in either 0.01% or 1% DMSO for comparison with the inhibitor treated cells.

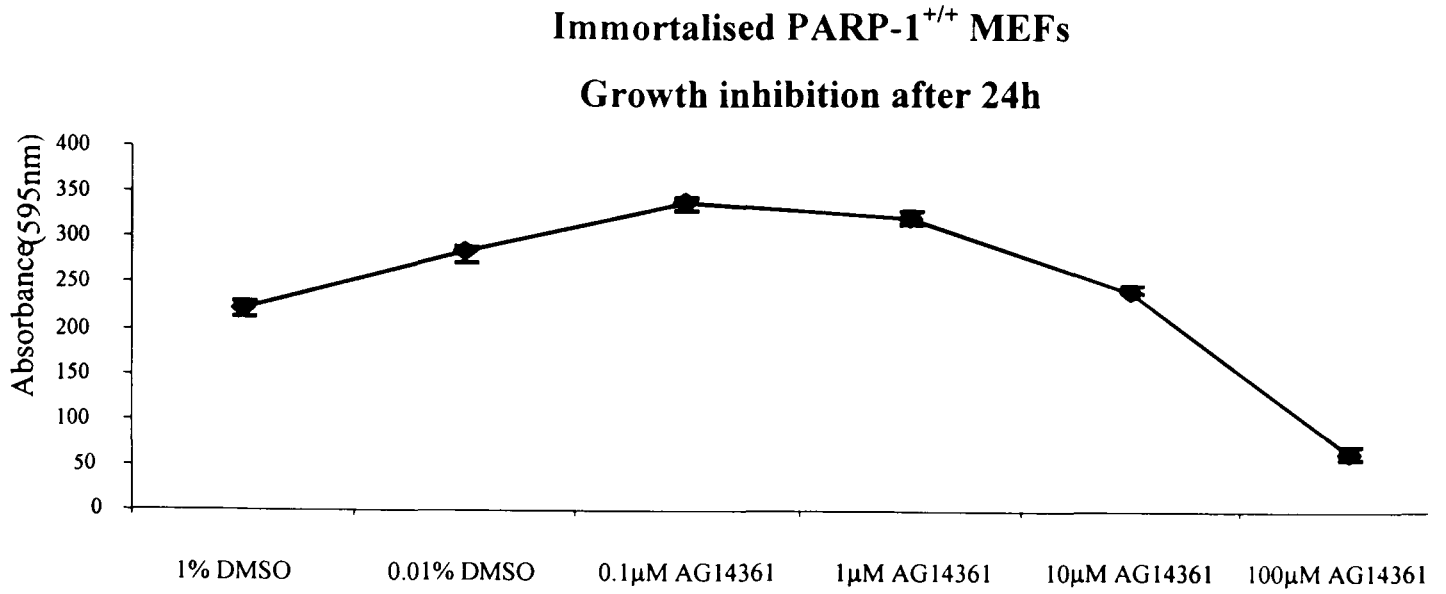


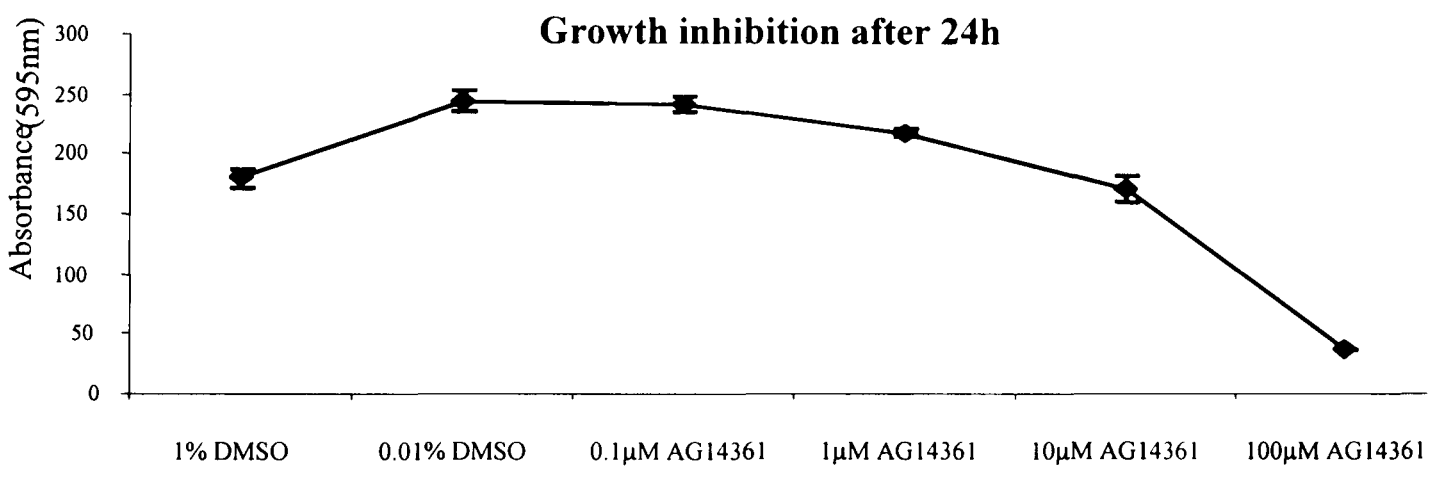


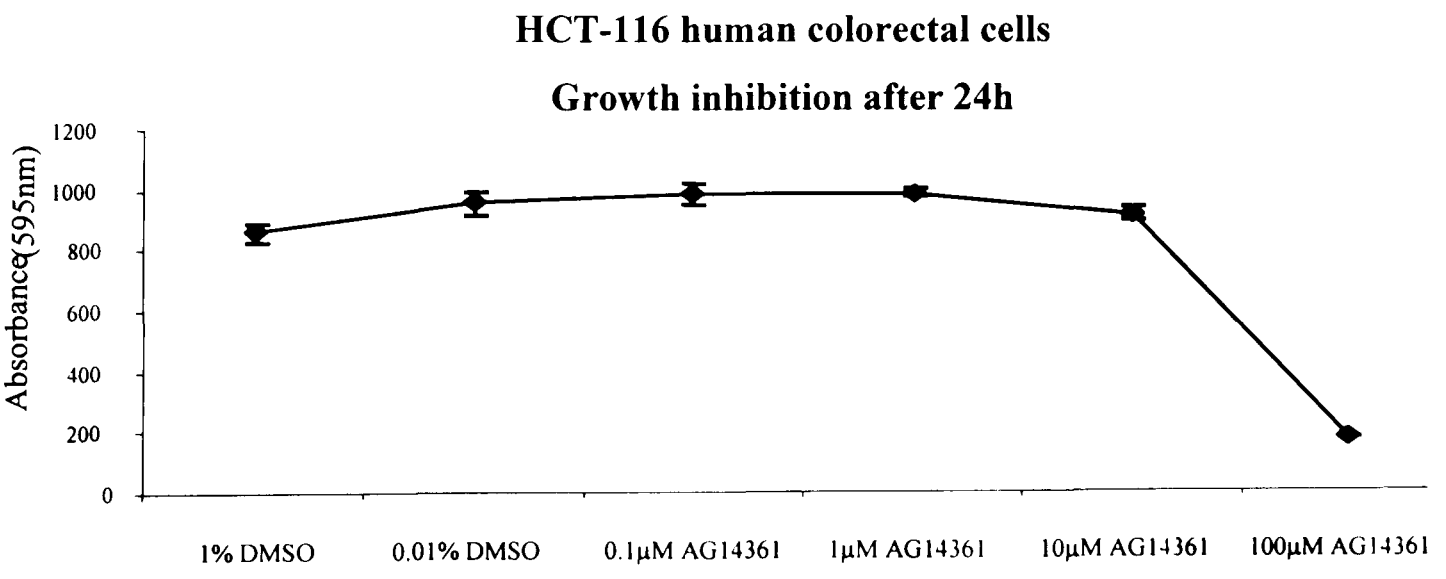


**Figure 3.10 SRB assays showing effect of 24 hours treatment with AG14361 on cellular growth**

### 3.2.6.2 Western blot showing basal p53 levels after AG14361 treatment

Western blot analysis of p53 levels was carried out at various time points after treatment of exponentially growing HCT-116 cells with 1μM AG14361. As can be seen in figure 3.11, AG14361 alone did not cause a change in p53 levels over a 24h period. In addition, no change was observed in the levels of the p53 target gene, mdm2 (results not shown). This suggests that AG14361 alone does not stress cells in any way that might result in an increase in p53 levels or its transcriptional activity. This information is obviously essential before including the compound in any experiments analysing p53 responses.

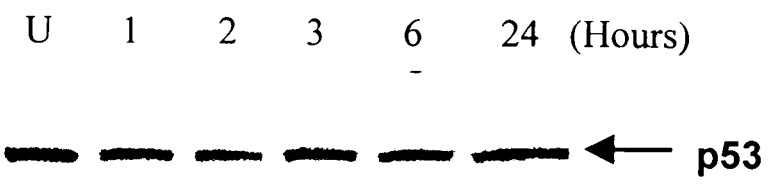


**Figure 3.11 Western blot analysis showing p53 levels over time after treatment of HCT-116 cells with 1μM AG14361**

## 3.3 Discussion

### 3.3.1 Summary of Results

The data presented in this chapter aimed to verify the techniques chosen to remove PARP-1 activity from cells. This involved confirming the genotype and phenotype of the PARP-1 MEFs, using Southern blotting and Western blotting, respectively. The data presented in this chapter confirmed the disruption of the PARP-1 gene in the knockout MEFs and Western blotting confirmed the lack of PARP-1 expression in these cells. A PARP permeabilised cell assay measuring the incorporation of [$^{32}$P]-NAD$^{+}$ into acid-precipitable material showed that the PARP-1$^{+/+}$ MEFs possessed a PARP activity that was stimulated by oligonucleotide. This activity was inhibited by including 1μM AG14361 in the assay. The same assay demonstrated that the PARP-1$^{-/-}$ MEFs possessed approximately 5% PARP

activity compared to their wild type counterparts. This activity was independent of added oligonucleotide but was also inhibited by AG14361. The effectiveness of AG14361 was also demonstrated in a different assay, using an immunoblotting technique for the measurement of ADP-ribose polymer. Finally, using SRB assays, 1μM AG14361 was shown to have no growth inhibitory effects during the time course of DNA damage experiments performed in the subsequent chapters (24h) . and did not alter the basal levels of p53 over the same time course.

### 3.3.2 Analysis of PARP permeabilised cell assay using radiolabelled $NAD^+$ in PARP-$1^{+/+}$ and PARP-$1^{-/-}$ MEFs

A PARP-permeabilized cell assay measuring the incorporation of counts from [$^{32}$P]-$NAD^+$ into acid-insoluble material showed that the PARP activity was >90% reduced in the PARP-$1^{-/-}$ MEFs, consistent with the disruption of the PARP-1 gene. However, it should be noted that the PARP-1 knockout cells did possess approximately 5% PARP activity, which cannot be attributed to PARP-1. It is likely that this activity is due to other members of the recently described PARP family, which now includes up to seven members (see Section 1.4.7).

This activity has been described previously in PARP-1 knockout MEFs (Shieh *et al.*, 1998), who showed that the residual activity was inducible by DNA damage. PARP- $1^{-/-}$ cells treated with 136μM MNNG were able to synthesise polymer, which was indistinguishable in structure to that synthesised in the PARP-1 wild-type cells. Also, this polymer production resulted in a decrease in intracellular $NAD^+$ concentration, suggesting that this activity is due to a PARP protein, but obviously not PARP-1. Interestingly, unlike the study mentioned above, the activity described here was not inducible by DNA ends.

However, it should be noted that Shieh *et al* used a different method for stimulating PARP activity, with damage to endogenous DNA being used rather than the introduction of an exogenous oligonucleotide. In addition Shieh and colleagues used a method for measuring PARP activity, which did not involve cellular permeabilization. Permeabilization has actually been shown to cause DNA damage and hence induce intracellular stress responses. Therefore, it is possible that the alternative PARP activity detected in this present study is a consequence of the permeabilization procedure, resulting in endogenous DNA damage. Alternatively, the oligonucleotide used in this study may not be suitable for the activation of the alternative PARP activity. Recent unpublished data in the Cancer Research Unit suggests that the oligonucleotide used (10 bp) is incapable of activating DNA-PK, which is known to be activated by DNA ends. Instead it was necessary to use a longer oligonucleotide to efficiently activate this kinase (Stephany Veuger, unpublished results). However, what is not in doubt is that the PARP-$1^{-/-}$ cells possess an alternative PARP activity, distinct from PARP-1, which is also inhibited by the PARP-1 inhibitor, AG14361.

Subsequent studies have attributed this activity to PARP-2 (Ame *et al.*, 1999), which was shown to be inducible by both DNA strand breaks and DNA damage. Another group assigned this activity to an alternative product of the PARP-1 gene, called sPARP-1 which lacks the DNA binding domain and as such has activity that is independent of strand breaks but can be induced by DNA damage (Sallmann *et al.*, 2000). The cloned cDNA for this PARP protein was identical to the catalytic domain of PARP-1 and consisted of 1732 base pairs. The authors proposed that sPARP-1 was produced by transcription of the PARP-1 gene from an alternative transcription start site, downstream of the disrupted area of exon 2 in these particular PARP-$1^{-/-}$ MEFs. Importantly, in the exon 4 PARP-1 knockout MEFs used in this thesis, the disrupted area of the PARP-1 gene is also upstream

of this putative alternative transcription start site. Therefore, sPARP-1 could, in theory, be produced in these cells. The characteristics of sPARP-1 described by Sallmann *et al.*, 2000 are more concurrent with the data presented here, however no specific attempts have been made to identify the enzyme responsible for the activity in the knockout cells used in this study. It should be noted that the PARP-1 antibody used, H-250, was raised against a C-terminal epitope of PARP-1 and should therefore detect any sPARP-1 present within cells. However, no such protein was detected in any of the cell lines used in this study (data not shown).

It is important to note, in terms of the interpretation of results, that 1μM AG14361 was able to inhibit the PARP activity in both the PARP-1 proficient and deficient MEFs. Assuming that the PARP activity detected in the PARP-$1^{-/-}$ MEFs is also present in the PARP-$1^{+/+}$ MEFs, then when the latter cells are treated with AG14361, more than one PARP activity is being inhibited. More specifically, PARP-1 will be inhibited, as will the other 'PARP activity' that has been detected in the PARP-1 knockout cells. Therefore, any effect observed in PARP-$1^{+/+}$ MEFs cannot automatically be attributed to PARP-1. However, the involvement of PARP-1 could be demonstrated if the effect was observed in the PARP-1 knockout MEFs. It will also be possible to determine whether the alternative PARP activity detected in the PARP-$1^{-/-}$ MEFs is involved in p53 regulation by treating these cells with AG14361 and DNA damage. In this situation, the alternative PARP activity will be inhibited and any effects observed cannot be due to PARP-1 in these cells. As the PARP activity in the PARP-$1^{-/-}$ MEFs has not yet been assigned to a particular PARP enzyme, only general conclusions can be derived.

As described in a previous section (Section 1.4.7), the PARP family members share significant sequence homology within the catalytic domain. As such, it is perhaps not surprising that an inhibitor that is competitive for $NAD^+$ binding to the catalytic domain of PARP-1, is also able to inhibit the catalytic activity of other PARP enzymes.

Having discussed the implications of treating PARP-1 proficient and deficient MEFs with AG14361, it should be noted at this stage that knocking out PARP-1 and its inhibition are two distinct phenomena. When inhibited, PARP-1 is still able to bind DNA strand breaks. However, it is likely to bind strand breaks permanently as it cannot perform its catalytic function and therefore cannot automodify itself and dissociate from the DNA. In PARP-$1^{-/-}$ knockout cells, there is no PARP-1 protein present and hence DNA strand breaks will remain vacant or will be occupied by other DNA-binding proteins. These facts will need to be considered when analysing any results.

### 3.3.3 Development of a PARP permeabilised cell assay using antibody detection of ADP-ribose polymer

The technique commonly used for the estimation of PARP activity (discussed in the previous section) has some limitations. For example, each sample requires 1 x $10^6$ cells. As each reaction is performed in triplicate, this means a minimum of 6 x $10^6$ cells are required for a simple +/- AG14361 inhibitor experiment. In addition, there is some concern whether the counts being measured by scintillation counting can be solely attributed to the activity of PARP-1. It is possible that other $NAD^+$-utilising metabolic pathways are responsible for some of the 'PARP activity' being measured. For example, ADP-ribosylation reactions are also carried out by mono(ADP-ribosyl) transferases and $NAD^+$ glycohydrolases, as well as other members of the PARP-1 family (e.g. PARP-2, V-

PARP etc). Therefore, some of the activity measured may be as a consequence of these enzymes rather than PARP-1. Also, where possible it is best to eliminate the use of radioactivity in experiments, for improved safety reasons and to reduce the disposal of radioactive waste. Finally, although label from the ADP-ribose moiety of NAD is incorporated into acid-insoluble counts, this does not itself constitute proof of ADP-ribose polymer formation. Therefore, a non-radioactive, immunoblotting method for the measurement of ADP-ribose polymer has been developed and validated.

The technique developed involves the permeabilisation of cells and activation of PARP-1 by oligonucleotide. However, non-radiolabelled NAD is used in the assay. To measure PARP-1 activity, samples are blotted onto membrane and an antibody used to detect the levels of ADP-ribose polymer synthesised in the individual reactions. As shown in Figure 3.6 the detection method for the assay was sensitive to purified polymer, with the intensity of dot changing in accordance with the amount of polymer bound to the membrane. In addition, no ADP-ribose polymer was detectable in the PARP-1 knockout cells and only in PARP-1 wild type cells treated with oligonucleotide was there any significant detectable polymer formation. There is a small amount of antibody binding evident, even in the presence of AG14361. This may be non-specific antibody binding, or because only de novo synthesis of polymer is inhibited in the actual assay, any pre-existing polymer in the cells prior to permeabilisation will not be affected.

One of the major benefits of this new method is that each reaction is performed on $5 \times 10^3$ cells, which is $1/20^{th}$ of the cell number required for the radiolabelled $NAD^+$ method. In addition, studies have shown that 5000 cells (or less) are the optimal number bound to the

membrane to allow detection of polymer without increasing the background signal too much. Therefore, it may be possible to scale down further the number of cells used per experiment. Affar *et al.*, 1998 used a 24-well dot-blot manifold and as such had to load more cells (up to 250,000) per well to optimise the signal.

As well as proving very useful throughout this project, this technique is now being optimised in the Cancer Research Unit for use in clinical trials of potent PARP-1 inhibitors, where patients are treated with PARP-1 inhibitors to potentiate the effects of chemo- and radio-therapy in tumour cells. Blood samples will be taken and peripheral blood lymphocytes of treated patients analysed to confirm inhibition of PARP-1 by the inhibitors. The relatively small amount of blood that can be taken from patients during sampling meant that the development of a technique involving smaller cell numbers was essential. Also, the optimisation of this technique for a 96-well format allows the testing of many samples during a single experiement.

The results above show that the immortalised PARP-1 MEFs can be used as a paired cell line, which are proficient and deficient in PARP-1. The effect of PARP-1 protein and activity on the DNA damage-induced p53 response can be analysed using these cell lines.

In addition to characterizing the PARP-1 MEFs, this chapter also aimed to show the effectiveness of AG14361 as an alternative strategy for the removal of PARP-1 activity. Results have been presented showing that AG14361 itself did not alter p53 levels or activity over time. Also, SRB assays showed that 1μM AG14361 was not growth inhibitory during the time course of the planned experiments. These observations are

essential when using the compound to analyse any modification of the DNA damage-inducible p53 response. As described in Sections 3.3.2 and 3.3.3, 1μM AG14361 also effectively inhibited PARP-1 activity in the assays described.

The results in this chapter have comprehensively characterized the PARP-1 MEFs as well as the PARP inhibitor AG14361. Both gene knockout and inhibitor strategies have been employed to remove PARP activity from cells in DNA damage response experiments, the results of which will be presented in the following chapter.

# CHAPTER 4

# P53 STATUS OF IMMORTALISED MEFS AND THE DERIVATION OF A PARP-1 STABLE TRANSFECTANT CELL LINE

## 4.1 Introduction and objectives:

A summary of data suggesting a functional relationship between PARP-1 and p53 has been presented in Chapter 1, Section 1.4.6. As described, different groups obtained apparently conflicting results when analysing the DNA damage-induced p53 response in the presence and absence of PARP-1. The principal aim of this thesis was to use both PARP-1 knockout cells and a novel potent PARP-1 inhibitor, AG14361, to remove PARP activity from cells and to analyse the DNA damage induced p53 response. However, it became apparent from initial DNA damaging experiments in this study that the immortalised PARP-$1^{+/+}$ MEFs were probably expressing mutant p53 whereas the PARP-1 knockout cells were expressing wild type p53. A second independently derived spontaneously immortalised MEF cell line pair was generated, but subsequent analysis revealed the same pattern in terms of p53 status in these cells.

Based on these results it appeared that the PARP-$1^{+/+}$ MEFs tend to develop p53 mutations during immortalisation whereas the PARP-$1^{-/-}$ MEFs do not. It was therefore decided that it may be futile to immortalise any further MEFs if the p53 in the PARP-$1^{+/+}$ cells was likely to become mutated. One option available was to perform experiments on primary MEFs. However, these cells have a substantially slower growth rate than immortalised cells (see Chapter 6) and are also more difficult to transfect. Transfection is an essential component of the luciferase reporter gene system, which was to be used to measure p53 activity. It was therefore decided to stably transfect the immortalised PARP-$1^{-/-}$ MEFs, which possessed wild-type p53, with a construct that expresses PARP-1. This would hopefully lead to the production of a paired cell line proficient and deficient in PARP-1 with wild type p53. In addition, these immortalised cells would grow well and be suitable for transfection studies using the reporter gene assay. Finally, and perhaps most importantly, the cell line pair would have identical genetic backgrounds, except of course for the stable transfected plasmid expressing PARP-1 protein.

Therefore, due to the mutant p53 status in the PARP-$1^{+/+}$ MEFs, the aim of this chapter was to produce a cell line pair proficient and deficient in PARP-1 that both expressed wild type p53. This was achieved by stable transfection of PARP-1 into the PARP-$1^{-/-}$ MEFs. This chapter also contains sequencing data concerning the p53 status (mutant or wild-type) of the immortalised MEFs. In addition, results are shown demonstrating the production of a PARP-1 stable transfectant, which has been validated in terms of PARP-1 expression and activity.

## 4.2 Results

### 4.2.1 The response of PARP-$1^{+/+}$ and PARP-$1^{-/-}$ MEFs to IR and UV

PARP-1 +/+ and -/- MEFs were plated at 5 x $10^5$ cells in 60mm tissue culture plates and incubated at 37°C for 24 hours. The cells were then treated with 2, 5 and 10Gy IR and 20, 50 and 100J/$m^2$ UV. Samples were taken after 3, 6 and 24h as well as an untreated (control) sample. Western blot analysis was performed on all cell lysates and the membranes probed for p53, mdm2, PARP-1 and actin (as a protein loading control), see figure 4.1.

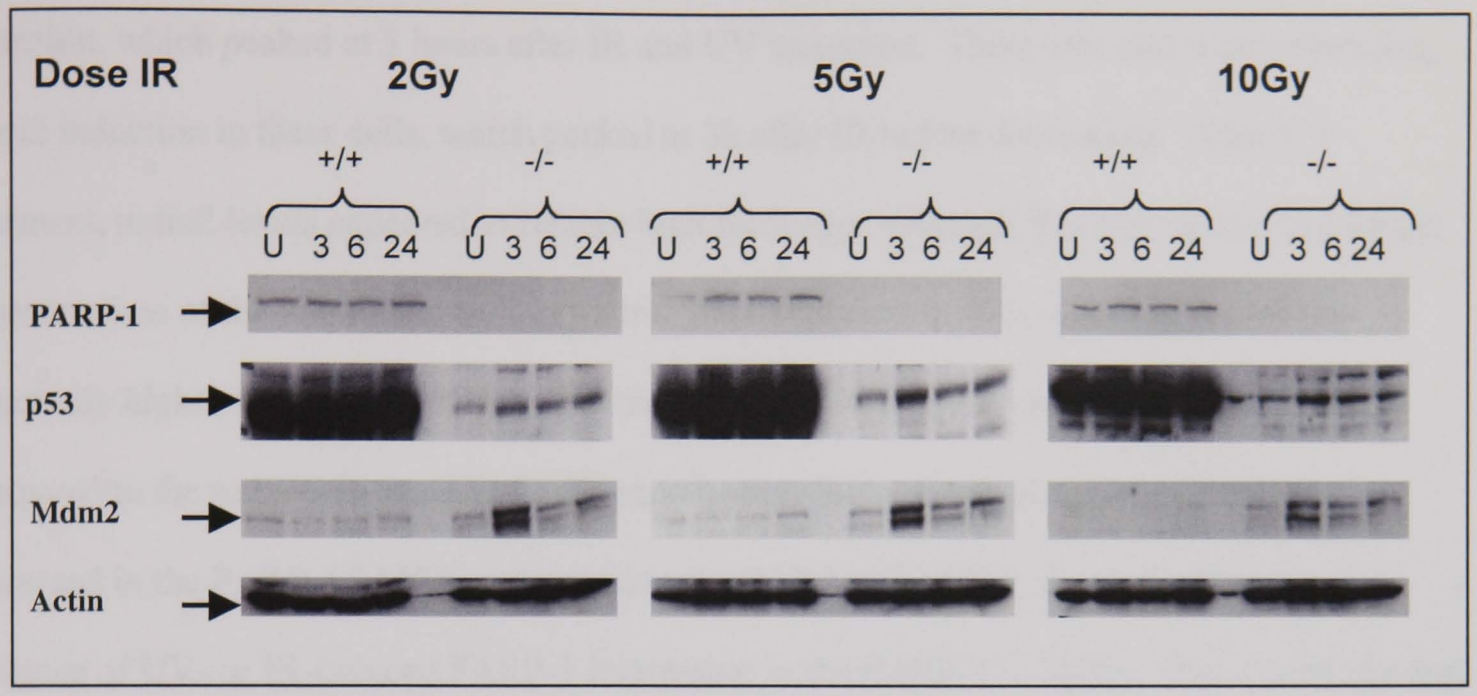


**Figure 4.1 Western blot analysis of immortalised PARP-1 MEFs in response to IR and UV.**

An initial observation from the Western blots was the very high levels of p53 in the PARP-$1^{+/+}$ cells. There was no apparent p53 induction in these cells, and despite the high p53 levels, there were only low levels of mdm2, which were not induced. This was true for both of the DNA damaging agents used at all doses. These observations are consistent with the expression of a

mutant and functionally inactivated p53. In contrast, the PARP-$1^{-/-}$ MEFs showed a p53 induction, which peaked at 3 hours after IR and UV treatment. There was also a corresponding mdm2 induction in these cells, which peaked at 3h after IR before decreasing. After UV treatment, mdm2 levels appeared to remain high for longer although this may be due to a longer exposure time of the membrane to X-ray film. This explanation is in accordance with the apparently higher basal levels of mdm2 in the PARP-$1^{-/-}$ MEFs used in the UV experiment compared to the same cells used in the IR experiment. Importantly, there is no PARP-1 expressed in the PARP-$1^{-/-}$ MEFs compared to the PARP-$1^{+/+}$ MEFs. Nor was there any evidence of UV- or IR-induced PARP-1 expression in the PARP-$1^{+/+}$ MEFs. The hypothesis that the PARP-$1^{+/+}$ MEFs were expressing mutant p53 was investigated by sequencing the p53 in these cells. The p53 in the PARP-$1^{-/-}$ MEFs was also analysed.

cDNA sequencing was performed according to the method described in Section 2.10. As can be seen below (figure 4.2), the results confirmed that the PARP-$1^{+/+}$ MEFs were expressing a mutant p53, with a single G to C base change in codon 278 producing an Asp to Glu amino acid substitution (GAC to GAG codon change). Codon 278 is within the DNA binding domain of p53 and a mutation in this area would be consistent with the observed lack of p53 target gene transactivation (i.e. the lack of mdm2 induction observed in figure 4.1). In addition, lack of mdm2 transactivation would mean less mdm2 mediated degradation of p53 and hence this would explain the very high p53 levels observed. The PARP-$1^{-/-}$ MEFs were found to express wild type p53, again consistent with the observed p53 induction by DNA damage (figure 4.1).

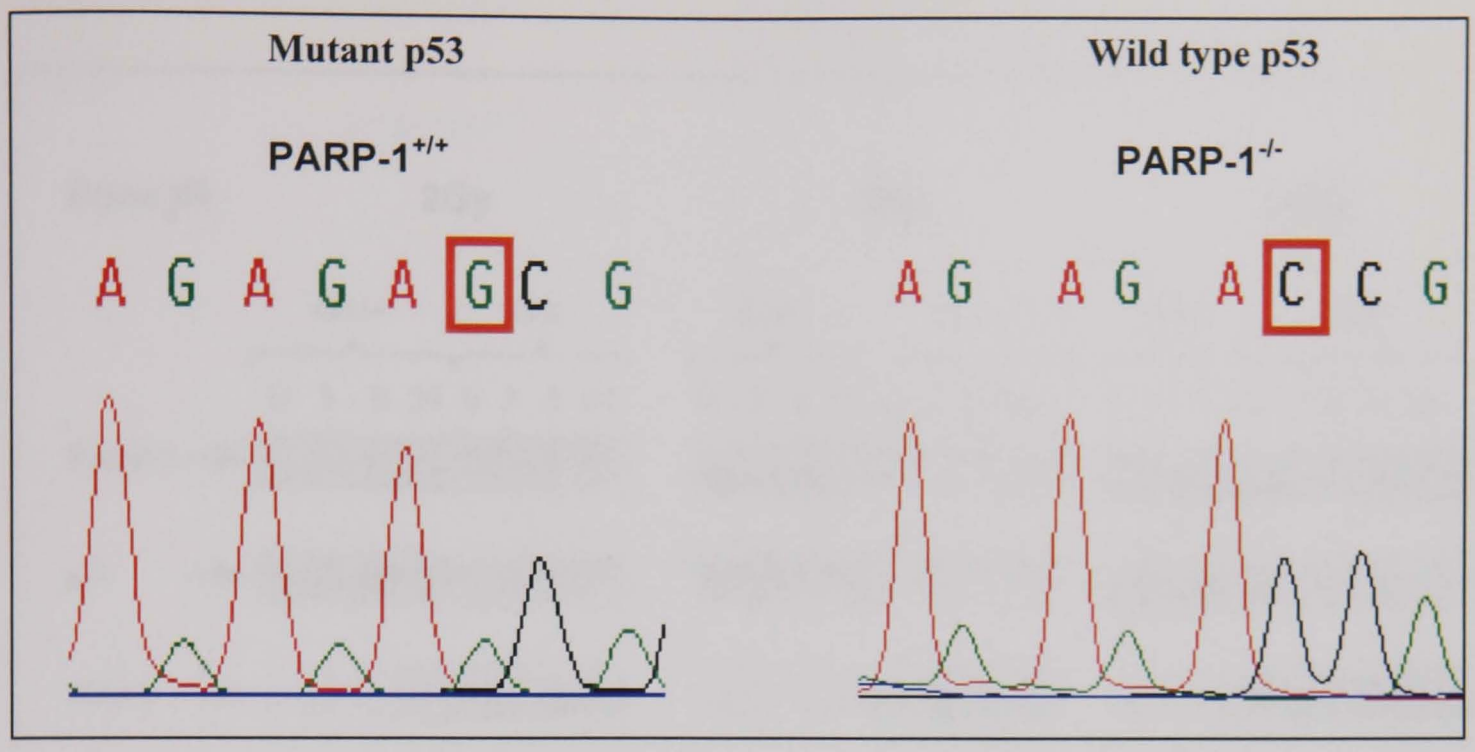


**Figure 4.2 Sequencing data highlighting the p53 mutation in the immortalised PARP-1$^{+/+}$ MEFs.** Mutation highlighted is a C – G change within codon 278, producing an Asp to Glu amino acid change (GAC to GAG codon change). PARP-1$^{-/-}$ MEFs express wild type p53.

Due to the presence of a p53 mutation in the immortalised PARP-1$^{+/+}$ MEFs, the above DNA damage experiments were repeated in a second independently derived immortalized MEF cell line pair from the same Gilbert de Murcia derived PARP-1 knockout mice (which will be hereafter be referred to as GPARP-1$^{+/+}$ and GPARP-1$^{-/-}$). Western blots and enzyme assays confirmed the lack of PARP-1 expression and activity in the GPARP-1$^{-/-}$ cells (data not shown). Unexpectedly, Western blot analysis in response to IR (figure 4.3) produced a very similar pattern of p53 and mdm2 induction as the previously described immortalized MEFs (figure 4.1).

Again, the PARP-1$^{+/+}$ MEFs showed very high levels of p53, no apparent induction and lack of p53 target gene (mdm2) transactivation, whereas again the PARP-1$^{-/-}$ cells showed both p53 and mdm2 induction, indicative of wild type p53.

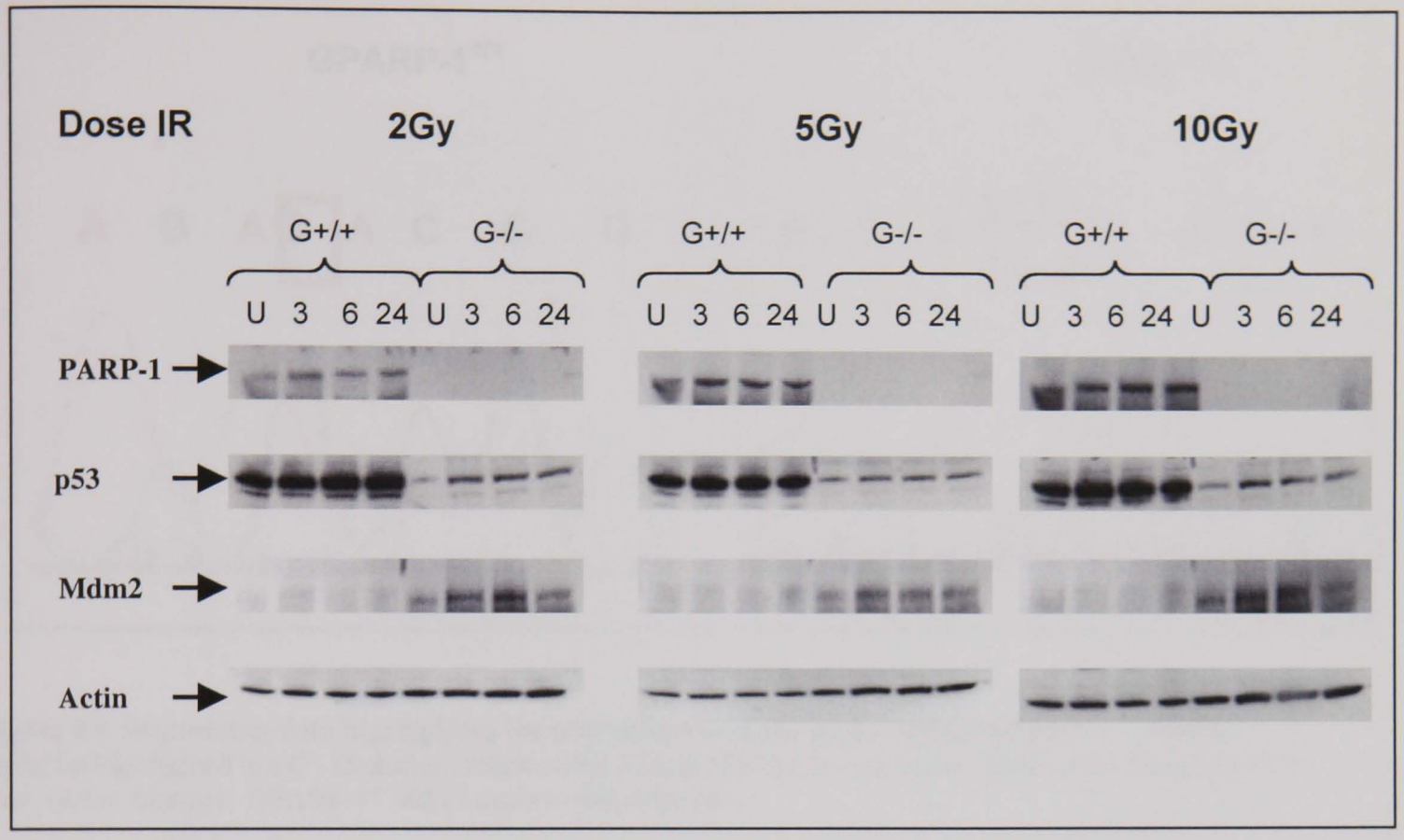


**Figure 4.3 Western blot analysis of GPARP-1 MEFs in response to IR.**
As for the other pair of immortalised MEFs, the GPARP-$1^{+/+}$ MEFs express a p53 with mutant characteristics whereas the GPARP-$1^{-/-}$ MEFs have p53 with wild type characteristics.

Subsequent cDNA sequencing of the p53 in the GPARP-1 MEFs revealed a mutant p53 in the GPARP-$1^{+/+}$ MEFs and a wild type p53 in the GPARP-$1^{-/-}$ MEFs (figure 4.4). Interestingly, this mutation was also in codon 278 but with a C to G base change, resulting in an amino acid change of Asp to Gln (GAC to CAC codon change).

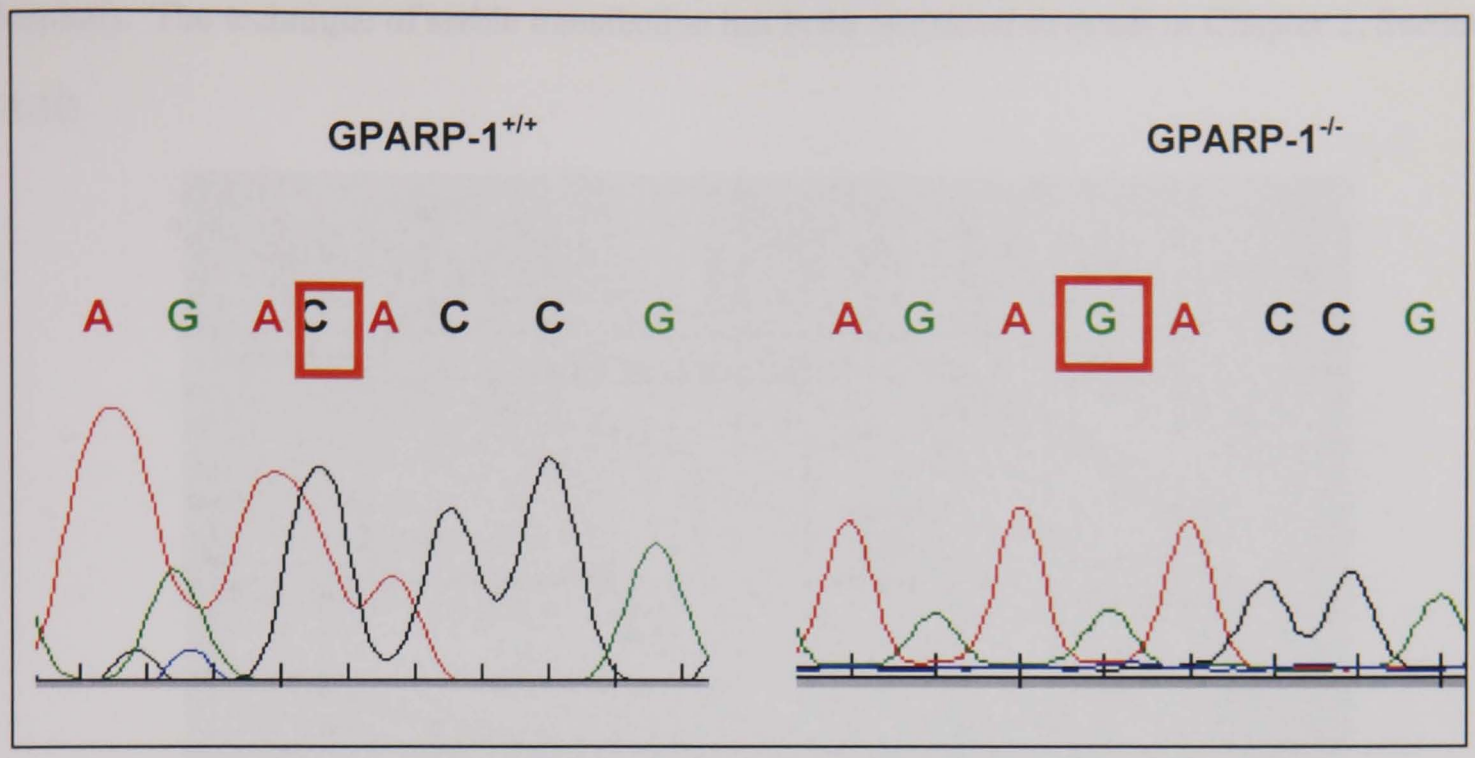


**Figure 4.4 Sequencing data highlighting the p53 mutation in the immortalised GPARP-1$^{+/+}$ MEFs.** Mutation highlighted is a C - G change within codon 278, producing an Asp to Gln amino acid change (GAC to CAC codon change). GPARP-1$^{-/-}$ MEFs express wild type p53.

This suggested the interesting possibility that PARP-1$^{+/+}$ MEFs tend to develop p53 mutations during immortalisation, but PARP-1$^{-/-}$ MEFs do not develop such mutations. This was investigated further in chapter 6. However, for the purposes of comparing the DNA damage induced p53 response in PARP-1$^{+/+}$ and PARP-1$^{-/-}$ MEFs, it was decided to stably transfect the wt p53 PARP-1$^{-/-}$ MEFs with a PARP-1 expression construct, as a means to generate a PARP-1 expressing immortalised MEF cell line.

### 4.2.2 The stable transfection of PARP-1$^{-/-}$ MEFs with a plasmid construct expressing PARP-1

The plasmid construct contained a 3.1kb fragment corresponding to human PARP-1 cDNA (van Gool *et al.*, 1997). This sequence has been inserted into a eukaryotic expression vector, downstream of a CMV promoter (figure 4.5; van Goole *et al.*, 1997). The plasmid (pPARP31) was kindly provided by Alexander Burkle (Department of Gerontology, Newcastle General

Hospital). The technique of stable transfection has been discussed in detail in Chapter 2, Section 2.1.10.

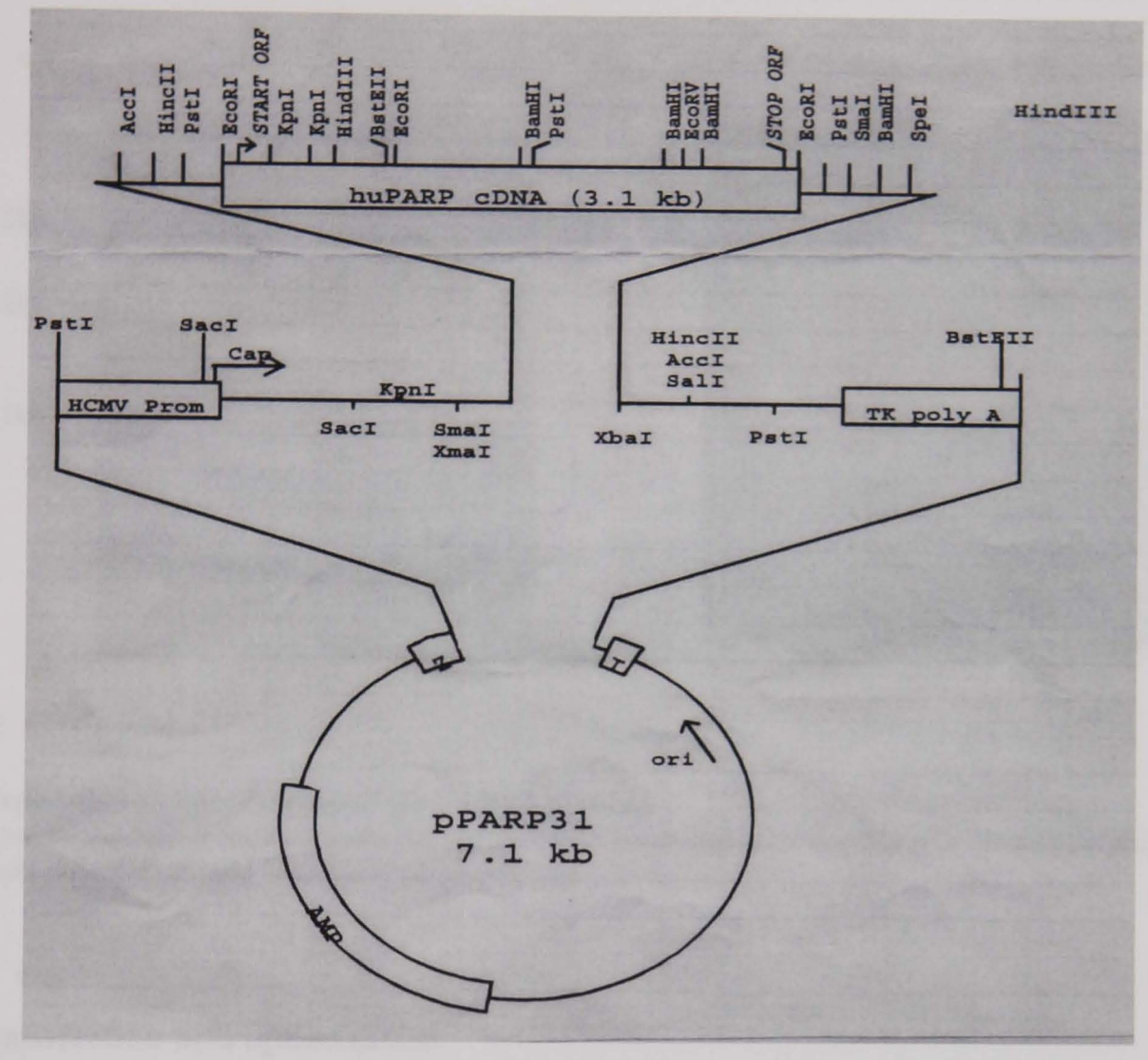


**Figure 4.5 Plasmid map of pPARP31**

### 4.2.3 Preparation of plasmid

The first step in the process of stable transfection was the preparation and purification of the pPARP31 plasmid, according to the methods described in Chapter 2, Section 2.2.1 To confirm isolation of the plasmid, it was subjected to *Eco*RI digestion and the products analysed by electrophoresis on a 0.8% agarose gel (Figure 4.6). The size of the resultant DNA fragments was estimated and should correspond to the predicted fragment sizes from the plasmid map (3.1, 2.0 and 1.1kb) The plasmid was diluted to 0.5µg/ml in distilled water and stored at –20°C.

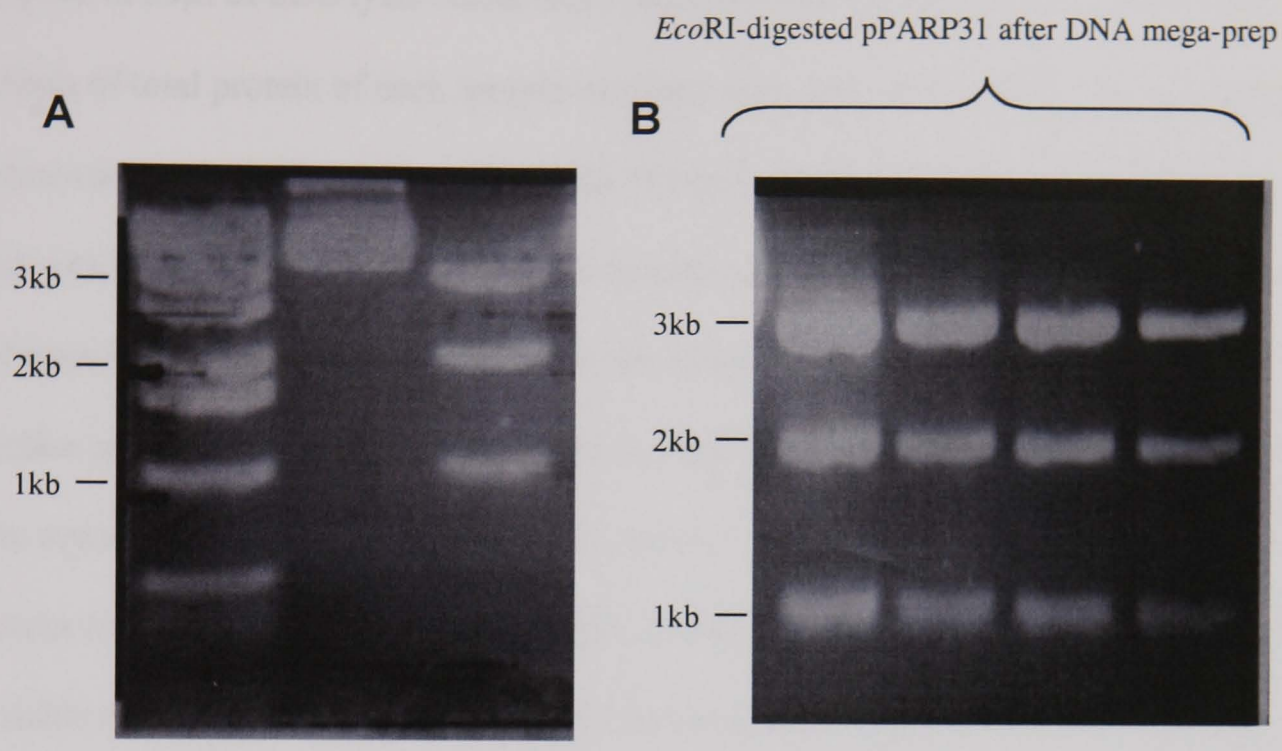


**Figure 4.6 Preparation and purification of the PARP-1 plasmid**
A. *Eco*RI digestion of plasmid showing isolation of the correct sized fragments according to the plasmid map. B. Sample of *Eco*RI digested plasmid after DNA Mega-prep (QIAGEN)

### 4.2.4 Transfection and optimisation

The conditions required for efficient transfection and hence expression of a plasmid differ, depending both upon the size of the plasmid and also the particular cell line to be transfected. Perhaps the most important factor is the ratio of the volume of transfection reagent used (FuGENE 6) to the amount of plasmid DNA, as it is the transfection reagent which acts as the 'vehicle' for transport of the plasmid DNA into cells.

PARP-$1^{-/-}$ MEFs were plated out at 1.5 x $10^5$ cells into 35mm tissue culture plates and grown for 24 hours. The cells were then transfected with the plasmid at three different ratios of transfection reagent (µl):DNA(µg). The ratios chosen were 3:2, 3:1 and 6:1, as recommended in the manufacturers protocol. Three blank plates were also transfected with an empty vector (i.e.

not containing the PARP-1 insert) at the same ratios. After 24 hours incubation, the six plates of cells were lysed in 50µl of SDS lysis buffer and a protein assay performed on the individual samples. 50µg of total protein of each sample was then separated on a 4-20% polyacrylamide gel before transfer to nitrocellulose membrane for Western blot analysis. The membrane was then probed with an anti-PARP-1 rabbit polyclonal antibody. As can be seen in Figure 4.7, the 3:2 ratio of transfection reagent:DNA resulted in the highest expression of PARP-1, with a gradual decline in expression when the ratio was increased. There is a slight difference in size between the transfected PARP-1 and the positive control, likely due to the purified positive control protein containing a tag to aid purification. It was therefore decided to use a 3:2 ratio in the actual stable transfection procedure to try and ensure good expression levels of PARP-1. As expected, the three blank samples contained no PARP-1.

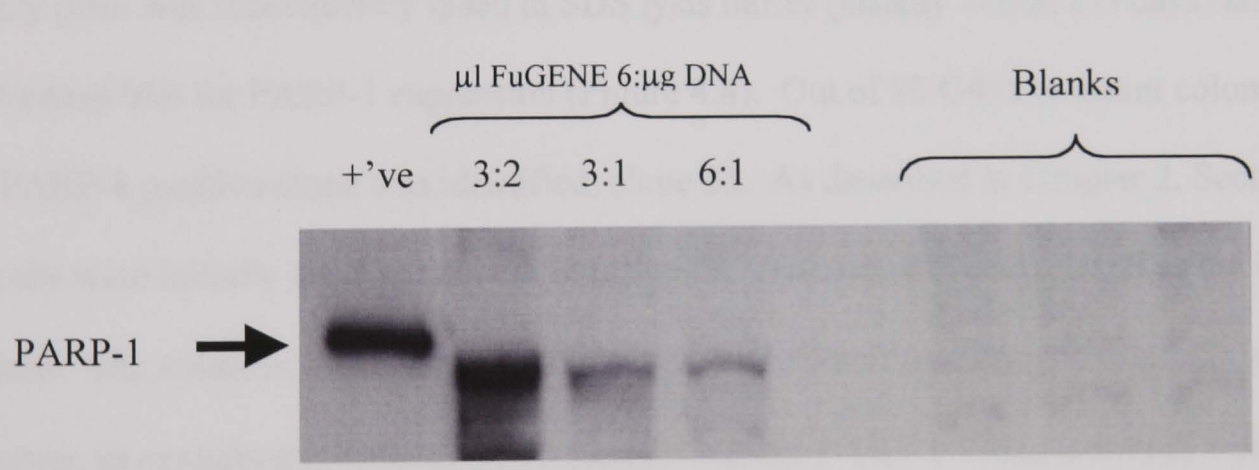


**Figure 4.7 Optimisation of the transfection conditions.**
Western blot showing levels of PARP-1 protein 24h post-transfection. The lanes show the effect of different ratios of FuGENE 6 (µl):µg of plasmid DNA used (lanes 2 – 4). Purified PARP-1 was used as a positive control (lane 1). Blanks consisted of PARP-$1^{-/-}$ MEFs transfected with an empty vector using the previously described FuGENE 6 :DNA ratios.

Stable transfection of the PARP-$1^{-/-}$ MEFs was achieved using the conditions described above. The cells were seeded onto two 35mm plates and transfected as before. It should be noted that the stable transfection procedure also included a co-transfected plasmid containing a neomycin (geneticin/G418) resistance gene (pCR3 plasmid) to select for transfected cells. After 24 hours

incubation in transfection mixture, the cells were trypsinised and counted before plating various numbers of cells into 15cm tissue culture plates, containing 600μg/ml G418. The cell numbers plated out were 100, 1000 and 10000. The aim of plating out low numbers of cells is that a colony will grow from a single cell and if this initial cell is stably transfected, a homogenous population of cells should be produced. In addition, it is important to be able to isolate individual colonies of cells. If a plate contains too many cells it may become impossible to isolate a single colony without contaminating the population with cells from a neighbouring colony. After approximately 10-14 days, colonies were present on the plates and were isolated using sterile cloning rings followed by trypsinisation. The cells were placed initially into a well of a 24 well tissue culture plate. When suitably confluent, they were transferred to two 35mm tissue culture plates, with the cells being split at 75% and 25% into the two plates. The higher density plate was subsequently lysed in SDS lysis buffer (usually within 2-3 days) and analysed by Western blot for PARP-1 expression (Figure 4.8). Out of 98 G418 resistant colonies isolated, one PARP-1 positive clone was identified, clone 23. As described in Chapter 2, Section 2.1.10, the cells were initially transfected with a neomycin resistance plasmid as well as the PARP-1 plasmid. The colonies were subsequently grown in medium containing 600μg/ml geneticin. However, as explained in Chapter 2, Section 2.1.10, the PARP-$1^{-/-}$ MEFs already contain a neomycin resistance cassette and hence will already be resistant to the antibiotic used. This may be the reason for isolating only one positive colony. Because of this oversight, it has also been necessary to perform additional experiments to confirm the homogeneity of the isolated stable transfectant and also to rule out the possibility of cross contamination by an alternative PARP-$1^{+/+}$ cell line. The positive clone was grown to sufficient numbers before re-plating the cells out for colonies, as before. This was to ensure that the stable transfectant cell line was indeed a homogenous population of cells, all expressing PARP-1. Several colonies were again isolated and analysed for PARP-1 expression using Western blotting (figure 4.8). All colonies isolated

were positive for PARP-1 and were grown for several weeks before freezing of 1 x $10^6$ aliquots of cells in liquid nitrogen.

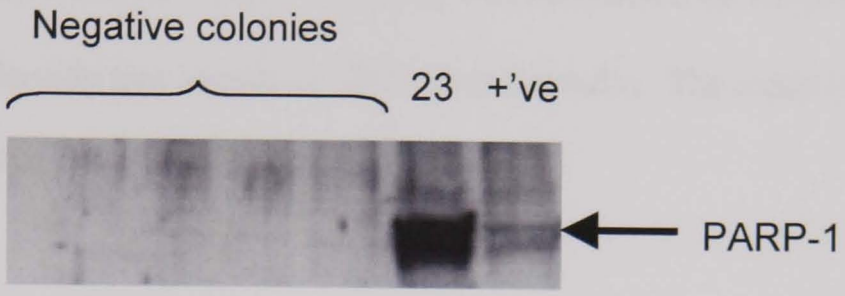


**Figure 4.8 Western blot showing identification of a positive clone for PARP-1 expression**

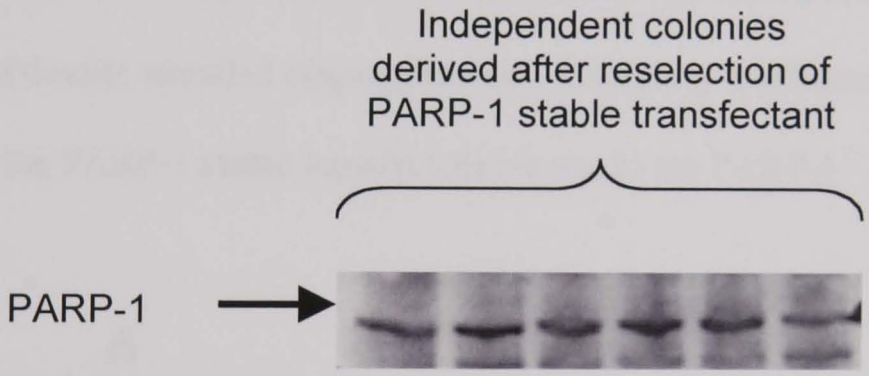


**Figure 4.9 Reselection of colonies confirming homogenous population of PARP-1 stably transfected cells**
Western blot analysis of six independent colonies derived after reselection of PARP-1 stable transfectant all show PARP-1 expression.

### 4.2.5 Validation of PARP-1 stable transfectant

The derived stably transfected cell line (hereafter referred to as clone 23) has been shown to express PARP-1 protein. However, in order to utilise this cell line in DNA damage experiments as a PARP-1 proficient counterpart of the PARP-$1^{-/-}$ MEFs, it was essential to demonstrate activity of the transfected enzyme. In addition it was necessary to demonstrate that the isolation of a PARP-1 proficient cell line was due to transfection and not simply cross-contamination of the culture by a different PARP-1 proficient cell line.

PARP-1 activity in the stably transfected cell line was demonstrated by performing a PARP permeabilised cell assay followed by immuno dot blot detection of ADP-ribose polymer (as described in Methods Section 2.8.2). PARP-1 activity was stimulated by the presence of a short double-stranded oligonucleotide that simulates DNA strand breaks. The assay was also performed using the PARP-$1^{-/-}$ MEFs at the same time.

As can be seen in Figure 4.10, clone 23 possessed PARP-1 activity which was activated by DNA ends and was also inhibited by treatment with 1μM AG14361. This was in contrast to the PARP-1 knockout MEFs, which did not synthesize any detectable ADP-ribose polymer in the presence of double stranded oligonucleotide. This assay confirmed the presence of PARP-1 activity in the PARP-1 stable transfectant but not in the PARP-$1^{-/-}$ cells.

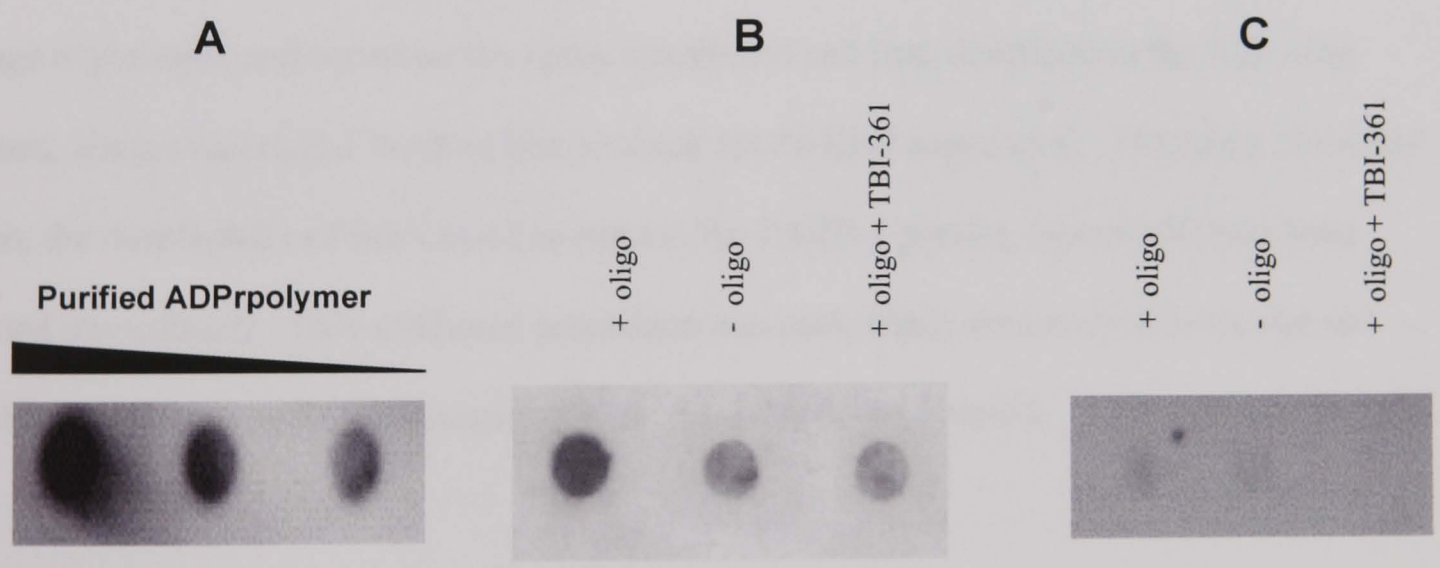


**Figure 4.10 Confirmation of PARP-1 activity in clone 23.**
Panel A is a positive control showing the decrease in dot intensity with decreasing amounts of purified ADP-ribose polymer. The central panel shows the oligonucleotide dependent PARP-1 activity in the stably transfected cell line (clone 23), which is abolished by treatment of cells with 1μM of the PARP-1 inhibitor AG14361. Panel C shows the relative lack of ADP-ribose polymer formation in the PARP-$1^{-/-}$ MEFs.

Although no obvious morphological or growth rate changes were apparent between clone 23 and PARP-1$^{-/-}$ MEFs, it was important to demonstrate that the stable transfectant was not a product of contamination. This was achieved by repeating the Southern blot analysis described in the previous chapter (Section 3.2.1). With the 0.8kb 5' probe described in Section 2.4.1, the clone 23 MEFs should still produce a smaller 3.3kb fragment when the genomic DNA is subjected to *Eco*RI digestion as the disrupted PARP-1 locus should remain unchanged. As can be seen below, the PARP-1 stable transfectant gives an identical Southern blot result as the PARP-1$^{-/-}$ cells. As no other PARP-1 proficient cell line would give rise to a fragment of this size the possibility of contamination is eliminated. A PARP-1$^{+/+}$ sample has also been included in the blot to act as a control. It should be noted that the PARP-1 stable transfectant lane does not contain any higher bands corresponding to those produced in the PARP-1 wild type MEFs. This is because the probe used is actually directed against intronic DNA whereas only PARP-1 cDNA (i.e. exonic) is present in the clone 23 MEFs. Therefore, no probe-specific fragment will be produced from *Eco*RI digestion of this plasmid. In addition, it should be noted that each DNA damage experiment performed on the stably transfected cell line, described in the following chapters, always included a Western blot to check for PARP-1 expression. Therefore, if for any reason, the transfected cell line ceased to express the PARP-1 protein, this would have been detected immediately. This additional precaution was particularly necessary since it was not possible to maintain antibiotic selection for the retention of the plasmid.

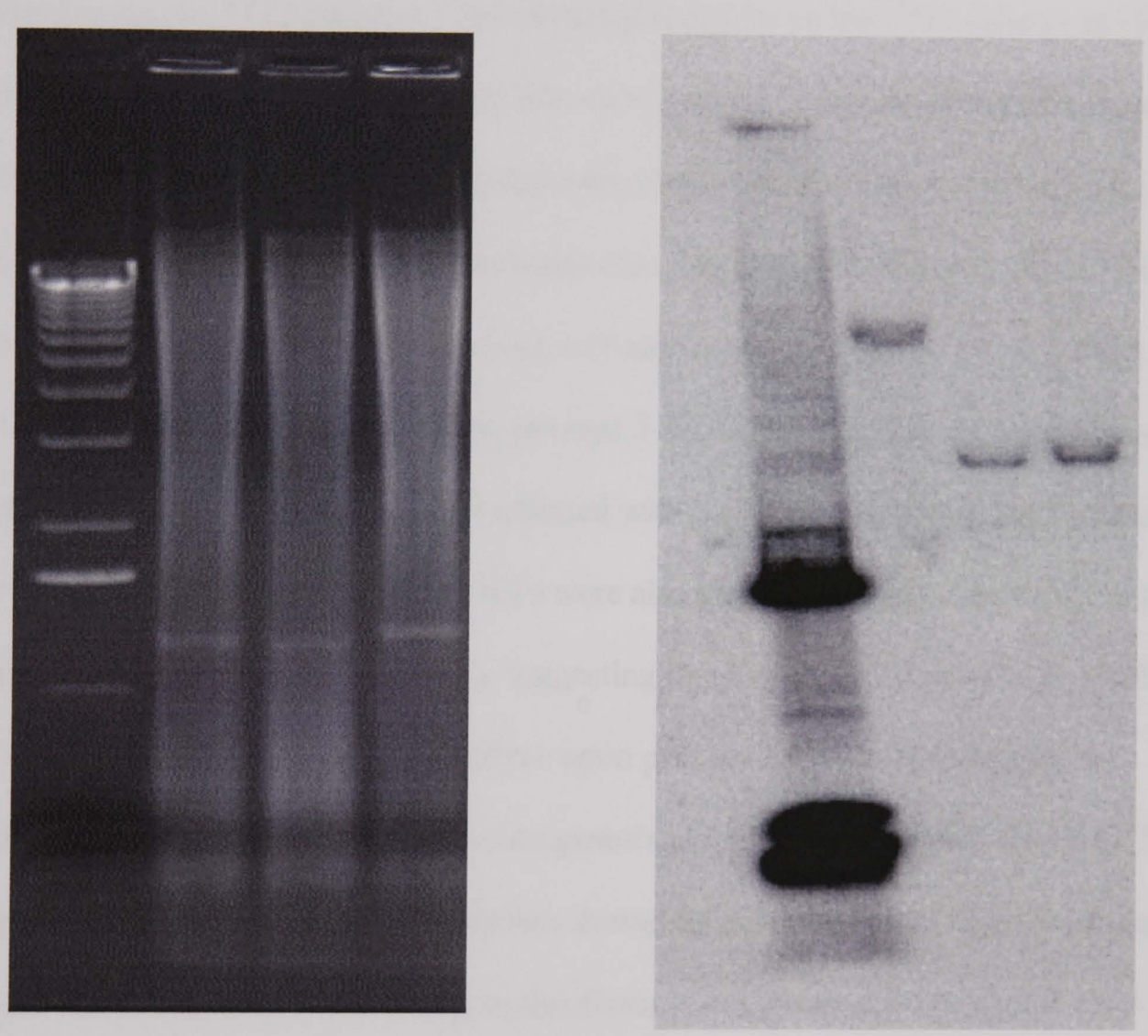


**Figure 4.11 Confirmation of homogenicity of clone 23 by Southern blotting**
The gel on the left shows efficient *Eco*RI digestion of genomic DNA from PARP-$1^{+/+}$, PARP-$1^{-/-}$ and clone 23 MEFs. The Southern blot on the right shows that clone 23 MEFs retain the 3.3kb band due to the disrupted endogenous PARP-1 locus in these cells. The Southern blot was probed with the 0.8kb probe that binds the 5' end of the PARP-1 gene.

## 4.3 Discussion

### 4.3.1 Mutant p53 status of PARP-$1^{+/+}$ MEFs

The initial experiments described in this chapter involved the DNA damage induced p53 response in the immortalised PARP-1 MEFs. An unexpected observation was made in that the

PARP-1$^{+/+}$ cells were found to express mutant p53 whereas the PARP-1$^{-/-}$ cells expressed wild type p53. A literature search regarding the loss of p53 function during immortalisation of MEFs revealed that this may be a common event. For example, Rittling and Denhardt, 1992, demonstrated the acquisition of p53 mutations in 2/3 independently derived MEF cell lines immortalised using the 3T12 protocol. This protocol is similar to the 3T3 method used in this thesis (see Chapter 2, Section 2.1.9), except that four times as many cells are re-plated into fresh medium upon sub-culturing. The p53 mutations detected were, like those in this thesis, within the DNA binding domain of p53. A further study demonstrated that the inactivation of p53 using antisense RNA allowed primary MEFs to form colonies in culture (Carnero *et al.*, 2000). Briefly, antisense RNA was introduced into passage 3 MEFs using a retrovirus delivery system and the cells plated out for colonies. Cells infected with an empty vector (i.e. not expressing antisense RNA) and uninfected primary MEFs were also plated out. Only those cells with inactivated p53 were able to form colonies, suggesting that loss of p53 function was sufficient to confer a transformed (immortalised) phenotype upon primary MEFs. On reflection, as immortalisation is an essential event in tumourigenesis and p53 mutation occurs in over 50% of cancers, perhaps the formation of p53 mutations during immortalisation of cells is not totally unexpected. However, what is interesting in this thesis is the observation that the PARP-1$^{-/-}$ cells do not appear to undergo the same genetic changes during immortalisation, and do not require inactivation, by mutation, of p53. Some other component regulating cellular growth and lifespan is likely to have been mutated for these cells to surpass the senescent phase. These observations have been made in two independently derived pairs of PARP-1 MEFs. It should also be noted that the mutations detected in the two independent PARP-1$^{+/+}$ MEF cell lines are in the same codon, 278 and it would seem unlikely that this is a coincidence. A different base is mutated, with the result of either an Asp to Glu or an Asp to Gln amino acid change in the two cell lines. Codon 278 is within the DNA binding domain of p53, suggesting selection for inactivation of the

transcriptional transactivation function of p53 during the immortalisation of PARP-$1^{+/+}$ MEFs. It is interesting that several studies in the literature have described lower p53 levels in the PARP-1 knockout MEFs compared with wild-type MEF controls and assigned this observation to a decreased stability of p53 in the absence of PARP-1 (Wesierska-Gadek *et al.*, 1999). However, no sequencing data is presented in these studies to indicate the p53 status of the PARP-$1^{+/+}$ MEFs. It may be that it is actually the PARP-$1^{+/+}$ cells expressing higher levels of p53 due to a mutation somewhere in that gene rather than the PARP-$1^{-/-}$ cells expressing less p53. Further studies into this interesting phenomenon have been performed and will be discussed in Chapter 6.

### 4.3.2 PARP-1 stable transfectant

The observations in the initial experiments that revealed the mutant p53 status of immortalised PARP-$1^{+/+}$ MEFs made it necessary to develop an alternative strategy to analyse p53 responses in PARP-1 proficient and deficient cells. This was achieved by stably transfecting the PARP-$1^{-/-}$ MEFs with a construct containing PARP-1 regulated by a eukaryotic promoter. This chapter has included data showing the derivation and validation of the transfected cell line, with both the presence and activity of PARP-1 being demonstrated. In addition, by re-plating clone 23 for colonies and analysing several of these, the possibility of the derived cell line being a heterogeneous population of cells has been eliminated. Also, to eliminate the possibility of cross contamination with a different PARP-1 proficient cell line during transfection, a Southern blot was performed. This Southern blot showed that the PARP-1 knockout cells had an identical *Eco*R1 restriction pattern to that seen in the PARP-1 stably transfected cell line. This is expected as the disrupted PARP-1 gene is still present in the derived cell line and hence will produce a 3.3kb fragment upon *Eco*RI digestion of the genomic DNA. To sum up, PARP-$1^{-/-}$ MEFs have been transfected with PARP-1 cDNA. These cells have been re-selected and the genetic

background of the cells confirmed, eliminating any possibility of heterogeneity or contamination of the cells.

The stable transfection procedure has produced a PARP-1 proficient cell line that is wild type in p53. This cell line was subsequently used in DNA damage response experiments, along with PARP-1 knockout MEFs and the human colorectal cell line, HCT-116, the details of which will be explained in the next chapter.

# CHAPTER 5

# THE DNA DAMAGE-INDUCED P53 RESPONSE IN THE PRESENCE AND ABSENCE OF PARP-1

## 5.1 Introduction and objectives

The data presented in chapters 3 and 4 have described and validated the techniques used to remove PARP-1 protein and/or activity from cells. PARP-$1^{-/-}$ MEFs have been shown to lack both PARP-1 protein and activity. In addition, the PARP-1 inhibitor, AG14361 has been shown to effectively inhibit PARP-1 activity in PARP-$1^{+/+}$ cell lines. Further data has been presented highlighting the need to derive a PARP-1 stably transfected cell line by the introduction of PARP-1 cDNA into the PARP-$1^{-/-}$ MEFs. Briefly, immortalised PARP-$1^{+/+}$ MEFs were found to express mutant p53 and hence could not be used to analyse p53 responses. The stably-transfected cell line has been shown to possess both PARP-1 protein and activity and as such has been used as the PARP-1 proficient counterpart (referred to hereafter as clone 23) of the PARP-$1^{-/-}$ MEFs in DNA damage experiments.

Several studies have been published which suggested a functional relationship between PARP-1 and p53. However, no consistent pattern was apparent when analysing the data in the literature. For example, there are discrepancies in results involving different PARP-$1^{-/-}$ cells as well as studies involving PARP-1 inhibitors (See Section 1.4.6 for details).

In summary, the p53 induction in PARP-$1^{-/-}$ MEFs disrupted in exon 1 was found to be identical to their wild type counterparts in response to IR (Masutani *et al.*,. 1999). In addition, the transcriptional transactivation activity of p53 was unaffected (as measured by Western blot analysis of p53 target genes). A reduced p53 induction was observed in the exon 2 PARP-1 knockout cells in response to IR (Agarwal *et al.*, 1997), with a corresponding reduction in p53 trasncriptional activity (measured by Western blot analysis and luciferase reporter gene assay). Finally, a recent publication using exon 4 knockout MEFs suggested differential regulation of p53 by PARP-1, depending upon the type of

DNA damaging agent used. When compared to PARP-$1^{+/+}$ MEFs, the PARP-$1^{-/-}$ cells showed a reduced p53 induction in response to IR but an enhanced p53 response after treatment with the monofunctional alkylating agent, MNU. In addition, several studies have been published using PARP-1 inhibitors and analysing the p53 response. As with the PARP-1 knockout studies, results have been inconsistent with some groups reporting an enhanced p53 response (Lu and Lane, 1993) and others reporting a reduced or delayed response (Wang *et al.,* 1998). It may be that differences between groups were due to different cell lines being used. Alternatively, different DNA damaging agents may activate p53 by different pathways, some involving PARP-1 and others not involving PARP-1. It also needs to be considered that different DNA damaging agents may activate PARP-1 to different extents, or that PARP-1 may be more or less implicated in the repair pathway involved, and thus may affect the strand break signalling levels (e.g. mediated by ATM) to p53. A similar situation is apparent when looking at the involvement of particular protein kinases in p53 activation in response to different DNA damaging agents. A more detailed description of the putative role of PARP-1 in p53 regulation has been provided in Section 1.4.6

Data presented in previous chapters has validated the use of PARP-$1^{-/-}$ cells and AG14361 as efficient means for the removal of PARP-1 activity from cells. Therefore the aim of this chapter was to use a combination of PARP-$1^{+/+}$ and PARP-$1^{-/-}$ MEFs and a potent PARP-1 inhibitor to try and clarify some of the conflicting data which exists within the literature. It should be emphasised that the inhibitor used in this study is approximately 1000-fold more potent than the previously most commonly used PARP-1 inhibitor, 3-aminobenzamide.

Experiments were carried out using immortalized clone 23 MEFs (PARP-1 proficient) and PARP-1$^{-/-}$ (PARP-1 deficient) MEFs as well as a human colorectal cell line, HCT-116, all of which have been demonstrated to contain wild-type p53 (see figures 5.4 – 5.6). The p53 response was analysed in response to a variety of DNA damaging agents, including IR, UV and the monofunctional alkylating agent, temozolomide. Each agent induces a distinct form of DNA damage, which is in turn repaired by a particular DNA repair pathway or combination of pathways. The hypothesis was that PARP-1$^{-/-}$ MEFs (or, alternatively, PARP-1 inhibited cells) would show an altered p53 response to their wild type, or PARP-1 active counterparts. In addition, the use of different DNA damaging agents may show that PARP-1 only regulates p53 in response to particular types of DNA damage.

Data presented in this chapter consists of Western blot analysis of the cell lines treated with DNA damaging agents in the presence or absence of 1μM AG14361. Western blots are included for p53 (to show any change in p53 protein levels), mdm2 (to demonstrate transcriptional activity of p53), PARP-1 and actin (to show equal protein loading in each lane). In addition, a luciferase- based reporter gene assay is used to measure p53 activity. Data is presented showing the validation of this assay before it was used in DNA damage response experiments.

## 5.2 Results

### 5.2.1 Validation of the luciferase reporter gene assay

A reporter gene assay is a technique involving the introduction of plasmid DNA into cells (Section 2.7). The plasmid usually contains a gene downstream of a promoter site, the expression of which can be readily measured. The plasmid used in this study contained a

luciferase gene downstream of the P2 promoter of the *MDM2* gene (pGL3-P2, generated by Laing, H, PhD thesis, Cancer Research Unit, University of Newcastle upon Tyne). The P2 promoter is p53-responsive, therefore introduction of this plasmid into cells should result in the production of luciferase in a p53-dependent manner. In addition, luciferase levels should increase in response to DNA damage due to the increased transcriptional activity of p53. To eliminate the possibility that increases in luciferase were simply due to increased transfection, a control plasmid, containing a β-galactosidase gene is co-transfected with the luciferase plasmid. The β-galactosidase gene is not downstream of a p53 responsive promoter (CMV promoter) and as such levels of β-galactosidase should not increase in response to DNA damage to the same extent as luciferase. An increase of β-galactosidase may be observed over time due to the constant transcription of the plasmid. Obviously, the rate of breakdown of this protein will determine whether increases are observed. That said, after DNA damage the luciferase levels should increase markedly compared to the β-galactosidase levels. To control for transfection efficiency, a ratio of luciferase/β-galactosidase is measured.

The first step in the validation of the assay was to show that the introduction of the P2 plasmid (containing the luciferase gene) resulted in luciferase expression when compared to the same plasmid without the P2 promoter site. HCT-116 cells were therefore transfected with either the P2 plasmid (pGL3-P2) or the empty vector (pGL3) along with the β-galactosidase plasmid. The empty vector consists of the pGL3 vector containing the luciferase gene but lacking the P2 promoter. Samples were taken after 24h, 30h and 48h and the samples analysed using a luminometer.

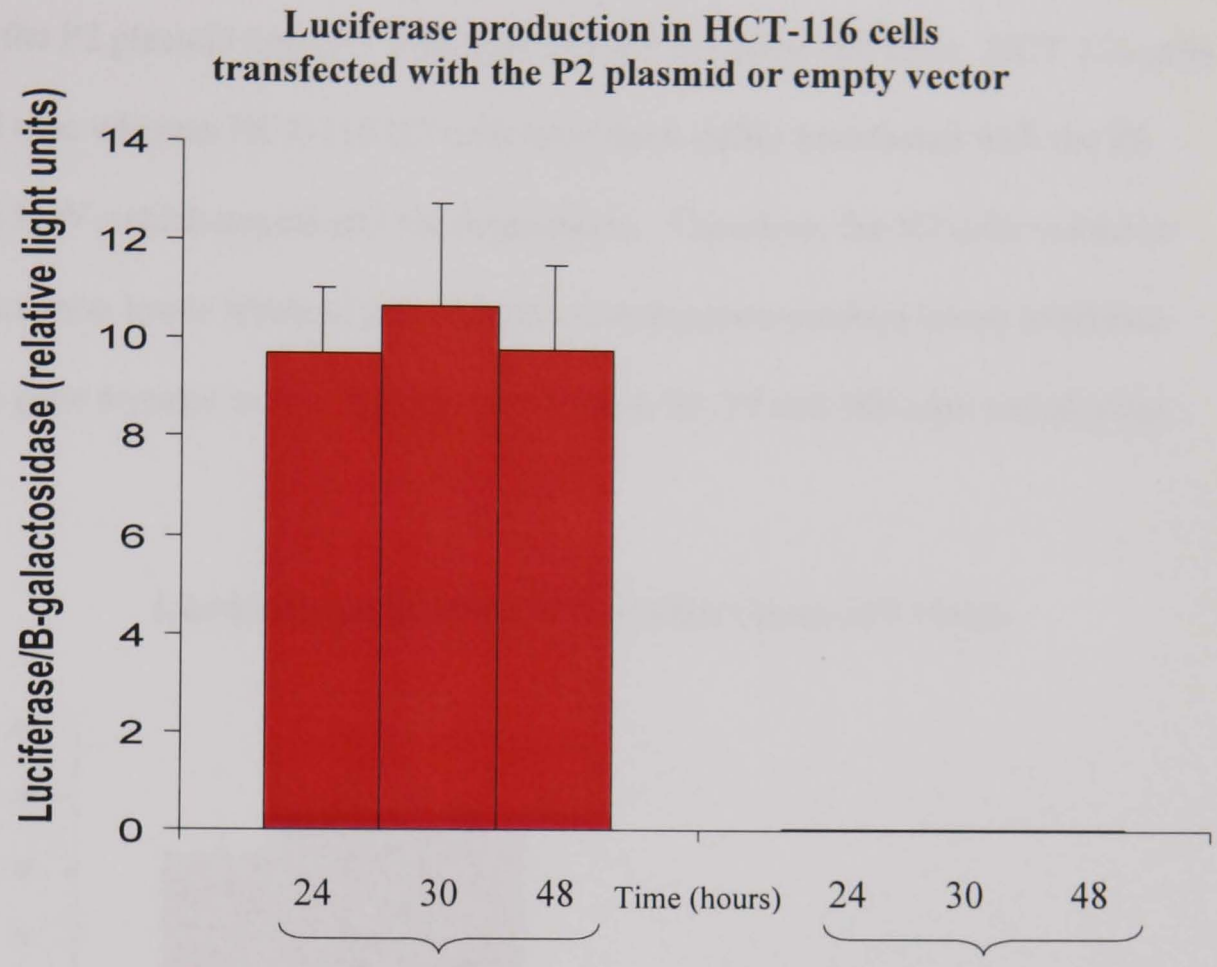


**Figure 5.1 The transfection of cells with the pGL3-P2 plasmid results in the expression of luciferase**
Cells transfected just with the pGL3 plasmid express approximately 400-fold less luciferase than cells transfected with the pGL3-P2 plasmid

Figure 5.1 above clearly shows the significant production of luciferase in cells transfected with the P2 plasmid. In contrast, the levels of luciferase produced from the plasmid without the P2 promoter (empty vector) are virtually undetectable (approximately 400-fold reduced) when plotted on the same graph. In addition, it should be noted that the ratio of luciferase/β-galactosidase did not increase over time in the absence of DNA damage. This is an important experiment as the assay was used in subsequent experiments where increases in the ratio was interpreted as increases in p53 activity.

The next and perhaps most important step in the validation process was to show that the expression of luciferase occurred in a p53-dependent manner. This was achieved by transfecting the P2 plasmid into p53 wild type and p53 deficient cell lines. HCT-116 cells are p53 wild type whereas HCT-116 N7 cells have been stably transfected with the E6 protein from HPV, which targets p53 for degradation. Therefore, the N7 cells would be expected to express lower levels of p53 and, as a consequence produce lower luciferase values in the gene reporter assay. Samples were taken 24, 30 and 48h after transfection.

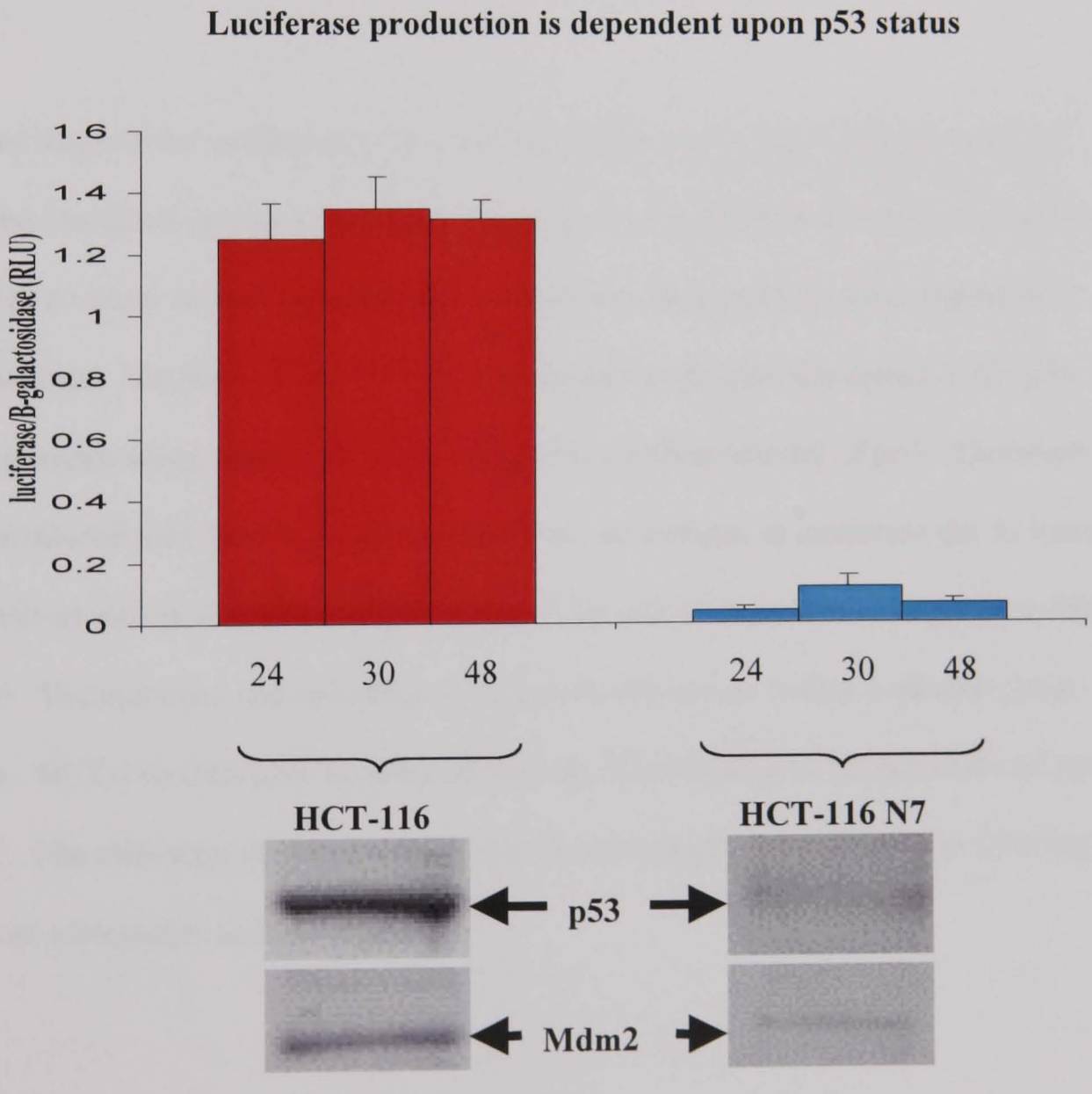


**Figure 5.2 Analysis of luciferase expression in p53 wild type and p53 deficient cell lines**
HCT-116 and HCT-116 N7 cells were transfected with pGL3-P2 and β-galactosidase plasmids and expression measured over time. P53 activity was estimated by calculating the ratio of luciferase: β-galactosidase. Parallel Western blot analysis shows the levels of p53 and mdm2 in the cell lines. This data is representative of two independent experiments.

As can be seen in figure 5.2, the HCT-116 N7 cells expressed much lower levels of p53 and mdm2 protein compared to the HCT-116 cells (shown by Western blot analysis). This reduced p53 level correlated with a greatly reduced level of luciferase in the HCT-116 N7 cells. It should be noted that this experiment has been repeated in a p53 mutant cell line (immortalised PARP-$1^{+/+}$, data not shown), which express very high p53 levels. However, because the p53 is mutated in the DNA binding domain, it is unable to bind the P2 promoter and only very low levels of luciferase were produced. This set of results clearly shows that the expression of luciferase was dependent upon both p53 levels and p53 status.

The final stage of the validation of the luciferase assay was to show that the levels of luciferase increased in response to DNA damage. As described in Section 1.2.2, p53 is subject to a variety of post-translational modifications that activate p53 in response to DNA damage. The basis of p53 activation is thought to involve disruption of the p53-mdm2 complex along with an increase in the DNA binding activity of p53. Therefore, cells transfected with the P2 plasmid should show an increase in luciferase due to increased p53 levels as well as increased DNA binding of the activated protein in response to DNA damage. The induction and activation of p53 normally occurs within 2-4h after DNA damage. HCT-116 cells were transfected with the P2 plasmid and incubated for 24 hours at 37°C. The cells were then exposed to 5Gy IR and samples taken after 3 and 6 hours, as well as an untreated (control) sample.

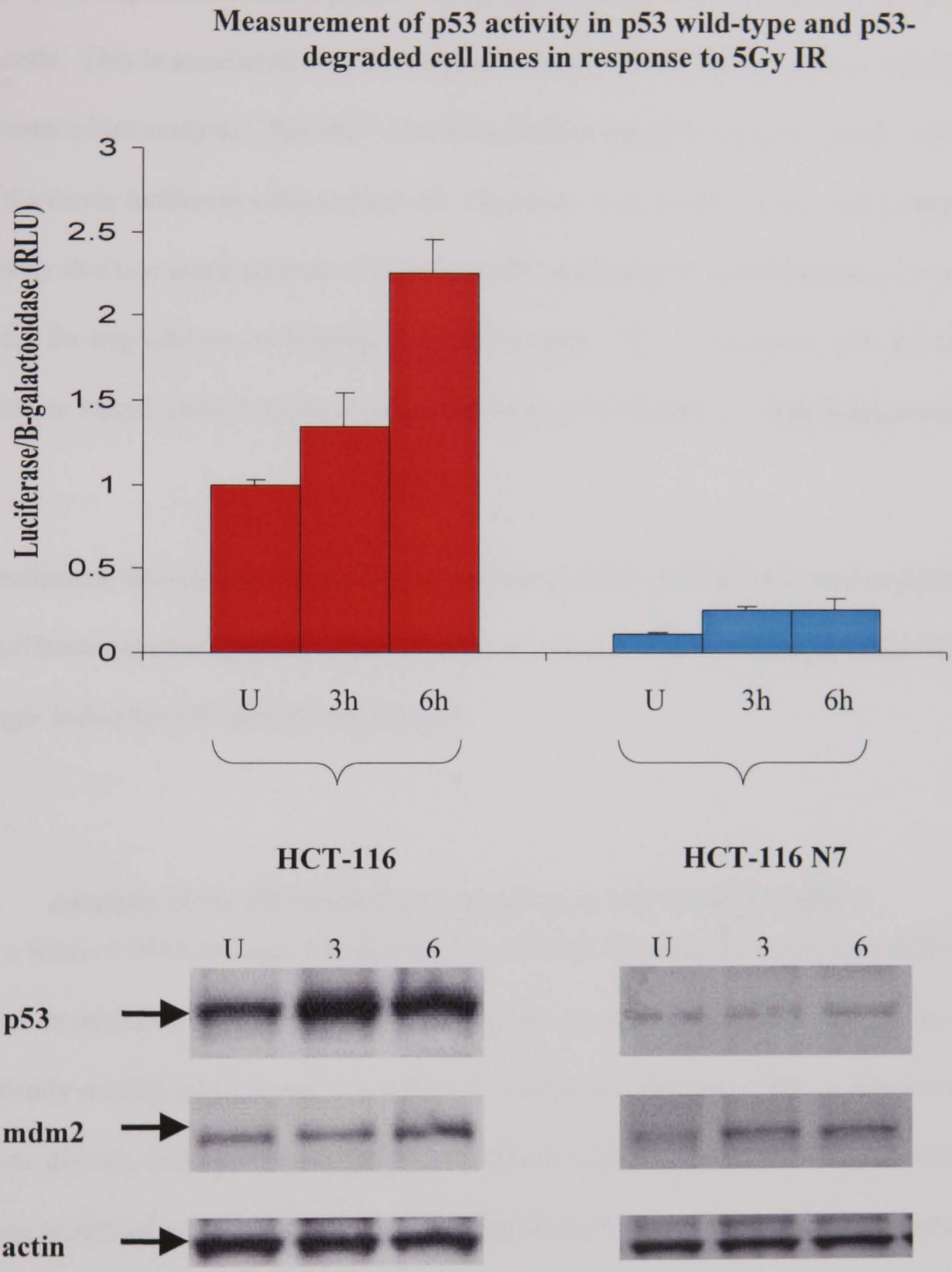


**Figure 5.3 The effect of IR on the production of luciferase**
HCT-116 or HCT-116 N7 cells were treated with 5Gy IR for 3 and 6h and luciferase:β-galactosidase values measured. Western blot analysis of p53 and mdm2 was performed in parallel.

Figure 5.3 shows that exposure of cells to a DNA damaging agent brings about an increase in luciferase expression, with a greater than 2-fold increase observed at 6h in the p53 wild-type cells. This is associated with an increase in both p53 and mdm2 protein, as measured by Western blot analysis. The HCT-116 N7 cells have much lower p53 levels, consistent with the lower luciferase values observed. However, there is an increase in luciferase after IR, likely due to a small amount of functional p53 within these cells that has not been targeted for degradation *via* binding of the E6 protein. This is consistent with the slight increase in mdm2 protein levels observed in these cells (Figure 5.3, right hand panel).

In conclusion, the validation experiments presented in this section have demonstrated that the luciferase reporter gene assay can be used as a sensitive and reliable indicator of DNA-damage- inducible p53 activity within cells.

### 5.2.2 Analysis of the IR induced p53 response in cells lacking PARP-1

IR is a form of DNA damage that directly induces both single and double stranded DNA breaks. In addition, free radicals (reactive oxygen species) are produced, which can chemically modify DNA bases via oxidation. Common products of this oxidation are thymine glycols, produced by oxidation of a thymine base. With such an array of DNA damage produced, repair involves several different pathways, some which may require PARP-1 and some not.

Studies to date have reported that animals or cells lacking PARP-1 are hypersensitive to IR (de Murcia *et al.*, 1997, Wang *et al.*, 1997), suggesting a positive survival function of PARP-1 in response to this type of damage. Under normal circumstances, PARP-1 is

thought to bind to certain breaks generated after IR and recruit other repair proteins to the site of damage. Additionally, PARP-1 has been implicated in recombinational repair, where it is thought that PARP-1 may bind to the double stranded ends of DNA and protect them from further damage by nucleases before the lesion is eventually repaired.

Studies into p53 activation in response to IR have focussed predominantly on the role of kinases. In particular, the ATM kinase is thought to activate p53 via direct phosphorylation of Ser15 and indirect phosphorylation of Ser20 (via activation of a second kinase, Chk2). In addition, ATM is believed to phosphorylate mdm2 on Ser395. All of these events may lead to the disruption of the p53-mdm2 complex and hence activation of p53. Several groups have also reported that PARP-1 is necessary for efficient p53 induction and activation in response to IR. Mechanisms proposed for this activity include protein-protein interaction between PARP-1 and p53 or poly(ADP-ribosylation) of p53. Contrary to this model, Lu and Lane, 1993, described an increased IR- induced p53 response in cells lacking PARP-1 activity due to PARP-1 inhibition. This increased accumulation of p53 was argued to be a consequence of the persistence of DNA strand breaks due to the lack of PARP-1 and the consequent inhibition of DNA repair, resulting in increased signalling to p53. A similar pattern of p53 induction has been observed in PARP-1$^{-/-}$ cells treated with alkylating agents (Oliver *et al.*, 1999; Beneke *et al.*, 2000).

The aim of this section, therefore, was to analyse the IR-induced p53 response in cells lacking PARP-1 through either inhibition or knocking out of the PARP-1 gene.

Clone 23 and PARP-1$^{-/-}$ MEFs or HCT-116 cells were co-transfected with the P2 and β-galactosidase plasmids and incubated for 24 hours. The cells were then treated with 5Gy IR and samples taken after 1, 2, 3 and 6 hours as well as an untreated (control) sample. These samples were used for the luciferase reporter gene assay. Western blot samples were also taken in parallel at the same time points but also included a 24-hour time point. Samples were analysed for p53 activity (by luciferase assay) and for levels of p53 and mdm2 protein (by Western blotting).

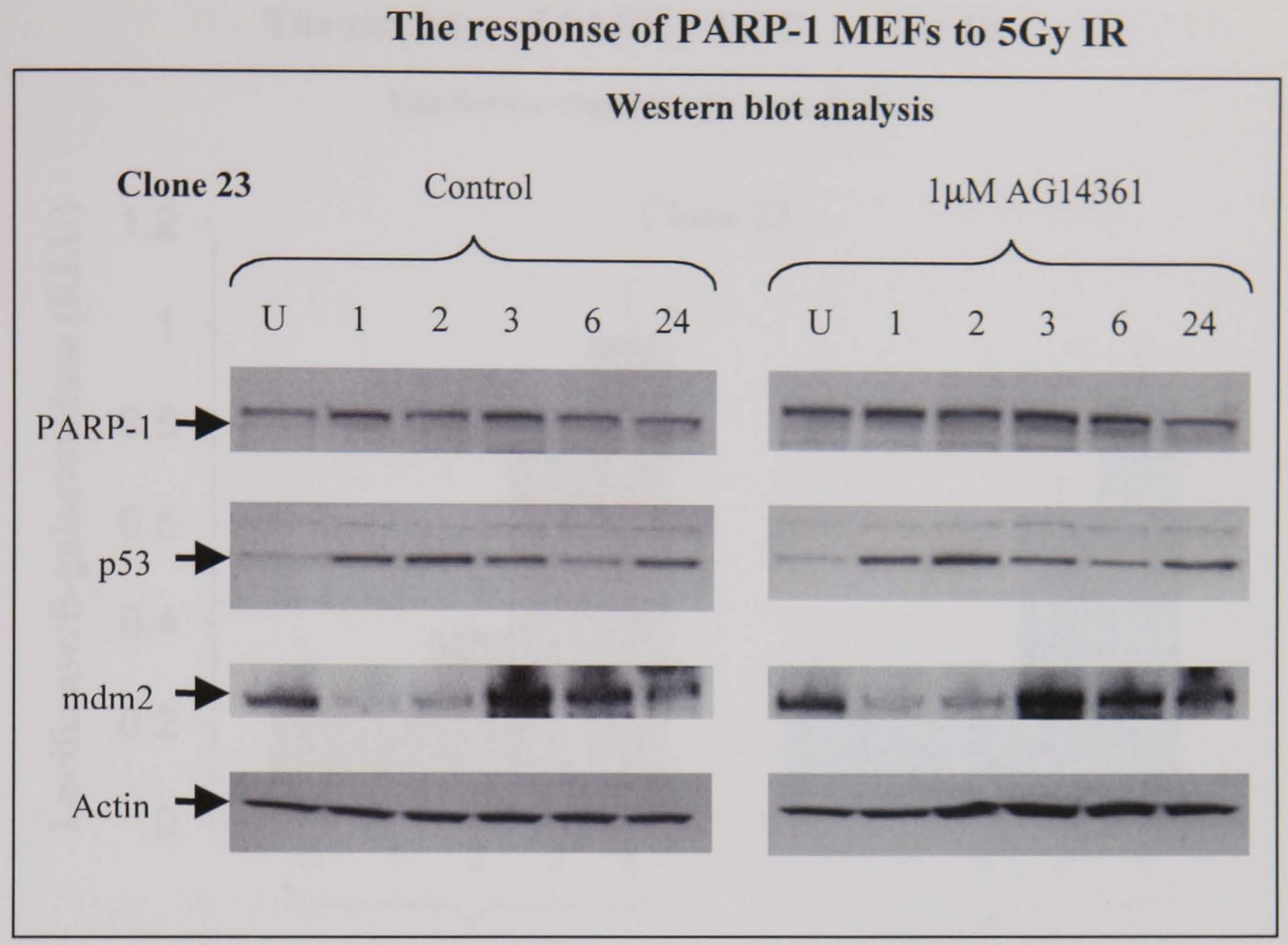


**Figure 5.4 The response of PARP-1 MEFs to 5Gy IR – Western blot analysis**
Samples were taken at 1, 2, 3, 6 and 24h post-IR and subject to Western blot analysis. Controls consist of cells treated with 0.01% DMSO

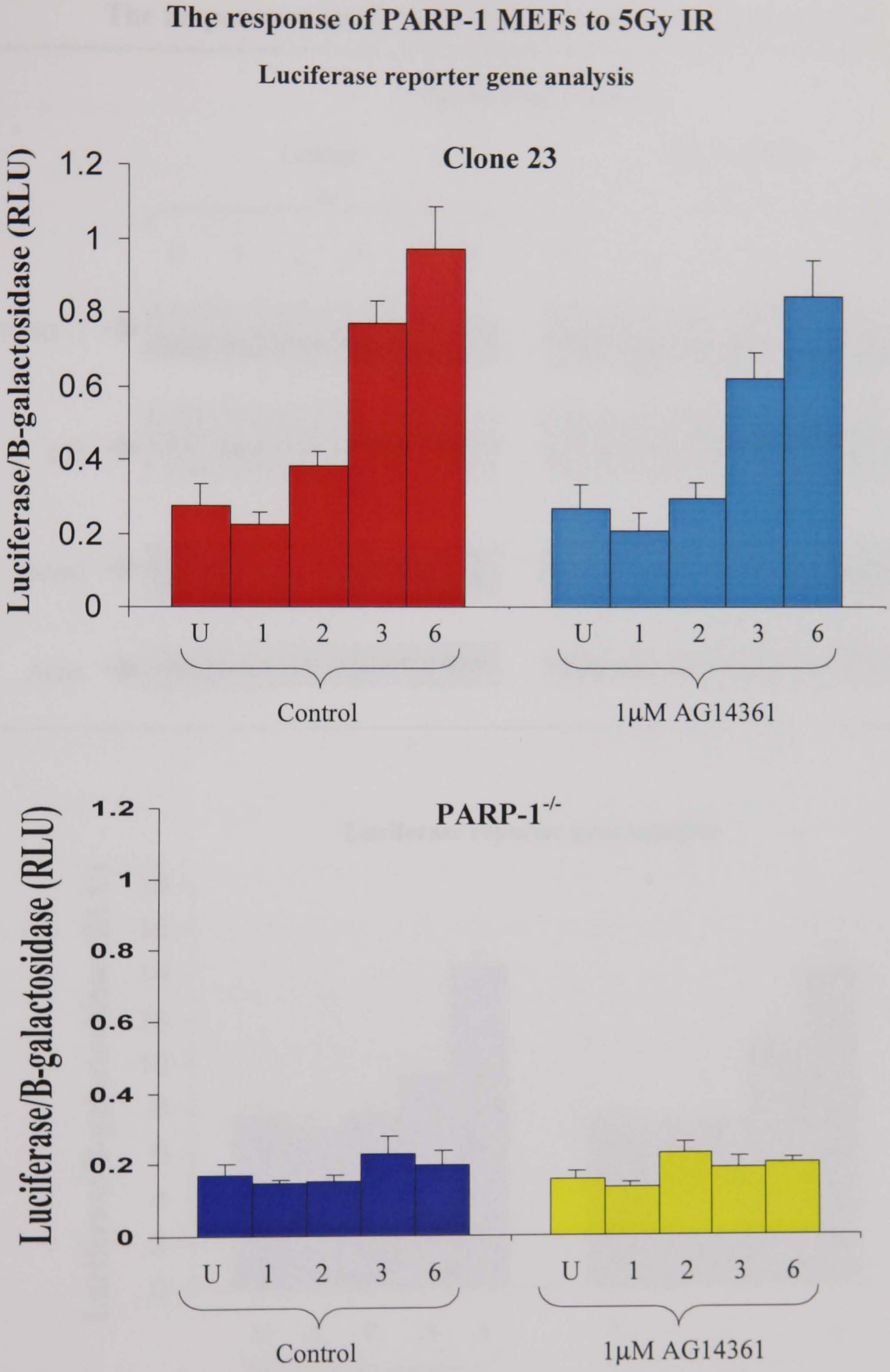


**Figure 5.5 Measurement of p53 activity in clone 23 and PARP-1$^{-/-}$ MEFs in response to 5Gy IR**
MEFs were treated with 5Gy IR and samples taken after 1,2,3 and 6h and luciferase:β-galactosidase values measured. Controls consisted of cells treated with 0.01% DMSO.

**The response of HCT-116 human colorectal cells to 5Gy IR**

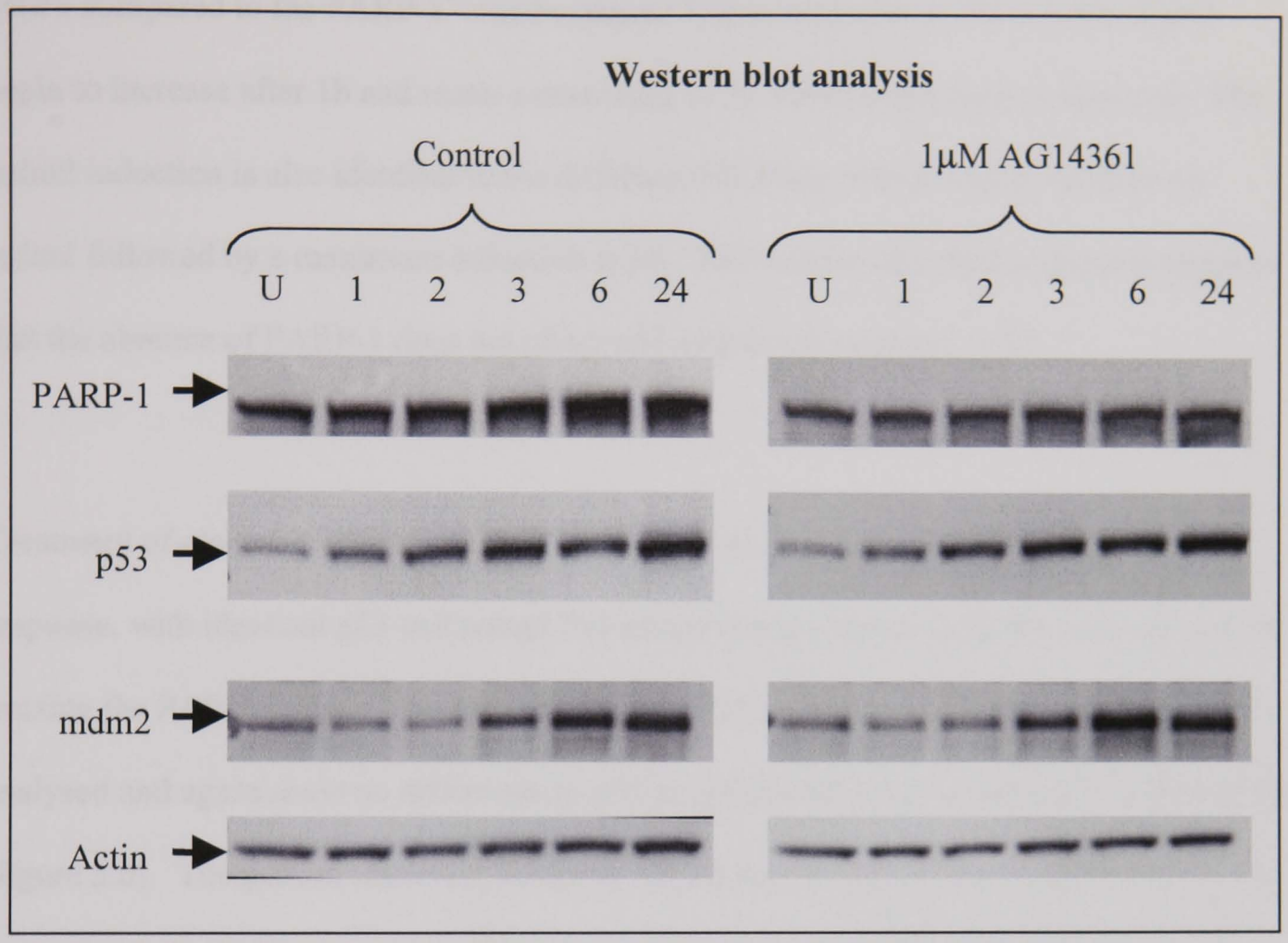


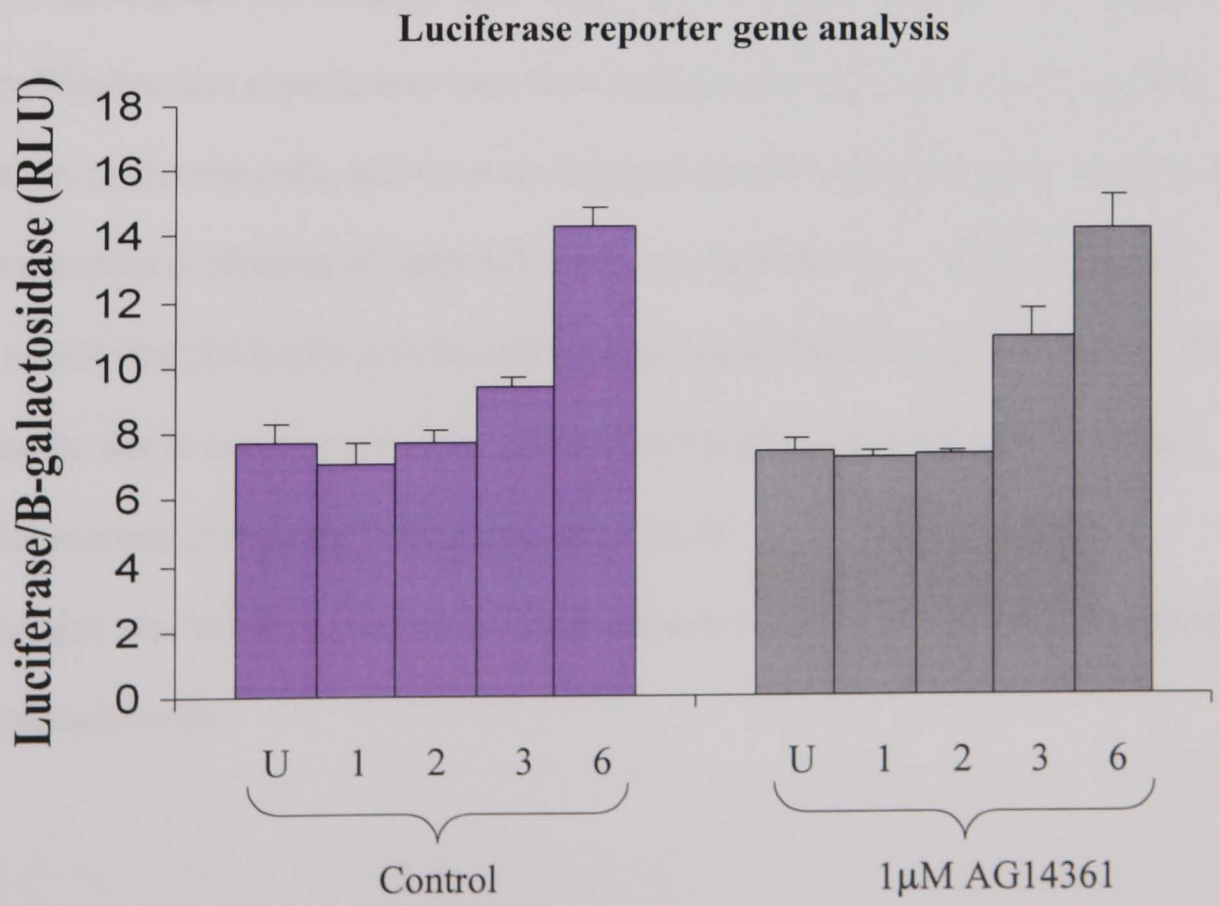


**Figure 5.6 The response of HCT-116 cells to 5Gy IR – Western blot and luciferase analysis**
Samples were taken at 1, 2, 3, 6 and 24h post-IR and subject to Western blot and luciferase analysis. Controls consist of cells treated with 0.01% DMSO

Western blot analysis reveals no significant difference in p53 induction in the clone 23 MEFs compared to the PARP-1$^{-/-}$ MEFs (figure 5.4) in response to IR. Levels of p53 begin to increase after 1h and reach a maximum at 2h before beginning to decrease. The mdm2 induction is also identical in the different cell lines, with an initial decrease in mdm2 followed by a maximum induction at 6h. This pattern of mdm2 induction suggests that the absence of PARP-1 does not affect p53 activity in response to IR.

Treatment of clone 23 MEFs with AG14361 also has no effect on the IR-induced p53 response, with identical p53 and mdm2 inductions being observed (figure 5.4). As well as treating the PARP-1 stable transfectant with AG14361, human HCT-116 cells have been analysed and again show no difference in p53 or mdm2 induction in response to 5Gy of IR (figure 5.6). The pattern observed, however, is different to that in the PARP-1 MEFs. For example, in the HCT-116 cells, p53 levels begin to increase at 1h and gradually increase up until 24h. In contrast, p53 levels in the PARP-1 MEFs peak at 2h before decreasing. Preliminary Western blot experiments have been performed in a second human cell line, A2780 ovarian carcinoma cells, and show an identical pattern of p53 response to HCT-116 cells in the presence or absence of 1μM AG14361. As described in a previous chapter, AG14361 inhibits the 5% PARP activity still present in the PARP-1 knockout MEFs. This activity must be due to one or more of the alternative PARP proteins recently described. Western blot analysis of PARP-1$^{-/-}$ MEFs treated with IR +/- AG14361 (figure 5.4) therefore suggest also that this alternative PARP activity is not involved in the regulation of p53 in response to IR.

The results of the luciferase reporter gene assay, measuring p53 activity suggest that PARP-1 is not involved in the activation of p53 in response to IR. PARP-1 proficient cells (both clone 23 MEFs and HCT-116 cells) treated with AG14361 show a very similar pattern of induction to cells without the inhibitor. In clone 23 MEFs, luciferase levels begin to increase at 3h and show an approximately three-fold increase at 6h (figure 5.5). The HCT-116 cells show a slight increase in p53-dependent luciferase activation at 3h which has approximately doubled at 6h (figure 5.6). In accordance with the Western blot analysis, p53 activity, as measured by luciferase production increases with mdm2 protein in all of the cells analysed. However, an unexpected result was obtained in the PARP-$1^{-/-}$ MEFs. As can be seen in figure 5.5, these cells showed no apparent increase in the luciferase/β-galactosidase ratio over the whole time period (6h) and had lower values overall compared to the PARP-1 proficient MEFs. For example, the untreated luciferase value in the clone 23 MEFs is 3899 RLU (figure 5.7), whereas the same sample in the PARP-$1^{-/-}$ MEFs has a luciferase value of just 380. A similar decrease is also observed in the β-galactosidase values in the PARP-$1^{-/-}$ MEFs compared to clone 23 MEFs. Initially this could be interpreted as an inability to efficiently activate p53 and hence reduced expression of luciferase in these cells. However, this would not be in agreement with the clear induction of mdm2 in the PARP-1 knockout Western blots. In addition, closer analysis of the raw data reveals that both the luciferase and β-galactosidase values (see figure 5.7) were dramatically lower (about 10-fold) than in the clone 23 MEFs. This suggests that the absence of PARP-1 protein adversely affects the transfection and/or the expression of the exogenous plasmids. As such, the luciferase data in the PARP-1 knockouts cannot be interpreted as an accurate representation of p53 activity within these cells. This observation will be discussed in more detail in Section 5.3.1. It should be noted that treatment of clone 23 MEFs with AG14361 did not have a similar effect on the

raw data values (see figure 5.7). Therefore the effect observed must be a consequence of the absence of PARP-1 protein rather than its activity. This effect has also been observed in response to all of the DNA damaging agents used, eliminating the possibility that it is a damage-specific effect.

**Luciferase and β-galactosidase raw data values after 5Gy IR treatment of clone 23 and PARP-1$^{-/-}$ MEFs**

| | Clone 23 | | | PARP-1$^{-/-}$ | | |
|---|---|---|---|---|---|---|
| | Luciferase | B-gal | Luc/B-gal | Luciferase | B-gal | Luc/B-gal |
| Untr | 2563 | 16662 | 0.153823 | 376 | 1850 | 0.203243 |
| | 5920 | 15332 | 0.386121 | 455 | 2265 | 0.200883 |
| | 3214 | 12273 | 0.261876 | 310 | 2917 | 0.106274 |
| 1h | 2928 | 14938 | 0.19601 | 301 | 1938 | 0.155315 |
| | 4944 | 16421 | 0.301078 | 337 | 2673 | 0.126076 |
| | 1562 | 12270 | 0.127302 | 369 | 2376 | 0.155303 |
| 2h | 4722 | 19381 | 0.243641 | 363 | 3422 | 0.106078 |
| | 3821 | 14164 | 0.269768 | 324 | 1897 | 0.170796 |
| | 4284 | 11333 | 0.378011 | 387 | 2228 | 0.173698 |
| 3h | 15034 | 19496 | 0.771133 | 368 | 2408 | 0.152824 |
| | 11023 | 20788 | 0.530258 | 443 | 2106 | 0.210351 |
| | 10993 | 19420 | 0.566066 | 573 | 1781 | 0.321729 |
| 6h | 20572 | 26590 | 0.773674 | 638 | 3256 | 0.195946 |
| | 39283 | 37684 | 1.042432 | 488 | 1847 | 0.264212 |
| | 23160 | 31514 | 0.734911 | 394 | 3129 | 0.125919 |

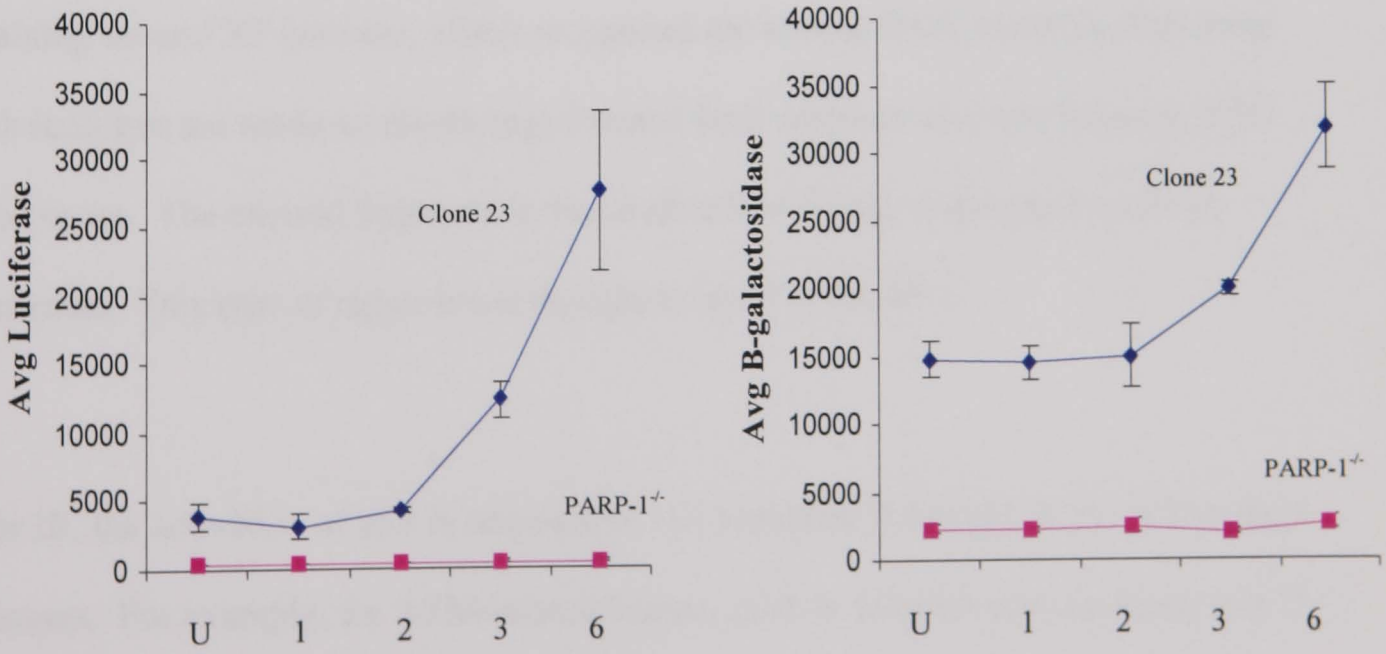


**Figure 5.7 Table and graph summarising the low luciferase and β-galactosidase values in PARP-1$^{-/-}$ MEFs compared to clone 23 MEFs**

In conclusion, the data presented in this section has shown that PARP-1 is not involved in the p53 response to IR. p53 induction and activity were identical in the presence and absence of PARP-1. However, with relation to previously published work, it cannot be excluded that the effects observed are cell line specific and PARP-1 may play a role in the regulation of p53 in other cell lines.

### 5.2.3 Analysis of the UV-induced p53 response in cells lacking PARP-1

The exposure of cells to UV radiation results in the distortion of genomic DNA by the formation of intra-strand linkages. Nucleic acid bases absorb the ultra violet light, with the resultant influx of energy inducing chemical changes. The most common photoproducts are the consequence of bond formation between adjacent pyrimidines within a strand of DNA, and of these the most frequent are cyclobutane dimers. The result of this bond formation is distortion of the normal helical structure of DNA, which may subsequently affect the efficiency of DNA transcription or replication. Pyrimidine dimers are repaired by nucleotide excision repair. This process involves a large multi-protein complex, containing several XP proteins, which recognises the altered DNA structure, following which incisions are made on the damaged strand both upstream and downstream of the altered bases. The excised fragment is removed before filling of the gap by a DNA polymerase. This type of repair is not thought to involve PARP-1.

As for IR, the activation of p53 in response to UV radiation is thought to be orchestrated by kinases. For example, the ATM-related kinase, ATR is induced after exposure to UV and phosphorylates p53 on Ser15 and Ser37, with the likely result of disrupting binding to mdm2. In addition, ATR brings about phosphorylation of two C-terminal residues,

increasing the DNA binding activity of p53. To date, PARP-1 has not been implicated in the p53 response to UV.

This section contains data analysing the UV-induced p53 response in cells lacking PARP-1 through either inhibition or disruption of the PARP-1 gene.

**The response of PARP-1 MEFs to 50J/m$^2$ ultra-violet radiation**

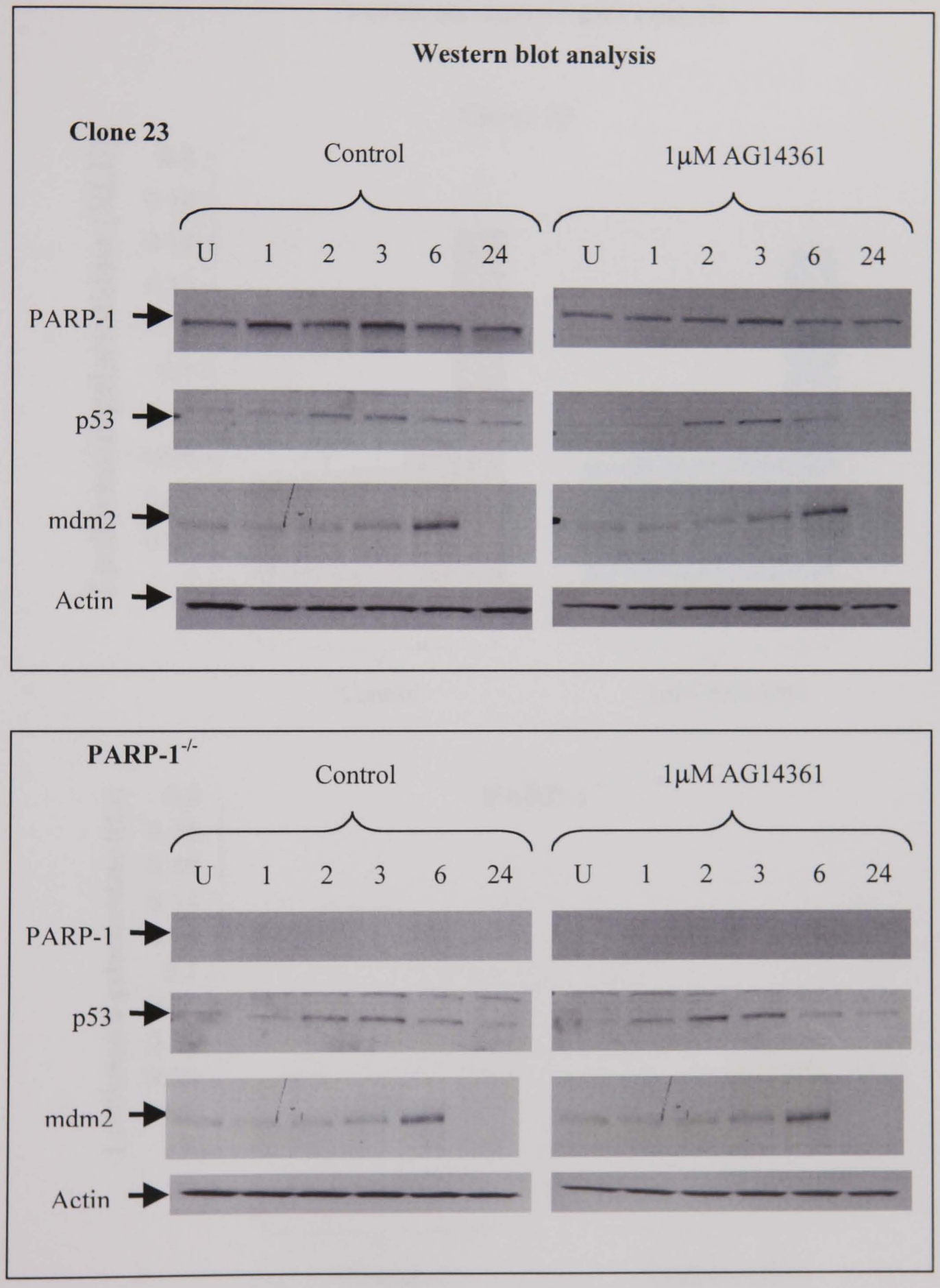


**Figure 5.8 The response of PARP-1 MEFs to 50J/m$^2$ UV – Western blot analysis**
Samples were taken at 1, 2, 3, 6 and 24h post-IR and subject to Western blot analysis. Controls consist of cells treated with 0.01% DMSO.

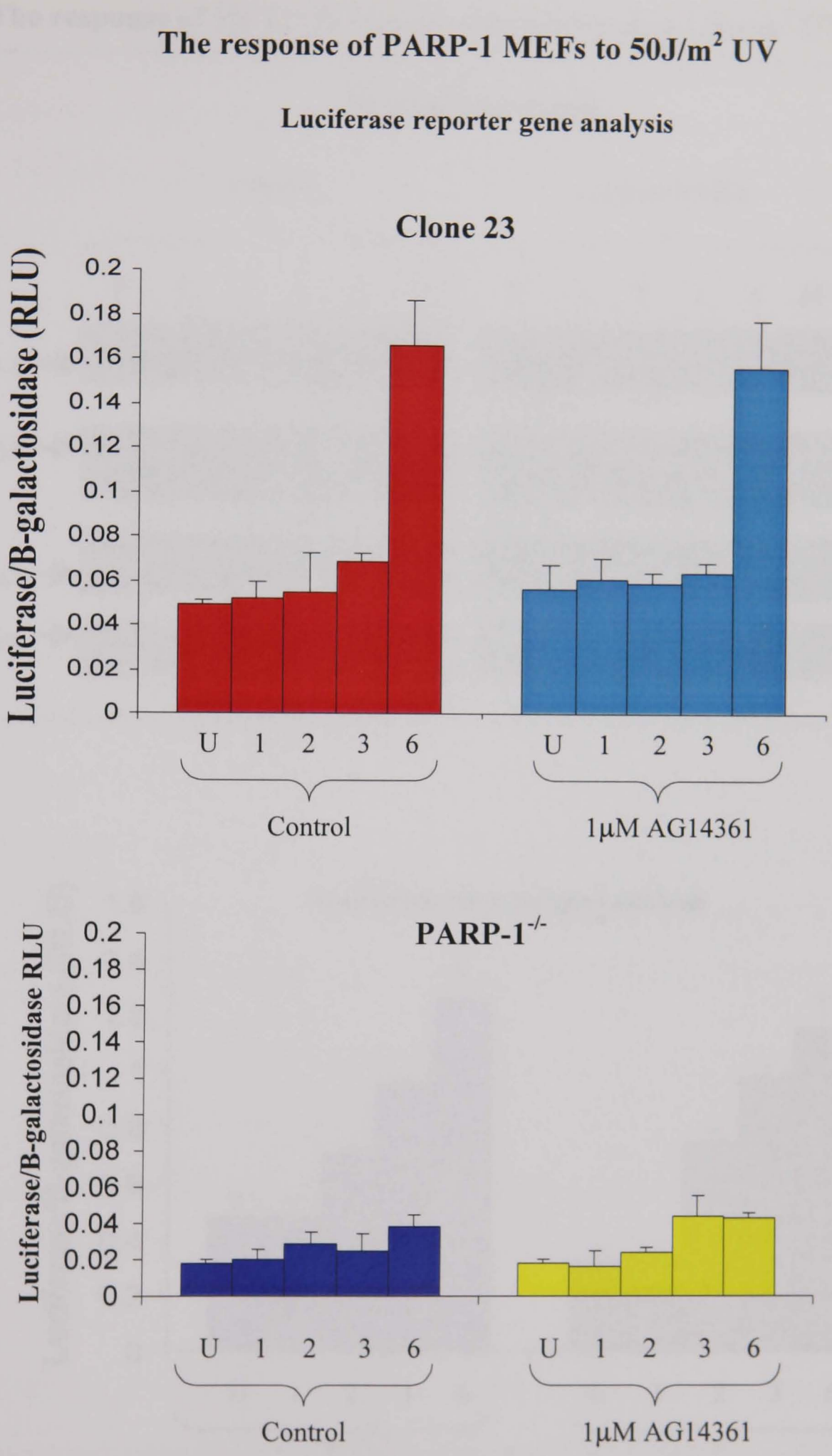


**Figure 5.9 p53 activity in clone 23 and PARP-1$^{-/-}$ MEFs in response to 50J/m$^2$ UV**
MEFs were treated with 50J/m$^2$ UV and samples taken after 1,2,3 and 6h and luciferase:β-galactosidase values measured. Controls consisted of cells treated with 0.01% DMSO.

**The response of HCT-116 human colorectal cells to 50J/m$^2$ UV**

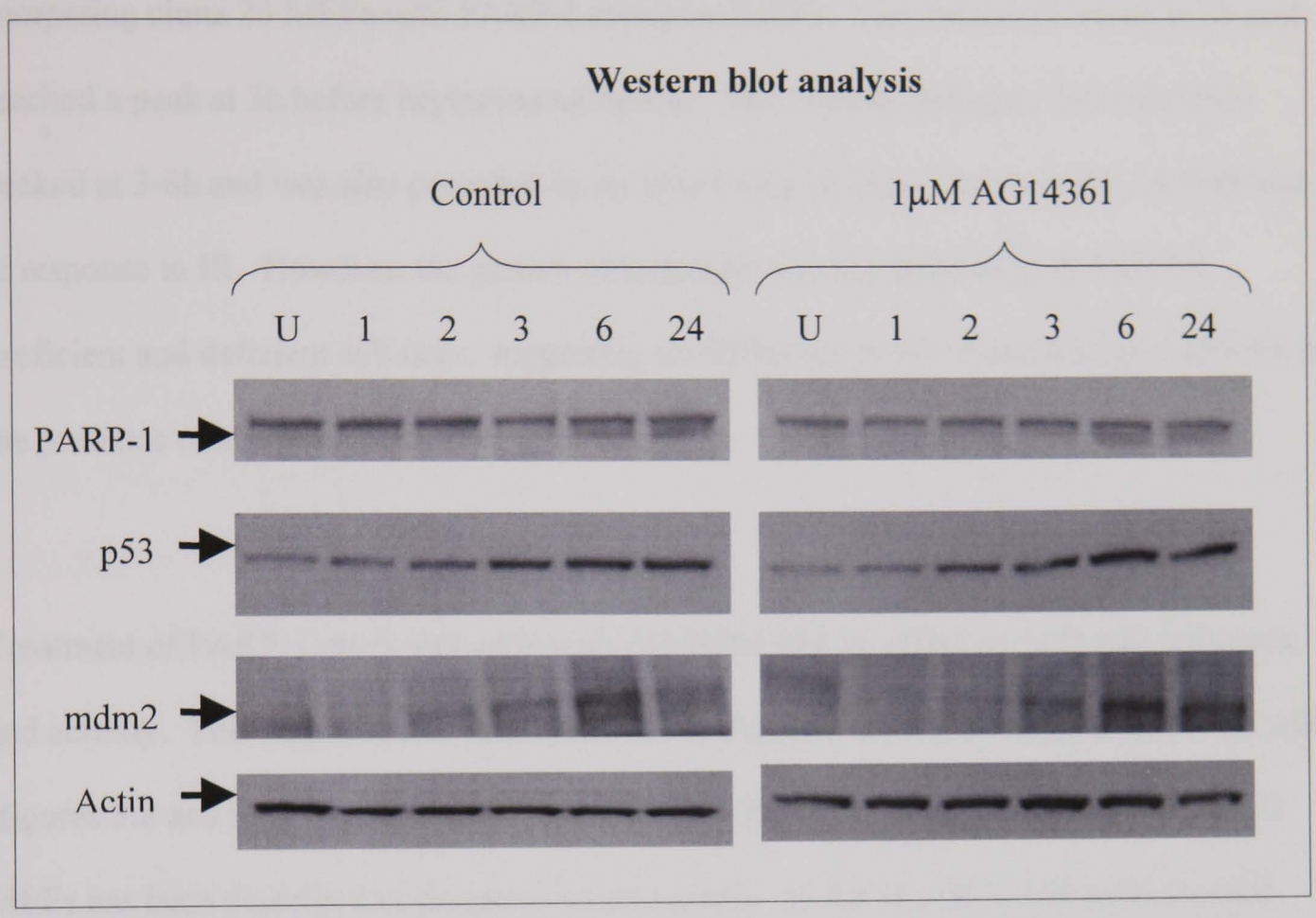


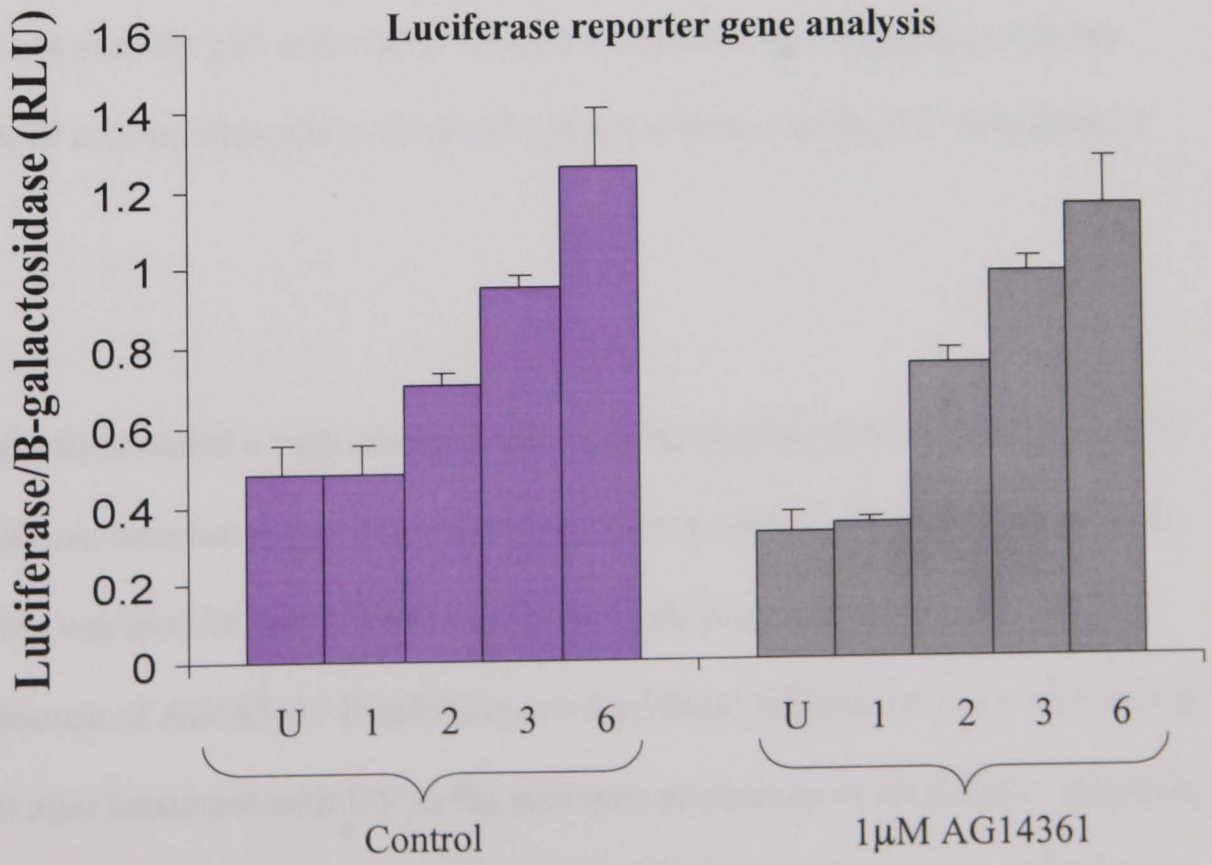


**Figure 5.10 The response of HCT-116 cells to 50J/m$^2$ – Western blot and luciferase analysis**
Samples were taken at 1, 2, 3, 6 and 24h post-UV and subject to Western blot and luciferase analysis. Controls consisted of cells treated with 0.01% DMSO.

Western blot analysis (figure 5.8) revealed no significant difference in p53 induction when comparing clone 23 MEFs with PARP-1 knockout MEFs. The induction began at 2h and reached a peak at 3h before beginning to decline. The corresponding mdm2 induction peaked at 3-6h and was also preceded by an initial drop in mdm2 levels at 1h, as observed in response to IR. However, the pattern of induction was the same in both PARP-1 proficient and deficient cell lines, suggesting no difference in p53 transcriptional activity in the presence or absence of PARP-1 protein.

Treatment of PARP-1 proficient cells with AG14361 had no effect on both p53 induction and activity. This response has been observed in clone 23 MEFs, as well as HCT-116 cells (figures 5.8 and 5.10, respectively). The pattern of p53 and mdm2 induction in clone 23 MEFs has been described in the previous paragraph. As for IR, HCT-116 cells showed different kinetics of p53 induction compared to the MEFs, with levels beginning to increase at 2h and increasing gradually up to 24h. Treatment of the PARP-$1^{-/-}$ cells with AG14361 did not alter the p53 and mdm2 induction in these cells, suggesting that the alternative PARP activity detected in these cells is not involved in the UV-induced p53 response.

Luciferase analysis revealed a very similar pattern to the response observed after IR, with the most significant increase apparent at 6h, in accordance with the Western blot analysis for mdm2. This was true for both PARP-1 proficient cell lines that were tested, in the presence or absence of AG14361. In addition, no significant differences were observed at any time point after treatment with UV in the presence or absence of AG14361. However, the PARP-$1^{-/-}$ MEFs, as was the case with IR, showed overall lower values. Analysis of

the raw data again showed reduced luciferase and β-galactosidase values (approximately 10-fold, data not shown), suggesting a requirement for PARP-1 protein to enable efficient transfection and/or expression of the plasmids in this cell line.

The luciferase and Western blot data presented in this section clearly show that neither PARP-1 protein nor activity are involved in the p53 response to UV light in the cell lines tested. This section of data is in agreement with Valenzuela *et al.*, 2002, who showed no difference in p53 induction or activity in response to UV-irradiation in PARP-$1^{+/+}$ and PARP-$1^{-/-}$ MEFs.

### 5.2.4 Analysis of the temozolomide-induced p53 response in cells lacking PARP-1

Temozolomide is a monofunctional alkylating agent that has been developed within the last ten years and is currently used in the treatment of certain human tumours, particularly malignant brain tumours (for a review of temozolomide structure and function, see Newlands *et al.*, 1997) Alkylating agents act by directly modifying DNA bases, predominantly in nucleophilic regions, with the principal lesion induced by temozolomide being N7-methylguanine. The damage produced is repaired by the base excision repair (BER) pathway (see Section 1.4.3). Although this process will be discussed as being one pathway, it should be noted that there are several variations, each specific for a different type of modified base. However, all of the pathways have features in common. For example, the damaged base is first recognised by a DNA glycosylase, which appears to diffuse along the minor groove of DNA. The base is then removed to create an abasic site. The damaged strand is then nicked by an AP endonuclease upstream of the abasic site. This creates a 3' OH overhang, which is essential for the synthesis of new DNA. This

synthesis is performed by DNA polymerase β, which displaces and nicks the damaged strand before sealing of the DNA strand by DNA ligase III.

Studies have shown that in the absence of PARP-1, cells or animals are particularly hypersensitive to treatment with alkylating agents (Wang *et al.,* 1998; de Murcia *et al.,* 1997; Delaney, *et al.,* 2002). It is thought that after the excision of the damaged base, PARP-1 binds to the single strand break as part of a BER complex (consisting at least of XRCC1, PARP-1 and DNA ligase III). The exact role of PARP-1 is unclear, however, a study has implicated PARP-1 in the DNA synthesis step (in association with XRCC1), possible by recruiting DNA polymerase to the site of damage (Dantzer *et al.,* 1999). Previous studies have identified an increased p53 response to alkylating agents in the absence of PARP-1 (de Murcia *et al.,* 1997 and Venezuela *et al.,* 2002). This altered response was explained in terms of a persistence of DNA damage due to the lack of PARP-1, subsequent impaired BER pathway and hence increased signalling to p53, possibly caused by hyperactivation of kinases such as ATM.

This section contains data analysing the temozolomide-induced p53 response in cells lacking PARP-1 through either inhibition or knocking out of the PARP-1 gene.

## The response of PARP-1 MEFs 0.5mM temozolomide

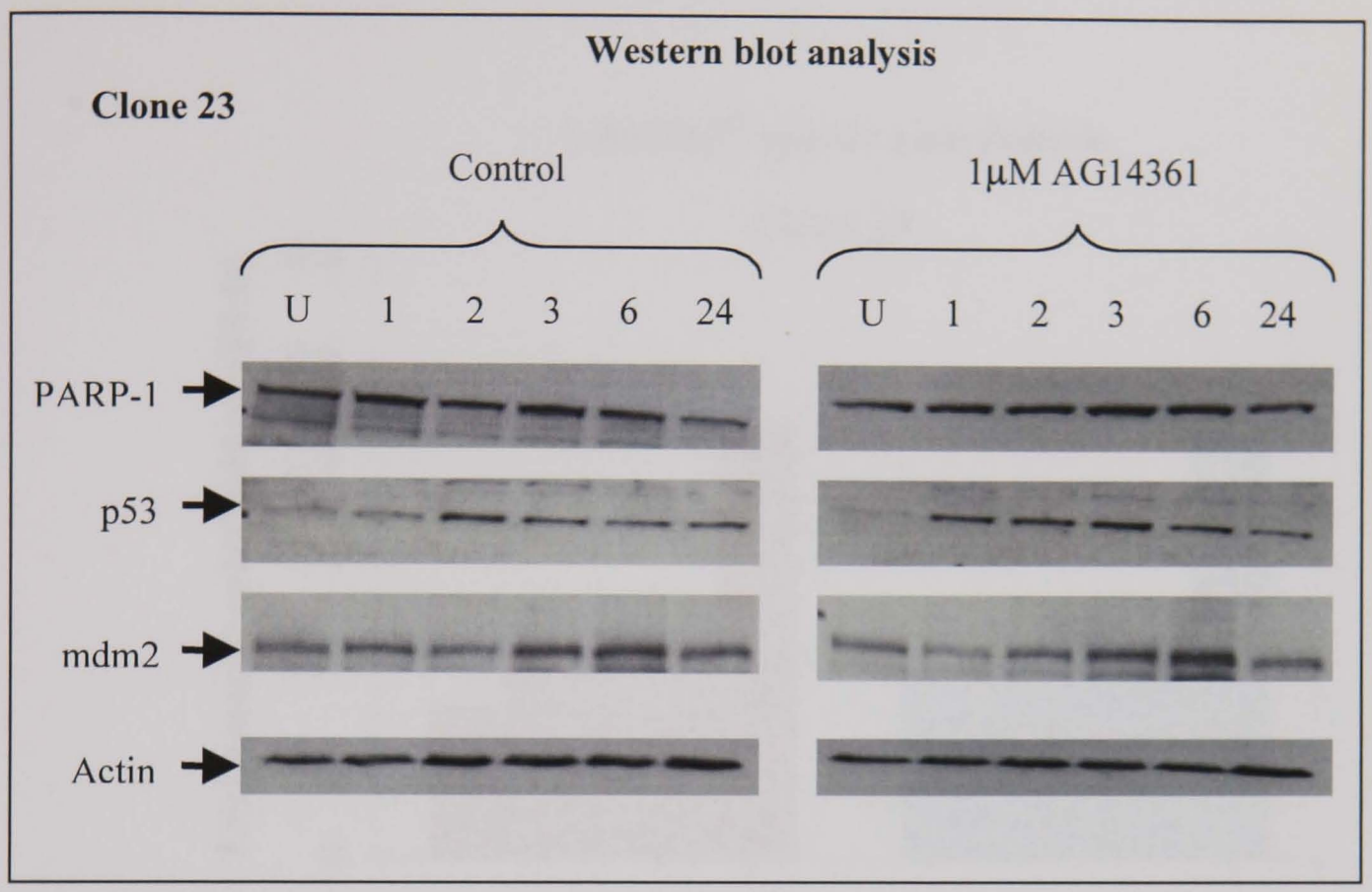


**Figure 5.11 The response of clone 23 and PARP-1$^{-/-}$ MEFs to 0.5mM temozolomide - Western blot analysis**
MEFs were treated with 0.5mM temozolomide and samples taken after 1, 2, 3 and 6h for Western blot analysis. Controls consist of cells treated with 0.01% DMSO

## The response of PARP-1 MEFs to 0.5mM temozolomide

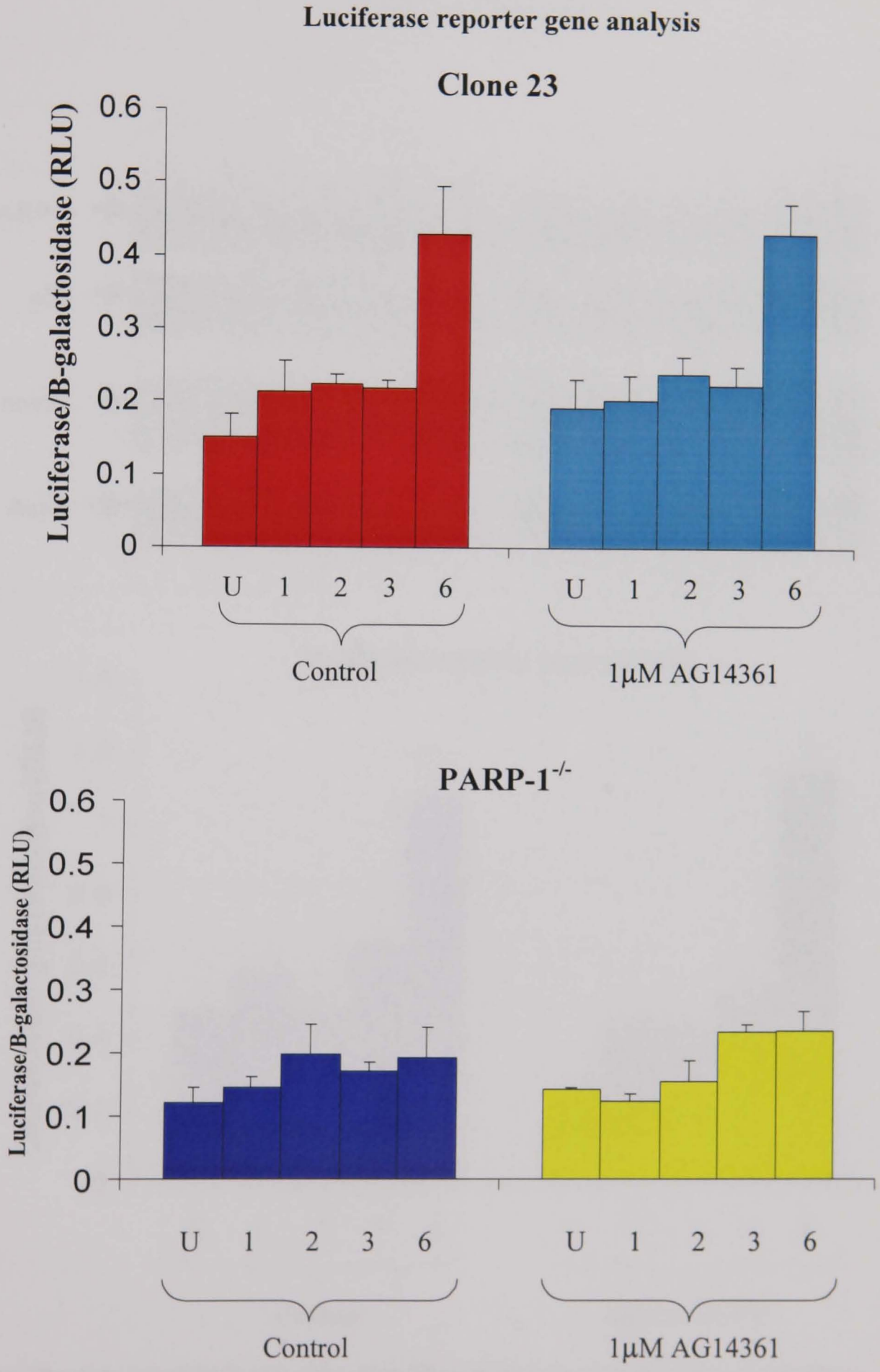


**Figure 5.12 p53 activity in clone 23 and PARP-1$^{-/-}$ MEFs after 0.5mM temozolomide treatment**
MEFs were treated with 0.5mM temozolomide and samples taken after 1,2,3 and 6h and luciferase: β-galactosidase values measured. Controls consist of cells treated with 0.01% DMSO

**The response of HCT-116 human colorectal cells to 0.5mM temozolomide**

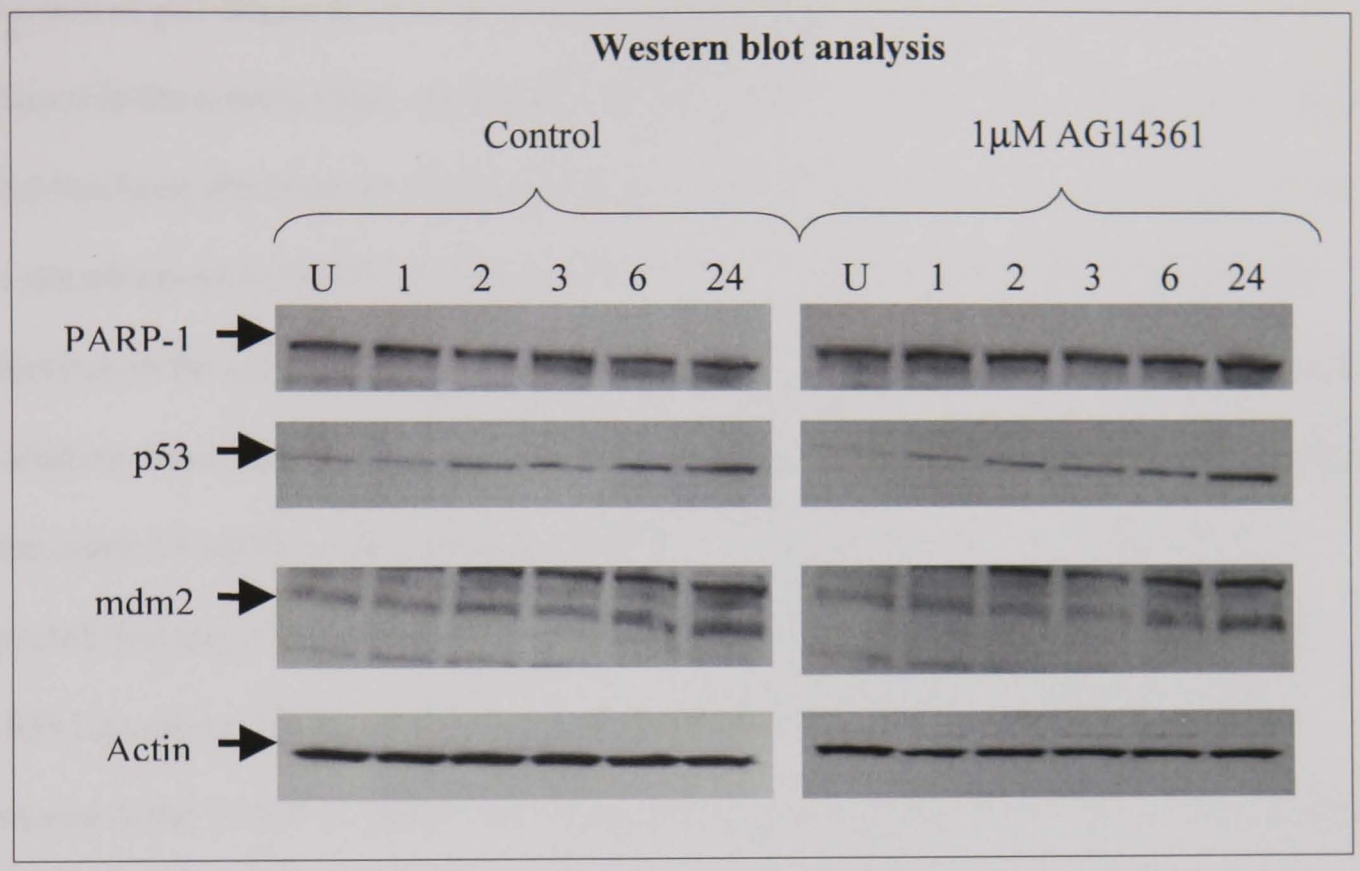


**Figure 5.13 The response of HCT-116 cells to 0.5mM temozolomide – Western blot and luciferase analysis**

Samples were taken at 1, 2, 3, 6 and 24h post-UV and subject to Western blot and luciferase analysis. Controls consist of cells treated with 0.01% DMSO

Treatment of PARP-1 proficient MEFs with 0.5mM temozolomide and AG14361 slightly increased the p53 induction when compared to the DMSO-treated control cells. The induction of p53 began at 1h in the inhibitor treated cells, whereas no induction was yet apparent in the control cells, and remained more elevated at 3 and 6h. Although this slight effect has been observed on three independent occasions, it should be noted that this effect was not observed in HCT-116 (figure 5.13). Instead, these cells exhibited identical p53 inductions in the presence or absence of PARP-1 activity when treated with temozolomide. In addition, there was no significant difference in mdm2 induction or luciferase production in the clone 23 MEFs in the presence or absence of AG14361. Finally, it might be expected that any effect observed with the PARP-1 inhibitor will also be evident in the PARP-1 knockout MEFs. However, as can be seen in figure 5.11, the p53 induction observed in the PARP-$1^{-/-}$ MEFs was almost identical to that in the DMSO-treated PARP-1 proficient MEFs, again suggesting that PARP-1 is not involved in the regulation of p53. Taken together, it seems that the increased p53 induction observed in the Western blot analysis of clone 23 MEFs may be due to expected minor variations that occur during experiments. However, it cannot be excluded that the effect is genuine and indeed has been observed previously in cells lacking PARP-1 treated with an alkylating agent (de Murcia *et al.*, 1997). If time had permitted, these experiments would have been further repeated to confirm these results. In additon, other alkylating agents, for example MNU and MNNG would have been used.

## 5.3 Discussion

This chapter addressed the main aim of this thesis, which was to investigate the hypothesis that PARP-1 functions as an upstream regulator of p53 in response to DNA damage. Previous studies suggesting such a relationship does exist have been described in detail in

Section 1.4.6 and also summarised at the start of this chapter. It is immediately obvious from these studies that the nature of any regulation of p53 by PARP-1 remains highly controversial, with some groups reporting a reduced p53 response in the absence of PARP-1 and other groups reporting an enhanced p53 response under similar circumstances. However, these studies have involved the use of different cell lines, a variety of DNA damaging agents and also several different mechanisms have been employed to remove PARP-1 activity from cells.

This chapter contains data analysing the p53 response in mouse as well as human cell lines. Also, a range of DNA damaging agents have been employed, to vary the DNA lesions induced and hence subsequent repair pathways utilised by the cell. In addition, two different methods for the removal of PARP-1 activity have been used, that is the knocking out of the PARP-1 gene and also the use of a novel potent PARP-1 inhibitor, AG14361. As described previously in this thesis, it is of note that AG14361 is more potent than any previous PARP-1 inhibitor used to analyse p53 responses. Furthermore, the most commonly used PARP-1 inhibitor in the p53-related literature, 3-AB is approximately 1000-fold less potent than the inhibitor used in this thesis. Finally, the generation of a PARP-1 stably transfected cell line produced a PARP-1 proficient and deficient cell line pair with identical genetic backgrounds. The p53 status of these MEFs has been confirmed as wild-type. It should be noted that previously published studies involving the use of immortalised PARP-1 MEFs have not analysed the p53 status of these cells. Taken together, a comprehensive set of data has been compiled addressing all of the major variables within the literature.

As well as analysing p53 levels and activity by Western blot analysis (by monitoring the levels of mdm2 and confirming normal p53 and mdm2 induction in the cell lines used), a luciferase reporter gene assay has been used to measure the transcriptional activity of p53. This assay is based on the transient transfection of a plasmid containing a luciferase gene downstream of the P2 promoter of *MDM2*. This P2 promoter is p53-responsive therefore, after DNA damage of the transfected cells, luciferase levels should increase in accordance with an increase in p53 activity. To control for transfection efficiency, a plasmid containing a β-galactosidase gene was co-transfected with the luciferase plasmid and a ratio of luciferase/β-galactosidase calculated to represent p53 activity. Before using the reporter gene assay to measure p53 activity, it was necessary to validate the assay. This was achieved by showing that the P2 promoter was necessary for the expression of luciferase by transfecting cells with the luciferase plasmid with and without the P2 promoter. Figure 5.1 shows that the plasmid containing the P2 promoter resulted in much greater expression of luciferase. Furthermore, it was shown that this luciferase expression was dependent on p53 status, with a p53 degraded cell line (HCT-116 N7) producing lower luciferase levels compared to the corresponding p53 wild-type cell line (HCT-116). Finally, it was necessary to show that the luciferase assay was responsive to DNA damage. Therefore, HCT-116 cells were treated with 5Gy IR and luciferase levels measured over a period of 6h. The data showed an increase in luciferase 6h after IR treatment, corresponding to an increase in p53 and mdm2 protein levels as measured by Western blot analysis (figure 5.3). This assay was therefore used as a validated measure of p53 activity in all subsequent DNA damage response experiments.

### 5.3.1 Analysis of the reduced luciferase and β-galactosidase levels observed in the luciferase assay in PARP-1$^{-/-}$ MEFs

Initial experiments using PARP-1 proficient and PARP-1$^{-/-}$ MEFs treated with 5Gy IR produced interesting results in the luciferase assay. Plotting of the results in a bar chart showed that the PARP-1 knockout MEFs had reduced luciferase/β-galactosidase values compared to the PARP-1 proficient cells. In addition, these values did not increase with time after DNA damage (figure 5.5). Initially this could be interpreted as a reduced p53 activity in the absence of PARP-1. However, closer analysis of the raw data values reveals a large reduction in both luciferase and β-galactosidase values (approximately 10-fold). This phenomenon has been described previously, with Agarwal *et al.*, 1997 describing a reduced luciferase expression in PARP-1$^{-/-}$ MEFs compared to their PARP-1$^{+/+}$ counterparts. However, the reduction observed was only 10%, whereas the reduction observed in this thesis was up to 90% in the actual raw data values compared to the PARP-1 proficient MEFs (see figure 5.6). The study of Agarwal *et al.*, 1997 showed only the data obtained from the calculation of ratios of luciferase to a transfection control (which was LacZ expression in that study). Therefore, it is possible that the raw data values (for luciferase and LacZ) may have decreased significantly compared to the PARP-1$^{+/+}$ MEFs. However, this would not significantly alter the resultant ratio. If the raw data values of such an experiment alter to the extent observed in this thesis, then the results could not be used as a reliable indicator of p53 activity. It should also be noted that the PARP-1 proficient MEFs used in this thesis were produced by the stable transfection of PARP-1 into the PARP-1 knockout MEFs. Therefore, these cells are predicted to be genetically identical except for the expression of PARP-1 in the stably transfected cell line, thus excluding the possibility that different genetic backgrounds of the cells were influencing the luciferase assay. Treatment of the PARP-1 stable transfectant with AG14361 did not alter the expression of luciferase or β-galactosidase, therefore the effect observed in the

PARP-1$^{-/-}$ cells is possibly a result of the lack of PARP-1 protein rather than activity. As described in section 1.4.5, PARP-1 protein has been implicated in the control of transcription, with studies showing that PARP-1 can bind and/or ADP-ribosylate several components of the transcriptional machinery. However, Western blot analysis of mdm2 revealed that the absence of PARP-1 protein did not influence the IR-induced increase in expression of this endogenous (as opposed to transfected) gene. Transcription of this gene relies upon the same promoter used in the luciferase assay (the P2 promoter of *MDM2*). Therefore, it appears that the observed decrease in plasmid expression in the PARP-1$^{-/-}$ MEFs was either due to reduced transfection efficiency or reduced expression, specifically, of exogenous plasmids in the absence of PARP-1 protein. These hypotheses are further supported by the fact that β-galactosidase values are also significantly reduced in the absence of PARP-1 protein. The fact that PARP-1 inhibition does not reduce luciferase or β-galactosidase values suggests that it may be that PARP-1 interacts with certain proteins, or indeed the exogenous DNA itself, resulting in stabilisation and/or expression of the plasmid gene. If time had permitted, this interesting observation would have been investigated further. For example, transient transfection of PARP-1 into PARP-1$^{-/-}$ MEFs may have resulted in an increase in luciferase expression. However, there would be no way of knowing what percentage of cells had actually been transiently transfected with PARP-1 in this system, making the interpretation of such results difficult.

### 5.3.2 Analysis of the p53 response to different DNA damaging agents in the presence and absence of PARP-1

The p53 response was analysed using Western blotting and a luciferase reporter gene assay. Three different DNA damaging agents were used, IR, UV and temozolomide. In addition, experiments were performed in MEFs (PARP-1 proficient and deficient) and

human HCT-116 cells. PARP-1 activity was abolished in the PARP-1 proficient mouse and human cells by treating with 1μM AG14361.

### 5.3.2.1 IR treatment

The PARP-1 proficient MEFs showed an identical p53 induction to the PARP-1 knockout MEFs, as measured by Western blot analysis (figure 5.4). In addition, the induction of the p53 target gene, mdm2 was identical. This indicates that PARP-1 is not required for the efficient induction or activation of p53 in response to IR. This result is in agreement with Masutani *et al.,* 1999, who observed similar responses in PARP-$1^{+/+}$ and PARP-$1^{-/-}$ MEFs treated with 8Gy IR. However, other studies have suggested a reduced p53 response in the absence of PARP-1 after treatment with IR. For example, after 5Gy IR treatment, PARP-$1^{-/-}$ MEFs (disrupted in exon 2) were found to have a reduced p53 induction (approximately 20% compared to PARP-$1^{+/+}$ MEFs) (Agarwal *et al.,* 1997). However, only 24h time points were analysed in this study, whereas p53 has usually been maximally induced between 2 and 4h before gradually returning to basal levels. This study also demonstrated that downstream effects of p53 were unaffected by this reduced p53, with PARP-1 knockout MEFs demonstrating an intact G1 arrest after IR. A similar study using different PARP-$1^{-/-}$ MEFs (disrupted in exon 4 as are those used in this thesis) also showed a reduced p53 response to 6Gy IR (Valenzuela *et al.,* 2002). In fact, in that study the p53 induction observed in the PARP-$1^{-/-}$ MEFs was barely detectable by Western blot analysis. In contrast, a massive p53 induction is observed in the PARP-$1^{+/+}$ MEFs, beginning at 2h and reaching a peak at 6h. Despite the huge difference in p53 induction, that same study did not show any difference in cell survival between immortalised PARP-1 proficient and deficient MEFs after IR treatment. Given that the principle role of p53 in the cell is to induce cell cycle arrest to allow time for DNA repair to occur or to induce apoptosis, the lack of an effect on cell survival is perhaps surprising. It may be important to the

interpretation of results that the two studies discussed in this section have both used primary MEFs to analyse p53 responses (immortalised MEFs were used for cell survival assays). As described in the next chapter (chapter 6) of this thesis, the primary PARP-$1^{-/-}$ MEFs investigated here grow much more slowly than the PARP-$1^{+/+}$ MEFs. A retardation of growth to this degree indicates that there is a major defect in one or more pathway(s) regulating cellular proliferation. This is very likely to have consequences in terms of how the cell responds to genotoxic stress *via* the activation of p53, which is itself important in the regulation of cellular proliferation. Results obtained in such circumstances may not be representative of the normal cellular response to DNA damage.

Studies have also been performed on immortalised MEFs. For example, basal p53 levels in immortalised PARP-$1^{-/-}$ MEFs (disrupted in exon 2) were substantially lower than in PARP-$1^{+/+}$ MEFs (Wesierska-Gadek *et al.*, 1999). In addition, a reduced p53 induction in response to doxorubicin (a topoisomerase II poison) was observed in the absence of PARP-1 in the same study. However, results presented in this thesis have suggested a propensity for the PARP-$1^{+/+}$ MEFs to undergo p53 mutations during immortalisation whereas the PARP-$1^{-/-}$ MEFs retain wild-type p53 (see Chapter 4, Section 4.2.1). Indeed, several studies have been published describing a tendency for MEFs generally to develop p53 mutations during immortalisation (Rittling and Denhardt, 1992; Jenkins *et al,* 1984; Harvey and Levine, 1991). The observed phenotype of the immortalised MEFs in this thesis, in terms of p53 expression, is higher basal levels in the p53 mutant PARP-$1^{+/+}$ MEFs compared to the p53 wild type PARP-$1^{-/-}$ MEFs. Therefore, when considering studies with immortalised MEFs, that do not present sequencing data, the possibility cannot be excluded that the cells are expressing mutant p53, which would abolish or alter the p53 induction usually observed in response to DNA damage. In this thesis, by the

transfection of PARP-1 into PARP-1 knockout MEFs, a cell line pair has been produced that both express wild type p53 but are either proficient or deficient in PARP-1. Therefore, the results presented in this thesis have circumvented the potential problems of p53 mutations which tend to be selected for during the immortalisation of MEFs. Also, the immortalised MEFs, by definition, have a faster growth rate than the primary MEFs, eliminating any of the potential problems encountered with very slow-growing primary cell lines (see Chapter 6 for further details). In addition, the results obtained in the PARP-1 knockout MEFs have been replicated using the PARP-1 inhibitor, AG14361, further supporting the conclusion that PARP-1 is not involved in the regulation of p53 in response to IR.

As briefly described above, 1μM AG14361 does not alter the p53 response after IR treatment. This was true in the clone 23 MEFs and also the human HCT-116 cells. Western blot analysis of p53 and mdm2 in both cell lines showed identical patterns of induction with or without 1μM AG14361. In addition, in the PARP-1 proficient cell lines, where transfection efficiencies were not reduced, and it was possible to derive conclusions from the luciferase reporter gene assay, again 1μM AG14361 did not affect the observed increase in p53 activity over time in both cell lines.

Previous studies analysing p53 responses after IR treatment using PARP-1 inhibitors have produced conflicting results. For example, Lu and Lane, 1993, observed an increased p53 response after treatment of cells with 3-AB and IR. The authors proposed that the increased p53 was due to a persistence of strand breaks, caused by PARP-1 inhibition and slowing of repair, resulting in increased signalling to p53. Conversely, Wang *et al.*, 1998,

showed that the p53 induction in glioblastoma cells treated with 3-AB was significantly reduced 1.5h after IR treatment. This corresponded with a reduction in the levels of both p21 and mdm2. However, the effect observed was only transient with no reduction in p53 evident at later time points. It should be strongly noted that both of the studies mentioned used 3-AB, a 1000-fold less potent and less specific PARP-1 inhibitor than AG14361, the inhibitor used in this thesis. Therefore, some of the effects observed with this inhibitor may be due to non-specific effects of the inhibitor (e.g. Hunting *et al.*, 1985), which is influencing the p53 response to IR. It also cannot be excluded that the differences observed are due to different cell lines being used in the studies described.

The results summarised in this section strongly suggest that PARP-1 is not involved in the IR-induced p53 response. Contradictory published data has been summarised, along with possible explanations for the contradictory data described. The results presented within this thesis allow conclusions to be derived, which will not have been influenced by such factors as the p53 status of immortalised MEFs or the probable lack of inhibitor specificity. Instead, PARP-1 proficient and deficient MEFs, with proven wild-type p53, have been used along with an inhibitor that has been shown to abolish ADP-ribose polymer formation at a concentration of 1μM. This is in marked contrast to the > millimolar concentrations of 3-AB required to achieve similar PARP-1 inhibition. As well as Western blot analysis, an intact cell reporter gene assay has been used to measure p53 activity. Taken together, a comprehensive set of data has been amassed showing that PARP-1 is not involved in the regulation of p53 in response to 5Gy IR.

The advantages of the cell lines (in terms of known p53 status in the MEFs) and inhibitor used, which have been described in this section, will also apply to the following sections where results of identical experiments with different DNA damaging agents are discussed.

### 5.3.2.2 Ultra violet radiation

The majority of studies analysing the involvement of PARP-1 in the cellular response to UV have suggested that PARP-1 is not involved in the repair of UV-induced damage, with no sensitisation to UV observed in the absence of PARP-1. In addition no poly-ADP-ribose was synthesised in response to UV treatment (Satoh *et al.,* 1993; Molinete *et al.,* 1993, Wang *et al.,* 1995). Contrary to these findings, several earlier studies showed that PARP-1 activity increases in human lymphoblastoid cell lines after UV treatment (see Section 1.4.3.2). Interestingly, this activation was abolished in xeroderma pigmentosum lymphoblast cells, which are unable to excise pyrimidine dimers (Berger *et al.,* 1980). This suggests that the strand break generated after dimer excision is able to activate PARP-1. It is therefore possible that this PARP-1 activation could influence the downstream activation of p53. However, the results presented in this thesis suggest this regulation does not occur in MEFs or the established HCT-116 cells.

PARP-1 proficient MEFs treated with $50J/m^2$ UV showed the same pattern of p53 and mdm2 inductions, both quantitatively and with the same time course, as PARP-1 knockout MEFs, as shown by Western blot analysis. This is in agreement with Valenzuela *et al.,* 2002, who showed an identical pattern of p53 induction in PARP-$1^{+/+}$ and PARP-$1^{-/-}$ MEFs after $40J/m^2$ UV. No conclusions could be derived from the luciferase assays comparing

the PARP-1 proficient and deficient MEFs in this thesis, for the reasons discussed in section 5.3.1.

Experiments involving the use of AG14361 to remove PARP-1 activity from PARP-1 proficient cell lines have also shown that PARP-1 is not involved in the p53 response to UV-irradiation. Both PARP-1 proficient MEFs and HCT-116 human colorectal cells showed identical patterns of p53 and mdm2 induction in the presence or absence of 1μM AG14361. In addition, luciferase assays measuring p53 activity in these cell lines also showed that AG14361 did not change the observed response to UV (figures 5.8 and 5.9).

Studies elsewhere showing an altered p53 response in the absence of PARP-1 after treatment with certain DNA damaging agents suggest one of two mechanistic explanations. Firstly, some groups suggest that the absence of PARP-1 leads to a prolongation of strand breaks in response to DNA damage and hence an increased p53 response, presumably due to e.g. increased ATM kinase signalling to p53. Such a response has been observed with IR and MNU (Lu and Lane, 1993; de Murcia *et al.*, 1997). This is obviously not a direct regulatory role of PARP-1 on p53. Rather, it is a side-effect due to an impaired DNA repair pathway in the absence of PARP-1, leading to persistence of DNA strand breaks. The fact that several studies have shown that PARP-1 is not involved in the repair of UV-induced DNA damage (Satoh *et al.*, 1993; Molinete *et al.*, 1993, Wang *et al.*, 1995) suggested that an increased p53 response to UV in the absence of PARP-1 would not be expected. This is in agreement with the results presented in this thesis. The second explanation provided for an altered p53 response to DNA damage is that PARP-1 is directly regulating p53, putatively by poly(ADP-ribosyl)ation or protein-protein interaction. Several studies have shown that PARP-1 is not activated in response to UV (Satoh *et al.*, 1993; Molinete *et al.*, 1993), suggesting that post-translational modification

of p53 by PARP-1 could not occur after exposure to UV, and hence the p53 response would not be altered in the absence of PARP-1. Again this is consistent with the results presented in this thesis.

### 5.3.2.3 Temozolomide treatment

Several studies have been published showing that animals and cells lacking PARP-1 are hypersensitive to treatment with alkylating agents, with the relevant data being summarised in Section 1.4.3 (Wang *et al.*, 1997; de Murcia *et al.*, 1997; Masutani *et al.*, 1999). The putative basis for this sensitivity was a defect in the base excision repair pathway that would usually repair lesions caused by alkylation damage, hence causing a potentiation of the DNA damage and the consequent decrease in survival. In such circumstances it might be expected that the prolongation of strand breaks would bring about an enhanced p53 response. This effect has indeed been observed in PARP-1 MEFs treated with MNU, a monofunctional alkylating agent (de Murcia *et al.*, 1997; Valenzuela *et al.*, 2002).

The data presented in this thesis did show a slight potentiation of the p53 induction in PARP-1 proficient MEFs treated with temozolomide and 1μM AG14361 when compared to control cells. This observation would be in agreement with those studies described earlier in this section. However, an enhanced p53 induction may be expected to bring about an increased mdm2 induction due to increased transcriptional transactivation activity of p53. However, this was not observed, since very similar mdm2 inductions were seen in the presence or absence of AG14361 in the PARP-1 proficient MEFs. The lack of a change in p53 transactivation activity is also demonstrated in the luciferase assay, where AG14361 clearly had no effect on the p53 activity in the clone 23 MEFs. It is important to

note that an increase in p53 activity depends upon a variety of post-translational modifications, including phosphorylation and acetylation on several amino acid residues. It therefore cannot be excluded that p53 levels are increasing, but the post-translational modifications required to increase DNA binding are not occurring. Despite this, a change in p53 response observed in the presence of AG14361 would perhaps be expected to occur in the PARP-1$^{-/-}$ MEFs also. However, as was seen in figure 5.12, the PARP-1$^{-/-}$ MEFs produced p53 and mdm2 inductions very similar to the control clone 23 MEFs. In addition, experiments performed in HCT-116 cells showed that both p53 levels and activity were unchanged in the presence and absence of 1μM AG14361. The enhanced p53 levels in clone 23 MEFs treated with AG14361 may be due to a cell-line specific effect that does not occur in HCT-116 cells. In addition, in the PARP-1 MEFs, the difference between inhibiting PARP-1 and knocking out PARP-1 may account for the apparent discrepancy between PARP-1 inhibited MEFs and PARP-1 knockout MEFs.

For example, in response to temozolomide treatment, strand breaks are generated in both PARP-1 proficient and deficient MEFs, as PARP-1 is not involved in the actual removal of the damaged base or the incision event at the AP site (Shall, 1984). In the clone 23 MEFs treated with AG14361, PARP-1 would bind to the strand break and remain bound due to inhibition of catalytic activity and hence lack of PARP-1 automodification which would result in its release. The bound PARP-1 may in turn block access of other repair enzymes to the site of damage and hence the strand break persists, potentially leading to hyperactivation of DNA damage response kinases, such as ATM or ATR, and increased signalling to p53. In this situation, the effect would not be observed in the PARP-1 knockout cells as access of repair enzymes to the strand break is not blocked by the presence of PARP-1. Although this hypothesis would explain the data obtained after

treatment of PARP-1 MEFs with temozolomide +/- AG14361, it is not in agreement with several published studies showing that PARP-1$^{-/-}$ MEFs have seriously inhibited repair of alkylation damage. If time had permitted the above experiments would have been repeated to try and confirm the described effect. It would then have been possible to design experiments to test the proposed model for increased p53 induction in the PARP-1 MEFs.

### 5.3.3 General conclusions

This chapter contains data that is relevant to the initial hypothesis of this thesis, which was that PARP-1 functions as an upstream regulator of p53. The data presented summarising the p53 response to UV was in accordance with those previously published data, which indicated the p53 response is independent of PARP-1. The p53 response observed after alkylating agent treatment was partially in agreement with published data, with PARP-1 proficient MEFs treated with AG14361 and temozolomide producing a slightly enhanced p53 induction compared to DMSO-treated control cells. However, such an observation was not repeated in the PARP-1 knockout MEFs. If time had permitted, an alternative alkylating agent would have been used, such as MNU, which has previously been shown to potentiate the p53 response in PARP-1 knockout MEFs compared to PARP-1 proficient MEFs. The involvement of PARP-1 in the p53 response to IR is perhaps the area of research where most studies have been performed. Curiously, these studies have not produced any firm or coherent conclusions regarding the nature of any regulation of p53 by PARP-1. In fact, different groups have produced opposing results, with some showing no involvement of PARP-1 and others suggesting a role for PARP-1 in the regulation of p53. There are many potential explanations for these discrepancies, including the different cell lines analysed and the different techniques used to remove PARP-1 activity from cells. With particular regard to this thesis, I have shown that the p53 status of immortalised

MEFs and the growth rates of primary MEFs should also be taken into consideration when performing experiments and when deriving conclusions from them. Of particular concern is the tendency of PARP-$1^{+/+}$ MEFs to develop p53 mutations during immortalisation: a phenomenon which interestingly was not observed in the PARP-$1^{-/-}$ MEFs. In addition, data within this thesis (Chapter 6) has shown a much reduced growth rate in the primary PARP-$1^{-/-}$ MEFs compared to their PARP-1 wild-type counterparts and raised doubts regarding their suitability for analysing p53 responses. Finally, doubts have been raised regarding the specificity of 3-AB, used in many studies analysing PARP-1 function. In this thesis, a very potent PARP-1 inhibitor (AG14361) has been used, which is significantly more potent than any other inhibitor that has been used to analyse p53 responses within the literature.

One or more of the factors mentioned above could influence the p53 response to DNA damage. However, data from this thesis would suggest that PARP-1 does not directly signal to, or modify p53 in the cell systems analysed. Any change in the p53 response that has been observed was after temozolomide treatment in PARP-1 inhibited MEFs, with the effect likely attributable to an impaired BER pathway.

# CHAPTER 6

# THE IMMORTALISATION OF PARP-1 MEFS

## 6.1 Introduction and objectives

The initial aim of this thesis was to use immortalised PARP-1$^{+/+}$ and PARP-1$^{-/-}$ MEFs to investigate the potential role of PARP-1 in the DNA damage-induced regulation of p53. The immortalisation procedure involves the isolation and growth in culture of primary MEFs obtained from the homogenisation of mouse embryos. These cells are then continuously passaged until they reach a stage of growth called senescence. This state is characterised by the halting of cellular growth. Senescent cells actually arrest with a G1 DNA content and cannot be stimulated to resume proliferation by mitogenic stimuli. Eventually, out of this population of essentially non-cycling cells, an immortalised sub-population of cells will grow. Several studies have been published implicating p53 in cellular senescence. For example, p53 transcriptional activity increases with the ageing of cells (Itahana *et al.*, 2001). In addition, wild type p53 is necessary for growth arrest in senescence (Sugrue *et al.*, 1997). Finally, a high percentage of cells that escape senescence have lost wild type p53 activity (see Section 6.3).

During this study, it was discovered that two independently derived lines of immortalised PARP-1$^{+/+}$ MEFs were expressing mutant p53 (Chapter 4, Section 4.2.1). However, the corresponding PARP-1$^{-/-}$ MEFs expressed wild type p53. Bearing in mind the putative role for p53 in cellular senescence and immortalisation, this was a very interesting observation. It suggests that, for some reason, the absence of PARP-1 bypasses the requirement of MEFs to mutate p53 during immortalisation. The PARP-1$^{-/-}$ MEFs have been described as being genetically unstable, characterised by an increase in sister chromatid exchanges (de Murcia *et al.*, 1997). Although the PARP-1$^{-/-}$ mice are not tumour prone, perhaps the genetically unstable cells adopt a mutation to a different gene, other than p53, allowing them to escape senescence. Alternatively, there may be a more functional explanation,

whereby PARP-1 and p53 may both have roles to play in senescence and immortalisation. In the absence of PARP-1 it may be necessary for the MEFs to retain wild type p53 whereas it may be beneficial to lose p53 function in the presence of PARP-1. In addition to being an interesting observation in this study, this finding may have relevance in terms of previously published data. As highlighted several times during this thesis, discrepancies exist regarding the role (if any) of PARP-1 in p53 regulation. In studies using immortalised MEFs, without directly sequencing the p53 and testing its functional integrity, it cannot be excluded that the PARP-$1^{+/+}$ MEFs possess a p53 with an altered function due to mutation or other mechanism of functional inactivation, such as amplification of MDM2.

The aim of this chapter was to demonstrate whether the p53 mutation was indeed a consequence of the immortalisation process. It was therefore necessary to show that both the primary MEFs and the PARP-1 mice, from which they were derived, expressed wild type p53. The p53 in primary PARP-1 MEFs was sequenced and also examined by Western blot analysis.

A further aim of this section was to repeat the immortalisation procedure in five independently derived PARP-$1^{+/+}$ and PARP-$1^{-/-}$ primary MEFs to gain a more statistically reliable figure, in terms of the p53 status in immortalised MEFs in the presence and absence of PARP-1.

As well as monitoring growth during the immortalisation experiments, observations were made regarding the morphological changes that occurred to the primary MEFs during the

course of the experiment. The cells were photographed at the pre-scenescent and scenescent phases.

As will be described in the following sections, all colonies of primary MEFs were lost before immortalisation had occurred, due to infection. Despite this, other significant and interesting observations were made during the growth of the cells. Most importantly, the PARP-$1^{-/-}$ cells had a greatly reduced growth rate compared to the PARP-$1^{+/+}$ MEFs.

Data presented in this chapter is in the form of Western blot analysis and cDNA sequencing to analyse the p53 status of PARP-1 cells or tissues. In addition cumulative growth curves are presented showing the effect of AG14361 on the long-term growth of primary and immortalised MEFs. Finally, photographs are included to demonstrate the morphological differences between primary and senescent MEFs.

## 6.2 Results

### 6.2.1 P53 expression and status in primary and immortalised PARP-1 MEFs

As previously described, the immortalised PARP-$1^{+/+}$ MEFs that were to be used in this study were found to be expressing mutant p53. This section reintroduces the data confirming the p53 status of these immortalised MEFs. In addition, corresponding data is presented from primary MEFs, demonstrating the expression of wild type p53 in both the PARP-$1^{+/+}$ and PARP-$1^{-/-}$ cells.

Western blot analysis was performed on cell lysates from two independently derived immortalised pairs of MEFs as well as on the primary MEFs. The levels of p53 expression

were measured. Frequently, p53 mutations are indicated by very high basal levels of p53 expression due to increased stability and resistance to mdm2-mediated degradation. In addition, cDNA sequencing of p53 was performed in all cell lines to complement the Western blot analysis.

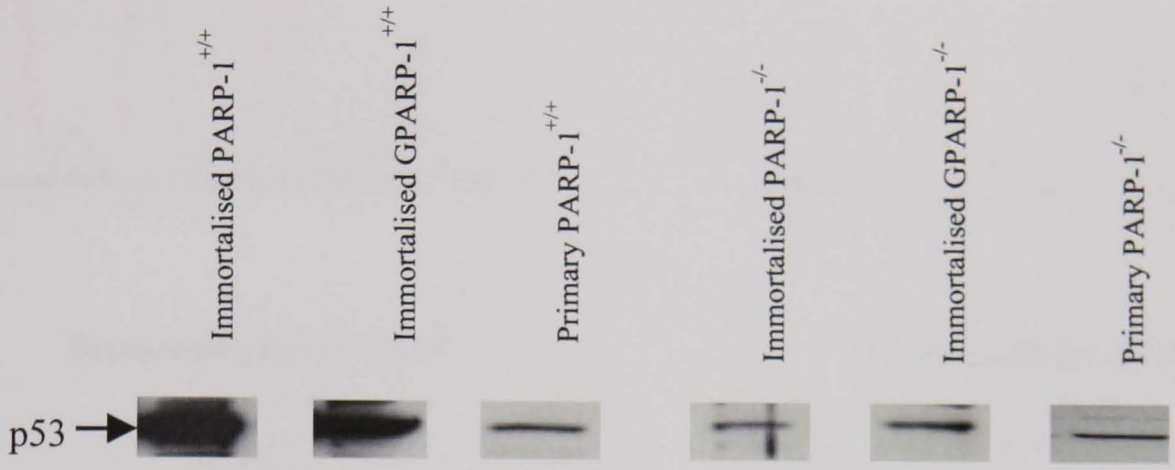


**Figure 6.1 Western blot analysis of p53 levels in untreated immortalised and primary PARP-1 MEFs**

Figure 6.1 shows that both of the independently derived immortalised PARP-$1^{+/+}$ MEFs express significantly higher p53 levels than the primary MEFs from which they were derived. It should be noted that all of the data presented in Figure 6.1 are from Western blots that were processed under identical conditions and the exposure times of the Western blots to X-ray film were constant. As described above, high basal levels of p53 are indicitive of a mutation within p53. Frequently this mutation increases the half life of p53, possibly by reducing mdm2-mediated degradation. Sequencing data for PARP-$1^{+/+}$ and GPARP-$1^{+/+}$ immortalised MEFs has been presented in Chapter 4, Section 4.2.1. However, for the purposes of this section, this data will be reintroduced and compared to additional data derived from the primary PARP-$1^{+/+}$ MEFs (passage 1).

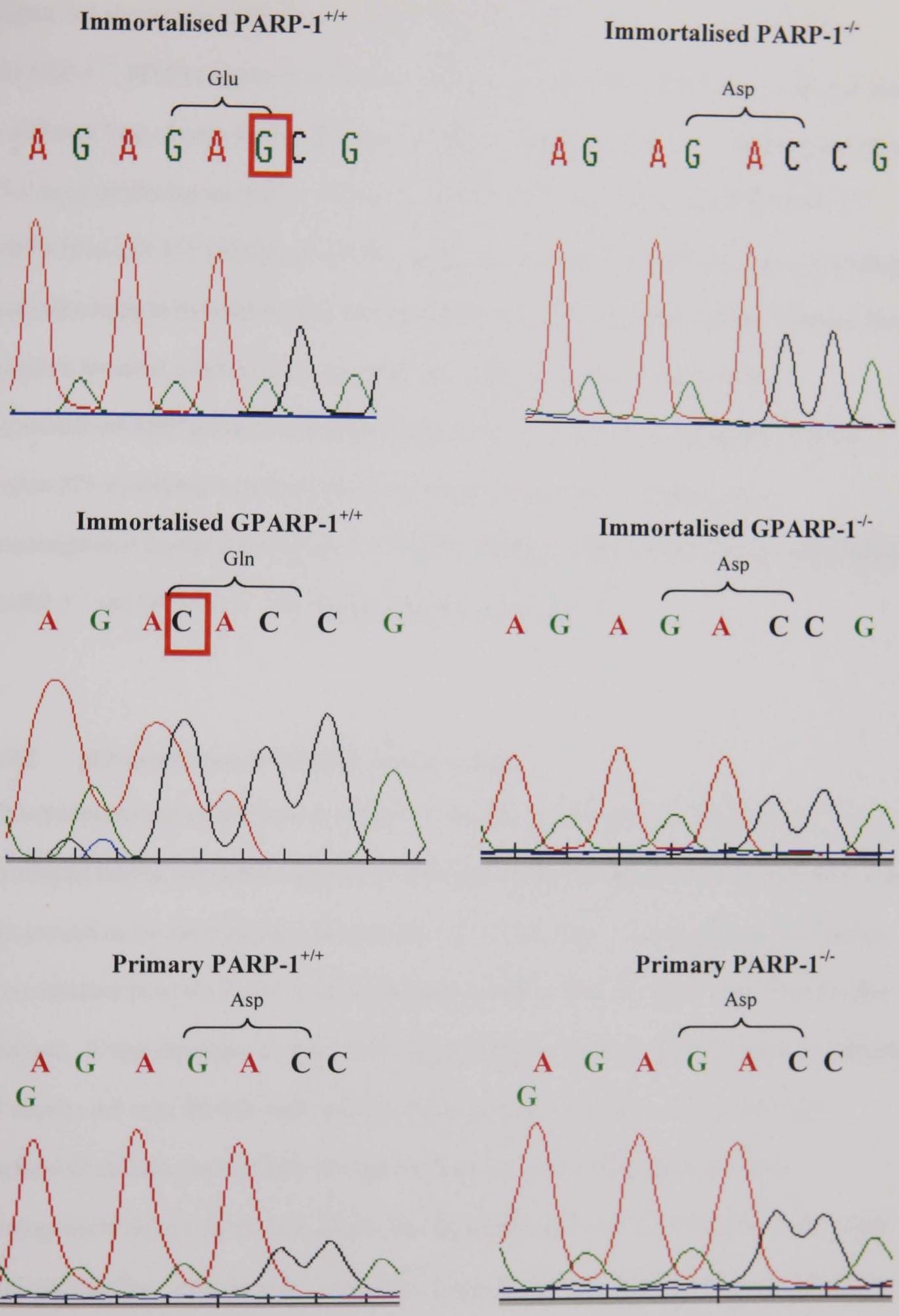


**Figure 6.2 p53 sequencing data from immortalised and primary PARP-1 MEFs**
Wild-type p53 contains an Asp residue at codon 278. Mutated bases are highlighted , with the resultant amino acid change also described.

Figure 6.2 shows that in the immortalised pairs of PARP-1 MEFs, the PARP-$1^{+/+}$ and GPARP-$1^{+/+}$ MEFs express mutant p53. Both have a mutation within codon 278, but with a different base change within that codon. The immortalised PARP-$1^{+/+}$ MEFs have a C to G change producing an Asp to Glu amino acid change. The immortalised GPARP-$1^{+/+}$ MEFs have a G to C change, producing an Asp to Gln amino acid change. It is surprising and interesting to note that both of the mutations are within the same codon. Western blot analysis revealed an inability to transactivate mdm2 in both of these PARP-$1^{+/+}$ immortalised MEF cell lines (Chapter 4, Sections 4.2.1 and 4.2.3), consistent with the codon 278 alterations representing loss of function mutations, abrogating the transcriptional transactivation function of p53. Figure 6.2 also shows that the immortalised PARP-$1^{-/-}$ and GPARP-$1^{-/-}$ MEFs both express wild-type p53.

### 6.2.2 p53 expression in PARP-1 mouse tissues

The data presented in the previous section clearly shows that p53 mutations have developed during cell culture, probably during the immortalisation process since they were not present in the early passage primary MEFs. As a further confirmation of this, tissues were isolated from the PARP-1 mice and analysed for p53 expression using Western blot analysis. It was important to check whether low basal p53 levels are expressed in a variety of tissues, not only for this study but also to validate other studies which have been performed on these mice within the Cancer Research Unit. Frozen tissues were homogenised using a pestle and mortar and liquid nitrogen, before being dissolved in hot SDS lysis buffer. After protein estimation, 50µg of total protein were subject to Western blot analysis. Tissues were isolated from three PARP-$1^{+/+}$ and PARP-$1^{-/-}$ mice and all samples analysed. As a control, samples from the relevant immortalised PARP-1 MEFs were also included on the Western blot.

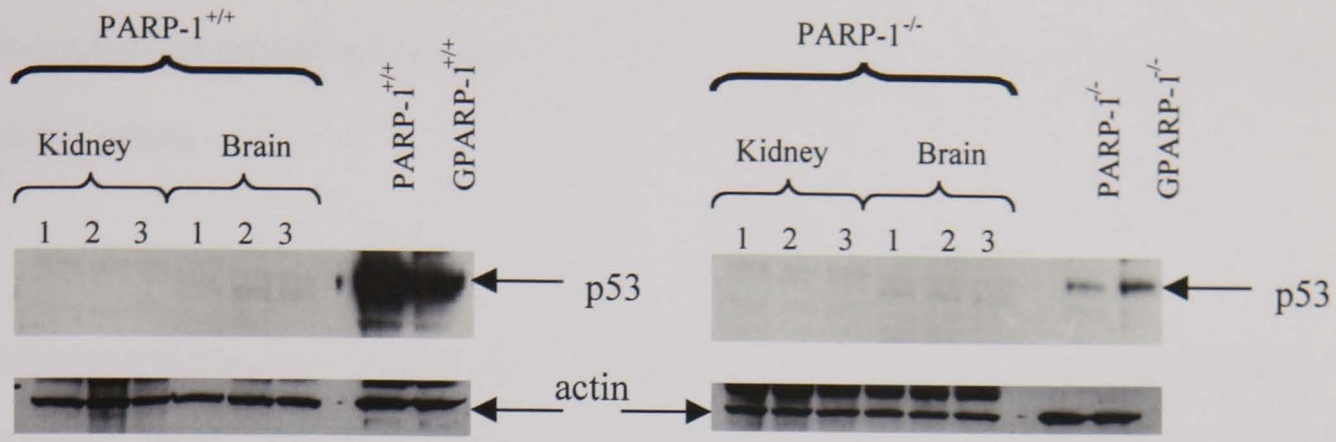


**Figure 6.3 Western blot analysis of p53 levels in PARP mouse tissues, probed with the rabbit polyclonal CM5 antibody**

As can be seen in the Western blots above (figure 6.3), tissues from the PARP-$1^{+/+}$ mice expressed very low levels of p53 compared to the immortalised +/+ MEFs derived from these mice. These lower levels were virtually undetectable and are indicative of wild type p53, further confirming that the p53 mutation has developed during cell culture. The tissues from the PARP-$1^{-/-}$ mice also possessed lower levels of p53 to the -/- MEFs derived from these mice. This may suggest that when placed in cell culture, which is a non-physiological situation, the MEFs become stressed and as a consequence slightly up-regulate p53.

### 6.2.3 The immortalisation of PARP-1 MEFs

The results presented earlier in this chapter show that two independently derived colonies of immortalised PARP-$1^{+/+}$ MEFs express mutant p53. This is in contrast to the corresponding immortalised PARP-$1^{-/-}$ MEFs that express wild type p53. In addition, it has been shown that the primary MEFs (both +/+ and -/-) express wild type p53. Therefore, it is possible that immortalisation of the PARP-$1^{+/+}$ MEFs involves selection for p53 mutations. In contrast, the absence of PARP-1 may allow the requirement to mutate

p53 during the immortalisation process to be bypassed. To test this hypothesis further, the immortalisation procedure was repeated using a greater number of independent colonies of PARP-1 MEFs.

The immortalisation process was set up according to the standard 3T3 protocol (Todaro and Green, 1963). Briefly, 1 x $10^6$ cells (passage 1) were placed into a 100mm tissue culture dish and allowed to grow for 3 days. The cells were then counted and re-plated at 1 x $10^6$ cells per plate. This process was repeated until the cells had reached senescence. This phase in cellular growth is characterised by a halting of proliferation. At this point, upon splitting, cell numbers had actually decreased. It was therefore decided to stop splitting every three days and to simply observe the cells, looking for evidence of transformed (immortalised) cells. Such areas are apparent in the form of dense patches of small cells, which is in contrast to the large, irregular-shaped senescent cells (see figure 6.5 for the morphology of cells). Five independent plates were set up for each of the PARP-$1^{+/+}$ MEFs, the PARP-$1^{-/-}$ MEFs and also PARP-$1^{+/+}$ MEFs grown in the presence of 1μM AG14361. By setting up five independent plates of $1^{st}$ passage cells and keeping them growing independently, it was ensured that any immortalised colonies eventually isolated that contain p53 mutations will have arisen by independent events. AG14361 will inhibit PARP-1 activity in these cells and, as in PARP-$1^{-/-}$ MEFs, may allow immortalisation without mutation of p53. The cell counts for all 15 independent colonies were plotted in the form of cumulative growth curves (Figure 6.4).

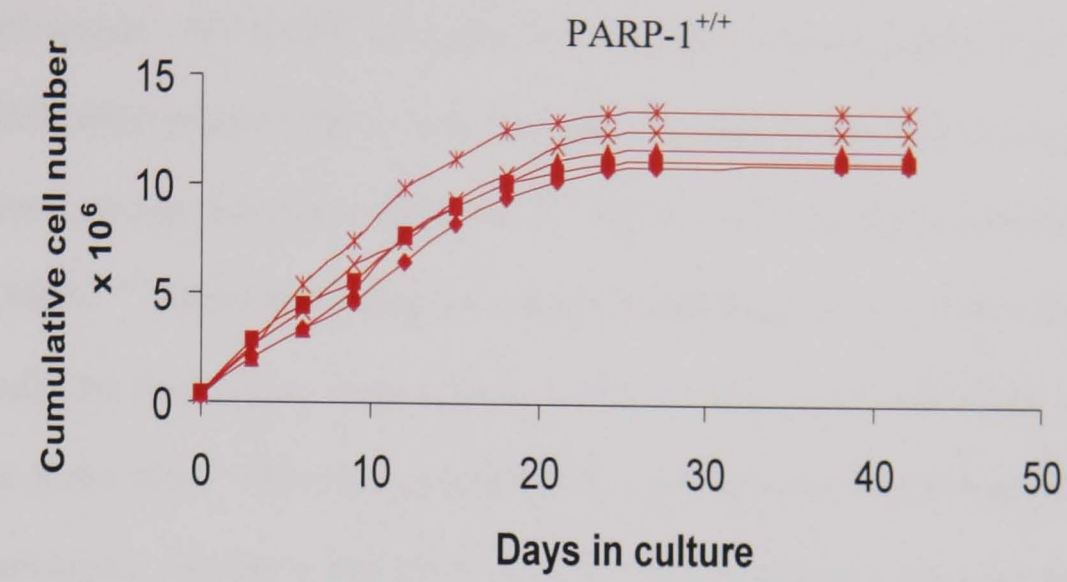


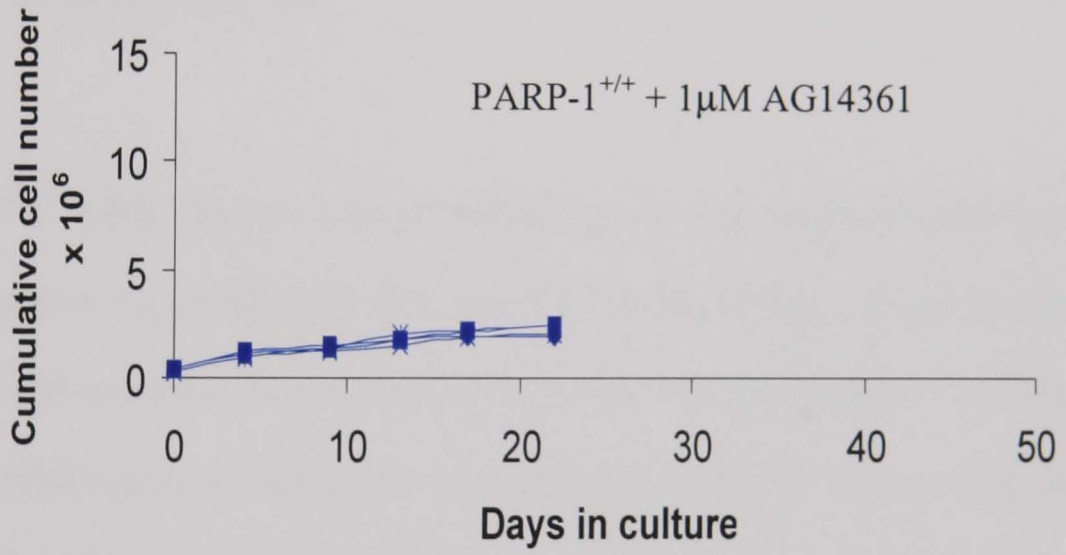


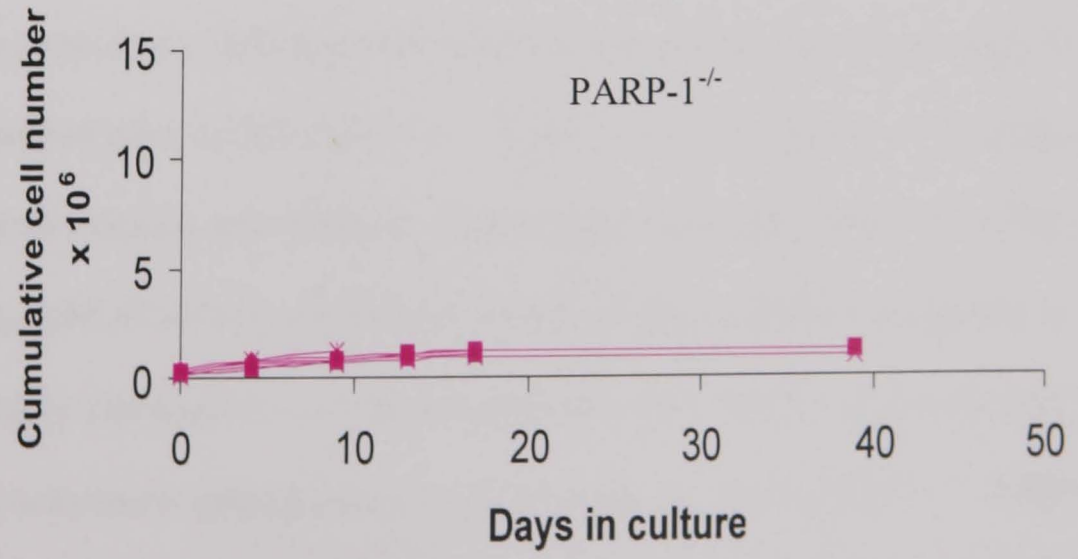


**Figure 6.4 Cumulative growth curves of primary PARP-1 MEFs**
Each symbol represents an independent plate. All curves are plotted on the same axes as the primary PARP-1$^{+/+}$ MEFs to highlight the differences in growth rates in the presence and absence of PARP-1. Note that some cells were lost to infection early in the attempted immortalisation process

As can be seen in figure 6.4, the primary PARP-$1^{+/+}$ MEFs grew with a constant growth rate for approximately 20 days, with an average doubling time of 40 hours. At this point, after around 12 cell doublings, cellular proliferation slowed dramatically, as the cells entered senescence. Associated with entry into senescence was a change in morphology, from small densely packed cells to large, flat and irregular shaped cells (see figure 6.5). Unfortunately, during senescence all PARP-$1^{+/+}$ MEFs were lost due to infection. One plate of PARP-$1^{+/+}$ MEFs showed signs of transformed areas of cells with several colonies evident under the microscope. This plate was split in order to spread the cells over the whole area of the plate. There was evidence of a small increase in cell number, indicative of immortalisation. However, this plate was also lost to infection before any analysis of p53 status could be carried out.

The PARP-$1^{-/-}$ MEFs showed a much reduced growth rate compared to the PARP-$1^{+/+}$ MEFs, despite being plated out at the same cell number initially. Because of this, these cells were split less often to try and allow the cell numbers to increase. Despite this, the PARP-$1^{-/-}$ MEFs grew extremely slowly, with a doubling time of around 200 hours. It appeared from microscopy that a significant proportion of the PARP-$1^{-/-}$ cells had entered a premature senescence, with the cells adopting a senescent morphology early in the immortalisation process (see figue 6.5). Again these cells were lost to infection before any immortalised colonies were derived. Interestingly, growth of PARP-$1^{+/+}$ MEFs in medium containing 1μM AG14361 retarded the growth of these cells (doubling time of approximately 180 hours) to a level comparable to the PARP-1 knockout cells. AG14361 also acted to induce a premature senescent morphology in the PARP-$1^{+/+}$ MEFs, with large, flat cells being apparent early in the immortalisation procedure. The PARP-$1^{+/+}$ MEFs did not adopt a scenescent morphology until day 20 of the immortalisation process. However,

both the PARP-1$^{-/-}$ and PARP-1$^{+/+}$ inhibitor-treated cells adopted this phenotype within 5-7 days of cell culture. Unfortunately, the inhibitor-treated cells were also lost due to infection before any immortalised cells had emerged. The difference in growth rate between primary PARP-1$^{+/+}$ and PARP-1$^{-/-}$ MEFs was not observed in the immortalised PARP-1 MEFs, where both the PARP-1 proficient and deficient MEFs grew with a doubling time of 20 hours (data not shown).

To eliminate any potential effect of the DMSO (in which AG14361 is dissolved) on cell growth, a control plate was set up containing 0.01% DMSO. These cells showed identical growth characteristics to the PARP-1$^{+/+}$ MEFs (data not shown).

Due to the time restraints involved in the completion of a PhD, it was impossible to repeat the above long-term experiment.

**Primary**

PARP-$1^{+/+}$ (day 2)

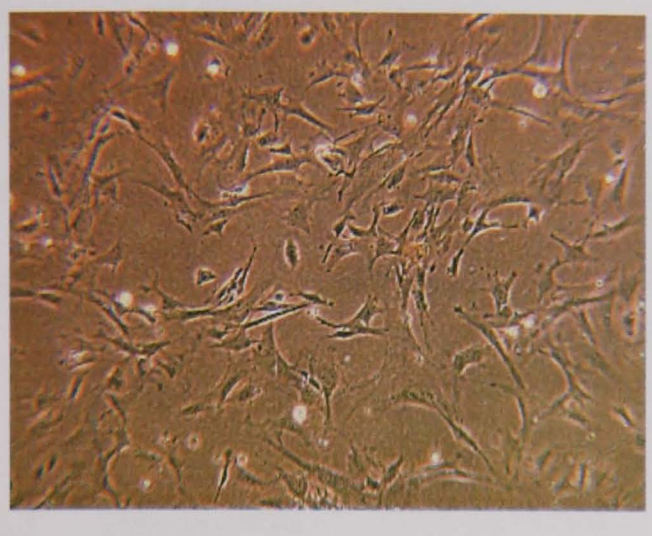

PARP-$1^{-/-}$ (day 2)

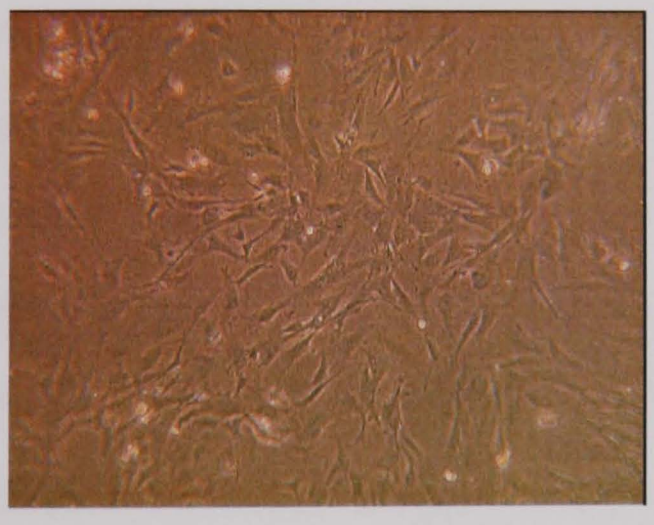

PARP-$1^{+/+}$ + 1μM AG14361 (day 2)

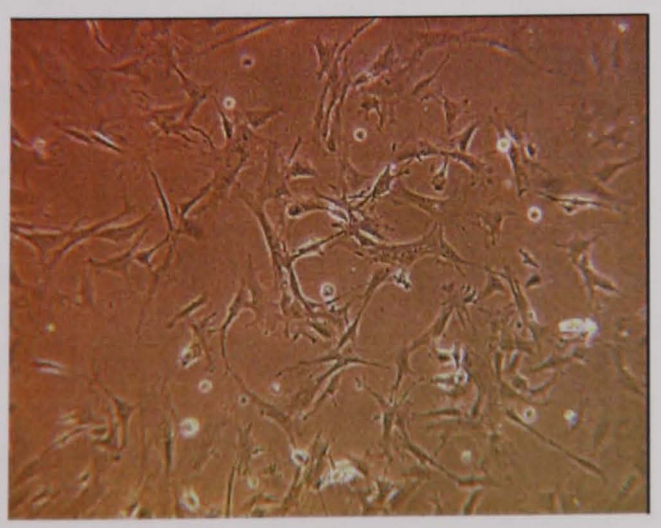

**Scenescent**

PARP-$1^{+/+}$ (day 20)

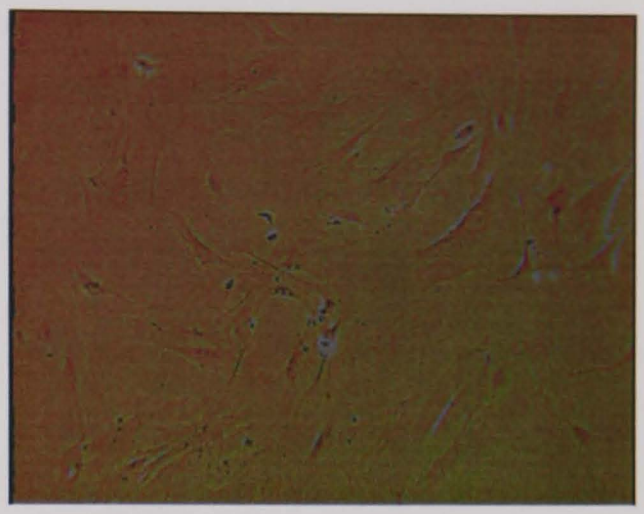

PARP-$1^{-/-}$ (day 7)

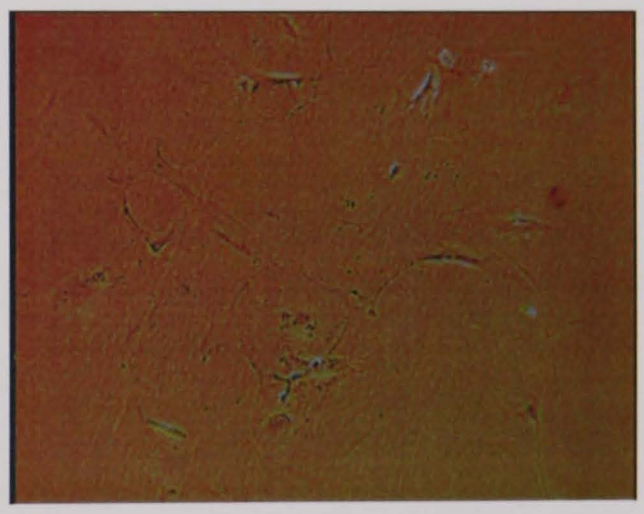

PARP-$1^{+/+}$ + 1μM AG14361 (day 7)

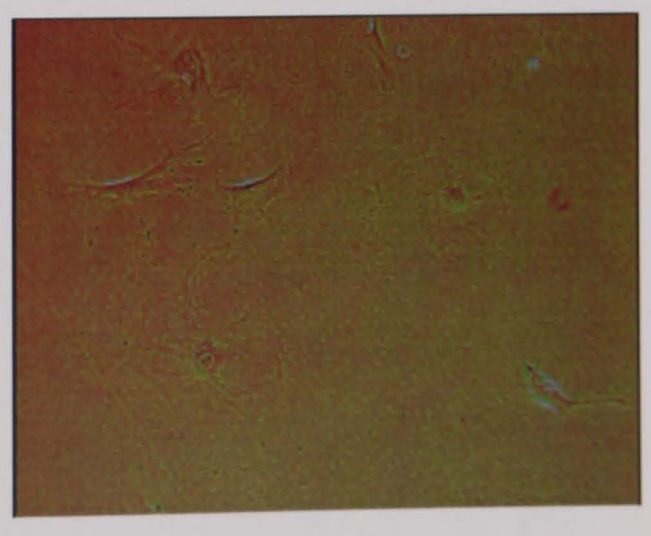

**Figure 6.5 Photographs showing the morphology of primary and scenescent PARP-1 MEFs**

Although the immortalisation experiment did not produce any immortalised cells from which p53 data could be derived, it did reveal interesting growth characteristics in the presence and absence of PARP-1. For instance, in the absence of PARP-1, either through knocking out the gene or through chemical inhibition by AG14361, the growth of primary MEFs was slowed dramatically. In addition, these cells appeared to enter a premature scenescence after only 5-7 days in cell culture.

## 6.3 Discussion

### 6.3.1 Summary of results

The data presented in this chapter has shown that the p53 mutation detected in two independently derived colonies of immortalised PARP-$1^{+/+}$ MEFs developed during cell culture. Western blot analysis showed that these cells expressed high basal levels of p53 compared to primary PARP-$1^{+/+}$ MEFs. In comparison, tissues derived from PARP-$1^{+/+}$ mice had virtually undetectable levels of p53 (figure 6.3). This Western blot data suggested that both the PARP-$1^{+/+}$ mice and primary MEFs were expressing wild-type p53. This was confirmed by cDNA sequencing, clearly showing the expression of wild-type p53 in primary PARP-$1^{+/+}$ MEFs whereas the immortalised PARP-$1^{+/+}$ MEFs were shown to be expressing mutant p53 (figure 6.2). Western blot data of primary and immortalised PARP-$1^{-/-}$ MEFs showed low basal levels of p53, as did data from PARP-$1^{-/-}$ tissues. This indication of wild-type p53 in these cells was confirmed by cDNA sequencing (figure 6.2). Taken together, this data showed that the p53 mutation detected in the two colonies of immortalised PARP-$1^{+/+}$ MEFs developed during cell culture. In addition, the data suggests that the absence of PARP-1 bypasses the requirement of MEFs to mutate p53 during immortalisation. An experiment was performed to test this hypothesis but cells

were lost to infection before analysis of p53 status could take place. Despite this, interesting data was obtained from this experiment, with cumulative growth curves showing that primary PARP-$1^{-/-}$ MEFs grew very much more slowly than the primary PARP-$1^{+/+}$ MEFs. In addition, the absence of PARP-1 appeared to induce a premature senescence, with PARP-$1^{-/-}$ MEFs adopting a morphology typical of senescence after only 5-7 days in cell culture (figure 6.5). The PARP-$1^{+/+}$ MEFs did not enter senescence until 20-22 days in culture. Significantly, a slower growth rate and apparent premature senescence were also observed in primary PARP-$1^{+/+}$ MEFs treated with 1μM AG14361.

### 6.3.2 Analysis of the p53 status of primary and immortalised PARP-1 MEFs

The initial aim of this thesis was to use immortalised PARP-$1^{+/+}$ and PARP-$1^{-/-}$ MEFs to analyse the requirement of PARP-1 in the DNA damage induced p53 response. However, initial experiments on two independently derived pairs of immortalised PARP-1 MEFs revealed that both colonies of PARP-$1^{+/+}$ MEFs were expressing mutant p53. It was shown in this chapter that these mutations occurred during cell culture by sequencing the p53 in primary PARP-$1^{+/+}$ MEFs and revealing that the p53 was wild type in these cells (figure 6.2). These primary MEFs are the pre-cursor cells for the immortalised PARP-$1^{+/+}$ MEFs, indicating that the p53 mutation had occurred during cell culture. A literature search regarding the immortalisation of MEFs revealed that the mutation of p53 was a fairly common event during immortalisation.

Under normal circumstances, primary MEFs will undergo a finite number of cell divisions before entering a phase called senescence (reviewed in Itahana *et al.*, 2001). At senescence, cells have stopped growing and have essentially withdrawn from the cell

cycle. Human cells are thought to enter senescence due to telomere shortening. Telomeres are sequences of repetitive DNA that cap the ends of linear chromosomes. During DNA replication, there is a stretch of DNA at the end of chromosomes that is not replicated, the area covered by the DNA polymerase bound to the DNA template. This stretch of unreplicated DNA can be up to 200bp in length. Therefore, telomeres act to protect the essential genomic information within chromosomes by capping the ends of chromosomes and hence it is this telomeric DNA that is not replicated rather than DNA containing genetic information. It was therefore hypothesised that the acquisition of one or more critically short telomeres results in human cells entering replicative senescence, to prevent the possible loss of genetic information during DNA replication. Supporting this hypothesis is the finding that prevention of telomere shortening by the ectopic expression of telomerase, which acts to elongate telomeres, resulted in the abrogation of senescence in some human cells (Bodnar *et al.*, 1998; Vaziri and Benchimol, 1998).

The putative role of telomere shortening in inducing senescence in human cells may not be true for mouse cells. For example, cells from laboratory mouse strains have very long telomeres and in some cases express telomerase. Despite this, mouse cells have a shorter replicative lifespan than human cells. The fact that mouse cells have longer telomeres than human cells but shorter replicative lifespan suggests that telomere shortening is not an important factor in the induction of scenescence in mouse cells (Wright and Shay, 2000). With particular relevance to this thesis, it should be noted that PARP-$1^{-/-}$ mice have been reported to have shorter telomeres compared to PARP-$1^{+/+}$ mice, with reductions in length of around 30% being observed (d'Adda di Fagagna *et al.*, 1999 and Tong *et al.*, 2001). Despite this, it should be noted that neither study makes reference to a premature scenescence in the absence of PARP-1 and no firm functional explanation is provided for

the apparent shortening of telomeres in PARP-$1^{-/-}$ mice. Other studies have proposed that cells enter scenescence due to the stressful conditions of cell culture (reviewed in Sherr and DePinho, 2000). Although most cells grow when placed into cell culture, it should be noted that the environment is far from physiological. For example, there is a disruption of cell-cell contacts, lack of heterotypic interactions between different cell types, persistent Ras activation by mitogens, hyperoxic conditions and contact with the plastic of the culture dish may all induce stress responses. One or more of these factors is likely to give rise to DNA damage and induce the relevant response within the cell and subsequent cell cycle arrest. As senescent cells arrest with a G1 content of DNA, it is possible that under permanent conditions of cellular stress, the mouse cells undergo a permanent cell cycle arrest. An example of the 'background' DNA damage that occurs during cell culture is provided by the observation that ATM null cells sustain a high level of chromosome breakage. In the presence of ATM, this damage would usually be repaired, however, this damage persists in the absence of ATM and induces a premature senescence in these cells (Westphal *et al.*, 1997).

Further support for the 'culture shock' hypothesis of cellular senescence may be provided by several studies showing that entry into senescence requires functional p53 (a stress response protein) and that subsequent immortalisation and exit from senescence requires loss of p53 function. Perhaps the simplest indication that p53 was required for senescence was provided by Harvey *et al.*, 1993, who studied the growth characteristics of $p53^{+/+}$ and $p53^{-/-}$ primary MEFs. Cumulative growth curves demonstrated that the $p53^{-/-}$ MEFs grew fairly rapidly and did not enter a senescent phase. However, cells possessing wild type p53 ($p53^{+/+}$) grew more slowly initially before entering senescence. This slower growth rate may be indicative of a permanent activation of a DNA damage response leading to slowing

of the cell cycle. Prolonged activation of this checkpoint may lead to long-term growth arrest in senescence. A further study showed that the introduction of wild-type p53 into human tumour cells lacking functional p53 was able to induce a senescent phenotype (Sugrue *et al.,* 1997). This study transfected a tumour cell line (expressing mutant p53) with an inducible plasmid construct containing wild type p53. The effect of expression of wild-type p53 was an apparent halting in cellular proliferation, associated with a change in cellular morphology. Cells adopted an increased and flattened morphology, with elongated cellular processes, consistent with the changes in cell shape associated with senescence (Hayflick and Moorhead, 1961).

Perhaps the most compelling evidence that p53 function is required for senescence is the common observation that immortalised cells that exit the senescent phase have lost p53 function (Harvey and Levine, 1991; Rittling and Denhardt, 1992). This loss of function may occur due to p53 mutation, or in the presence of wild type p53, be associated with a mutation to the tumour suppressor, $p19^{ARF}$ ($p14^{ARF}$ in humans). $p19^{ARF}$ binds to mdm2 and prevents the inhibitory action of mdm2 upon p53. Therefore, in the absence of $p19^{ARF}$, mdm2 is able unapposed to inhibit the function of p53. Mutation of p53 during immortalisation was demonstrated by Rittling and Deinhardt, 1992. This study showed that two independently derived colonies of immortalised MEFs expressed mutant p53, with the mutations being evident in the DNA binding domain. The cells were derived using a 3T12 protocol, where four times as many cells are re-plated at each sub-culture compared to the 3T3 protocol described in Section 2.1.9. A more recent report analysing the p53 status of immortalised MEFs generated by a 3T3 protocol demonstrated a mutation in 2/3 independent colonies (Kim *et al.,* 2001). One mutation was a missense mutation, resulting in a Pro to Arg change at amino acid 275 (very close to the site of mutations detected in

this thesis, amino acid 278). The other mutation was a nonsense mutation at amino acid 173, changing Cys to a stop codon. Interestingly, the third group of immortalised MEFs, with wild type p53, did not produce detectable levels of p53 mRNA or protein, as measured by Northern blot and immunoprecipitation. This observation was due to a destabilisation of p53 mRNA and protein in these cells, by an unknown mechanism, but with the result of losing the p53 expression.

From the data summarised above, it is perhaps not surprising that the two immortalised PARP-$1^{+/+}$ MEF cell lines derived in this thesis possess p53 mutations. In addition, the fact that immortalisation is an essential step in tumour formation and that over 50% of tumours possess p53 mutations, perhaps make the observation not entirely unexpected. However, it was interesting to find that two immortalised PARP-$1^{-/-}$ MEF cell lines both expressed wild type p53. It should be noted that loss of p53 function is not an essential step in immortalisation and also that several other cellular changes are required for cells to become immortal. For example, rodent cells can be immortalised by the introduction of cellular oncogenes such as *c-myc* and c-Ha-*Ras*, suggesting that the activation of certain oncogenes can result in or contribute to immortalisation. It may be that cells can become immortalised by undergoing a certain set of mutations, with one mutational event triggering another. In the PARP-$1^{-/-}$ MEFs, a set of genes may be mutated, which do not include p53. As stated earlier, $p19^{ARF}$ is frequently found to be mutated, deleted or epigenetically inactivated by methylation in immortalised cells expressing wild-type p53. It may be that the immortalised PARP-$1^{-/-}$ MEFs lost $p19^{ARF}$ function rather than p53 during immortalisation. It would be interesting to measure the expression levels of various genes or proteins implicated in immortalisation in both the PARP-1 +/+ and -/- MEFs. This could be achieved by cDNA microarray analysis and Western blotting and any interesting findings investigated further by sequencing of the particular gene. As described

earlier, this type of analysis may reveal that different 'sets' of genes were involved in the immortalisation process in the PARP-$1^{+/+}$ and PARP-$1^{-/-}$ MEFs and hence may suggest a role for PARP-1 in a particular immortalisation pathway.

### 6.3.3 The growth rates of primary PARP-1 MEFs

The observation that immortalised PARP-$1^{+/+}$ MEFs tend to undergo p53 mutations during immortalisation whereas PARP-$1^{-/-}$ MEFs do not was investigated further by attempting to isolate several independent immortalised colonies of PARP-1 MEFs. As described in Section 2.1.9, five plates of PARP-$1^{+/+}$ MEFs, five plates of PARP-$1^{-/-}$ MEFs and five plates of PARP-$1^{+/+}$ MEFs grown in the presence of 1μM AG14361 were set up for long term growth according to the 3T3 protocol. Unfortunately, all cells were lost due to infection before any immortalised colonies were derived. Despite this, several interesting observations were made regarding the growth rates and time to reach senescence of the primary MEFs. As can be seen in figure 6.4, the growth rates of the PARP-$1^{-/-}$ MEFs were massively slower than the PARP-$1^{+/+}$ MEFs. Interestingly, treatment of the PARP-$1^{+/+}$ MEFs with 1μM AG14361 slowed growth to a similar extent to that observed in the PARP-$1^{-/-}$ MEFs. This effect was not due to the DMSO content of the medium as a control plate of PARP-$1^{+/+}$ MEFs grown in the presence of 0.01% DMSO grew with the same rate as the untreated PARP-$1^{+/+}$ MEFs. Interestingly, the inhibition of PARP-1 and knocking out of PARP-1 in primary MEFs appeared to bring about a premature senescence, as observed by the morpholological changes described in the previous section.

There are several possible explanations for the different growth rates in the presence and absence of PARP-1. Before discussing these possibilities, it should be noted that all of the

cells were plated out at the same initial cell number and grown under identical growth conditions. In addition, all cells were grown at the same time and were split at the same time until the cells reached senescence.

One characteristic of primary MEFs is an inability to proliferate when plated at low densities. Therefore, it could be argued that the PARP-$1^{-/-}$ MEFs have simply been plated out at too low a density and, as such, have ceased proliferating. However, PARP-$1^{+/+}$ MEFs were plated out at the same initial cell number and yet were able to grow much faster than the PARP-$1^{-/-}$ MEFs. The fact that AG14361 significantly retarded the growth rate of the PARP-$1^{+/+}$ MEFs may suggest that the absence of PARP-1 function decreases the plating efficiency of primary MEFs. In this situation, despite plating out identical cell numbers of PARP-$1^{+/+}$ and PARP-$1^{-/-}$ MEFs, fewer of the latter cells would adhere to the plate and hence the effective cell density would be lower. If a particular cell density threshold had not been met then the PARP-$1^{-/-}$ MEFs may enter a premature senescence. A similar situation would arise in the PARP-$1^{+/+}$ MEFs treated with AG14361. This hypothesis could be tested by plating at a range of initial densities up to 50% confluence.

A different study has previously described a slower growth rate in primary PARP-$1^{-/-}$ MEFs (disrupted in exon 2) than PARP-$1^{+/+}$ MEFs (Wang *et al.*, 1995), although the difference reported was not as great as that in this thesis. For two days in culture, the growth rates of the primary PARP-$1^{+/+}$ and PARP-$1^{-/-}$ MEFS were significantly different. However, after 14 days in culture, the cumulative cell number of PARP-$1^{-/-}$ MEFs was approximately 50% of the PARP-$1^{+/+}$ MEFs, consistent with a decreased growth rate in the PARP-$1^{-/-}$ cells. Wang *et al*, 1995, used slightly different conditions for the analysis of

growth rates, with 1 x $10^5$ cells/well in a 6-well plate. However, this does not represent a greater cell density than that used in this thesis and therefore cannot be used as an explanation for the greater decrease in proliferation in the PARP-$1^{-/-}$ MEFs observed in this study. Wang *et al*, 1995, also makes no mention of a premature senescence in PARP-$1^{-/-}$ MEFs, again at odds with observations made in this thesis.

It was described in Section 6.3.2 that primary MEFs may enter senescence as a result of 'culture shock', caused by persistent DNA damage brought about by the non-physiological environment that the cells are grown in. For example, the hyperoxic conditions could lead to oxidative damage to DNA, such as is inflicted by IR under oxic conditions. With reference to this hypothesis, it is interesting to note that primary ATM$^{-/-}$ MEFs, that are defective in the repair of DNA damage, grow more slowly than their ATM$^{+/+}$ counterparts. Xu and Baltimore, 1996, generated ATM$^{-/-}$ mice by homologous recombination. These mice and also cells derived from them were shown to be hypersensitive to the effects of IR, indicating a role for ATM in the response to this type of DNA damage. In addition, this study showed a 60-80% decrease in cellular proliferation and a premature entry into senescence in ATM$^{-/-}$ MEFs compared to ATM$^{+/+}$ MEFs. A similar premature senescence has also been observed in fibroblasts derived from AT patients (Shiloh *et al.*, 1985). The characteristics of the ATM$^{-/-}$ MEFs may be particularly relevant to this chapter, bearing in mind the similar putative role of PARP-1 in the response to DNA damage. For example, ATM$^{-/-}$ and PARP-$1^{-/-}$ mice and cells have both been shown to be hypersensitive to IR (Xu and Baltimore, 1996; de Murcia *et al.*, 1997). As described previously, cells grown in culture are subject to constant DNA damage. Under normal circumstances, this damage is repaired and cells continue to proliferate. However, in the absence of ATM or PARP-1, this damage is likely to persist due to defective DNA repair pathways. This may result in a slowing of the cell cycle hence the reduced proliferation of PARP-$1^{-/-}$ and ATM$^{-/-}$ MEFs.

Interestingly, Xu and Baltimore showed that $ATM^{-/-}$ MEFs progress more slowly through the G1/S phase border than $ATM^{+/+}$ MEFs. This was demonstrated by synchronizing ATM MEFs by serum starvation before release into medium containing 10% FBS for 24 hours. FACS analysis revealed that 74% of $ATM^{+/+}$ MEFs were in S-phase compared to 51% of $ATM^{-/-}$ MEFs. This observation may also be in agreement with the culture shock hypothesis, whereby $ATM^{-/-}$ MEFs are less proficient in repairing the DNA damage during cell culture, resulting in a higher proportion of cells in G1, possibly mediated by p53 activation. With reference to a putative role of p53, it is interesting to note that the growth retardation observed in $ATM^{-/-}$ MEFs is abolished by additionally knocking out p53 to produce $ATM^{-/-}$ $p53^{-/-}$ MEFs (Westphal *et al.*, 1997).

Importantly, other studies have shown a reduced growth rate in cells lacking other proteins involved in genetic stability. For example, Deans *et al.*, 2000 showed that $Xrcc2^{-/-}$ mice were embryonic lethal (Xrcc2 has been implicated in homologous recombination repair). This same study went on to generate embryonic stem cells disrupted in *Xrcc2* and showed that these cells entered a premature senescence, with complete growth arrest at or before passage 4 in culture. Similar findings have been observed for disruptions of both *Rad51* (Lim and Hasty, 1996) and *Brca2* (Sharan *et al.*, 1997). The observed phenotype in all of these cell types could be explained by the accumulation of DNA damage caused by the stressful conditions of cell culture (and inefficient repair due to lack of important repair proteins) leading to the induction of cellular checkpoints causing a slowing or halting of the cell cycle.

Although a lot of data discussed in this section has involved ATM, it is likely to be relevant to this study due to certain similarities between $ATM^{-/-}$ and $PARP\text{-}1^{-/-}$ MEFs. For example, both sets of MEFs are hypersensitive to IR due to defective repair pathways. The culture shock hypothesis of MEF senescence would suggest greater endogenous DNA damage in $ATM^{-/-}$ MEFs. This in turn would be in agreement with the observed build up of cells in G1 in the absence of ATM, possibly due to a p53-mediated cell cycle arrest. This would obviously slow the growth rate of $ATM^{-/-}$ MEFs. It would be interesting to analyse the DNA content of $PARP\text{-}1^{+/+}$ and $PARP\text{-}1^{-/-}$ by FACS analysis to see whether results were similar to $ATM^{+/+}$ and $ATM^{-/-}$ MEFs. Finally, although the principle aim of this chapter, to analyse the p53 status of immortalised MEFs, was not achieved, interesting data was derived suggesting a potential role of PARP-1 in the proliferation of primary MEFs. Due to time restrictions involved in the completion of a PhD only tentative conclusions can be made. However, future work involving FACS analysis will provide greater detail on the nature of the growth retardation in the $PARP\text{-}1^{-/-}$ MEFs. In addition, it would be interesting to analyse the expression levels of several genes involved in cellular proliferation by cDNA microarray analysis to try and identify differences between the $PARP\text{-}1^{+/+}$ and $PARP\text{-}1^{-/-}$ MEFs. Any differences could be confirmed by treatment of primary $PARP\text{-}1^{+/+}$ MEFs with 1μM AG14361, and may provide a definitive link between PARP-1 and the control of cellular proliferation.

# CHAPTER 7

# GENERAL SUMMARY AND FUTURE OBJECTIVES

## 7.1 Summary

The aim of this chapter is to summarise this entire thesis, from the initial introductory chapter through to the final results chapter. By doing this it is hoped that the reasons for proposing the original hypothesis are clear and also by summarising relevant results sections, to highlight the stepwise nature in which experiments were performed.

This thesis has been structured to initially emphasise the central role of p53 in the cellular response to DNA damage. There are two major responses to DNA damage, cell cycle arrest and apoptosis, the aims of which are to either halt the cell cycle to allow efficient repair of the DNA damage, or, in the presence of high levels of damage, the cell is programmed to die *via* the apoptotic pathway. Both of these responses can be mediated by p53, and function to prevent the propagation of DNA damage during cellular replication. Loss of control over cell cycle arrest or apoptosis ultimately leads to the formation of a cancerous cell, where DNA damage is propagated and mutations to essential regulatory genes occur. In this situation, the tumour cells are able to continually evolve and acquire new mutations, resulting in metastasis and the likely death of the organism harbouring the tumour. With this in mind, it is therefore essential to understand the mechanisms involved in the regulation of the tumour suppressor protein, p53.

Data has been summarised showing the negative regulation of p53 by mdm2. Mdm2 binds to the N-terminal transcriptional transactivation domain of p53, blocking the interaction of

p53 with components of the transcriptional machinery. This prevents the transcription of several p53-target genes, including *Mdm2* itself and $p21^{waf\text{-}1}$. In addition, mdm2 targets p53 for proteasomal degradation *via* a ubiquitin-mediated pathway. The result of this is that a negative feedback loop exists, whereby p53 induces the expression of mdm2, then mdm2 blocks p53 function and down-regulates p53 protein levels. It is therefore hypothesised that activation of p53 in response to DNA damage requires the alleviation of the inhibition imposed by mdm2.

In addition, data has been summarised showing the putative regulation of p53 by phosphorylation. The use of phospho-specific antibodies and site directed mutagenesis has identified more than 20 phosphorylation sites on p53, with the majority being mapped to the N-terminus. It is believed that Ser15 and Ser20 are particularly important in the activation of p53, with DNA damage activated kinases targeting these residues with the result of disrupting the p53-mdm2 complex.

P53 has also been shown to be post-translationally modified by acetylation. In response to DNA damage, an acetyl-transferase, p300, binds the N-terminal of p53 and targets residues within the C-terminal for acetylation. This results in an increased DNA binding activity of p53 and hence increased transcription of p53 target genes.

The roles of mdm2, phosphorylation and acetylation in the regulation of p53 have been fairly well studied. However, there are a variety of other post-translational modifications that putatively occur, including sumoylation and, with particular respect to this thesis, poly(ADP-ribosylation), performed by the enzyme PARP-1.

PARP-1 is activated rapidly in response to DNA damage and is involved in the BER pathway to repair damage to DNA brought about principally by alkylating agents. In addition, PARP-1 is thought to play a role in the repair of IR-induced damage, with animals lacking PARP-1 being hypersensitive to the effects of this type of DNA damage. It is not known whether PARP-1 is involved in the repair of the major cytotoxic lesion of IR, DSBs, or whether a different subset of lesions induced by IR are involved (for example, thymine glycols and 8-hydroxyguanine). Several studies analysing the DNA damage response in the absence of PARP-1 have implicated this enzyme as an upstream regulator of p53. However, as has been stressed throughout this thesis, the nature of any regulation remains controversial. For example, studies have been published showing a decreased p53 response in the absence of PARP-1, whereas others have shown an enhanced p53 response. In addition, there are also studies showing no difference in the p53 response in the presence and absence of PARP-1. It should be noted that a lot of these studies have analysed the response to different DNA damaging agents. In addition, several studies have utilised different methods to remove PARP-1 from cells. For example three independent colonies of PARP-$1^{-/-}$ mice have been generated, disrupted in exons 1, 2 or 4 of PARP-1. Also, a dominant-negative strategy, involving the overexpression of the PARP-1 DBD, chemical inhibition of PARP-1 and antisense RNA strategies have all been used to remove PARP-1 activity from cells. With particular relevance to this thesis, the most commonly used PARP-1 inhibitor in the literature, 3-AB is approximately 1000-fold less potent than the PARP-1 inhibitor used in this study, AG14361. Therefore, AG14361 may be expected to be more specific and, as such, any effects on p53 induction that were observed in this thesis could more confidently be attributed to PARP-1 inhibition.

Therefore, the principal aim of this thesis was to clarify some of the conflicting data that exists in the literature regarding the potential regulation of p53 by PARP-1. This was to be achieved using a combination of PARP-$1^{-/-}$ MEFs and a novel, potent PARP-1 inhibitor. As well as analysing the p53 response by Western blot analysis, a p53-responsive luciferase reporter gene assay was validated to measure the transcriptional transactivation activity of p53. Finally, the response to a variety of DNA damaging agents was analysed, to investigate whether PARP-1 regulated p53 in a DNA damage-specific manner.

The initial experiments in this thesis aimed to characterise the PARP-$1^{-/-}$ MEFs and the PARP-1 inhibitor, AG14361. The MEFs were characterised using a combination of Southern blotting, Western blotting and an enzymatic assay measuring PARP-1 activity. The generation of the PARP-$1^{-/-}$ mice involved the insertion of a neomycin resistance cassette into exon 4 of PARP-1 using homologous recombination. In the wild type PARP-1 locus, there are two *Eco*RI sites, separated by 9.6kb. Therefore, upon *Eco*RI digestion of purified genomic DNA, a fragment of 9.6kb was produced. This fragment was separated from the other DNA fragments by agarose gel electrophoresis. In the PARP-$1^{-/-}$ MEFs, disruption of the PARP-1 locus introduced an extra *Eco*RI site, with the result that restriction enzyme digestion produces a smaller, 3.3kb fragment. After agarose gel electrophoresis, the DNA was transferred to a nylon membrane before incubation of the membrane with a radiolabelled probe. This probe binds the N-terminal of the PARP-1 locus, which is present in both the PARP-$1^{+/+}$ and PARP-$1^{-/-}$ MEFs, therefore subsequent autoradiography revealed bands of 9.6kb and 3.3kb, respectively, confirming the disruption of the PARP-1 locus in the PARP-$1^{-/-}$ MEFs.

The MEFs were further characterised by Western blot analysis with a PARP-1 specific antibody clearly showing the presence of a band corresponding to PARP-1 in the PARP-$1^{+/+}$ MEFs and the absence of a similar band in the PARP-$1^{-/-}$ MEFs.

The final step in the characterisation of the PARP-1 MEFs was to assay PARP-1 activity in the cells. A PARP-1 permeabilised cell assay measuring the incorporation of radiolabelled $NAD^+$ into acid-precipitable material confirmed PARP-1 activity in the PARP-$1^{+/+}$ MEFs. This activity was stimulated by DNA ends, included in the assay as a short double-stranded oligonucleotide, and was abolished by treatment of the cells with 1μM AG14361. The PARP-$1^{-/-}$ MEFs possessed < 5% PARP activity compared to the PARP-$1^{+/+}$ MEFs. In addition, this activity was not stimulated by DNA ends but was abolished by 1μM AG14361. From this assay, it was concluded that the PARP-$1^{-/-}$ MEFs possessed an alternative PARP activity that cannot be attributed to PARP-1 and is likely due to one or more other PARP family member (e.g. PARP-2, tankyrase and sPARP-1). It has therefore been shown that AG14361 is also able to inhibit the activity of this other PARP activity.

To further confirm that the activity measured by the radiolabelled $NAD^+$ method was indeed due to synthesis of ADP-ribose polymer, a modified assay was developed and validated. This assay did not involve the use of radiolabelled $NAD^+$ and could be performed on a much smaller cell number than the previous assay. After PARP-1 stimulation, the permeabilised cells were bound to a nylon membrane using a dot-blot apparatus and polymer detected using an ADP-ribose polymer-specific monoclonal antibody. This assay was shown to detect purified polymer. In addition, AG14361 was shown to virtually abolish polymer formation in PARP-1 proficient cells and PARP-$1^{-/-}$ MEFs gave rise to only minimal amounts of ADP-ribose polymer.

The PARP permeabilised cell assay (both the radiolabelled $NAD^+$ and immuno dot-blot method) demonstrated the effectiveness of AG14361 at removing PARP-1 activity from PARP-1 proficient cells. However, before using AG14361 in DNA damage response experiments, it was essential to show that the PARP-1 inhibitor itself was not growth inhibitory during the time course of experiments. Therefore, SRB assays were performed in PARP-$1^{+/+}$ and PARP-$1^{-/-}$ MEFs, as well as human HCT-116 cells. No growth inhibition was observed up to 72h after treatment with 1μM AG14361 in all cell lines, compared to a DMSO-treated control. It was also important to show that AG14361 does not stress the cells in such a way that a p53 response is induced. Therefore, Western blot analysis of p53 levels in HCT-116 cells treated with 1μM AG14361 was performed, with no change in p53 levels observed over the course of a 24-hour treatment period.

Having characterised the PARP-1 MEFs and AG14361, the next aim was to treat PARP-$1^{+/+}$ and PARP-$1^{-/-}$ MEFs with DNA damaging agents (such as IR and UV) and analyse p53 levels using Western blotting. These experiments were performed on immortalised MEFs, with subsequent Western blot analysis revealing very high p53 levels in PARP-$1^{+/+}$ cells, which were not induced by DNA damage. In addition, there was virtually undetectable levels of Mdm2 in these cells. These characteristics were indicative of mutant p53, with subsequent cDNA sequencing confirming this belief. The PARP-$1^{-/-}$ MEFs showed both a p53 and Mdm2 induction after IR or UV treatment and were shown to express wild type p53 by cDNA sequencing. Obviously, it was futile to analyse p53 responses in cells expressing mutant p53, therefore, the DNA damage experiments were repeated in a second independently derived pair of immortalised PARP-1 MEFs. Interestingly, Western blot and cDNA analysis again revealed a mutant p53 in the PARP-

$1^{+/+}$ MEFs and wild type p53 in the PARP-$1^{-/-}$ MEFs. The mutations detected in the two colonies of PARP-$1^{+/+}$ MEFs were in the same amino acid (278), but at a different site in the codon. The primary PARP-1 MEFs from which these cells were derived were shown to express wild type p53; therefore the p53 mutation has developed during cell culture and was a likely consequence of the immortalisation procedure. This set of data led to the hypothesis that the absence of PARP-1 bypasses the requirement to mutate p53 during the immortalisation of MEFs, a hypothesis that was tested in chapter 6.

In order to produce a PARP-1 proficient MEF cell line expressing wild type p53, it was decided to stably transfect immortalised PARP-$1^{-/-}$ MEFs with a plasmid construct expressing PARP-1. The stable transfection procedure resulted in the isolation of one PARP-1 positive colony, which was bulked up and aliquots frozen. This stable transfectant, termed clone 23, was shown to express PARP-1 protein and possess PARP-1 activity that was stimulated by DNA ends, using the immuno dot-blot technique.

It was now possible to perform DNA damage experiments on clone 23 and PARP-$1^{-/-}$ MEFs and analyse the p53 response to a variety of DNA damaging agents. In addition, the effect of AG14361 on the p53 response in these cells was analysed, as was the p53 response in human HCT-116 cells. Firstly, cells were treated with 5Gy IR, with no difference in p53 or mdm2 induction observed between clone 23 and PARP-$1^{-/-}$ MEFs. Analysis of the luciferase assay results in these cells revealed that the PARP-$1^{-/-}$ MEFs had significantly lower luciferase and β-galactosidase values than the clone 23 MEFs. The ratio of these values, which was used to estimate p53 activity, was also lower in the PARP-$1^{-/-}$ cells, with no induction over time. This apparent lack of p53 activation was in contrast to the clear mdm2 induction observed in Western blots. This pattern was also observed in

response to two other DNA damaging agents and suggests that PARP-1 may be required for the efficient transfection and/or transcription of exogenous plasmids. As an alternative method to remove PARP-1 activity, cells were treated with 1μM AG14361. Again no difference was observed in p53 induction or activity in all cell lines in the presence or absence of AG14361. Interestingly, PARP-1 inhibition in clone 23 MEFs did not alter the expression of the luciferase or β-galactosidase plasmids suggesting that PARP-1 protein rather than activity is involved in the efficient expression of exogenous plasmids.

The second type of DNA damage used was UV. Cells were treated with 50J/m$^2$ UV and analysed by Western blot and luciferase analysis. As for IR, no difference in p53 induction or activity was observed between clone 23 and PARP-1$^{-/-}$ MEFs. Furthermore, treatment of all cells (PARP-1 MEFs and HCT-116 cells) with 1μM AG14361 did not alter the observed p53 response to UV.

The final type of DNA damaging agent used was temozolomide, a monofunctional alkylating agent. The induction of p53 in clone 23 MEFs was slightly potentiated by treatment with 1μM AG14361. Similar results have been described in the literature using different alkylating agents and PARP-1 inhibitors. This effect was attributed to the persistence of strand breaks in the absence of PARP-1 activity and hence increased signalling to p53. However, the altered p53 induction observed in this thesis was not evident in the PARP-1$^{-/-}$ MEFs, perhaps suggesting a distinction between PARP-1 inhibition and knocking out PARP-1 in cells. In addition, AG14361 did not alter the p53 activity after temozolomide treatment, as measured by mdm2 Western blot and luciferase assay. Finally, HCT-116 cells showed identical p53 induction and activity after temozolomide treatment in the presence and absence of PARP-1 activity.

The final results chapter aimed to analyse the p53 status of independently derived colonies of immortalised PARP-$1^{+/+}$ and PARP-$1^{-/-}$ MEFs. This was to be achieved by isolating 5 independent immortalised colonies of both MEF cell lines according to the 3T3 protocol. In addition, five plates of primary PARP-$1^{+/+}$ MEFs were grown in the presence of 1μM AG14361 to see whether PARP-1 inhibition would mimic results obtained with PARP-1 knockout MEFs. Unfortunately all cells were lost due to infection before any p53 sequence analysis could be performed. However, interesting data was obtained regarding the growth rate of primary MEFs in the presence and absence of PARP-1.

Primary PARP-$1^{+/+}$ MEFs grew with a constant growth rate for approximately 20 days in culture (doubling time of 40 hours), before reaching senescence, when cellular propagation slowed dramatically. In contrast, PARP-$1^{-/-}$ MEFs grew much more slowly (doubling time of around 200 hours), with cells appearing to enter a premature senescence after only 5-7 days in cell culture. Interestingly, similar observations were made in primary PARP-$1^{+/+}$ MEFs grown in the presence of 1μM AG14361, with cells growing with a doubling time of approximately 180 hours, and appearing to enter senescence after only 5-7 days in cell culture. These results may suggest a role for PARP-1 in maintaining the normal growth of primary MEFs. Alternatively, the reduced growth rate may be due to the slowing of the cell cycle in response to increased levels of endogenous DNA damage in the absence of PARP-1. Interestingly, immortalised PARP-$1^{+/+}$ and PARP-$1^{-/-}$ MEFs show similar growth rates and AG14361 has no effect on the growth of immortalised PARP-1 proficient MEFs. Immortalised cells, by definition, have lost control over some aspect of normal cellular growth. Perhaps the normal cellular response to endogenous DNA damage has been lost, such that the absence of PARP-1 no longer triggers the slowing of cellular growth. A similar effect on cell growth and senescence has been observed in ATM$^{-/-}$ MEFs. Like

PARP-1, ATM is a DNA damage responsive enzyme, perhaps supporting a model where increased endogenous DNA damage in the absence of PARP-1 (or ATM) leads to a slowing of cellular growth.

Taken together, this thesis contains a comprehensive set of data investigating the potential role of PARP-1 in the regulation of p53. Importantly, sequencing data has been presented showing that the immortalised PARP-1 MEFs used in DNA damage experiments were expressing wild-type p53. Some of the studies in the literature have described altered p53 responses in the absence of PARP-1 in immortalised MEFs, without presenting sequencing data showing the status of the p53 gene. Given the tendency of MEFs to develop p53 mutations during immortalisation (see Chapter 6), such results should be interpreted with care. In addition, the production of a PARP-1 stably transfected MEF cell line has ensured that the comparison between the presence and absence of PARP-1 on p53 responses has been made in cell lines with identical genetic backgrounds. Data obtained in PARP-$1^{-/-}$ MEFs has also been supported by the use of a potent PARP-1 inhibitor, AG14361. As described several times during this thesis, AG14361 is approximately 1000-fold more potent than the most commonly used PARP-1 inhibitor in the literature, 3-AB. Therefore AG14361 is likely to be more specific and the responses observed using this inhibitor can more confidently be attributed to an inhibition of PARP-1, rather than some of the other enzymes that have been shown to be inhibited by 3-AB.

Having used well-characterised cell lines and a potent PARP-1 inhibitor, the primary conclusion from this thesis is that PARP-1 does not have a major direct causal link with DNA damage induced signalling to p53, in response to IR, UV or the monofunctional alkylating agent, temozolomide. A slight effect was observed in clone 23 MEFs treated

with AG14361 but the enhanced p53 induction is likely to be due to a persistence of strand breaks and increased signalling (e.g. by ATM) to p53.

## 7.2 Future objectives

If time had permitted, the main area of this thesis that warranted further investigation was the immortalisation of PARP-1 MEFs. The interesting observation that two independent colonies of immortalised PARP-$1^{+/+}$ MEFs expressed mutant p53 whereas the PARP-$1^{-/-}$ MEFs expressed wild type p53 led to the hypothesis that the absence of PARP-1 bypasses the requirement to mutate p53 during immortalisation of MEFs. However, due to the loss of cells to infection, this hypothesis was not tested. Because of the long-term nature of immortalisation, this experiment could not be repeated during the time-scale of a PhD.

In addition, the interesting observations on the growth rates of primary PARP-1 MEFs could be investigated further. For instance, if the proposed model of increased endogenous DNA damage in the absence of PARP-1 is correct, it might be expected that PARP-$1^{-/-}$ MEFs will contain higher levels of p53. This could be tested by Western blot analysis of p53 levels throughout the immortalisation experiment. In addition, increased levels of endogenous DNA damage in PARP-$1^{-/-}$ MEFs may lead to a checkpoint response and the build up of cells in G1 or G2 phases of the cell cycle. This hypothesis could be tested by comparing the cell cycle profile of PARP-$1^{+/+}$ and PARP-$1^{-/-}$ MEFs using FACS analysis.

Finally, cDNA microarray analysis of primary PARP-$1^{+/+}$ and PARP-$1^{-/-}$ MEFs might reveal altered expression of certain genes involved in the regulation of cell growth. Any findings from such an experiment could be investigated further by Western blot analysis of protein levels within cells.

# REFERENCES


Adamietz, P. & Rudolph, A. (1984). ADP-ribosylation of nuclear proteins in vivo. Identification of histone H2B as a major acceptor for mono- and poly(ADP-ribose) in dimethyl sulfate-treated hepatoma AH 7974 cells. *J Biol Chem*, **259,** 6841-6.

Affar, E.B., Duriez, P.J., Shah, R.G., Sallmann, F.R., Bourassa, S., Kupper, J.H., Burkle, A. & Poirier, G.G. (1998). Immunodot blot method for the detection of poly(ADP-ribose) synthesized in vitro and in vivo. *Anal Biochem*, **259,** 280-3.

Agarwal, M.L., Agarwal, A., Taylor, W.R., Wang, Z.Q., Wagner, E.F. & Stark, G.R. (1997). Defective induction but normal activation and function of p53 in mouse cells lacking poly-ADP-ribose polymerase. *Oncogene*, **15,** 1035-41.

Aktas, H., Cai, H. & Cooper, G.M. (1997). Ras links growth factor signaling to the cell cycle machinery via regulation of cyclin D1 and the Cdk inhibitor p27KIP1. *Molecular & Cellular Biology*, **17,** 3850-7.

Alarcon, R., Koumenis, C., Geyer, R.K., Maki, C.G. & Giaccia, A.J. (1999). Hypoxia induces p53 accumulation through MDM2 down-regulation and inhibition of E6-mediated degradation. *Cancer Res*, **59,** 6046-51.

Alkhatib, H.M., Chen, D.F., Cherney, B., Bhatia, K., Notario, V., Giri, C., Stein, G., Slattery, E., Roeder, R.G. & Smulson, M.E. (1987). Cloning and expression of cDNA for human poly(ADP-ribose) polymerase. *Proc Natl Acad Sci*, **84**, 1224-8

Althaus, F.R. (1992). Poly ADP-ribosylation: a histone shuttle mechanism in DNA excision repair. *J Cell Sci*, **102,** 663-70.

Althaus, F.R. & Richter, C. (1987). ADP-ribosylation of proteins. Enzymology and biological significance. *Mol Biol Biochem Biophys*, **37,** 1-237.

Alvarez-Gonzalez, R. (1988). 3'-Deoxy-NAD+ as a substrate for poly(ADP-ribose)polymerase and the reaction mechanism of poly(ADP-ribose) elongation. *J Biol Chem*, **263,** 17690-6.

Ame, J.C., Rolli, V., Schreiber, V., Niedergang, C., Apiou, F., Decker, P., Muller, S., Hoger, T., Menissier-de Murcia, J. & de Murcia, G. (1999). PARP-2, A novel mammalian DNA damage-dependent poly(ADP-ribose) polymerase. *J Biol Chem*, **274,** 17860-8.

Andreason, G.L. & Evans, G.A. (1988). Introduction and expression of DNA molecules in eukaryotic cells by electroporation. *Biotechniques*, **6,** 650-60.

Appella, E. & Anderson, C.W. (2001). Post-translational modifications and activation of p53 by genotoxic stresses. *European Journal of Biochemistry*, **268,** 2764-72.

Ashcroft, M., Kubbutat, M.H. & Vousden, K.H. (1999). Regulation of p53 function and stability by phosphorylation. *Molecular & Cellular Biology*, **19,** 1751-8.

Ashcroft, M., Taya, Y. & Vousden, K.H. (2000). Stress signals utilize multiple pathways to stabilize p53. *Molecular & Cellular Biology*, **20,** 3224-33.

Attardi, L.D. & Jacks, T. (1999). The role of p53 in tumour suppression: lessons from mouse models. *Cellular & Molecular Life Sciences*, **55,** 48-63.

Babiychuk, E., Cottrill, P.B., Storozhenko, S., Fuangthong, M., Chen, Y., O'Farrell, M.K., Van Montagu, M., Inze, D. & Kushnir, S. (1998). Higher plants possess two structurally different poly(ADP-ribose) polymerases. *Plant J*, **15,** 635-45.

Banin, S., Moyal, L., Shieh, S., Taya, Y., Anderson, C.W., Chessa, L., Smorodinsky, N.I., Prives, C., Reiss, Y., Shiloh, Y. & Ziv, Y. (1998). Enhanced phosphorylation of p53 by ATM in response to DNA damage. *Science*, **281,** 1674-7.

Barak, Y., Gottlieb, E., Juven-Gershon, T. & Oren, M. (1994). Regulation of mdm2 expression by p53: alternative promoters produce transcripts with nonidentical translation potential. *Genes & Development*, **8,** 1739-49.

Barak, Y., Juven, T., Haffner, R. & Oren, M. (1993). mdm2 expression is induced by wild type p53 activity. *EMBO Journal*, **12,** 461-8.

Beneke, S., Alvarez-Gonzalez, R. & Burkle, A. (2000). Comparative characterisation of poly(ADP-ribose) polymerase-1 from two mammalian species with different life span. *Exp Gerontol*, **35**, 989-1002.

Benjamin, R.C. & Gill, D.M. (1980). ADP-ribosylation in mammalian cell ghosts. Dependence of poly(ADP-ribose) synthesis on strand breakage in DNA. *J Biol Chem*, **255,** 10493-501.

Berger, N.A., Sikorski, G.W., Petzold, S.J. & Kurohara, K.K. (1980). Defective poly(adenosine diphosphoribose) synthesis in xeroderma pigmentosum. *Biochemistry*, **19**, 289-93

Berghammer, H., Ebner, M., Marksteiner, R. & Auer, B. (1999). pADPRT-2: a novel mammalian polymerizing(ADP-ribosyl)transferase gene related to truncated pADPRT homologues in plants and Caenorhabditis elegans. *FEBS Lett*, **449**, 259-63.

Blasina, A., Paegle, E.S. & McGowan, C.H. (1997). The role of inhibitory phosphorylation of CDC2 following DNA replication block and radiation-induced damage in human cells. *Molecular Biology of the Cell*, **8,** 1013-23.

Blattner, C., Tobiasch, E., Litfen, M., Rahmsdorf, H.J. & Herrlich, P. (1999). DNA damage induced p53 stabilization: no indication for an involvement of p53 phosphorylation. *Oncogene*, **18,** 1723-32.

Bodnar, A.G., Ouellette, M., Frolkis, M., Holt, S.E., Chiu, C.P., Morin, G.B., Harley, C.B., Shay, J.W., Lichtsteiner, S. & Wright, W.E. (1998). Extension of life-span by introduction of telomerase into normal human cells. *Science*, **279,** 349-52.

Bottger, A., Bottger, V., Sparks, A., Liu, W.L., Howard, S.F. & Lane, D.P. (1997). Design of a synthetic Mdm2-binding mini protein that activates the p53 response in vivo. *Current Biology*, **7,** 860-9.

Bottger, V., Bottger, A., Garcia-Echeverria, C., Ramos, Y.F., van der Eb, A.J., Jochemsen, A.G. & Lane, D.P. (1999). Comparative study of the p53-mdm2 and p53-MDMX interfaces. *Oncogene*, **18,** 189-99.

Boulton, S., Pemberton, L.C., Porteous, J.K., Curtin, N.J., Griffin, R.J., Golding, B.T. & Durkacz, B.W. (1995). Potentiation of temozolomide-induced cytotoxicity: a comparative study of the biological effects of poly(ADP-ribose) polymerase inhibitors. *Br J Cancer*, **72,** 849-56.

Burnette, W.N. (1981). "Western blotting": electrophoretic transfer of proteins from sodium dodecyl sulfate--polyacrylamide gels to unmodified nitrocellulose and radiographic detection with antibody and radioiodinated protein A. *Anal Biochem*, **112,** 195-203.

Burzio, L.O., Riquelme, P.T. & Koide, S.S. (1979). ADP ribosylation of rat liver nucleosomal core histones. *J Biol Chem*, **254,** 3029-37.

Butler, A.J. & Ordahl, C.P. (1999). Poly(ADP-ribose) polymerase binds with transcription enhancer factor 1 to MCAT1 elements to regulate muscle-specific transcription. *Mol Cell Biol*, **19,** 296-306.

Calabrese, C.R., Batey, M.A., Thomas, H.D., Durkacz, B.W., Wang, L.Z., Kyle, S., Skalitzky, D., Li, J., Zhang, C., Boritzki, T., Maegley, K., Calvert, A.H., Hostomsky, Z., Newell, D.R. & Curtin, N.J. (2003). Identification of Potent Nontoxic Poly(ADP-Ribose) Polymerase-1 Inhibitors: Chemopotentiation and Pharmacological Studies. *Clin Cancer Res*, **9,** 2711-2718.

Caldecott, K.W., Aoufouchi, S., Johnson, P. & Shall, S. (1996). XRCC1 polypeptide interacts with DNA polymerase beta and possibly poly (ADP-ribose) polymerase, and DNA ligase III is a novel molecular 'nick-sensor' in vitro. *Nucleic Acids Res.* **24,** 4387-94.

Canman, C.E., Lim, D.S., Cimprich, K.A., Taya, Y., Tamai, K., Sakaguchi, K., Appella, E., Kastan, M.B. & Siliciano, J.D. (1998). Activation of the ATM kinase by ionizing radiation and phosphorylation of p53. *Science*, **281,** 1677-9.

Carnero, A., Hudson, J.D., Hannon, G.J. & Beach, D.H. (2000). Loss-of-function genetics in mammalian cells: the p53 tumor suppressor model. *Nucleic Acids Res*, **28,** 2234-41.

Chambon, P., Weil, J.D., Doly, J., Strosser, M.T. & Mandel, P. (1966). On the formation of a novel adenylic compound by enzymatic extracts of rat liver nuclei. *Biochem Biophys Res Commun*, **25,** 638-643.

Chambon, P., Weil, J.D. & Mandel, P. (1963). Nicotinamide mononucleotide activation of a new DNA-dependant polyadenylic acid synthesizing nuclear enzyme. *Biochemical and Biophysical Research Communications*, **11,** 39-43.

Chehab, N.H., Malikzay, A., Appel, M. & Halazonetis, T.D. (2000). Chk2/hCds1 functions as a DNA damage checkpoint in G(1) by stabilizing p53. *Genes & Development*, **14,** 278-88.

Chehab, N.H., Malikzay, A., Stavridi, E.S. & Halazonetis, T.D. (1999). Phosphorylation of Ser-20 mediates stabilization of human p53 in response to DNA damage. *Proceedings of the National Academy of Sciences of the United States of America*, **96,** 13777-82.

Chen, J., Lin, J. & Levine, A.J. (1995). Regulation of transcription functions of the p53 tumor suppressor by the mdm-2 oncogene. *Molecular Medicine*, **1,** 142-52.

Chen, J., Marechal, V. & Levine, A.J. (1993). Mapping of the p53 and mdm-2 interaction domains. *Molecular & Cellular Biology*, **13,** 4107-14.

Chen, L., Agrawal, S., Zhou, W., Zhang, R. & Chen, J. (1998). Synergistic activation of p53 by inhibition of MDM2 expression and DNA damage. *Proceedings of the National Academy of Sciences of the United States of America*, **95,** 195-200.

Chiarugi, A. (2002). Poly(ADP-ribose) polymerase: killer or conspirator? The 'suicide hypothesis' revisited. *Trends Pharmacol Sci*, **23,** 122-9.

Chu, G. (1997). Double strand break repair. *J Biol Chem*, **272,** 24097-100.

Colman, M.S., Afshari, C.A. & Barrett, J.C. (2000). Regulation of p53 stability and activity in response to genotoxic stress. *Mutation Research*, **462,** 179-88.

D'Adda di Fagagna, F., Prakash Hande, M., Tong, W., Lansdorp, P.M., Wang, Z.Q. & Jackson, S.P. (1999). Functions of poly(ADP-ribose) polymerase in controlling telomere length and chromosomal stability. *Nat Gen*, **23**, 76-80

D'Amours, D., Desnoyers, S., D'Silva, I. & Poirier, G.G. (1999). Poly(ADP-ribosyl)ation reactions in the regulation of nuclear functions. *Biochem J*, **342,** 249-68.

Dantzer, F., Schreiber, V., Niedergang, C., Trucco, C., Flatter, E., De La Rubia, G., Oliver, J., Rolli, V., Menissier-de Murcia, J. & de Murcia, G. (1999). Involvement of poly(ADP-ribose) polymerase in base excision repair. *Biochimie*, **81,** 69-75.

de Murcia, J.M., Niedergang, C., Trucco, C., Ricoul, M., Dutrillaux, B., Mark, M., Oliver, F.J., Masson, M., Dierich, A., LeMeur, M., Walztinger, C., Chambon, P. & de Murcia, G. (1997). Requirement of poly(ADP-ribose) polymerase in recovery from DNA damage in mice and in cells. *Proc Natl Acad Sci U S A*, **94,** 7303-7.

de Toledo, S.M., Azzam, E.I., Dahlberg, W.K., Gooding, T.B. & Little, J.B. (2000). ATM complexes with HDM2 and promotes its rapid phosphorylation in a p53-independent manner in normal and tumor human cells exposed to ionizing radiation. *Oncogene*, **19,** 6185-93.

Deans, B., Griffin, C.S., Maconochie, M. & Thacker, J. (2000). Xrcc2 is required for genetic stability, embryonic neurogenesis and viability in mice. *Embo J*, **19,** 6675-85.

Delaney, C.A., Wang, L.Z., Kyle, S., White, A.W., Calvert, A.H., Curtin, N.J., Durkacz, B.W., Hostomsky, Z. & Newell, D.R. (2000). Potentiation of temozolomide and topotecan growth inhibition and cytotoxicity by novel poly(adenosine diphosphoribose) polymerase inhibitors in a panel of human tumor cell lines. *Clin Cancer Res*, **6,** 2860-7.

DelGiudice, R.A. & Hopps, H.E. (1978). *Mycoplasma infection of Cell Cultures*, 57-69.

Delia, D., Mizutani, S., Panigone, S., Tagliabue, E., Fontanella, E., Asada, M., Yamada, T., Taya, Y., Prudente, S., Saviozzi, S., Frati, L., Pierotti, M.A. & Chessa, L. (2000). ATM protein and p53-serine 15 phosphorylation in ataxia-telangiectasia (AT) patients and at heterozygotes. *British Journal of Cancer*, **82,** 1938-45.

Donehower, L.A., Harvey, M., Slagle, B.L., McArthur, M.J., Montgomery, C.A., Jr., Butel, J.S. & Bradley, A. (1992). Mice deficient for p53 are developmentally normal but susceptible to spontaneous tumours. *Nature*, **356,** 215-21.

Dulic, V., Kaufmann, W.K., Wilson, S.J., Tlsty, T.D., Lees, E., Harper, J.W., Elledge, S.J. & Reed, S.I. (1994). p53-dependent inhibition of cyclin-dependent kinase activities in human fibroblasts during radiation-induced G1 arrest. *Cell*, **76,** 1013-23.

Durkacz, B.W., Omidiji, O., Gray, D.A. & Shall, S. (1980). (ADP-ribose)n participates in DNA excision repair. *Nature*, **283,** 593-6.

Durkacz, B.W., Shall, S. & Irwin, J. (1981). The effect of inhibition of (ADP-ribose)n biosynthesis on DNA repair assayed by the nucleoid technique. *Eur J Biochem*, **121,** 65-9.

Dynan, W.S. & Yoo, S. (1998). Interaction of Ku protein and DNA-dependent protein kinase catalytic subunit with nucleic acids. *Nucleic Acids Res*, **26,** 1551-9.

Eguchi, Y., Shimizu, S. & Tsujimoto, Y. (1997). Intracellular ATP levels determine cell death fate by apoptosis or necrosis. *Cancer Res*, **57,** 1835-40.

el-Deiry, W.S., Tokino, T., Velculescu, V.E., Levy, D.B., Parsons, R., Trent, J.M., Lin, D., Mercer, W.E., Kinzler, K.W. & Vogelstein, B. (1993). WAF1, a potential mediator of p53 tumor suppression. *Cell*, **75,** 817-25.

Elledge, S.J., Richman, R., Hall, F.L., Williams, R.T., Lodgson, N. & Harper, J.W. (1992). CDK2 encodes a 33-kDa cyclin A-associated protein kinase and is expressed before CDC2 in the cell cycle. *Proceedings of the National Academy of Sciences of the United States of America*, **89,** 2907-11.

Enari, M., Sakahira, H., Yokoyama, H., Okawa, K., Iwamatsu, A. & Nagata, S. (1998). A caspase-activated DNase that degrades DNA during apoptosis, and its inhibitor ICAD. *Nature*, **391,** 43-50.

Fakharzadeh, S.S., Trusko, S.P. & George, D.L. (1991). Tumorigenic potential associated with enhanced expression of a gene that is amplified in a mouse tumor cell line. *EMBO Journal*, **10,** 1565-9.

Feinberg, A.P. & Vogelstein, B. (1983). A technique for radiolabeling DNA restriction endonuclease fragments to high specific activity. *Anal Biochem*, **132,** 6-13.

Foo, S.Y. & Nolan, G.P. (1999). NF-kappaB to the rescue: RELs, apoptosis and cellular transformation. *Trends Genet*, **15,** 229-35.

Freedman, D.A., Epstein, C.B., Roth, J.C. & Levine, A.J. (1997). A genetic approach to mapping the p53 binding site in the MDM2 protein. *Molecular Medicine*, **3,** 248-59.

Friedberg, E.C. (1995). Out of the shadows and into the light: the emergence of DNA repair. *Trends Biochem Sci*, **20,** 381.

Fuchs, S.Y., Adler, V., Buschmann, T., Wu, X. & Ronai, Z. (1998). Mdm2 association with p53 targets its ubiquitination. *Oncogene*, **17,** 2543-7.

Goodwin, P.M., Lewis, P.J., Davies, M.I., Skidmore, C.J. & Shall, S. (1978). The effect of gamma radiation and neocarzinostatin on NAD and ATP levels in mouse leukaemia cells. *Biochim Biophys Acta*, **543,** 576-82.

Gradwohl, G., Menissier de Murcia, J.M., Molinete, M., Simonin, F., Koken, M., Hoeijmakers, J.H. & de Murcia, G. (1990). The second zinc-finger domain of poly(ADP-ribose) polymerase determines specificity for single-stranded breaks in DNA. *Proc Natl Acad Sci U S A*, **87,** 2990-4.

Graham, F.L. & van der Eb, A.J. (1973). A new technique for the assay of infectivity of human adenovirus 5 DNA. *Virology*, **52,** 456-67.

Griffin, R.J., Curtin, N.J., Newell, D.R., Golding, B.T., Durkacz, B.W. & Calvert, A.H. (1995a). The role of inhibitors of poly(ADP-ribose) polymerase as resistance-modifying agents in cancer therapy. *Biochimie*, **77,** 408-22.

Griffin, R.J., Pemberton, L.C., Rhodes, D., Bleasdale, C., Bowman, K., Calvert, A.H., Curtin, N.J., Durkacz, B.W., Newell, D.R., Porteous, J.K. & et al. (1995b). Novel potent inhibitors of the DNA repair enzyme poly(ADP-ribose)polymerase (PARP). *Anticancer Drug Des*, **10,** 507-14.

Haines, D.S., Landers, J.E., Engle, L.J. & George, D.L. (1994). Physical and functional interaction between wild-type p53 and mdm2 proteins. *Molecular & Cellular Biology*, **14,** 1171-8.

Hannon, G.J., Casso, D. & Beach, D. (1994). KAP: a dual specificity phosphatase that interacts with cyclin-dependent kinases. *Proceedings of the National Academy of Sciences of the United States of America*, **91,** 1731-5.

Harvey, D.M. & Levine, A.J. (1991). p53 alteration is a common event in the spontaneous immortalization of primary BALB/c murine embryo fibroblasts. *Genes Dev*, **5,** 2375-85.

Harvey, M., Sands, A.T., Weiss, R.S., Hegi, M.E., Wiseman, R.W., Pantazis, P., Giovanella, B.C., Tainsky, M.A., Bradley, A. & Donehower, L.A. (1993). In vitro growth characteristics of embryo fibroblasts isolated from p53-deficient mice. *Oncogene*, **8,** 2457-67.

Hassa, P.O. & Hottiger, M.O. (1999). A role of poly (ADP-ribose) polymerase in NF-kappaB transcriptional activation. *Biol Chem*, **380,** 953-9.

Haupt, Y., Maya, R., Kazaz, A. & Oren, M. (1997). Mdm2 promotes the rapid degradation of p53. *Nature*, **387,** 296-9.

Hauschildt, S., Ulmer, A.J., Flad, H.D., Heyden, T. & Heine, H. (1998). ADP-ribosylation: role in LPS-induced phosphorylation of two cytosolic proteins (p36/38) in monocytes. *Prog Clin Biol Res*, **397,** 147-55.

Hayflick, L. & Moorhead, P.S. (1961). The limited in vitro lifespan of human diploid cell strains. *Experimental Cell Research*, **25,** 585-621.

Heuval, S. & Harlow, E. (1993). Distinct roles for cyclin-dependent kinases in cell cycle control. *Science*, **262**, 2050-4

Hirai, H., Roussel, M.F., Kato, J.Y., Ashmun, R.A. & Sherr, C.J. (1995). Novel INK4 proteins, p19 and p18, are specific inhibitors of the cyclin D-dependent kinases CDK4 and CDK6. *Molecular & Cellular Biology*, **15,** 2672-81.

Hirao, A., Kong, Y.Y., Matsuoka, S., Wakeham, A., Ruland, J., Yoshida, H., Liu, D., Elledge, S.J. & Mak, T.W. (2000). DNA damage-induced activation of p53 by the checkpoint kinase Chk2. *Science*, **287,** 1824-7.

Honda, R., Tanaka, H. & Yasuda, H. (1997). Oncoprotein MDM2 is a ubiquitin ligase E3 for tumor suppressor p53. *FEBS Letters*, **420,** 25-7.

Honda, R. & Yasuda, H. (1999). Association of p19(ARF) with Mdm2 inhibits ubiquitin ligase activity of Mdm2 for tumor suppressor p53. *EMBO Journal*, **18,** 22-7.

Hu, Y., Benedict, M.A., Ding, L. & Nunez, G. (1999). Role of cytochrome c and dATP/ATP hydrolysis in Apaf-1-mediated caspase-9 activation and apoptosis. *EMBO Journal*, **18,** 3586-95.

Hunting, D.J., Gowans, B.J. & Henderson, J.F. (1985). Specificity of inhibitors of poly(ADP-ribose) synthesis. Effects on nucleotide metabolism in cultured cells. *Mol Pharmacol*, **28,** 200-6.

Hupp, T.R. & Lane, D.P. (1994). Allosteric activation of latent p53 tetramers. *Current Biology*, **4,** 865-75.

Itahana, K., Dimri, G. & Campisi, J. (2001). Regulation of cellular senescence by p53. *Eur J Biochem*, **268,** 2784-91.

Jackson, M.W. & Berberich, S.J. (2000). MdmX protects p53 from Mdm2-mediated degradation. *Mol Cell Biol*, **20,** 1001-7.

Jackson, S.P. (2002). Sensing and repairing DNA double-strand breaks. *Carcinogenesis*, **23,** 687-96.

James, M.R. & Lehmann, A.R. (1982). Role of poly(adenosine diphosphate ribose) in deoxyribonucleic acid repair in human fibroblasts. *Biochemistry*, **21**, 4007-13.

Jeffrey, P.D., Russo, A.A., Polyak, K., Gibbs, E., Hurwitz, J., Massague, J. & Pavletich, N.P. (1995). Mechanism of CDK activation revealed by the structure of a cyclinA-CDK2 complex. *Nature*, **376,** 313-20.

Jenkins, J.R., Rudge, K. & Currie, G.A. (1984). Cellular immortalization by a cDNA clone encoding the transformation-associated phosphoprotein p53. *Nature*, **312,** 651-4.

Johnson, T.M., Yu, Z.X., Ferrans, V.J., Lowenstein, R.A. & Finkel, T. (1996). Reactive oxygen species are downstream mediators of p53-dependent apoptosis. *Proceedings of the National Academy of Sciences of the United States of America*, **93,** 11848-52.

Jones, S.N., Roe, A.E., Donehower, L.A. & Bradley, A. (1995). Rescue of embryonic lethality in Mdm2-deficient mice by absence of p53. *Nature*, **378,** 206-8.

Kannan, P., Yu, Y., Wankhade, S. & Tainsky, M.A. (1999). PolyADP-ribose polymerase is a coactivator for AP-2-mediated transcriptional activation. *Nucleic Acids Res*, **27,** 866-74.

Kastan, M.B., Onyekwere, O., Sidransky, D., Vogelstein, B. & Craig, R.W. (1991). Participation of p53 protein in the cellular response to DNA damage. *Cancer Research*, **51,** 6304-11.

Kato, J., Matsushime, H., Hiebert, S.W., Ewen, M.E. & Sherr, C.J. (1993). Direct binding of cyclin D to the retinoblastoma gene product (pRb) and pRb phosphorylation by the cyclin D-dependent kinase CDK4. *Genes & Development*, **7,** 331-42.

Kawai, H., Nie, L., Wiederschain, D. & Yuan, Z.M. (2001). Dual role of p300 in the regulation of p53 stability. *Journal of Biological Chemistry*, **276,** 45928-32.

Kawamitsu, H., Hoshino, H., Okada, H., Miwa, M., Momoi, H. & Sugimura, T. (1984). Monoclonal antibodies to poly(adenosine diphosphate ribose) recognize different structures. *Biochemistry*, **23,** 3771-7.

Khosravi, R., Maya, R., Gottlieb, T., Oren, M., Shiloh, Y. & Shkedy, D. (1999). Rapid ATM-dependent phosphorylation of MDM2 precedes p53 accumulation in response to DNA damage. *Proceedings of the National Academy of Sciences of the United States of America*, **96,** 14973-7.

Kickhoefer, V.A., Siva, A.C., Kedersha, N.L., Inman, E.M., Ruland, C., Streuli, M. & Rome, L.H. (1999). The 193-kD vault protein, VPARP, is a novel poly(ADP-ribose) polymerase. *J Cell Biol*, **146,** 917-28.

Kim, H., You, S., Farris, J., Foster, L.K. & Foster, D.N. (2001). Post-transcriptional inactivation of p53 in immortalized murine embryo fibroblast cells. *Oncogene*, **20,** 3306-10.

Koff, A., Giordano, A., Desai, D., Yamashita, K., Harper, J.W., Elledge, S., Nishimoto, T., Morgan, D.O., Franza, B.R. & Roberts, J.M. (1992). Formation and activation of a cyclin E-cdk2 complex during the G1 phase of the human cell cycle. *Science*, **257,** 1689-94.

Koniaras, K., Cuddihy, A.R., Christopoulos, H., Hogg, A. & O'Connell, M.J. (2001). Inhibition of Chk1-dependent G2 DNA damage checkpoint radiosensitizes p53 mutant human cells. *Oncogene*, **20,** 7453-63.

Kovesdi, I., Reichel, R. & Nevins, J.R. (1987). Role of an adenovirus E2 promoter binding factor in E1A-mediated coordinate gene control. *Proceedings of the National Academy of Sciences of the United States of America*, **84,** 2180-4.

Kreimeyer, A., Wielckens, K., Adamietz, P. & Hilz, H. (1984). DNA repair-associated ADP-ribosylation in vivo. Modification of histone H1 differs from that of the principal acceptor proteins. *J Biol Chem*, **259,** 890-6.

Kubbutat, M.H., Ludwig, R.L., Levine, A.J. & Vousden, K.H. (1999). Analysis of the degradation function of Mdm2. *Cell Growth & Differentiation*, **10,** 87-92.

Kubota, Y., Nash, R.A., Klungland, A., Schar, P., Barnes, D.E. & Lindahl, T. (1996). Reconstitution of DNA base excision-repair with purified human proteins: interaction between DNA polymerase beta and the XRCC1 protein. *Embo J*, **15,** 6662-70.

Kuerbitz, S.J., Plunkett, B.S., Walsh, W.V. & Kastan, M.B. (1992). Wild-type p53 is a cell cycle checkpoint determinant following irradiation. *Proceedings of the National Academy of Sciences of the United States of America*, **89,** 7491-5.

Kupper, J.H., de Murcia, G. & Burkle, A. (1990). Inhibition of poly(ADP-ribosyl)ation by overexpressing the poly(ADP-ribose) polymerase DNA-binding domain in mammalian cells. *J Biol Chem*, **265,** 18721-4.

Kupper, J.H., Muller, M., Jacobson, M.K., Tatsumi-Miyajima, J., Coyle, D.L., Jacobson, E.L. & Burkle, A. (1995). trans-dominant inhibition of poly(ADP-ribosyl)ation sensitizes cells against gamma-irradiation and N-methyl-N'-nitro-N-nitrosoguanidine but does not limit DNA replication of a polyomavirus replicon. *Mol Cell Biol*, **15,** 3154-63.

Kurosaki, T., Ushiro, H., Mitsuuchi, Y., Suzuki, S., Matsuda, M., Matsuda, Y., Katunuma, N., Kangawa, K., Matsuo, H., Hirose, T. & et al. (1987). Primary structure of human poly(ADP-ribose) synthetase as deduced from cDNA sequence. *J Biol Chem*, **262,** 15990-7.

Lambert, P.F., Kashanchi, F., Radonovich, M.F., Shiekhattar, R. & Brady, J.N. (1998). Phosphorylation of p53 serine 15 increases interaction with CBP. *Journal of Biological Chemistry*, **273,** 33048-53.

Lazebnik, Y.A., Kaufmann, S.H., Desnoyers, S., Poirier, G.G. & Earnshaw, W.C. (1994). Cleavage of poly(ADP-ribose) polymerase by a proteinase with properties like ICE. *Nature*, **371,** 346-7.

Lees-Miller, S.P., Sakaguchi, K., Ullrich, S.J., Appella, E., & Anderson, C.W. (1992). Human DNA-activated protein kinase phosphorylates serines 15 and 37 in the amino-terminal transactivation domain of human p53. *Mol Cell Biol*, **12**, 5041-9

Le Page, C., Sanceau, J., Drapier, J.C. & Wietzerbin, J. (1998). Inhibitors of ADP-ribosylation impair inducible nitric oxide synthase gene transcription through inhibition of NF kappa B activation. *Biochem Biophys Res Commun*, **243,** 451-7.

Lefebvre, P. & Laval, F. (1989). Potentiation of N-methyl-N'-nitro-N-nitrosoguanidine-induced O6-methylguanine-DNA-methyltransferase activity in a rat hepatoma cell line by poly (ADP-ribose) synthesis inhibitors. *Biochem Biophys Res Commun*, **163,** 599-604.

Leist, M., Single, B., Castoldi, A.F., Kuhnle, S. & Nicotera, P. (1997). Intracellular adenosine triphosphate (ATP) concentration: a switch in the decision between apoptosis and necrosis. *J Exp Med*, **185,** 1481-6.

Lengauer, C., Kinzler, K.W. & Vogelstein, B. (1998). Genetic instabilities in human cancers. *Nature*, **396,** 643-9.

Li, P., Nijhawan, D., Budihardjo, I., Srinivasula, S.M., Ahmad, M., Alnemri, E.S. & Wang, X. (1997). Cytochrome c and dATP-dependent formation of Apaf-1/caspase-9 complex initiates an apoptotic protease cascade. *Cell*, **91,** 479-89.

Li, R. & Botchan, M.R. (1993). The acidic transcriptional activation domains of VP16 and p53 bind the cellular replication protein A and stimulate in vitro BPV-1 DNA replication. *Cell*, **73,** 1207-21.

Li, Y., Jenkins, C.W., Nichols, M.A. & Xiong, Y. (1994). Cell cycle expression and p53 regulation of the cyclin-dependent kinase inhibitor p21. *Oncogene*, **9,** 2261-8.

Lill, N.L., Grossman, S.R., Ginsberg, D., DeCaprio, J. & Livingston, D.M. (1997). Binding and modulation of p53 by p300/CBP coactivators. *Nature*, **387,** 823-7.

Lim, D.S. & Hasty, P. (1996). A mutation in mouse rad51 results in an early embryonic lethal that is suppressed by a mutation in p53. *Mol Cell Biol*, **16,** 7133-43.

Lin, J., Chen, J., Elenbaas, B. & Levine, A.J. (1994). Several hydrophobic amino acids in the p53 amino-terminal domain are required for transcriptional activation, binding to mdm-2 and the adenovirus 5 E1B 55-kD protein. *Genes & Development*, **8,** 1235-46.

Liu, L., Scolnick, D.M., Trievel, R.C., Zhang, H.B., Marmorstein, R., Halazonetis, T.D. & Berger, S.L. (1999). p53 sites acetylated in vitro by PCAF and p300 are acetylated in vivo in response to DNA damage. *Molecular & Cellular Biology*, **19,** 1202-9.

Long, J.J., Leresche, A., Kriwacki, R.W. & Gottesfeld, J.M. (1998). Repression of TFIIH transcriptional activity and TFIIH-associated cdk7 kinase activity at mitosis. *Molecular & Cellular Biology*, **18,** 1467-76.

Lotem, J., Peled-Kamar, M., Groner, Y. & Sachs, L. (1996). Cellular oxidative stress and the control of apoptosis by wild-type p53, cytotoxic compounds, and cytokines. *Proceedings of the National Academy of Sciences of the United States of America*, **93,** 9166-71.

Lu, H. & Levine, A.J. (1995). Human TAFII31 protein is a transcriptional coactivator of the p53 protein. *Proceedings of the National Academy of Sciences of the United States of America*, **92,** 5154-8.

Lu, X. & Lane, D.P. (1993). Differential induction of transcriptionally active p53 following UV or ionizing radiation: defects in chromosome instability syndromes? *Cell*, **75,** 765-78.

Martin, K., Trouche, D., Hagemeier, C., Sorensen, T.S., La Thangue, N.B. & Kouzarides, T. (1995). Stimulation of E2F1/DP1 transcriptional activity by MDM2 oncoprotein. *Nature*, **375,** 691-4.

Martin, S.J. & Green, D.R. (1995). Protease activation during apoptosis: death by a thousand cuts? *Cell*, **82,** 349-52.

Martinez, J.D., Craven, M.T., Joseloff, E., Milczarek, G. & Bowden, G.T. (1997). Regulation of DNA binding and transactivation in p53 by nuclear localization and phosphorylation. *Oncogene*, **14,** 2511-20.

Masson, M., Niedergang, C., Schreiber, V., Muller, S., Menissier-de Murcia, J. & de Murcia, G. (1998). XRCC1 is specifically associated with poly(ADP-ribose)

polymerase and negatively regulates its activity following DNA damage. *Mol Cell Biol*, **18,** 3563-71.

Masutani, M., Nozaki, T., Nishiyama, E., Shimokawa, T., Tachi, Y., Suzuki, H., Nakagama, H., Wakabayashi, K. & Sugimura, T. (1999). Function of poly(ADP-ribose) polymerase in response to DNA damage: gene-disruption study in mice. *Molecular & Cellular Biochemistry*, **193,** 149-52.

Matsui, T., Segall, J., Weil, P.A. & Roeder, R.G. (1980). Multiple factors required for accurate initiation of transcription by purified RNA polymerase II. *J Biol Chem*, **255,** 11992-6.

Mazen, A., Menissier-de Murcia, J., Molinete, M., Simonin, F., Gradwohl, G., Poirier, G. & de Murcia, G. (1989). Poly(ADP-ribose)polymerase: a novel finger protein. *Nucleic Acids Res*, **17,** 4689-98.

McCullough, A.K., Dodson, M.L. & Lloyd, R.S. (1999). Initiation of base excision repair: glycosylase mechanisms and structures. *Annu Rev Biochem*, **68,** 255-85.

Meek, D.W. (1994). Post-translational modification of p53. *Seminars in Cancer Biology*, **5,** 203-10.

Menard, L. & Poirier, G.G. (1987). Rapid assay of poly(ADP-ribose) glycohydrolase. *Biochem Cell Biol*, **65,** 668-73.

Mendoza-Alvarez, H. & Alvarez-Gonzalez, R. (2001). Regulation of p53 sequence-specific DNA-binding by covalent poly(ADP-ribosyl)ation. *J Biol Chem*, **276,** 36425-30.

Menissier-de Murcia, J., Molinete, M., Gradwohl, G., Simonin, F. & de Murcia, G. (1989). Zinc-binding domain of poly(ADP-ribose)polymerase participates in the recognition of single strand breaks on DNA. *J Mol Biol*, **210,** 229-33.

Miwa, M. & Sugimura, T. (1971). Splitting of the ribose-ribose linkage of poly(adenosine diphosphate-robose) by a calf thymus extract. *J Biol Chem*, **246,** 6362-4.

Molinete, M., Vermeulen, W., Burkle, A., Menissier-de Murcia, J., Kupper, J.H., Hoeijmakers, J.H. & de Murcia, G. (1993). Overproduction of the poly(ADP-ribose) polymerase DNA-binding domain blocks alkylation-induced DNA repair synthesis in mammalian cells. *Embo J*, **12,** 2109-17.

Morgan, D.O. (1995). Principles of CDK regulation. *Nature*, **374,** 131-4.

Mueller, P.R., Coleman, T.R., Kumagai, A. & Dunphy, W.G. (1995). Myt1: a membrane-associated inhibitory kinase that phosphorylates Cdc2 on both threonine-14 and tyrosine-15. *Science*, **270,** 86-90.

Muller, M., Strand, S., Hug, H., Heinemann, E.M., Walczak, H., Hofmann, W.J., Stremmel, W., Krammer, P.H. & Galle, P.R. (1997). Drug-induced apoptosis in hepatoma cells is mediated by the CD95 (APO-1/Fas) receptor/ligand system and involves activation of wild-type p53. *Journal of Clinical Investigation*, **99,** 403-13.

Nduka, N., Skidmore, C.J. & Shall, S. (1980). The enhancement of cytotoxicity of N-methyl-N-nitrosourea and of gamma-radiation by inhibitors of poly(ADP-ribose) polymerase. *Eur J Biochem*, **105,** 525-30.

Newlands, E.S., Stevens, M.F., Wedge, S.R., Wheelhouse, R.T. & Brock, C. (1997). Temozolomide: a review of its discovery, chemical properties, pre-clinical development and clinical trials. *Cancer Treat Rev*, **23,** 35-61.

Nie, J., Sakamoto, S., Song, D., Qu, Z., Ota, K. & Taniguchi, T. (1998). Interaction of Oct-1 and automodification domain of poly(ADP-ribose) synthetase. *FEBS Lett*, **424,** 27-32.

Nurse, P. (1990). Universal control mechanism regulating onset of M-phase. *Nature*, **344,** 503-8.

Ogata, N., Ueda, K., Kawaichi, M. & Hayaishi, O. (1981). Poly(ADP-ribose) synthetase, a main acceptor of poly(ADP-ribose) in isolated nuclei. *J Biol Chem*, **256,** 4135-7.

Ohashi, Y., Itaya, A., Tanaka, Y., Yoshihara, K., Kamiya, T. & Matsukage, A. (1986). Poly(ADP-ribosyl)ation of DNA polymerase beta in vitro. *Biochem Biophys Res Commun*, **140,** 666-73.

Oliver, F.J., Menissier-de Murcia, J., Nacci, C., Decker, P., Andriantsitohaina, R., Muller, S., de la Rubia, G., Stoclet, J.C. & de Murcia, G. (1999). Resistance to endotoxic shock as a consequence of defective NF-kappaB activation in poly (ADP-ribose) polymerase-1 deficient mice. *Embo J*, **18,** 4446-54.

Olson, D.C., Marechal, V., Momand, J., Chen, J., Romocki, C. & Levine, A.J. (1993). Identification and characterization of multiple mdm-2 proteins and mdm-2-p53 protein complexes. *Oncogene*, **8,** 2353-60.

Parant, J.M., Reinke, V., Mims, B. & Lozano, G. (2001). Organization, expression and localization of the murine mdmx gene and psudogene. Gene, **270**, 277-83

Parker, L.L. & Piwnica-Worms, H. (1992). Inactivation of the p34cdc2-cyclin B complex by the human WEE1 tyrosine kinase. *Science*, **257,** 1955-7.

Petersen, B.O., Lukas, J., Sorensen, C.S., Bartek, J. & Helin, K. (1999). Phosphorylation of mammalian CDC6 by cyclin A/CDK2 regulates its subcellular localization. *EMBO Journal*, **18,** 396-410.

Pleschke, J.M., Kleczkowska, H.E., Strohm, M. & Althaus, F.R. (2000). Poly(ADP-ribose) binds to specific domains in DNA damage checkpoint proteins. *J Biol Chem*, **275,** 40974-80.

Polyak, K., Xia, Y., Zweier, J.L., Kinzler, K.W. & Vogelstein, B. (1997). A model for p53-induced apoptosis. *Nature*, **389,** 300-5.

Pomerantz, J., Schreiber-Agus, N., Liegeois, N.J., Silverman, A., Alland, L., Chin, L., Potes, J., Chen, K., Orlow, I., Lee, H.W., Cordon-Cardo, C. & DePinho, R.A. (1998). The Ink4a tumor suppressor gene product, p19Arf, interacts with MDM2 and neutralizes MDM2's inhibition of p53. *Cell*, **92,** 713-23.

Rankin, P.W., Jacobson, M.K., Mitchell, V.R. & Busbee, D.L. (1980). Reduction of nicotinamide adenine dinucleotide levels by ultimate carcinogens in human lymphocytes. *Cancer Res*, **40,** 1803-7.

Ray, L.S., Chatterjee, S., Berger, N.A., Grishko, V.I., LeDoux, S.P. & Wilson, G.L. (1996). Catalytic activity of poly(ADP-ribose) polymerase is necessary for repair of N-methylpurines in nontranscribed, but not in transcribed, nuclear DNA sequences. *Mutat Res*, **363,** 105-14.

Rich, T., Allen, R.L. & Wyllie, A.H. (2000). Defying death after DNA damage. *Nature*, **407,** 777-83.

Richardson, C. & Jasin, M. (2000). Frequent chromosomal translocations induced by DNA double-strand breaks. *Nature*, **405,** 697-700.

Riquelme, P.T., Burzio, L.O. & Koide, S.S. (1979). ADP ribosylation of rat liver lysine-rich histone in vitro. *J Biol Chem*, **254,** 3018-28.

Rittling, S.R. & Denhardt, D.T. (1992). p53 mutations in spontaneously immortalized 3T12 but not 3T3 mouse embryo cells. *Oncogene*, **7,** 935-42.

Roth, J., Dobbelstein, M., Freedman, D.A., Shenk, T. & Levine, A.J. (1998). Nucleo-cytoplasmic shuttling of the hdm2 oncoprotein regulates the levels of the p53 protein via a pathway used by the human immunodeficiency virus rev protein. *EMBO Journal*, **17,** 554-64.

Ruscetti, T., Lehnert, B.E., Halbrook, J., Le Trong, H., Hoekstra, M.F., Chen, D.J. & Peterson, S.R. (1998). Stimulation of the DNA-dependent protein kinase by poly(ADP-ribose) polymerase. *J Biol Chem*, **273,** 14461-7.

Ryan, K.M., Phillips, A.C. & Vousden, K.H. (2001). Regulation and function of the p53 tumor suppressor protein. *Current Opinion in Cell Biology*, **13,** 332-7.

Saikumar, P., Dong, Z., Mikhailov, V., Denton, M., Weinberg, J.M. & Venkatachalam, M.A. (1999). Apoptosis: definition, mechanisms, and relevance to disease. *Am J Med*, **107,** 489-506.

Sakahira, H., Enari, M. & Nagata, S. (1998). Cleavage of CAD inhibitor in CAD activation and DNA degradation during apoptosis. *Nature*, **391,** 96-9.

Saleh, A., Srinivasula, S.M., Acharya, S., Fishel, R. & Alnemri, E.S. (1999). Cytochrome c and dATP-mediated oligomerization of Apaf-1 is a prerequisite for procaspase-9 activation. *Journal of Biological Chemistry*, **274,** 17941-5.

Sallmann, F.R., Vodenicharov, M.D., Wang, Z.Q. & Poirier, G.G. (2000). Characterization of sPARP-1. An alternative product of PARP-1 gene with poly(ADP-ribose) polymerase activity independent of DNA strand breaks. *J Biol Chem*, **275,** 15504-11.

Sanger, F. (1981). Determination of nucleotide sequences in DNA. *Science*, **214,** 1205-10.

Satoh, M.S. & Lindahl, T. (1992). Role of poly(ADP-ribose) formation in DNA repair. *Nature*, **356,** 356-8.

Satoh, M.S., Poirier, G.G. & Lindahl, T. (1993). NAD(+)-dependent repair of damaged DNA by human cell extracts. *J Biol Chem*, **268,** 5480-7.

Schraufstatter, I.U., Hinshaw, D.B., Hyslop, P.A., Spragg, R.G. & Cochrane, C.G. (1986). Oxidant injury of cells. DNA strand-breaks activate polyadenosine diphosphate-ribose polymerase and lead to depletion of nicotinamide adenine dinucleotide. *J Clin Invest*, **77,** 1312-20.

Schreiber, V., Ame, J.C., Dolle, P., Schultz, I., Rinaldi, B., Fraulob, V., Menissier-de Murcia, J. & de Murcia, G. (2002). Poly(ADP-ribose) polymerase-2 (PARP-2) is required for efficient base excision DNA repair in association with PARP-1 and XRCC1. *J Biol Chem*, **277,** 23028-36.

Scolnick, D.M., Chehab, N.H., Stavridi, E.S., Lien, M.C., Caruso, L., Moran, E., Berger, S.L. & Halazonetis, T.D. (1997). CREB-binding protein and p300/CBP-associated factor are transcriptional coactivators of the p53 tumor suppressor protein. *Cancer Research*, **57,** 3693-6.

Serrano, M., Hannon, G.J. & Beach, D. (1993). A new regulatory motif in cell-cycle control causing specific inhibition of cyclin D/CDK4. *Nature*, **366,** 704-7.

Shall, S. (1984). Inhibition of DNA repair by inhibitors of nuclear ADP-ribosyl transferase. *Nucleic Acids Symp Ser*, 143-91.

Shall, S. & de Murcia, G. (2000). Poly(ADP-ribose) polymerase-1: what have we learned from the deficient mouse model? *Mutat Res*, **460,** 1-15.

Sharan, S.K., Morimatsu, M., Albrecht, U., Lim, D.S., Regel, E., Dinh, C., Sands, A., Eichele, G., Hasty, P. & Bradley, A. (1997). Embryonic lethality and radiation hypersensitivity mediated by Rad51 in mice lacking Brca2. *Nature*, **386,** 804-10.

Sheikh, M.S., Burns, T.F., Huang, Y., Wu, G.S., Amundson, S., Brooks, K.S., Fornace, A.J., Jr. & el-Deiry, W.S. (1998). p53-dependent and -independent regulation of the death receptor KILLER/DR5 gene expression in response to genotoxic stress and tumor necrosis factor alpha. *Cancer Research*, **58,** 1593-8.

Sherr, C.J. (1995). D-type cyclins. *Trends in Biochemical Sciences*, **20,** 187-90.

Sherr, C.J. & DePinho, R.A. (2000). Cellular senescence: mitotic clock or culture shock? *Cell*, **102,** 407-10.

Sherr, C.J. & Roberts, J.M. (1995). Inhibitors of mammalian G1 cyclin-dependent kinases. *Genes & Development*, **9,** 1149-63.

Shieh, S.Y., Ahn, J., Tamai, K., Taya, Y. & Prives, C. (2000). The human homologs of checkpoint kinases Chk1 and Cds1 (Chk2) phosphorylate p53 at multiple DNA damage-inducible sites. *Genes & Development*, **14,** 289-300.

Shieh, S.Y., Ikeda, M., Taya, Y. & Prives, C. (1997). DNA damage-induced phosphorylation of p53 alleviates inhibition by MDM2. *Cell*, **91,** 325-34.

Shieh, S.Y., Taya, Y. & Prives, C. (1999). DNA damage-inducible phosphorylation of p53 at N-terminal sites including a novel site, Ser20, requires tetramerization. *EMBO Journal*, **18,** 1815-23.

Shieh, W.M., Ame, J.C., Wilson, M.V., Wang, Z.Q., Koh, D.W., Jacobson, M.K. & Jacobson, E.L. (1998). Poly(ADP-ribose) polymerase null mouse cells synthesize ADP-ribose polymers. *J Biol Chem*, **273,** 30069-72.

Shiloh, Y., Tabor, E. & Becker, Y. (1985). In vitro phenotype of ataxia-telangiectasia (AT) fibroblast strains: clues to the nature of the "AT DNA lesion" and the molecular defect in AT. *Kroc Found Ser*, **19,** 111-21.

Shvarts, A., Bazuine, M., Dekker, P., Ramos, Y.F., Steegenga, W.T., Merckx, G., van Ham, R.C., van der Houven van Oordt, W., van der Eb, A.J. & Jochemsen, A.G. (1997). Isolation and identification of the human homolog of a new p53-binding protein, Mdmx. *Genomics*, **43,** 34-42.

Sigalas, I., Calvert, A.H., Anderson, J.J., Neal, D.E. & Lunec, J. (1996). Alternatively spliced mdm2 transcripts with loss of p53 binding domain sequences: transforming ability and frequent detection in human cancer. *Nature Medicine*, **2,** 912-7.

Siliciano, J.D., Canman, C.E., Taya, Y., Sakaguchi, K., Appella, E., & Kastan, M.B. (1997). DNA damage induces phosphorylation of the amino terminus of p53. *Genes Dev*, **11**, 3471-81

Simbulan-Rosenthal, C.M., Rosenthal, D.S., Ding, R., Bhatia, K. & Smulson, M.E. (1998). Prolongation of the p53 response to DNA strand breaks in cells depleted of PARP by antisense RNA expression. *Biochem Biophys Res Commun*, **253,** 864-8.

Skehan, P., Storeng, R., Scudiero, D., Monks, A., McMahon, J., Vistica, D., Warren, J.T., Bokesch, H., Kenney, S., & Boyd, M.R. (1990). New colorimetric cytotoxicity assay for anti-cancer drug screening. *J Natl Cancer Inst,* **82**, 1107-12

Skidmore, C.J., Davies, M.I., Goodwin, P.M., Halldorsson, H., Lewis, P.J., Shall, S. & Zia'ee, A.A. (1979). The involvement of poly(ADP-ribose) polymerase in the degradation of NAD caused by gamma-radiation and N-methyl-N-nitrosourea. *Eur J Biochem*, **101,** 135-42.

Slattery, E., Dignam, J.D., Matsui, T. & Roeder, R.G. (1983). Purification and analysis of a factor which suppresses nick-induced transcription by RNA polymerase II and its identity with poly(ADP-ribose) polymerase. *J Biol Chem*, **258,** 5955-9.

Smith, S., Giriat, I., Schmitt, A. & de Lange, T. (1998). Tankyrase, a poly(ADP-ribose) polymerase at human telomeres. *Science*, **282,** 1484-7.

Solomon, M.J., Glotzer, M., Lee, T.H., Philippe, M. & Kirschner, M.W. (1990). Cyclin activation of p34cdc2. *Cell*, **63,** 1013-24.

Southern, E.M. (1979). Analysis of restriction-fragment patterns from complex deoxyribonucleic acid species. *Biochem Soc Symp*, **44,** 37-41.

Sugimura, T., Fujimura, S., Hasegawa, S. & Kawamura, Y. (1967). Polymerization of the adenosine 5'-diphosphate ribose moiety of NAD by rat liver nuclear enzyme. *Biochim Biophys Acta*, **138,** 438-41.

Sugrue, M.M., Shin, D.Y., Lee, S.W. & Aaronson, S.A. (1997). Wild-type p53 triggers a rapid senescence program in human tumor cells lacking functional p53. *Proc Natl Acad Sci U S A*, **94,** 9648-53.

Suto, M.J., Turner, W.R., Arundel-Suto, C.M., Werbel, L.M. & Sebolt-Leopold, J.S. (1991). Dihydroisoquinolinones: the design and synthesis of a new series of potent inhibitors of poly(ADP-ribose) polymerase. *Anticancer Drug Des*, **6,** 107-17.

Szabo, C. (1996). The pathophysiological role of peroxynitrite in shock, inflammation, and ischemia-reperfusion injury. *Shock*, **6,** 79-88.

Szabo, C. (1998). Role of poly(ADP-ribose)synthetase in inflammation. *Eur J Pharmacol*, **350,** 1-19.

Tao, W. & Levine, A.J. (1999). P19(ARF) stabilizes p53 by blocking nucleo-cytoplasmic shuttling of Mdm2. *Proc Natl Acad Sci U S A*, **96,** 6937-41.

Taylor, W.R. & Stark, G.R. (2001). Regulation of the G2/M transition by p53. *Oncogene*, **20,** 1803-15.

Thut, C.J., Chen, J.L., Klemm, R. & Tjian, R. (1995). p53 transcriptional activation mediated by coactivators TAFII40 and TAFII60. *Science*, **267,** 100-4.

Thut, C.J., Goodrich, J.A. & Tjian, R. (1997). Repression of p53-mediated transcription by MDM2: a dual mechanism. *Genes & Development*, **11,** 1974-86.

Todaro, G.J. & Green, H. (1963). Quantitative studies of the growth of mouse embryo cells in culture and their development into established lines. *J Cell Biol*, **17,** 299-313.

Tong, W., Prakash Hande, M., Lansdorp, P.M. & Wang, Z.Q. (2001). DNA strand break-sensing molecule poly(ADP-ribose) polymerase cooperates with p53 in telomere function, chromosomal stability and tumour suppression. *Mol Cell Biol*, **21,** 4046-54.

Trucco, C., Oliver, F.J., de Murcia, G. & Menissier-de Murcia, J. (1998). DNA repair defect in poly(ADP-ribose) polymerase-deficient cell lines. *Nucleic Acids Res*, **26,** 2644-9.

Valenzuela, M.T., Guerrero, R., Nunez, M.I., Ruiz De Almodovar, J.M., Sarker, M., de Murcia, G. & Oliver, F.J. (2002). PARP-1 modifies the effectiveness of p53-mediated DNA damage response. *Oncogene*, **21,** 1108-16.

van den Heuvel, S. & Harlow, E. (1993). Distinct roles for cyclin-dependent kinases in cell cycle control. *Science*, **262,** 2050-4.

Van Gool, L., Meyer, R., Tobiasch, E., Cziepluch, C., Jauniaux, J.C., Mincheva, A., Lichter, P., Poirier, G.G., Burkle, A. & Kupper, J.H. (1997). Overexpression of human poly(ADP-ribose) polymerase in transfected hamster cells leads to increased poly(ADP-ribosyl)ation and cellular sensitization to gamma irradiation. *Eur J Biochem*, **244,** 15-20.

Vaziri, H. & Benchimol, S. (1998). Reconstitution of telomerase activity in normal human cells leads to elongation of telomeres and extended replicative life span. *Curr Biol*, **8,** 279-82.

Vaziri, H., West, M.D., Allsopp, R.C., Davison, T.S., Wu, Y.S., Arrowsmith, C.H., Poirier, G.G. & Benchimol, S. (1997). ATM-dependent telomere loss in aging human diploid fibroblasts and DNA damage lead to the post-translational activation of p53 protein involving poly(ADP-ribose) polymerase. *EMBO Journal*, **16,** 6018-33.

Vispe, S., Yung, T.M., Ritchot, J., Serizawa, H. & Satoh, M.S. (2000). A cellular defense pathway regulating transcription through poly(ADP-ribosyl)ation in response to DNA damage. *Proc Natl Acad Sci U S A*, **97,** 9886-91.

Vogel, H., Lim, D.S., Karsenty, G., Finegold, M. & Hasty, P. (1999). Deletion of Ku86 causes early onset of senescence in mice. *Proc Natl Acad Sci U S A*, **96,** 10770-5.

Vousden, K.H. & Lu, X. (2002). Live or let die: the cell's response to p53. *Nature Reviews. Cancer.*, **2,** 594-604.

Wang, X., Ohnishi, K., Takahashi, A. & Ohnishi, T. (1998). Poly(ADP-ribosyl)ation is required for p53-dependent signal transduction induced by radiation. *Oncogene*, **17,** 2819-25.

Wang, Z.Q., Auer, B., Stingl, L., Berghammer, H., Haidacher, D., Schweiger, M. & Wagner, E.F. (1995). Mice lacking ADPRT and poly(ADP-ribosyl)ation develop normally but are susceptible to skin disease. *Genes Dev*, **9,** 509-20.

Wang, Z.Q., Stingl, L., Morrison, C., Jantsch, M., Los, M., Schulze-Osthoff, K. & Wagner, E.F. (1997). PARP is important for genomic stability but dispensable in apoptosis. *Genes Dev*, **11,** 2347-58.

Weber, J.D., Taylor, L.J., Roussel, M.F., Sherr, C.J. & Bar-Saagi, D. (1999). Nucleolar Arf sequesters Mdm2 and activates p53. *Nat Cell Biol*, **1**, 20-6.

Weinfeld, M., Chaudhry, M.A., D'Amours, D., Pelletier, J.D., Poirier, G.G., Povirk, L.F. & Lees-Miller, S.P. (1997). Interaction of DNA-dependent protein kinase and poly(ADP-ribose) polymerase with radiation-induced DNA strand breaks. *Radiat Res*, **148,** 22-8.

Wesierska-Gadek, J., Bugajska-Schretter, A. & Cerni, C. (1996a). ADP-ribosylation of p53 tumor suppressor protein: mutant but not wild-type p53 is modified. *J Cell Biochem*, **62,** 90-101.

Wesierska-Gadek, J. & Schmid, G. (2000). Overexpressed poly(ADP-ribose) polymerase delays the release of rat cells from p53-mediated G(1) checkpoint. *J Cell Biochem*, **80,** 85-103.

Wesierska-Gadek, J., Schmid, G., Cerni, C. & Bugajska-Schretter, A. (1996b). ADP-ribosylation of wild-type p53 in vitro: binding of p53 protein to specific p53 consensus sequence prevents its modification

ADP-ribosylation of p53 tumor suppressor protein: mutant but not wild-type p53 is modified. *Biochem Biophys Res Commun*, **224,** 96-102.

Wesierska-Gadek, J., Wang, Z.Q. & Schmid, G. (1999). Reduced stability of regularly spliced but not alternatively spliced p53 protein in PARP-deficient mouse fibroblasts. *Cancer Res*, **59,** 28-34.

Westphal, C.H., Schmaltz, C., Rowan, S., Elson, A., Fisher, D.E. & Leder, P. (1997). Genetic interactions between atm and p53 influence cellular proliferation and irradiation-induced cell cycle checkpoints. *Cancer Res*, **57,** 1664-7.

Whitacre, C.M., Hashimoto, H., Tsai, M.L., Chatterjee, S., Berger, S.J. & Berger, N.A. (1995). Involvement of NAD-poly(ADP-ribose) metabolism in p53 regulation and its consequences. *Cancer Res*, **55,** 3697-701.

Wielckens, K., George, E., Pless, T. & Hilz, H. (1983). Stimulation of poly(ADP-ribosyl)ation during Ehrlich ascites tumor cell "starvation" and suppression of concomitant DNA fragmentation by benzamide. *J Biol Chem*, **258,** 4098-104.

Wielckens, K., Schmidt, A., George, E., Bredehorst, R. & Hilz, H. (1982). DNA fragmentation and NAD depletion. Their relation to the turnover of endogenous mono(ADP-ribosyl) and poly(ADP-ribosyl) proteins. *J Biol Chem*, **257,** 12872-7.

Wolf, B.B. & Green, D.R. (1999). Suicidal tendencies: apoptotic cell death by caspase family proteinases. *Journal of Biological Chemistry*, **274,** 20049-52.

Woo, R.A., McLure, K.G., Lees-Miller, S.P., Rancourt, D.E. & Lee, P.W. (1998). DNA-dependent protein kinase acts upstream of p53 in response to DNA damage. *Nature*, **394,** 700-4.

Wood, R.D., Mitchell, M., Sgouros, J. & Lindahl, T. (2001). Human DNA repair genes. *Science*, **291,** 1284-9.

Wright, W.E. & Shay, J.W. (2000). Telomere dynamics in cancer progression and prevention: fundamental differences in human and mouse telomere biology. *Nat Med*, **6,** 849-51.

Wu, G.S., Burns, T.F., McDonald, E.R., 3rd, Jiang, W., Meng, R., Krantz, I.D., Kao, G., Gan, D.D., Zhou, J.Y., Muschel, R., Hamilton, S.R., Spinner, N.B., Markowitz, S., Wu, G. & el-Deiry, W.S. (1997). KILLER/DR5 is a DNA damage-inducible p53-regulated death receptor gene. *Nature Genetics*, **17,** 141-3.

Wu, L. & Levine, A.J. (1997). Differential regulation of the p21/WAF-1 and mdm2 genes after high-dose UV irradiation: p53-dependent and p53-independent regulation of the mdm2 gene. *Molecular Medicine*, **3,** 441-51.

Wu, X., Bayle, J.H., Olson, D. & Levine, A.J. (1993). The p53-mdm-2 autoregulatory feedback loop. *Genes & Development*, **7,** 1126-32.

Xiao, Z.X., Chen, J., Levine, A.J., Modjtahedi, N., Xing, J., Sellers, W.R. & Livingston, D.M. (1995). Interaction between the retinoblastoma protein and the oncoprotein MDM2. *Nature*, **375,** 694-8.

Xu, Y. & Baltimore, D. (1996). Dual roles of ATM in the cellular response to radiation and in cell growth control. *Genes Dev*, **10,** 2401-10.

Yoshihara, K., Itaya, A., Tanaka, Y., Ohashi, Y., Ito, K., Teraoka, H., Tsukada, K., Matsukage, A. & Kamiya, T. (1985). Inhibition of DNA polymerase alpha, DNA polymerase beta, terminal deoxynucleotidyl transferase, and DNA ligase II by poly(ADP-ribosyl)ation reaction in vitro. *Biochem Biophys Res Commun*, **128,** 61-7.

Zhang, Y. & Xiong, Y. (2001). A p53 amino-terminal nuclear export signal inhibited by DNA damage-induced phosphorylation. *Science*, **292,** 1910-5.

Ziegler, M. & Oei, S.L. (2001). A cellular survival switch: poly(ADP-ribosyl)ation stimulates DNA repair and silences transcription. *Bioessays*, **23,** 543-8.

Zou, H., Henzel, W.J., Liu, X., Lutschg, A. & Wang, X. (1997). Apaf-1, a human protein homologous to C. elegans CED-4, participates in cytochrome c-dependent activation of caspase-3. *Cell*, **90,** 405-13.

# Appendix A
# Buffers and reagents

**Reagents for Western blot analysis**

**a) Electrode buffer**

| | |
|---|---|
| Tris | 25mM |
| Glycine | 200mM |
| SDS | 0.1% |

**b) Western blotting buffer**

| | |
|---|---|
| Tris | 25mM |
| Glycine | 200mM |
| Methanol | 20% |

**c) TBS-Tween**

| | |
|---|---|
| Tris | 50mM |
| NaCl | 0.15M |
| Tween20 | 0.1% |

**d) SDS lysis buffer**

| | |
|---|---|
| Tris | 62.5mM (pH 6.8 with HCl) |
| SDS | 2% |
| Glycerol | 10% |
| Distilled water | 15.5ml |

**Reagents for agarose gel electrophoresis**

**a) Tris-borate EDTA (TBE)**

| | |
|---|---|
| Tris-borate | 45mM |
| EDTA | 1mM |

**b) Loading buffer**

| | |
|---|---|
| Glycerol | 800µl |
| 0.5M EDTA | 40µl |
| Distilled water | 1160µl |

**Reagents for Southern blotting**

**a) 20 X SSC**

| | |
|---|---|
| NaCl | 175.3g |
| Na citrate | 88.2g |
| Distilled $H_2O$ | 800ml — pH to 7 with NaOH and make to 1000ml with $H_2O$ |

**b) Gilbert s solution**

| | |
|---|---|
| 1M $Na_2HPO_4$ | 152.5ml (pH 7.0) |

| | |
|---|---|
| 1M $NaH_2PO_4$ | 97.5ml (pH 7.0) |
| 0.5M EDTA | 1ml (pH 8.0) |
| $dH_2O$ | 74ml |
| BSA | 5g |

Filter sterilise then add 175ml of 20% SDS

**Reagents for PARP permeabilised cell assay measuring the incorporation of [$^{32}$P]-$NAD^+$**

**a) Isotonic buffer**

| | |
|---|---|
| HEPES | 40mM |
| KCl | 130mM |
| Dextran | 4% w/v |
| EGTA | 2mM |
| $MgCl_2$ | 2.3mM |
| Sucrose | 225mM |
| DTT | 2.5mM |

adjusted to pH 7.8 with NaOH/HCl

**Reagents for PARP permeabilised cell assay by antibody recognition**

**a) Permeabilisation buffer**

| | |
|---|---|
| Tris.HCL | 10mM |
| EDTA | 1mM |
| $MgCl_2$ | 4mM |
| 2-mercaptoethanol | 30mM |

pH to 7.8

supplemented with 0.015% digitonin

**b) Reaction buffer**

| | |
|---|---|
| Tris.Hcl | 100mM |
| $NAD^+$ | 1mM |
| $MgCl_2$ | 120mM |

pH to 7.8

# Appendix B
# Publications & presentations

Jowsey *et al.*, (2002). Proc Amer Assoc Cancer Res. *p53 accumulation and p53-mediated transcriptional transactivation in response to ionizing radiation is independent of poly(ADP-ribose) polymerase-1.* **Vol 43,** Poster 5640

Jowsey *et al.*, (2001). Proc Amer Assoc Cancer Res. *Poly(ADP-ribose) polymerase as an upstream regulator of p53 and mdm2.* **Vol 42,** Poster 1161

Jowsey *et al.*, (2001). Br J Cancer. *The dependence of p53 induction and activity on poly(ADP-ribose) polymerase-1.* **Vol 85,** Poster 183

British Institute of Radiology: DNA damage & response meeting; March 1st 2002

A fifteen minute oral communication entitled *"p53 accumulation and p53 mediated transcriptional transactivation in response to ionizing radiation is independent of poly(ADP-ribose) polymerase-1"*